（Ⅱ）-A Structural analysis

(Ⅱ)-A. Structural analysis

A.1 Structural design

A.1.1 General description

A Type B(U) packaging consists of an inner shell, an outer shell, and a fuel basket as shown in (Ⅰ)-Fig.C.1.

The inner shell consists of a shell containing a fuel basket and a lid.

Fuel basket No.1 is the rectangular type as shown in (Ⅰ)-Fig.C.8. A basket for rectangular elements or wrapped KUCA fuels can contain up to ten elements.

Fuel basket No.2 is also the rectangular type as shown in (Ⅰ)-Fig.C.9. The basket can contain up to 1 spectrum converter.

After being placed in the fuel basket, the fuel elements, wrapped KUCA fuels and spectrum converter are fixed by a spacer made of silicone rubber.

Inner shell combined with its lid forms containment boundary as shown in (Ⅰ)-Fig.C.3 and also works as a pressure vessel against inner pressure. Inner lid attached to inner shell by inner lid bolts keep containment of its joint using double O-ring system.

Outer shell with its lid forms containment boundary as shown in (Ⅰ)-Fig.C.4.

Heat insulator and shock absorber are filled between inner shell and outer shell. Outer lid attached to outer shell with outer lid bolts keep containment of its joint using Gasket.

Inner lid would never be opened by any possible contingency since it is covered by outer lid during transport. Outer lid bolt has a lock and a seal so that they would show evidence that it has not been opened.

This packaging is lifted and tied down with 4 eye-plates shown in (Ⅰ)-Fig.C.5.

The package is tie_down to tie down device shown in (Ⅰ)-Fig.C.2 with eye-plates during transport.

A.1.2 Design standards

The design standards for the packaging are based on the "Public Notification and Section Ⅲ-Subsec, NB of ASME. Analytical standard are determined for each set of test conditions.

(1) Analytical standards

(Ⅱ)-Table A.1 shows the various test conditions for the design standards corresponding to the items being analyzed. The analytical standards will be determined on the basis of the mechanical properties of the materials shown in section (Ⅱ)-A.3 and the temperatures shown in section (Ⅱ)-B.

The design standard value in which distortion level has no influence on the packaging's containment under accident test conditions is used for the inner lid clamping bolts, which are essential for the containment boundary. Yield stress is used as the analytical standard for the hoisting and clamping device in accordance with the "Public Notification". Penetration resistance is chosen as the analytical standard for the collision during the penetration test.

Welding efficiency is 1.0 for welding parts inspected by radiation method and 0.45 for other welding parts.

Symbols of the design standard value in Tables are as follows;

Sm ; Design stress intensity value

Sy ; Yield point of the designh

Su ; Design tensile strength

Sa ; Alternative peak stress

N ; Number of cycles

Na ; Allowable number of cycles

DF ; Accumulative usage factor (= N/Na)

(2) Combinations of design load

Combinations of design load are determined on conditions (structure temperature, material, safety factor, etc.) of each components shown in (Ⅱ)-Table.A.2 and (Ⅱ)-Table.A.3.

(3) Margin for safety

Margin of safety (MS) is obtained as follows.

$$\text{Margin for safety (MS)} = \frac{\text{The design standard value}}{\text{Analytical value}} - 1$$

According to the design standards described above, (Ⅱ)-Table A.4 (1/24) ～(24/24) shows conditions of structural analysis, analytical item and method, etc.

(Ⅱ)-Table A.1 Design standard for structural analysis

Pm; General primary membrane stress
PL; Local primary membrane stress
Pb; Primary bending stress
Q ; Secondary stress
F ; Peak stress
DF; Accumulative usage factor

Condition	Item	Component / Position to be evaluated	Primary stress		Primary+secon-dary Stress	Primary+secon-dary+peak stress
			Pm(PL)	PL+Pb	PL+Pb+Q	PL+Pb+Q+F
Routine transport	Lifting device	Eye plate	<Sy	<Sy	—	—
	Tie-down device	Eye plate	<Sy	<Sy	—	—
	Pressure	Package	Withstanding the effect of changing ambient pressure.			
	Vibration	Package	Withstanding the effect of vibration during transport.			
Normal conditions of transport	Thermal test	Inner shell	<Sm	<1.5Sm	<3Sm	Fatigue evaluation (DF<1)
		Inner lid	<2/3Sy	<Sy	<Sy	
		Inner lid bolt				
	Water spray test	Package	Withstanding the water spray test.			
	Free drop test (1.2m height)	Inner shell	<Sm	<1.5Sm	<3Sm	—
		Fuel basket				
		Inner lid	<2/3Sy	<Sy	<Sy	—
		Inner lid bolt				
		Fuel element/plate				
	Stacking test	Inner shell	<Sm	<1.5Sm	<3Sm	—
		Inner lid	<2/3Sy	<Sy	<Sy	
	Penetrating test	Outer shell	No penetration			
Accident conditions of transport	Drop test Ⅰ (9m height)	Inner shell	$<\frac{2}{3}$Su	<Su	—	—
		Fuel basket				
		Inner lid	<2/3Sy	<Sy	—	—
		Inner lid bolt				
		Fuel element/plate				
	Drop test Ⅱ (1m height penetration)	Outer shell	No penetration			
		Inner shell	$<\frac{2}{3}$Su	<Su	—	—
		Inner lid	<2/3Sy	<Sy	—	
	Thermal test	Inner shell	$<\frac{2}{3}$Su	<Su	—	—
		Inner lid	<2/3Sy	<Sy	—	
		Inner lid bolt				
	Water immersion (15m depth)	Inner shell	$<\frac{2}{3}$Su	<Su	—	—
		Inner lid	<2/3Sy	<Sy	—	

Note: The same criteria for stress evaluation are used for both Type B(U) packages and fissile packages.

"fuel plate" includes spectrum converter

(Ⅱ)-Table A.2 Design load, combination of load (1/2)

Require-ment	Condition	Item	Component / Position to be evaluated	Load				
				Mass*	Internal pressure	External pressure	Thermal expansion	Other
B(U) package	Routine transport	Lifting device	Eye plate	△	—	—	—	—
		Tie-down device	Eye plate	△	—	—	—	—
		Pressure	Package	—	○	○	—	○
		Vibration	Package	—	—	—	—	△
	Normal conditions of transport	Thermal test	Inner shell	—	△	—	—	—
			Inner lid	—	△	—	—	—
			Inner lid bolt	—	○	—	○	○
		Water spray test	Package	—	—	—	—	△
		Free Drop test (1.2m height)	Inner shell	○	○	—	—	—
			Fuel basket	△	—	—	—	—
			Inner lid	○	○	—	—	—
			Inner lid bolt	○	○	—	○	○
			Fuel element/plate	△	—	—	—	—
		Penetrating test	Outer shell	—	—	—	—	△
		Stacking test	Inner shell	○	○	—	—	—
	Accident conditions of transport	Drop test Ⅰ (9m height)	Inner shell	○	○	—	—	—
			Fuel basket	△	—	—	—	—
			Inner lid	○	○	—	—	—
			Inner lid bolt	○	○	—	—	○
			Fuel element/plate	△	—	—	—	—
		Drop test Ⅱ (1m height penetration)	Outer shell	△	—	—	—	—
			Inner shell	○	○	—	—	—
			Inner lid	○	○	—	—	—
		Thermal test	Inner shell	—	△	—	—	—
			Inner lid	—	△	—	—	—
			Inner lid bolt	—	○	—	—	○
		Water immersion (15m depth)	Inner shell	—	—	△	—	—
			Inner lid	—	—	△	—	—

○: Analyzed under combination of load. △: Analyzed under single load.

＊: Mass does not mean weight simply but means mass (force) considering impact force such as given (mass) × (acceleration).

Note: “fuel plate” includes spectrum converter

(Ⅱ)-Table A.2 Design load, combination of load (2/2)

Require-ment	Condition	Item	Component / Position to be evaluated	Load				
				Mass*	Internal pressure	External pressure	Thermal expansion	Other
Fissile packages	Normal conditions of transport	Water spray test	Package	—	—	—	—	△
		Free drop test (1.2m height)	Inner shell	○	○	—	—	—
			Fuel basket	△	—	—	—	—
			Inner lid	○	○	—	—	—
			Inner lid bolt	○	○	—	○	○
			Fuel element/plate	△	—	—	—	—
		Stacking test	Inner shell	○	○	—	—	—
		Penetrating test	Outer shell	—	—	—	—	△
	Accident conditions of transport	Drop test Ⅰ (9m height)	Inner shell	○	○	—	—	—
			Fuel basket	△	—	—	—	—
			Inner lid	○	○	—	—	—
			Inner lid bolt	○	○	—	—	○
			Fuel element/plate	△	—	—	—	—
		Drop test Ⅱ (1m height penetration)	Outer shell	△	—	—	—	—
			Inner shell	○	○	—	—	—
			Inner lid	○	○	—	—	—
		Thermal test	Inner shell	—	△	—	—	—
			Inner lid	—	△	—	—	—
			Inner lid bolt	—	○	—	—	○
		Water immersion (0.9m depth)	Inner shell	—	—	△	—	—
			Inner lid	—	—	△	—	—

○: Analyzed under combination of load. △: Analyzed under single load.

* : Mass does not mean weight simply but means mass (force) considering impact force such as given (mass) × (acceleration).

Note: "fuel plate" includes spectrum converter

(Ⅱ)-Table A.3 Load conditions (1/2)

Require-ment	Condition	Item	Component / Position to be evaluated	Load				
				Mass*	Internal pressure	External pressure	Thermal expan-sion	Other
B(U) Package	Routine transport	Lifting device	Eye plate	×3 times $=6.99\times10^{3}$N	—	—	—	—
		Tie-down device	Eye plate	×2[g] (up, down, front, back) ×1[g] (Left, right)	—	—	—	—
		Pressure	Package	—	9.81×10^{-2}MPa	60kPa	—	Initial clamping force 5.89×10^{4}N
		Vibration	Package	—	—	—	—	—
	Normal conditions of transport	Thermal test	Inner shell	—	9.81×10^{-2}MPa	—	—	—
			Inner lid	—	9.81×10^{-2}MPa	—	—	—
			Inner lid bolt	—	9.81×10^{-2}MPa	—	75(℃)	Initial clamping force 5.89×10^{4}N
		Water spray test	Package	—	—	—	—	—
		Free drop test (1.2m height)	Inner shell	×Acceleration =254.1[g] (for horizontal drop) =250.6[g] (for vertical drop) =90.8[g] (for corner drop)	9.81×10^{-2}MPa	—	—	—
			Fuel basket		—	—	—	—
			Inner lid		9.81×10^{-2}MPa	—	—	—
			Inner lid bolt		9.81×10^{-2}MPa	—	75(℃)	Initial clamping force 5.89×10^{4}N
			Fuel element/plate		—	—	—	—
		Stacking test	Inner shell	×5 times+Self weight	9.81×10^{-2}MPa	—	—	—
		Penetrating test	Outer shell	—	—	—	—	6kg Bar drop
	Accident conditions of transport	Drop test Ⅰ (9m height)	Inner shell	×Acceleration =367.0[g] (for horizontal drop) =388.4[g] (for vertical drop) =310.9[g] (for corner drop)	9.81×10^{-2}MPa	—	—	—
			Fuel basket		—	—	—	—
			Inner lid		9.81×10^{-2}MPa	—	—	—
			Inner lid bolt		9.81×10^{-2}MPa	—	—	Initial clamping force 5.89×10^{4}N
			Fuel element/plate		—	—	—	—
		Drop test Ⅱ (1m height penetration)	Outer shell	Self weight ×1m drop on mild steel bar	—	—	—	—
			Inner shell	×Acceleration =72.1g(Horizontal) =147.1[g](Vertical)	9.81×10^{-2}MPa	—	—	—
			Inner lid		9.81×10^{-2}MPa	—	—	—
		Thermal test	Inner shell	—	9.81×10^{-2}MPa	—	—	—
			Inner lid	—	9.81×10^{-2}MPa	—	—	—
			Inner lid bolt	—	9.81×10^{-2}MPa	—	—	Initial clamping force 5.89×10^{4}N
		Water immersion (15m depth)	Inner shell	—	—	147kPa	—	—
			Inner lid	—	—	147kPa	—	—

* : Mass does not mean weight simply but means mass (force) considering impact force such as given (mass) × (acceleration).

(Ⅱ)-Table A.3 Load conditions (2/2)

Require-ment	Condition	Item	Component / Position to be evaluated	Load: Mass*	Load: Internal pressure	Load: External pressure	Load: Thermal expan-sion	Load: Other
Fissile package	Normal conditions of transport	Water spray test	Package	—	—	—	—	Water spray
		Free drop test (1.2m height)	Inner shell	×Acceleration =254.1[g] (for horizontal drop) =250.6[g] (for vertical drop) =90.8[g] (for corner drop)	9.81×10^{-2}MPa	—	—	—
			Fuel basket		—	—	—	—
			Inner lid		9.81×10^{-2}MPa	—	—	—
			Inner lid bolt		9.81×10^{-2}MPa	—	75(℃)	Initial clamping force 5.89×10^{4}N
			Fuel element/plate		—	—	—	—
		Stacking test	Inner shell	×5 times+Self weight	9.81×10^{-2}MPa	—	—	—
		Penetrating test	Outer shell	—	—	—	—	6kg bar drop
	Accident conditions of transport	Drop test Ⅰ (9m height)	Inner shell	×Acceleration =379.0[g] (for horizontal drop) =446.2[g] (for vertical drop) =332.3[g] (for corner drop)	9.81×10^{-2}MPa	—	—	—
			Fuel basket		—	—	—	—
			Inner lid		9.81×10^{-2}MPa	—	—	—
			Inner lid bolt		9.81×10^{-2}MPa	—	—	Initial clamping force 5.89×10^{4}N
			Fuel element/plate		—	—	—	—
		Drop test Ⅱ (1m height penetration)	Outer shell	Self weight 1m drop on mild steel bar	—	—	—	—
			Inner shell	×Acceleration =72.1g(Horizontal) =147.0[g](Vertical)	9.81×10^{-2}MPa	—	—	—
			Inner lid		9.81×10^{-2}MPa	—	—	—
		Thermal test	Inner shell	—	9.81×10^{-2}MPa	—	—	—
			Inner lid	—	9.81×10^{-2}MPa	—	—	—
			Inner lid bolt	—	9.81×10^{-2}MPa	—	—	Initial clamping force 5.89×10^{4}N
		Water immersion (0.9m depth)	Inner shell	—	—	9 kPa	—	—
			Inner lid	—	—	9 kPa	—	—

＊ : Mass does not mean weight simply but means mass (force) considering impact force such as given (mass) × (acceleration).

Symbols;

σ	: Principal stress	τ_t	: Torsional stress
σ_b	: Bending stress	F	: Load
σ_c	: Compressive stress	P	: Pressure
τ	: Shear stress	A	: Cross section

(Ⅱ)-Table A.4 Design conditions, analytical methods of structural analysis (1/24)

Requirement	Condition	Item	Design condition						Analytical methods		Remark
			Reference figure	Material	Temp.	Design load			Applied formula or element	Standard	
						Type	Loading factor	Element			
B(U) package	Routine transport	1. Chemical and galvanic reaction									
		(1) Chemical reaction	—	—	—	Corrosion	—	Activation difference of electric position	no chemical reaction	Nil	
		(2) Galvanic reaction	—	—	—	Corrosion	—		no galvanic reaction	Nil	
		2. Strength at low temperature									
		(1) Body	—	SUS304	-40℃	Material	1	Degradation	Allowable lowest temperature	No brittle fracture -40℃	
		(2) Bolt	—	SUS630	-40℃	Material	1	Degradation	Allowable lowest temperature		
		(3) O-ring	—	Silicon-rubber	-40℃	Material	1	Degradation	Allowable lowest temperature		
		3. Containment system									
		(1) Inner lid	(Ⅰ)-Fig.C.3	SUS630	75℃	Opening due to contingency	—	Possibility of contingency	—	Nil	
		4. Lifting device							M:Bending moment t:Plate thickness b:Width of eye plate		
		(1) Eye plate	(Ⅱ)-Fig.A.9	SUS304	75℃	Mass of package	3	Bending stress	$\sigma_b = \frac{6M}{tb^2}$	Sy	
							3	Shear stress	$\tau = \frac{F}{A}$	0.6Sy	
								Combined stress	$\sigma = \sqrt{\sigma_b^2 + 4\tau^2}$	S	
		5. Tie-down device									
		(1) Eye plate	(Ⅱ)-Fig.A.11	SUS304	75℃	Mass of package	2	Bending stress	$\sigma_b = \frac{6M}{tb^2}$	Sy	
			(Ⅱ)-Fig.A.12				2	Shear stress	$\tau = \frac{F}{A}$	0.6Sy	
								Combined stress	$\sigma = \sqrt{\sigma_b^2 + 4\tau^2}$	S	

Symbols;

σ	: Principal stress	τ_t	: Torsional stress
σ_b	: Bending stress	F	: Load
σ_c	: Compressive stress	P	: Pressure
τ	: Shear stress	A	: Cross section

(Ⅱ)-Table A.4 Design conditions, analytical methods of structural analysis (2/24)

Requirement	Condition	Item	Design condition						Analytical methods		Remark
			Reference figure	Material	Temp.	Design load			Applied formula or element	Standard	
						Type	Loading factor	Element			
B(U) package	Routine transport	6. Pressure									
		(1) Frame of Inner shell	—	SUS304	75℃	Reduction of ambient pressure 60kPa	1	Combined stress	$\sigma_\theta = \frac{P \cdot Dm}{2t}$, $\sigma_z = \frac{P \cdot Dm}{4t}$, $\sigma_r = -\frac{P}{2}$ Formula for thin cylinder	Note 1	Note 1: Design standard of each stress component is determined using Sm. Note 2: Analysis standard of each stress component is determined using Sy. Note 3: Initial margin of tightening is about 1.1mm.
		(2) Inner bottom plate	—	SUS304	75℃		1	Combined stress	$\sigma_\theta = \pm 0.225 \frac{P \cdot a^2}{h^2}$, $\sigma_r = \pm 0.75 \frac{P \cdot a^2}{h^2}$, $\sigma_z = -P$ Formula for fixed disc		
		(3) Inner shell lid	—	SUS630	75℃		1	Combined stress	$\sigma_\theta = \sigma_r = \mp 1.24 \frac{P \cdot a^2}{h^2}$, $\sigma_z = -P$ Formula for simply supported disc	Note 2	
		(4) Inner shell lid bolt	—	SUS630	75℃	Initial bolt load	1	Tensile stress	$\sigma_t = \frac{F}{Ar}$		
						Internal pressure	1	Tensile stress	$\sigma_t = \frac{F}{n \cdot Ar}$		
		(5) Displacement of inner O-ring part of inner shell lid	—	SUS630	75℃	Internal pressure	1	Displacement	$\omega = \frac{P \cdot a^4}{64} \times \left(1 - \frac{r^2}{a^2}\right) \times \left(\frac{5+\nu}{1+\nu} - \frac{r^2}{a^2}\right)$ Formula for displacement of O-ring part	Note 3	
		7. Vibration (1) Package (2) Fuel basket	(Ⅱ)-Fig.A.14	SUS304	75℃	Vibration	1	Resonance	$f_u = \sqrt{\frac{1}{2\pi}} \cdot \sqrt{\frac{k}{m}}$ f_u :characteristic frequency	No resonance	

Symbols;

σ	: Principal stress	τ_t	: Torsional stress
σ_b	: Bending stress	F	: Load
σ_c	: Compressive stress	P	: Pressure
τ	: Shear stress	A	: Cross section

(Ⅱ)-Table A.4 Design conditions, analytical methods of structural analysis (3/24)

Requirement	Condition	Item	Design condition						Analytical methods		Remark
			Reference figure	Material	Temp.	Design load			Applied formula or element	Standard	
						Type	Loading factor	Element			
B(U) package	Normal test conditions	1. Thermal condition 1.1 Thermal expansion (1) Gap between basket and inner shell	(Ⅱ)-Fig.A.15	SUS304	approx. 62/63℃	Thermal expansion	1	Compression	Presense of gap between inner shell and basket.	Free	—
		1.2 Stress Calculation (1) Frame of Inner shell	(Ⅱ)-Fig.A.16 (Ⅱ)-Fig.A.17	SUS304	75℃	Internal pressure	1	Combined Stress	Formula for thin cylinder	Note 1	Note 1: Design standard of each stress component is determined using Sm. Note 2: Analysis standard of each stress component is determined using Sy. Note 3: Initial margin of tightening is about 1.1mm.
		(2) Inner bottom plate	(Ⅱ)-Fig.A.18	SUS304	75℃	Internal pressure	1	Combined Stress	Formula for fixed disc	Note 1	
		(3) Inner shell lid	(Ⅱ)-Fig.A.19	SUS630	75℃	Internal pressure	1	Combined Stress	Formula for simply supported disc	Note 2	
		(4) Inner shell lid bolt	(Ⅱ)-Fig.A.21	SUS630	75℃	Initial bolt load Internal pressure Thermal expansion	1	Tensile stress Tensile stress Tensile stress	$\sigma_t = \frac{F}{Ai}$ $\sigma_t = \frac{F}{n \cdot Ai}$ Negrigible	Note 2	
		(5) Displacement of O-ring part of inner lid	(Ⅱ)-Fig.A.20	SUS630	75℃	Internal pressure	1	Displacement	Formula for displacement of O-ring part	Note 3	
		2. Water spray test				Water spray	1	Absorption Water-repellent	Absorption Water-repellent	Nil Good	

Symbols;

σ	: Principal stress	τ_t	: Torsional stress
σ_b	: Bending stress	F	: Load
σ_c	: Compressive stress	P	: Pressure
τ	: Shear stress	A	: Cross section

(Ⅱ)-Table A.4 Design conditions, analytical methods of structural analysis (4/24)

Requirement	Condition	Item	Design condition						Analytical methods		Remark
			Reference figure	Material	Temp.	Design load			Applied formula or element	Standard	
						Type	Loading factor	Element			
B(U) package	Normal test conditions	3. Free drop 3.1 Horizontal drop (1) Deformation of shock absorber	(Ⅱ)-Fig.A.35 (Ⅱ)-Fig.A.36	—	—	Horizontal drop from 1.2m height	1	Deformation	$\delta = \delta_0 - \delta_H$ δ_0: Minimum thickness before drop δ_H: Deformation δ : Thickness after drop	Note 1	Note 1: Effect of deformation will be judged in thermal test.
		(2) Frame of Inner shell	(Ⅱ)-Fig.A.37	SUS304	75℃	ditto	1	Bending stress	$\sigma_b = \frac{M}{Z}$		Note 2: Analytical standard of each stress component is determined using Sm.
		(3) Inner bottom plate	(Ⅱ)-Fig.A.38	SUS304	75℃	ditto	1	Shear stress	$\tau = \frac{F}{A}$	Note 2	
		(4) Upper part of inner shell (Inner lid)	(Ⅱ)-Fig.A.39	SUS630	75℃	ditto	1	Shear stress	$\tau = \frac{F}{A}$		
		(5) Inner shell lid bolt	(Ⅱ)-Fig.A.40	SUS630	75℃	ditto	1	Bending stress	$\sigma_b = \frac{M \cdot L_{max}}{1}$		Note 3: Analysis standard of each stress component is determined using Sy.
		(6) Fuel basket	(Ⅱ)-Fig.A.41	SUS304	75℃	ditto	1	Bending stress	$\sigma_b = \frac{M}{Z}$		
		(7) Fuel element/plate	(Ⅱ)-Fig.A.42～44	AG3NE	75℃	ditto	1	Bending stress	$\sigma_b = \frac{M}{Z}$	Note 3	
							1	Compression stress	$\sigma_c = \frac{W}{a(h_2 - h_1)}$		
		(Spectrum Converter)		A6061P (T6)			1	Buckling stress	$\sigma_y = \sigma_{cr}\left(1 + \frac{e}{r}\sec\frac{L}{2K}\sqrt{\frac{\sigma_{cr}}{E}}\right)$ σ_y : Yield stress σ_{cr} : buckling stress E : modulus of direct elasticity K : radius-of-gyration of area L : length r : section modulus/cross section e : eccentricity	Note 4	Note 4: Analysis standard is Sy.
		(8) Fuel element hold down part	(Ⅱ)-Fig.A.45	A6061P (T6)	75℃	ditto	1	Bending stress	$\sigma_b = \frac{M}{Z}$	Note 5	Note 5: Analysis standard of each stress component is determined using Sy.

Note: Bolt stress due to internal pressure and initial bolt load is obtained from the design condition and formula described in “1.2 Stress calculation”.

Symbols;

σ	: Principal stress	τ_t	: Torsional stress
σ_b	: Bending stress	F	: Load
σ_c	: Compressive stress	P	: Pressure
τ	: Shear stress	A	: Cross section

(Ⅱ)-Table A.4 Design conditions, analytical methods of structural analysis (5/24)

Requirement	Condition	Item	Design condition						Analytical methods		Remark
			Reference figure	Material	Temp.	Design load			Applied formula or element	Standard	
						Type	Loading factor	Element			
B(U) package	Normal test conditions	3.2 Vertical drop (Bottom side)	(Ⅱ)-Fig.A.46								Note 1: Effect of deformation will be judged in thermal test. Note 2: Analytical standard of each stress component is determined using Sm. Note 3: Analysis standard of each stress component is determined using Sy.
		(1) Deformation of shock absorber	(Ⅱ)-Fig.A.47	—	—	Vertical drop (Bottom side) from 1.2m height	1	Deformation	$\delta = \delta_0 - \delta_V$ δ_0: Minimum thickness before drop δ_V: Deformation δ : Thickness after drop	Note 1	
		(2) Frame of Inner shell	(Ⅱ)-Fig.A.48	SUS304	75℃	ditto	1	Compression stress	$\sigma_c = \frac{F}{A}$	Note 2	
		(3) Inner bottom plate	(Ⅱ)-Fig.A.49	SUS304	75℃	ditto	1	Combined stress	Formula for fixed disc		
		(4) Inner shell lid	(Ⅱ)-Fig.A.50	SUS630	75℃	ditto	1	Combined stress	Formula for simply supported disc	Note 3	
		(5) Inner shell lid bolt	—	SUS630	75℃	ditto	1	—	—		
		(6) Fuel Element/plate	(Ⅱ)-Fig.A.51～53	AG3NE	75℃	ditto	1	Shear stress	$\tau = \frac{F}{2(h_2 - h_1)b}$	Note 3	
		(Spectrum Converter)		A6061P (T6)			1	Tensile stress	$\sigma_t = \frac{W_o}{A}$		
							1	Compression stress	$\sigma_c = \frac{W}{A}$		
		(7) Fuel element hold down part	(Ⅱ)-Fig.A.54	A6061P (T6)	75℃	ditto	1	Compression stress	$\sigma_c = \frac{W}{A}$		

Symbols;

σ	: Principal stress	τ_t	: Torsional stress
σ_b	: Bending stress	F	: Load
σ_c	: Compressive stress	P	: Pressure
τ	: Shear stress	A	: Cross section

(Ⅱ)-Table A.4 Design conditions, analytical methods of structural analysis (6/24)

Requirement	Condition	Item	Design condition						Analytical methods		Remark
			Reference figure	Material	Temp.	Design load			Applied formula or element	Standard	
						Type	Loading factor	Element			
B(U) package	Normal test condition	3.3 Vertical drop (Lid side)	(Ⅱ)-Fig.A.55								Note 1: Effect of deformation will be judged in thermal test.
		(1) Deformation of shock absorber	(Ⅱ)-Fig.A.56	—	—	Vertical drop (Lid side) from 1.2m height	1	Deformation	$\delta = \delta_0 - \delta_V$ δ_0: Minimum thickness before drop δ_V: Deformation δ : Thickness after drop	Note 1	
		(2) Frame of Inner shell	(Ⅱ)-Fig.A.57	SUS304	75℃	ditto	1	Compression stress	$\sigma_c = \frac{F}{A}$	Note 2	Note 2: Analytical standard of each stress component is determined using Sm. Note 3: Analysis standard of each stress component is determined using Sy.
		(3) Inner bottom plate	(Ⅱ)-Fig.A.58	SUS304	75℃	ditto	1	Combined stress	Formula for fixed disc		
		(4) Inner shell lid	(Ⅱ)-Fig.A.59	SUS630	75℃	ditto	1	Combined stress	Formula for simply supported disc	Note 3	
		(5) Inner shell lid bolt		SUS630	75℃	ditto	1	Tensile stress	$\sigma_t = \frac{R}{n \cdot Ai}$		
		(6) Fuel Element/plate	(Ⅱ)-Fig.A.60～62	AG3NE	75℃	ditto	1	Shear stress	$\tau = \frac{F}{2(h_2 - h_1)b}$	Note 3	
		(Spectrum Converter)		A6061P (T6)			1	Tensile stress	$\sigma_t = \frac{W_o}{A}$		
							1	Compression stress	$\sigma_c = \frac{W}{A}$		
		(7) Fuel element hold down part	(Ⅱ)-Fig.A.63	A6061P (T6)	75℃	ditto	1	Compression stress	$\sigma_c = \frac{W}{A}$		
		3.4 Corner drop	(Ⅱ)-Fig.A.63			Corner drop from 1.2m drop (Lid side)	1	Analyzed for each item of para.5.1～5.3 above from horizontal and vertical component of impact			
		(1) Inner shell lid bolt	(Ⅱ)-Fig.A.64	SUS630	75℃			Bending stress	$\sigma_{max} = \sigma_V + \sigma_H$ $\sigma_V = \frac{N_V \cdot W \cdot L_V \cdot \ell_{VMAX}}{2\Sigma \ell^2 \cdot A_r}$ $\sigma_H = \frac{N_H \cdot W \cdot L_H \cdot \ell_{HMAX}}{2\Sigma \ell^2 \cdot A_r}$	Note 3	
		3.5 Inclined drop	(Ⅱ)-Fig.A.65～68	—	—	Inclined drop from 1.2m height		Analyzed for each item of para.5.1～5.3 above from horizontal and vertical component of impact			

Symbols;

σ	: Principal stress	τ_t	: Torsional stress
σ_b	: Bending stress	F	: Load
σ_c	: Compressive stress	P	: Pressure
τ	: Shear stress	A	: Cross section

(Ⅱ)-Table A.4 Design conditions, analytical methods of structural analysis (7/24)

Requirement	Condition	Item	Design condition						Analytical methods		Remark
			Reference figure	Material	Temp.	Design load			Applied formula or element	Standard	
						Type	Loading factor	Element			
B(U) package	Normal test condition	4. Stacking test									
		(1) Frame of Inner shell	(Ⅱ)-Fig.A.72	SUS304	75℃	Mass of package	×5+Self weight	Bending stress	$\sigma_Z = \frac{F+m\cdot g}{A}$	Note 1	Note 1: Design standard of each stress component is determined using Su.
		(2) Inner shell lid	(Ⅱ)-Fig.A.71	SUS630	75℃	Mass of package	×5+Self weight	Combined stress	Formula for simply supported disc	Note 2	Note 2: Analysis standard of each stress component is determined using Sy.
		5. Penetration test (1) Outer shell	(Ⅱ)-Fig.A.72, 73	SUS304	75℃	Impact of mild steel bar	×1	Absorbed energy	$E_2 = \frac{1}{2}\tau_{Cr}\cdot\pi\cdot d\cdot t^2$ (τ_{Cr}: Shear strength)=0.6Su	No penetration	
		6. Free drop on each corner or each rim									Not applicable

Symbols;

σ	: Principal stress	τ_t	: Torsional stress
σ_b	: Bending stress	F	: Load
σ_c	: Compressive stress	P	: Pressure
τ	: Shear stress	A	: Cross section

(Ⅱ)-Table A.4 Design conditions, analytical methods of structural analysis (8/24)

Requirement	Condition	Item	Design condition						Analytical methods		Remark
			Reference figure	Material	Temp.	Design load			Applied formula or element	Standard	
						Type	Loading factor	Element			
B(U) package	Accident test conditions	1. Drop test Ⅰ 1.1 Vertical drop (Bottom side) (1) Deformation of shock absorber	(Ⅱ)-Fig.A.75	—	—	Vertical drop (Bottom side) from 9m height	1	Deformation	$\delta = \delta_0 - \delta_V$ δ_0: Minimum thickness before drop δ_V: Deformation δ : Thickness after drop	Note 1	Note 1: Effect of deformation will be judged in thermal test.
		(2) Frame of Inner shell		SUS304	75℃	ditto	1	Compression stress	$\sigma_c = \frac{W}{A}$	Note 3	Note 2: Analytical standard of each stress component is determined using Su.
		(3) Inner bottom plate		SUS304	75℃	ditto	1	Combined stress	Formula for fixed disc		
		(4) Inner shell lid		SUS630	75℃	ditto	1	Combined stress	Formula for simply supported disc	Note 2	
		(5) Inner shell lid bolt		SUS630	75℃	ditto	1	——	——		Note 3: Analysis standard of each stress component is determined using Sy.
		(6) Fuel element/plate		AG3NE	75℃	ditto	1	Shear stress	$\tau = \frac{F}{2(h_2 - h_1)b}$	Note 2	
		(Spectrum Converter)		A6061P (T6)			1	Tensile stress	$\sigma_t = \frac{W_o}{A}$		
							1	Compression stress	$\sigma_c = \frac{W}{A}$		
		(7) Fuel element hold down part		A6061P (T6)	75℃	ditto	1	Compression stress	$\sigma_c = \frac{W}{A}$		

Symbols;

σ	: Principal stress	τ_t	: Torsional stress
σ_b	: Bending stress	F	: Load
σ_c	: Compressive stress	P	: Pressure
τ	: Shear stress	A	: Cross section

(Ⅱ)-Table A.4 Design conditions, analytical methods of structural analysis (9/24)

Requirement	Condition	Item	Design condition						Analytical methods		Remark
			Reference figure	Material	Temp.	Design load			Applied formula or element	Standard	
						Type	Loading factor	Element			
B(U) package	Accident test conditions	1.2 Vertical drop (Lid side)									Note 1: Effect of deformation will be judged in thermal test. Note 2: Analytical standard of each stress component is determined using Su. Note 3: Analysis standard of each stress component is determined using Sy.
		(1) Deformation of shock absorber	(Ⅱ)-Fig.A.76	—	—	Vertical drop (Lid side) from 9m height	1	Deformation	$\delta = \delta_0 - \delta_V$ δ_0: Minimum thickness before drop δ_V: Deformation δ : Thickness after drop	Note 1	
		(2) Frame of Inner shell		SUS304	75℃	ditto	1	Compression stress	$\sigma_c = \frac{F}{A}$	Note 2	
		(3) Inner bottom plate		SUS304	75℃	ditto	1	Combined stress	Formula for fixed disc		
		(4) Inner shell lid		SUS630	75℃	ditto	1	Combined stress	Formula for simply supported disc	Note 3	
		(5) Inner shell lid bolt		SUS630	75℃	ditto	1	Tensile stress	$\sigma_t = \frac{F}{n \cdot Ai}$		
		(6) Fuel element/plate (Spectrum Converter)		AG3NE A6061P (T6)	75℃	ditto	1	Shear stress	$\tau = \frac{F}{2(h_2 - h_1)b}$		
							1	Tensile stress	$\sigma_t = \frac{W_o}{A}$		
							1	Compression stress	$\sigma_c = \frac{W}{A}$		
		(7) Fuel element hold down part		A6061P (T6)	75℃	ditto	1	Compression stress	$\sigma_c = \frac{W}{A}$		

Symbols;

σ	: Principal stress	τ_t	: Torsional stress
σ_b	: Bending stress	F	: Load
σ_c	: Compressive stress	P	: Pressure
τ	: Shear stress	A	: Cross section

(Ⅱ)-Table A.4 Design conditions, analytical methods of structural analysis (10/24)

Requirement	Condition	Item	Design condition						Analytical methods		Remark
			Reference figure	Material	Temp.	Design load			Applied formula or element	Standard	
						Type	Loading factor	Element			
B(U) package	Accident test conditions	1.3 Horizontal drop									
		(1) Deformation of shock absorber	(Ⅱ)-Fig.A.77	—	—	Horizontal drop from 9m height	1	Deformation	$\delta = \delta_0 - \delta_H$ δ_0: Minimum thickness before drop δ : Thickness after drop δ_H: Deformation	Note 1	Note 1: Effect of deformation will be judged in thermal test.
		(2) Frame Of Inner shell		SUS304	75℃	ditto	1	Bending stress	$\sigma_b = \frac{M}{Z}$	Note 3	Note 2: Analytical standard of each stress component is determined using Su. Note 3: Analytical standard of each stress component is determined using Sy. Note 4: Analysis standard is σ_{cr}.
		(3) Inner bottom plate		SUS304	75℃	ditto	1	Combined stress	Formula for fixed disc		
		(4) Upper part of inner shell (Inner lid)		SUS630	75℃	ditto	1	Shear stress	$\tau = \frac{F}{A}$	Note 2	
		(5) Inner shell lid bolt		SUS630	75℃	ditto	1	Bending stress	$\sigma_b = \frac{M \cdot \ell_{max}}{I}$		
		(6) Fuel basket		SUS304	75℃	ditto	1	Bending stress	$\sigma_b = \frac{M}{Z}$		
		(7) Fuel element/plate (Spectrum Converter)		AG3NE A6061P (T6)	75℃	ditto	1	Bending stress	$\sigma_b = \frac{M}{Z}$		
							1	Compression stress	$\sigma_c = \frac{W}{a(h_2 - h_1)}$		
							1	Buckling stress	$\sigma_y = \sigma_{cr}\left(1 + \frac{e}{r}\sec\frac{L}{2K}\sqrt{\frac{\sigma_{cr}}{E}}\right)$ σ_y : Yield stress σ_{cr} : buckling stress E : modulus of direct elasticity K : radius-of-gyration of area L : length r : section modulus/cross section e : eccentricity	Note 4	
		(8) Fuel element hold down part		A6061P (T6)	75℃	ditto	1	Bending stress	$\sigma_b = \frac{M}{Z}$	Note 2	

Symbols;

σ	: Principal stress	τ_t	: Torsional stress
σ_b	: Bending stress	F	: Load
σ_c	: Compressive stress	P	: Pressure
τ	: Shear stress	A	: Cross section

(Ⅱ)-Table A.4 Design conditions, analytical methods of structural analysis (11/24)

Requirement	Condition	Item	Design condition						Analytical methods		Remark
			Reference figure	Material	Temp.	Design load			Applied formula or element	Standard	
						Type	Loading factor	Element			
B(U) package	Accident test conditions	1.4 Corner drop	(Ⅱ)-Fig.A.78			Corner drop from 9m height	1	Analyzed for each item of para.8.1～8.3 above from horizontal and vertical component of impact			Note 1: Analytical standard of each stress component is determined using Sy.
		(1) Inner lid bolt		SUS630	75℃	Corner drop from 9m height (Lid side)	1	Bending stress	$\sigma_{max} = \sigma_V + \sigma_H$ $\sigma_V = \frac{N_V \cdot W \cdot L_V \cdot \ell_{VMAX}}{2\Sigma \ell^2 \cdot A_r}$ $\sigma_H = \frac{N_H \cdot W \cdot L_H \cdot \ell_{HMAX}}{2\Sigma \ell^2 \cdot A_r}$	Note 1	
		1.5 Inclined drop	(Ⅱ)-Fig.A.79～(Ⅱ)-Fig.A.82			Inclined drop from 9m height	1	Analyzed for each item of para.8.1～8.3 above from horizontal and vertical component of impact			

Symbols;

σ	: Principal stress	τ_t	: Torsional stress
σ_b	: Bending stress	F	: Load
σ_c	: Compressive stress	P	: Pressure
τ	: Shear stress	A	: Cross section

(Ⅱ)-Table A.4 Design conditions, analytical methods of structural analysis (12/24)

Requirement	Condition	Item	Design condition						Analytical methods		Remark
			Reference figure	Material	Temp.	Design load			Applied formula or element	Standard	
						Type	Loading factor	Element			
B(U) package	Accident test conditions	2. Drop test Ⅱ 2.1 Penetration	(Ⅱ)-Fig.A.83								
		(1) Outer lid	(Ⅱ)-Fig.A.84	SUS304	75℃	Drop onto a mild bar from 1m height	1	Penetration energy		No Penetration	
		(2) Outer bottom plate		SUS304	75℃	ditto	1	Penetration energy			
		(3) Frame of Outer shell		SUS304	75℃	ditto	1	Penetration energy			
		3. Thermal test 3.1 Thermal expansion									Note 1: Analytical standard of each stress component is determined using Su. Note 2: Analytical standard of each stress component is determined using Sy. Note 3: Initial margin of tightening is about 1.1mm.
		(1) Gap between inner shell and fuel basket		SUS304	500/ 225℃	Thermal expansion	1	Compression	Presense of gap between inner shell and basket	free	
		3.2 Stress by pressure									
		(1) frame of Inner shell		SUS304	500℃	Internal pressure	1	Combined Stress	Formula for thin cylinder	Note 1	
		(2) Inner bottom plate		SUS304	500℃	Internal pressure	1	Combined Stress	Formula for fixed disc		
		(3) Inner shell lid		SUS630	225℃	Internal pressure	1	Combined Stress	Formula for simple support disc		
		(4) Inner shell lid bolt		SUS630	225℃	Initial torque	1	Tensile stress	$\sigma_t = \frac{F}{Ai}$	Note 2	
					225℃	Internal pressure	1	Tensile stress	$\sigma_t = \frac{F}{n \cdot Ai}$		
		(5) Displacement of O-ring part of inner lid		SUS630	225℃	Internal pressure	1	Displacement	Formula for displacement of O-ring part	Note 3	

Symbols;

σ	: Principal stress	τ_t	: Torsional stress
σ_b	: Bending stress	F	: Load
σ_c	: Compressive stress	P	: Pressure
τ	: Shear stress	A	: Cross section

(Ⅱ)-Table A.4 Design conditions, analytical methods of structural analysis (13/24)

Requirement	Condition	Item	Design condition						Analytical methods		Remark
			Reference figure	Material	Temp.	Design load			Applied formula or element	Standard	
						Type	Loading factor	Element			
B(U) package	Accident test conditions	4. Water immersion test 4.1 Water immersion (15m depth)	(Ⅱ)-Fig.A.85								Note 1: Analytical standard of each stress component is determined using Su. Note 2: Analytical standard of each stress component is determined using Su. Note 3: Initial margin of tightening is about 1.1mm.
		(1) Frame of Inner shell	(Ⅱ)-Fig.A.88	SUS304	──	External pressure	1	Combined Stress	Formula for thin cylinder	Note 1	
		(2) Inner bottom plate	(Ⅱ)-Fig.A.89	SUS304	──	External pressure	1	Combined Stress	Formula for fixed disc	Note 1	
		(3) Inner shell lid	(Ⅱ)-Fig.A.90	SUS630	──	External pressure	1	Combined Stress	Formula for simply supported disc	Note 2	
		(4) Buckling of inner shell	(Ⅱ)-Fig.A.86	SUS304	──	External pressure	1	Buckling stress	$P_e = \frac{4B \cdot t}{2D_o}$ B : Buckling factor D_0: Outer diameter of inner shell	Note 1	
		(5) Displacement of O-ring part of inner lid	(Ⅱ)-Fig.A.91	SUS630	──	External pressure	1	Displacement	Formula for displacement of O-ring part	Note 3	

Symbols;

σ	: Principal stress	τ_t	: Torsional stress
σ_b	: Bending stress	F	: Load
σ_c	: Compressive stress	P	: Pressure
τ	: Shear stress	A	: Cross section

(Ⅱ)-Table A.4 Design conditions, analytical methods of structural analysis (14/24)

Requirement	Condition	Item	Design condition						Analytical methods		Remark
			Reference figure	Material	Temp.	Design load			Applied formula or element	Standard	
						Type	Loading factor	Element			
Fissile package	Normal test conditions	1. Water spray test				Water spray	1	Absorption Water-repellent	Absorption Water-repellent	Nil Good	

Symbols;

σ	: Principal stress	τ_t	: Torsional stress
σ_b	: Bending stress	F	: Load
σ_c	: Compressive stress	P	: Pressure
τ	: Shear stress	A	: Cross section

(Ⅱ)-Table A.4 Design conditions, analytical methods of structural analysis (15/24)

Requirement	Condition	Item	Design condition						Analytical methods		Remark
			Reference figure	Material	Temp.	Design load			Applied formula or element	Standard	
						Type	Loading factor	Element			
Fissile package	Normal test conditions	2. Free drop 2.1 Horizontal drop									Note 1: Effect of deformation will be judged in thermal test.
		(1) Deformation of shock absorber	(Ⅱ)-Fig.A.95	—	—	Horizontal drop from 1.2m height	1	Deformation	$\delta = \delta_0 - \delta_H$ δ_0: Minimum thickness before drop δ_H: Deformation δ : Thickness after drop	Note 1	
		(2) Frame of Inner shell	—	SUS304	75℃	ditto	1	Bending stress	$\sigma_b = \frac{M}{Z}$	Note 2	Note 2: Analytical standard of each stress component is determined using Sm.
		(3) Inner shell bottom plate	—	SUS304	75℃	ditto	1	Shear stress	$\tau = \frac{F}{A}$		
		(4) Upper part of inner shell (Inner lid)	—	SUS630	75℃	ditto	1	Shear stress	$\tau = \frac{F}{A}$		
		(5) Inner shell lid bolt	—	SUS630	75℃	ditto	1	Bending stress	$\sigma_b = \frac{M \cdot L_{max}}{1}$	Note 3	Note 3: Analysis standard of each stress component is determined using Sy.
		(6) Fuel basket	—	SUS304	75℃	ditto	1	Bending stress	$\sigma_b = \frac{M}{Z}$		
		(7) Fuel element/plate	—	AG3NE	75℃	ditto	1	Bending stress	$\sigma_b = \frac{M}{Z}$		
		(Spectrum Converter)		A6061P (T6)			1	Compression stress	$\sigma_c = \frac{W}{a(h_2 - h_1)}$		
							1	Buckling stress	$\sigma_y = \sigma_{cr}\left(1 + \frac{e}{r}\sec\frac{L}{2K}\sqrt{\frac{\sigma_{cr}}{E}}\right)$ σ_y : Yield stress σ_{cr} : buckling stress E : modulus of direct elasticity K : radius-of-gyration of area L : length r : section modulus/cross section e : eccentricity	Note 4	Note 4: Analysis standard is σ_{cr}.
		(8) Fuel element hold down part	—	A6061P (T6)	75℃	ditto	1	Bending stress	$\sigma_b = \frac{M}{Z}$	Note 5	Note 5: Analysis standard of each stress component is determined using Sy.

Symbols;

σ	: Principal stress	τ_t	: Torsional stress
σ_b	: Bending stress	F	: Load
σ_c	: Compressive stress	P	: Pressure
τ	: Shear stress	A	: Cross section

(Ⅱ)-Table A.4 Design conditions, analytical methods of structural analysis (16/24)

Requirement	Condition	Item	Design condition						Analytical methods		Remark
			Reference figure	Material	Temp.	Design load			Applied formula or element	Standard	
						Type	Loading factor	Element			
Fissile package	Normal test conditions	2.2 Vertical drop 2.2.1 Vertical drop (Bottom side)									Note 1: Effect of deformation will be judged in thermal test. Note 2: Analytical standard of each stress component is determined using Sm. Note 3: Analysis standard of each stress component is determined using Sy.
		(1) Deformation of shock absorber	(Ⅱ)-Fig.A.96	—	—	Vertical drop (Bottom side) from 1.2m height	1	Deformation	$\delta = \delta_0 - \delta_V$ δ_0: Minimum thickness before drop δ_V: Deformation δ : Thickness after drop	Note 1	
		(2) Frame of Inner shell	—	SUS304	75℃	ditto	1	Compression stress	$\sigma_c = \frac{F}{A}$	Note 2	
		(3) Inner shell bottom plate	—	SUS304	75℃	ditto	1	Combined stress	Formula for fixed disc	Note 2	
		(4) Inner shell lid	—	SUS630	75℃	ditto	1	Combined stress	Formula for simply supported disc	Note 3	
		(5) Inner shell lid bolt	—	SUS630	75℃	ditto	1	—	—	Note 3	
		(6) Fuel element/plate	—	AG3NE	75℃	ditto	1	Shear stress	$\tau = \frac{F}{2(h_2 - h_1)b}$	Note 3	
		(Spectrum Converter)		A6061P (T6)			1	Tensile stress	$\sigma_t = \frac{W_o}{A}$	Note 3	
							1	Compression stress	$\sigma_c = \frac{W}{A}$	Note 3	
		(7) Fuel element hold down part	—	A6061P (T6)	75℃	ditto	1	Compression stress	$\sigma_c = \frac{W}{A}$	Note 3	

Symbols;

σ	: Principal stress	τ_t	: Torsional stress
σ_b	: Bending stress	F	: Load
σ_c	: Compressive stress	P	: Pressure
τ	: Shear stress	A	: Cross section

(Ⅱ)-Table A.4 Design conditions, analytical methods of structural analysis (17/24)

Requirement	Condition	Item	Design condition						Analytical methods		Remark
			Reference figure	Material	Temp.	Design load			Applied formula or element	Standard	
						Type	Loading factor	Element			
Fissile package	Normal test condition	2.2.2 Vertical drop (Lid side)									Note 1: Effect of deformation will be judged in thermal test. Note 2: Analytical standard of each stress component is determined using Sm. Note 3: Analysis standard of each stress component is determined using Sy.
		(1) Deformation of shock absorber	—	—	—	Vertical drop (Lid side) from 1.2m height	1	Deformation	$\delta = \delta_0 - \delta_V$ δ_0: Minimum thickness before drop δ_V: Deformation δ : Thickness after drop	Note 1	
		(2) Frame of Inner shell	—	SUS304	75℃	ditto	1	Compression stress	$\sigma_c = \frac{F}{A}$	Note 2	
		(3) Inner shell bottom plate	—	SUS304	75℃	ditto	1	Combined stress	Formula for fixed disc		
		(4) Inner shell lid	—	SUS630	75℃	ditto	1	Combined stress	Formula for simply supported disc	Note 3	
		(5) Inner shell lid bolt	—	SUS630	75℃	ditto	1	Tensile stress	$\sigma_t = \frac{R}{n \cdot Ar}$		
		(6) Fuel Element/plate	—	AG3NE	75℃	ditto	1	Shear stress	$\tau = \frac{F}{2(h_2 - h_1)b}$	Note 3	
		(Spectrum Converter)		A6061P (T6)			1	Tensile stress	$\sigma_t = \frac{W_o}{A}$		
							1	Compression stress	$\sigma_c = \frac{W}{A}$		
		(7) Fuel element hold down part	—	A6061P (T6)	75℃	ditto	1	Compression stress	$\sigma_c = \frac{W}{A}$		
		2.3 Corner drop	—	—	—	Corner drop from 1.2m drop		Analyzed for each item of para.3.1～3.3 above from horizontal and vertical component of impact			
		(1) Inner lid bolt	—	SUS630	75℃	Corner drop from 1.2m drop (Lid side)	1	Bending stress	$\sigma_{max} = \sigma_V + \sigma_H$ $\sigma_V = \frac{N_V \cdot W \cdot L_V \cdot \ell_{VMAX}}{2\Sigma \ell^2 \cdot A_r}$ $\sigma_H = \frac{N_H \cdot W \cdot L_H \cdot \ell_{HMAX}}{2\Sigma \ell^2 \cdot A_r}$	Note 3	

(Ⅱ)-Table A.4 Design conditions, analytical methods of structural analysis (18/24)

Symbols;

σ	: Principal stress	τ_t	: Torsional stress
σ_b	: Bending stress	F	: Load
σ_c	: Compressive stress	P	: Pressure
τ	: Shear stress	A	: Cross section

Requirement	Condition	Item	Design condition						Analytical methods		Remark
			Reference figure	Material	Temp.	Design load			Applied formula or element	Standard	
						Type	Loading factor	Element			
Fissile package	Normal test condition	3. Stacking test (1) Frame of Inner shell	—	SUS304	75℃	Mass of package	×5+Self weight	Bending stress	$\sigma_Z = \frac{F+m\cdot g}{A}$	Note 1	Note 1: Analysis standard of each stress component is determined using Su. Note 2: Analysis standard of each stress component is determined using Sy.
		(2) Inner shell lid	—	SUS630	75℃	Mass of package	×5+Self weight	Combined stress	Formula for simply supported disc	Note 2	
		4. Penetration test (1) Outer shell	—	SUS304	75℃	Impact on mild steel bar	1	Absorbed energy	$E_2 = \frac{1}{2}\tau_{Cr}\cdot\pi\cdot d\cdot t^2$ (τ_{Cr}: Shear strength)=0.6Su	No penetration	

Symbols;

σ	: Principal stress	τ_t	: Torsional stress
σ_b	: Bending stress	F	: Load
σ_c	: Compressive stress	P	: Pressure
τ	: Shear stress	A	: Cross section

(Ⅱ)-Table A.4 Design conditions, analytical methods of structural analysis (19/24)

Requirement	Condition	Item	Design condition						Analytical methods		Remark
			Reference figure	Material	Temp.	Design load			Applied formula or element	Standard	
						Type	Loading factor	Element			
Fissile package	Accident test conditions	1. Drop test Ⅰ 1.1 Vertical drop 1.1.1 Vertical drop (Bottom side)									Note 1: Effect of deformation will be judged in thermal test. Note 2: Analytical standard of each stress component is determined using Su. Note 3: Analysis standard of each stress component is determined using Sy.
		(1) Deformation of shock absorber	—	—	—	Vertical drop (Bottom side) from 9m height	1	Deformation	$\delta = \delta_0 - \delta_V$ δ_0: Minimum thickness before drop δ_V: Deformation δ : Thickness after drop	Note 1	
		(2) Frame of Inner shell	—	SUS304	75℃	ditto	1	Compression stress	$\sigma_c = \frac{W}{A}$	Note 3	
		(3) Inner shell bottom plate	—	SUS304	75℃	ditto	1	Combined stress	Formula for fixed disc		
		(4) Inner shell lid	—	SUS630	75℃	ditto	1	Combined stress	Formula for simply supported disc	Note 2	
		(5) Inner shell lid bolt	—	SUS630	75℃	ditto	1	—	—		
		(6) Fuel element/plate (Spectrum Converter)	—	AG3NE A6061P (T6)	75℃	ditto	1	Shear stress	$\tau = \frac{F}{2(h_2 - h_1)b}$	Note 2	
							1	Tensile stress	$\sigma_t = \frac{W_o}{A}$		
							1	Compression stress	$\sigma_c = \frac{W}{A}$		
		(7) Fuel element hold down part	—	A6061P (T6)	75℃	ditto	1	Compression stress	$\sigma_c = \frac{W}{A}$		

Symbols;

σ	: Principal stress	τ_t	: Torsional stress
σ_b	: Bending stress	F	: Load
σ_c	: Compressive stress	P	: Pressure
τ	: Shear stress	A	: Cross section

(Ⅱ)-Table A.4 Design conditions, analytical methods of structural analysis (20/24)

Requirement	Condition	Item	Design condition						Analytical methods		Remark
			Reference figure	Material	Temp.	Design load			Applied formula or element	Standard	
						Type	Loading factor	Element			
Fissile package	Accident test conditions	1.1.2 Vertical drop (Lid side) (1) Deformation of shock absorber	—	—	—	Vertical drop (Lid side) from 9m height	1	Deformation	$\delta = \delta_0 - \delta_V$ δ_0: Minimum thickness before drop δ_V: Deformation δ : Thickness after drop	Note 1	Note 1: Effect of deformation will be judged in thermal test.
		(2) Frame of Inner shell	—	SUS304	75℃	ditto	1	Compression stress	$\sigma_c = \frac{F}{A}$	Note 2	Note 2: Analytical standard of each stress component is determined using Su.
		(3) Inner shell bottom plate	—	SUS304	75℃	ditto	1	Combined stress	Formula for fixed disc		
		(4) Inner shell lid	—	SUS630	75℃	ditto	1	Combined stress	Formula for simply supported disc		
		(5) Inner shell lid bolt	—	SUS630	75℃	ditto	1	Tensile stress	$\sigma_t = \frac{F}{n \cdot Ar}$		
		(6) Fuel element/plate	—	AG3NE	75℃	ditto	1	Shear stress	$\tau = \frac{F}{2(h_2 - h_1)b}$		Note 3: Analysis standard of each stress component is determined using Sy.
		(Spectrum Converter)		A6061P (T6)			1	Tensile stress	$\sigma_t = \frac{W_o}{A}$	Note 3	
							1	Compression stress	$\sigma_c = \frac{W}{A}$		
		(7) Fuel element hold down part	—	A6061P (T6)	75℃	ditto	1	Compression stress	$\sigma_c = \frac{W}{A}$		

Symbols;

σ	: Principal stress	τ_t	: Torsional stress
σ_b	: Bending stress	F	: Load
σ_c	: Compressive stress	P	: Pressure
τ	: Shear stress	A	: Cross section

(Ⅱ)-Table A.4 Design conditions, analytical methods of structural analysis (21/24)

Requirement	Condition	Item	Design condition						Analytical methods		Remark
			Reference figure	Material	Temp.	Design load			Applied formula or element	Standard	
						Type	Loading factor	Element			
Fissile package	Accident test conditions	1.2 Horizontal drop									
		(1) Deformation of shock absorber	—	—	—	Horizontal drop from 9m height	1	Deformation	$\delta = \delta_0 - \delta_H$ δ_0: Minimum thickness before drop δ : Thickness after drop δ_H: Deformation	Note 1	Note 1: Effect of deformation will be judged in thermal test.
		(2) Frame of Inner shell	—	SUS304	75℃	ditto	1	Bending stress	$\sigma_b = \frac{M}{Z}$	Note 2	Note 2: Analytical standard of each stress component is determined using Su.
		(3) Inner shell bottom plate	—	SUS304	75℃	ditto	1	Combined stress	Formula for fixed disc		
		(4) Upper part of inner shell (Inner lid)	—	SUS630	75℃	ditto	1	Shear stress	$\tau = \frac{F}{A}$		
		(5) Inner shell lid bolt	—	SUS630	75℃	ditto	1	Bending stress	$\sigma_b = \frac{M \cdot \ell_{max}}{I}$	Note 3	Note 3: Analytical standard of each stress component is determined using Sy.
		(6) Fuel basket	—	SUS304	75℃	ditto	1	Bending stress	$\sigma_b = \frac{M}{Z}$		
		(7) Fuel element/plate	—	AG3NE	75℃	ditto	1	Bending stress	$\sigma_b = \frac{M}{Z}$		
		(Spectrum Converter)		A6061P (T6)			1	Compression stress	$\sigma_c = \frac{W}{a(h_2 - h_1)}$		
							1	Buckling stress	$\sigma_y = \sigma_{cr}\left(1 + \frac{e}{r}\sec\frac{L}{2K}\sqrt{\frac{\sigma_{cr}}{E}}\right)$ σ_y : Yield stress σ_{cr} : buckling stress E : modulus of direct elasticity K : radius-of-gyration of area L : length r : section modulus/cross section e : eccentricity	Note 4	Note 4: Analytical standard is σ_{cr}.
		(8) Fuel element hold down part	—	A6061P (T6)	75℃	ditto	1	Bending stress	$\sigma_b = \frac{M}{Z}$	Note 3	

Symbols;

σ	: Principal stress	τ_t	: Torsional stress
σ_b	: Bending stress	F	: Load
σ_c	: Compressive stress	P	: Pressure
τ	: Shear stress	A	: Cross section

(Ⅱ)-Table A.4 Design conditions, analytical methods of structural analysis (22/24)

Requirement	Condition	Item	Design condition						Analytical methods		Remark
			Reference figure	Material	Temp.	Design load			Applied formula or element	Standard	
						Type	Loading factor	Element			
Fissile package	Accident test conditions	1.3 Corner drop	—			Corner drop from 9m height	1	Analyzed for each item of para.1.1 and 1.2 above from horizontal and vertical component of impact		—	Note 1: Analytical standard of each stress component is determined using Sy.
		(1) Inner shell lid bolt		SUS630	75℃	Corner drop from 9m height (Lid side)	1	Bending stress	$\sigma_{max} = \sigma_V + \sigma_H$ $\sigma_V = \frac{N_V \cdot W \cdot L_V \cdot \ell_{VMAX}}{2\Sigma \ell^2 \cdot Ai}$ $\sigma_H = \frac{N_H \cdot W \cdot L_H \cdot \ell_{HMAX}}{2\Sigma \ell^2 \cdot Ai}$	Note 1	

Symbols;

σ	: Principal stress	τ_t	: Torsional stress
σ_b	: Bending stress	F	: Load
σ_c	: Compressive stress	P	: Pressure
τ	: Shear stress	A	: Cross section

(Ⅱ)-Table A.4 Design conditions, analytical methods of structural analysis (23/24)

Requirement	Condition	Item	Design condition						Analytical methods		Remark
			Reference figure	Material	Temp.	Design load			Applied formula or element	Standard	
						Type	Loading factor	Element			
Fissile package	Accident teset conditions	2. Drop test Ⅱ 2.1 Penetration									
		(1) Outer shell lid	—	SUS304	75℃	Drop onto a mild bar from 1m height	1	Penetration energy		No Penetration	
		(2) Outer shell bottom plate	—	SUS304	75℃	ditto	1	Penetration energy		No Penetration	
		(3) Frame of Outer shell	—	SUS304	75℃	ditto	1	Penetration energy		No Penetration	
		3. Thermal test 3.1 Thermal expansion									Note 1: Analytical standard of each stress component is determined using Su. Note 2: Analytical standard of each stress component is determined using Sy. Note 3: Initial margin of tightening is about 1.1mm.
		(1) Gap between inner shell and fuel basket	—	SUS304	500/ 225℃	Thermal expansion	1	Compression	Presence of gap between shell and basket	free	
		3.2 Stress by pressure									
		(1) Frame of Inner shell	—	SUS304	500℃	Internal pressure	1	Combined Stress	Formula for thin cylinder	Note 1	
		(2) Inner shell bottom plate	—	SUS304	500℃	Internal pressure	1	Combined Stress	Formula for fixed disc		
		(3) Inner shell lid		SUS630	225℃	Internal pressure	1	Combined Stress	Formula for simply supported disc		
		(4) Inner shell lid bolt	—	SUS630	225℃	Initial torque	1	Tensile stress	$\sigma_t = \frac{F}{Ai}$	Note 2	
					225℃	Internal pressure	1	Tensile stress	$\sigma_t = \frac{F}{n \cdot Ai}$		
		(5) Displacement of O-ring part of inner lid	—	SUS630	225℃	Internal pressure	1	Displacement	Formula for displacement of O-ring part	Note 3	

(Ⅱ)-Table A.4 Design conditions, analytical methods of structural analysis (24/24)

Symbols;

σ	: Principal stress	τ_t	: Torsional stress
σ_b	: Bending stress	F	: Load
σ_c	: Compressive stress	P	: Pressure
τ	: Shear stress	A	: Cross section

Requirement	Condition	Item	Design condition						Analytical methods		Remark
			Reference figure	Material		Design load			Applied formula or element	Standard	
						Type	Loading factor	Element			
Fissile package	Accident test conditions	4. Water immersion test 4.1 Water immersion (0.9m depth)									Note 1: Analytical standard of each stress component is determined using Su. Note 2: Analytical standard of each stress component is determined using Su. Note 3: Initial margin of tightening is about 1.1mm
		(1) Frame of Inner shell	—	SUS304		External pressure	1	Combined stress	Formula for thin cylinder	Note 1	
		(2) Inner shell bottom plate	—	SUS304		External pressure	1	Combined stress	Formula for fixed disc	Note 1	
		(3) Inner shell lid		SUS630		External pressure	1	Combined stress	Formula for simply supported disc	Note 2	
		(4) Buckling of inner shell	—	SUS304		External pressure	1	Buckling stress	$P_e = \frac{4B \cdot t}{2D_o}$ B : Buckling factor D_0: Outer diameter of inner shell	Note 1	
		(5) Displacement of O-ring part of inner lid	—	SUS630		External pressure	1	Displacement	Formula for displacement of O-ring part	Note 3	

A.2 Weight and center of gravity

As indicated in (Ⅰ)-Table-C.3, the package weighs 950 kg in maximum. Its center of gravity is shown in (Ⅱ)-Fig.A.1.

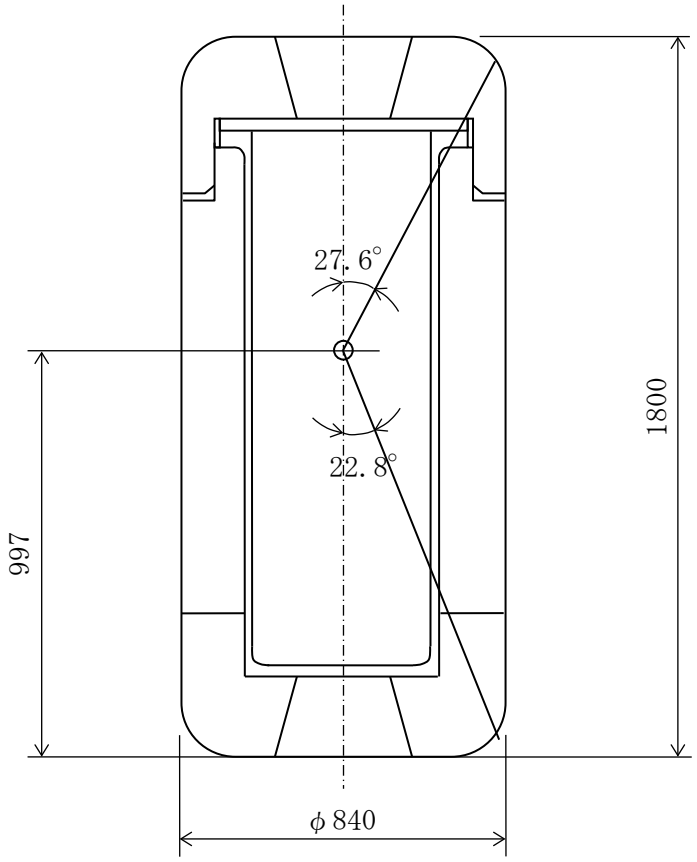

(Ⅱ)-Fig.A.1 Position of center of gravity

A.3 Mechanical properties of materials

(Ⅱ)-Table.A.5 is a list of the mechanical properties of the materials used in the analysis.

(Ⅱ)-Table.A.6 shows the mechanical properties of the materials to be used as analytic references.

In addition, the value based on the current appropriate source is indicated in (). Even in a case where values based on these current, appropriate sources are used for mechanical property of major members etc. of this shipping cask, it is confirmed that the impact on the analysis result will be minimal, and there will be no problem for safety.

Mechanical properties of stainless steel and aluminum alloy versus temperature is indicated in (Ⅱ)-Fig.A.2, (Ⅱ)-Fig.A.3, (Ⅱ)-Fig.A.4, and (Ⅱ)-Fig.A.5.

(Ⅱ)-Fig.A.6 and (Ⅱ)-Fig.A.7 show a design fatigue curve for the analysis.

A stress-strain curve of balsa used as a shock absorber is indicated in (Ⅱ)-Fig.A.8. The figures are quoted from references shown later.

(Ⅱ)-Table.A.5 Mechanical properties of materials

Material	Code	Main application parts	Modulus of longitudinal elasticity E [N/mm²]	Linear expansion factor α [1/℃]	Design tensile strength Su [N/mm²]	Design yield strength Sy [N/mm²]	Design stress intensity Sm [N/mm²]	Poisson's ratio ν	Stress-strain diagram
[2] Stainless steel (austenitic)	SUS304	Main body of inner shell Main body of outer shell and outer lid Fuel basket	(Ⅱ)-Fig.A.2 (4/5)	(Ⅱ)-Fig.A.2 (5/5)	(Ⅱ)-Fig.A.2 (1/5)	(Ⅱ)-Fig.A.2 (2/5)	(Ⅱ)-Fig.A.2 (3/5)	0.3	—
[2] Stainless steel precipitation hardened type	SUS630 H1150	Inner lid Inner lid clamping bolt Outer lid clamping bolt	(Ⅱ)-Fig.A.3 (3/4)	(Ⅱ)-Fig.A.3 (4/4)	(Ⅱ)-Fig.A.3 (1/4)	(Ⅱ)-Fig.A.3 (2/4)	(Ⅱ)-Fig.A.4 (1/1)	0.3	—
[14] Aluminum alloy	AG3NE	Fuel element (A) Fuel plate	—	—	—	(Ⅱ)-Fig.A.5 (1/1)	—	0.3	—
[4] Balsa	—	Shock absorber	—	—	—	—	—	—	(Ⅱ)-Fig.A.8

Stainless steel: see Literature [2]
Aluminum alloy : see Literature [14]
Balsa : see Literature [4]

Numbers shown in brackets ( ) indicate the number of the sheets for the Figure No.

(Ⅱ)-Table.A.6 Mechanical properties of materials to be used as design standards

No.	Evaluated position	Material	- Normal conditions - Normal test conditions - Accident test conditions (excluding thermal tests)						Accident test conditions (only for thermal tests)					
			T	Sm	Sy	Su	E	α	T	Sm	Sy	Su	E	α
1	Inner shell main body	SUS304	75	137	183 (180)	466	1.92 (1.91)	16.71 (15.9)	500	—	—	387	—	—
2	Inner lid	SUS630	75	311 (310)	688 (687)	847 (846)	1.99 (1.92)	9.38 (11.3)	225	—	612	—	—	—
3	Fuel basket	SUS304	75	137	183 (180)	466	1.92 (1.91)	16.71 (15.9)	—	—	—	—	—	—
4	Outer shell main body	SUS304	75	137	183 (180)	466	1.92 (1.91)	16.71 (15.9)	—	—	—	—	—	—
5	Outer lid	SUS304	75	137	183 (180)	466	1.92 (1.91)	16.71 (15.9)	—	—	—	—	—	—
6	Inner lid clamping bolt	SUS630	75	229	688 (687)	847	1.99 (1.92)	9.38 (11.3)	225	—	612	—	—	—
7	Outer lid clamping bolt	SUS630	75	229	688 (687)	847	1.99 (1.92)	9.38 (11.3)	—	—	—	—	—	—
8	Fuel element (A) Fuel plate	AG3NE	75	—	63.8 63.7	167	0.697	25.7	—	—	—	—	—	—
9	Fuel element (B)	JRR-4B type fuel plate	75	—	63.8	88.3	—	—	—	—	—	—	—	—
10	Fuel element hold down part Spectrum Converter	A6061P(T6)	75	—	245	295	—	—	—	—	—	—	—	—

T: Temperature [℃] Sm: Design stress intensity [N/mm^2] Sy: Design yield point [N/mm^2] Su: Design tensile strength [N/mm^2]

E: Modulus of longitudinal elasticity [×10^{5}N/mm^2] α: Linear expansion factor [×10^{-6}℃$^{-1}$]

( ): Code for Nuclear Power generation Facilities: Rules on of Materials Nuclear Power Plants (2012 edition) of the Japan Society of mechanical Engineers

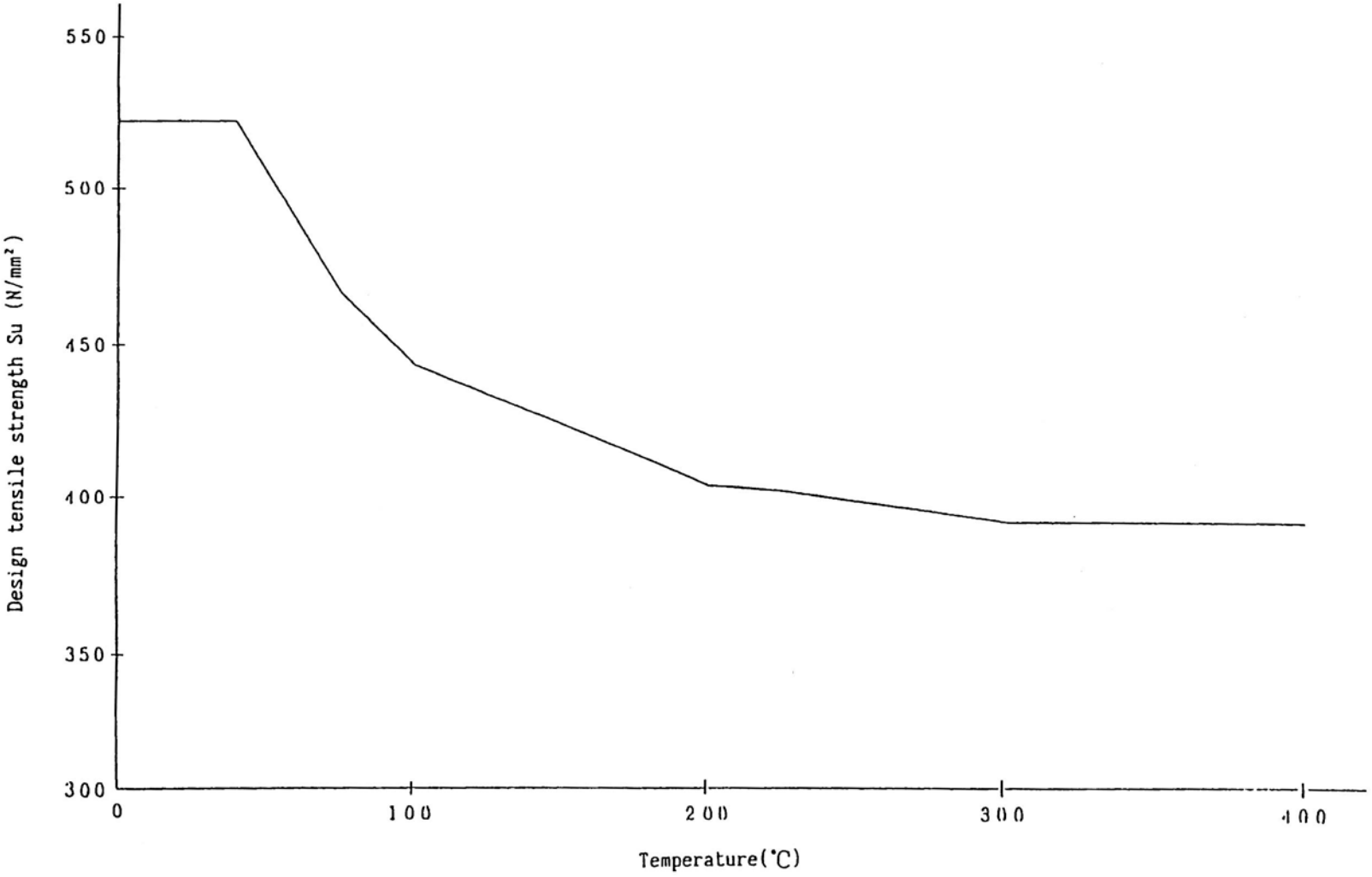

(Ⅱ)-Fig.A.2 Variations in mechanical properties of SUS304 according to changes in temperature (1/5)

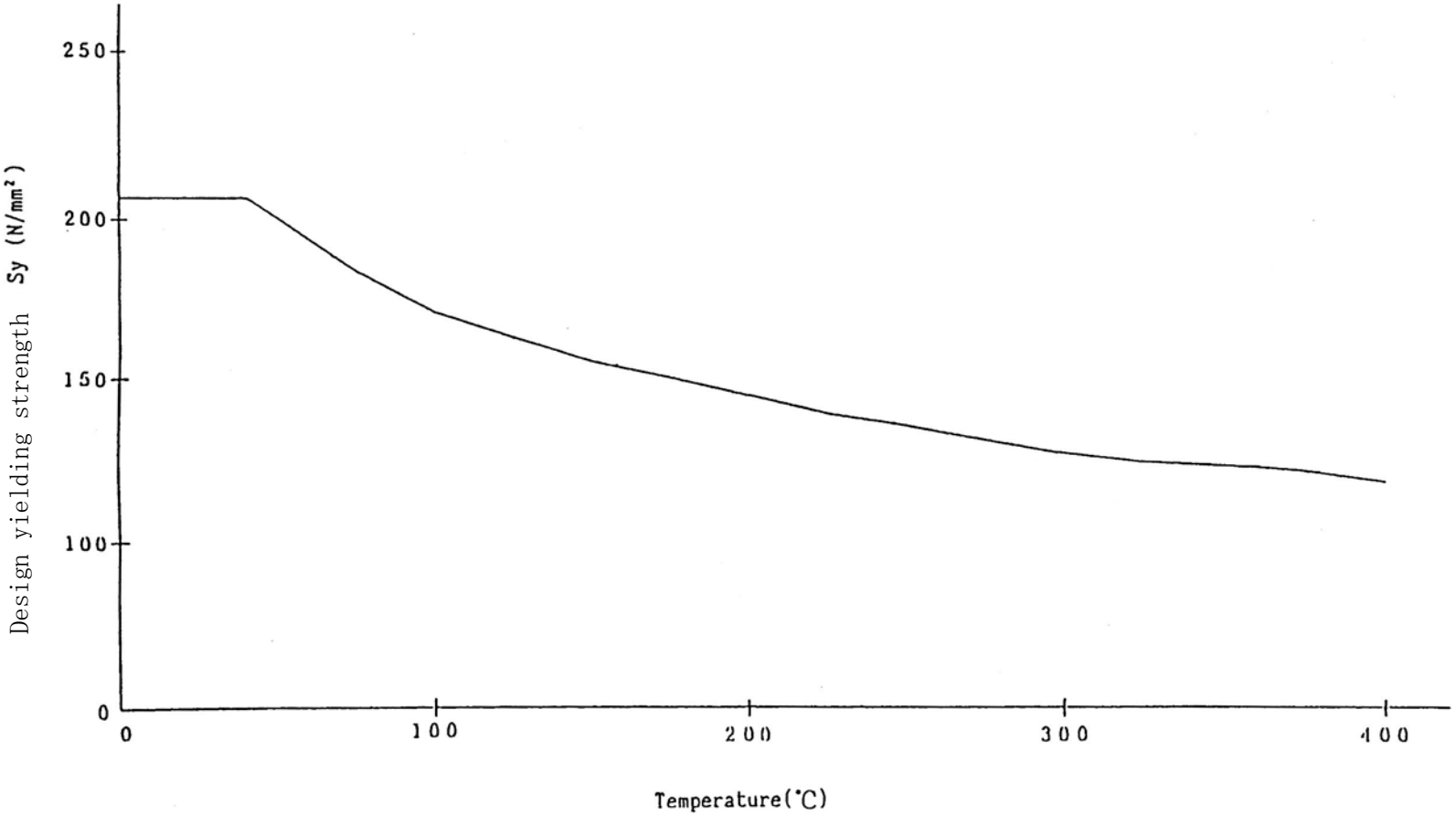

(Ⅱ)-Fig.A.2 Variations in mechanical properties of SUS304 according to changes in temperature (2/5)

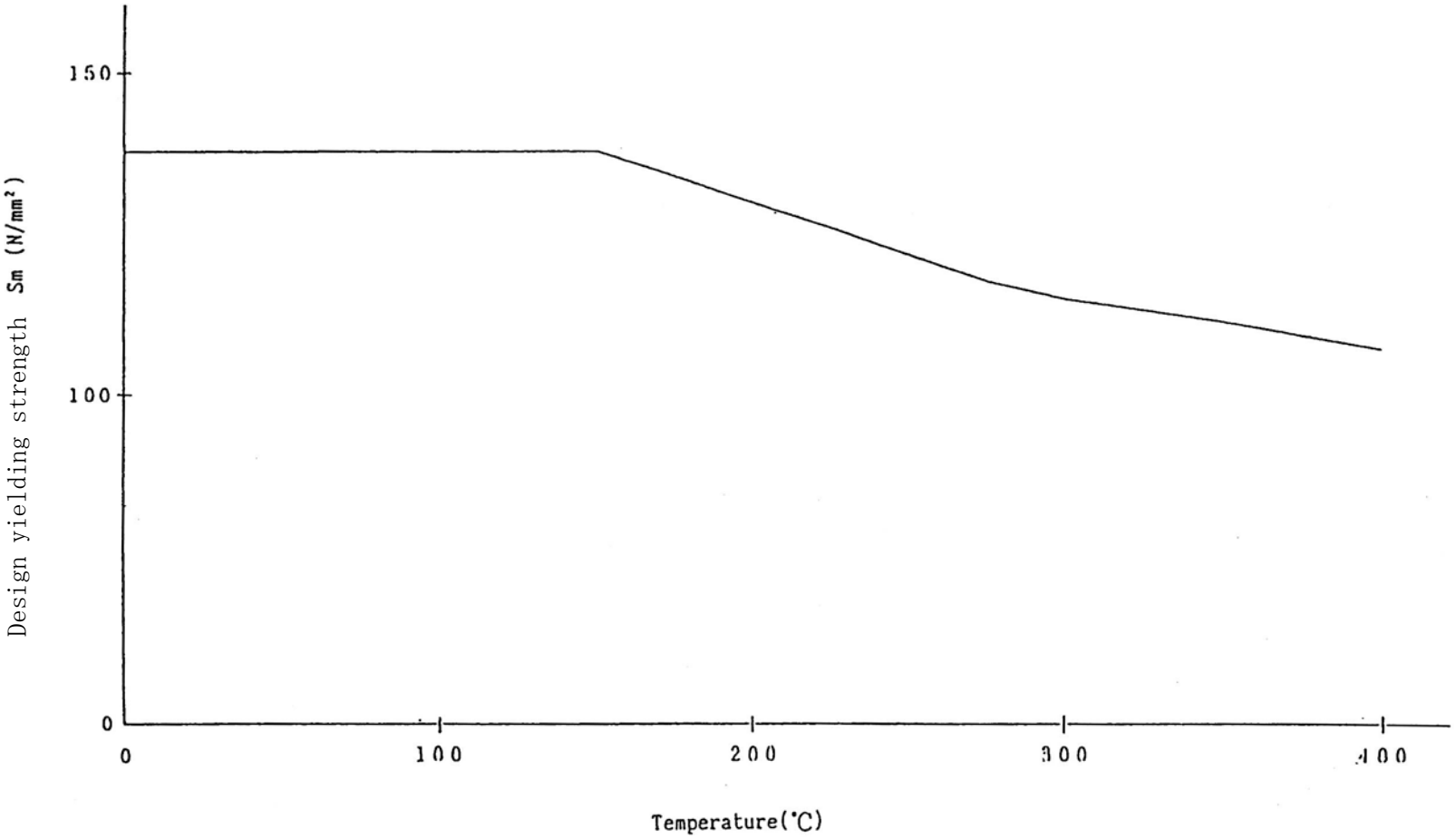

(Ⅱ)-Fig.A.2 Variations in mechanical properties of SUS304 according to changes in temperature (3/5)

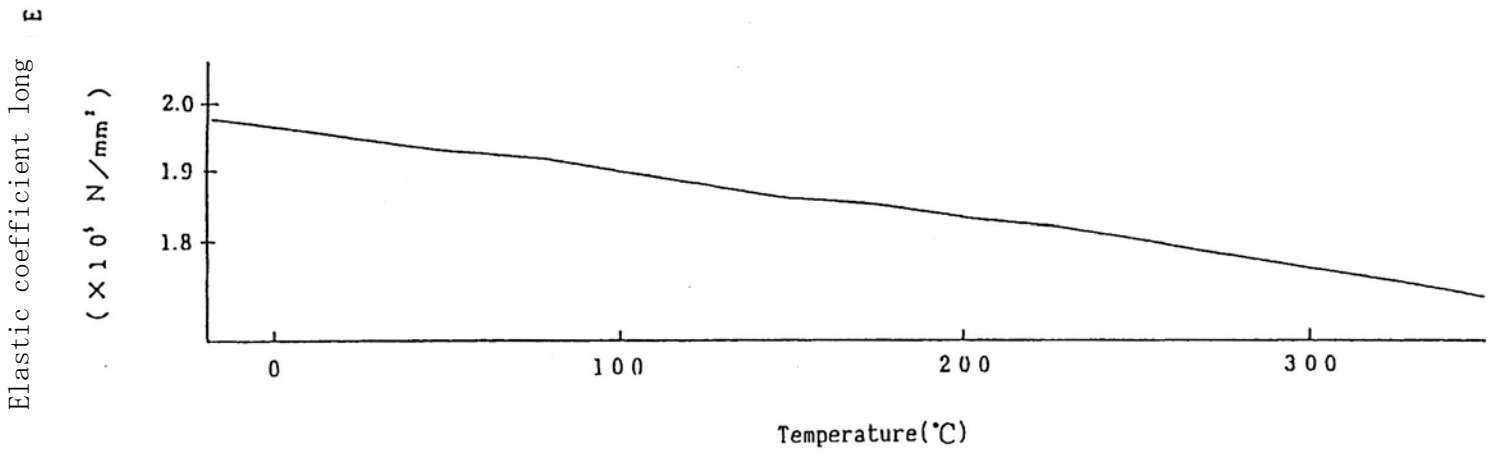

(Ⅱ)-Fig.A.2 Variations in mechanical properties of SUS304 according to changes in temperature (4/5)

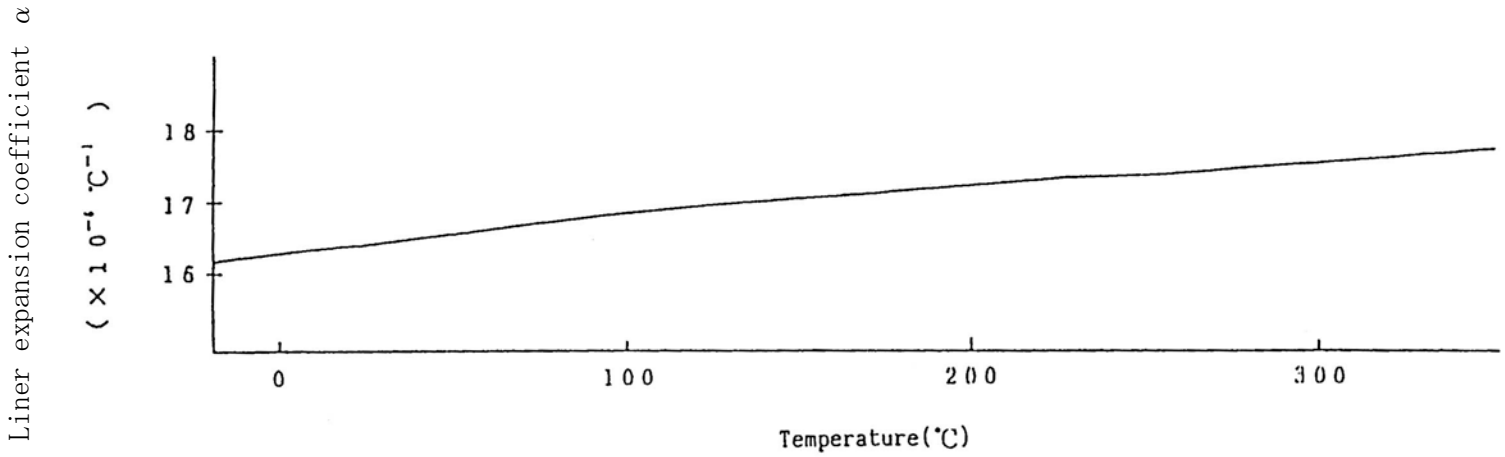

(Ⅱ)-Fig.A.2 Variations in mechanical properties of SUS304 according to changes in temperature (5/5)

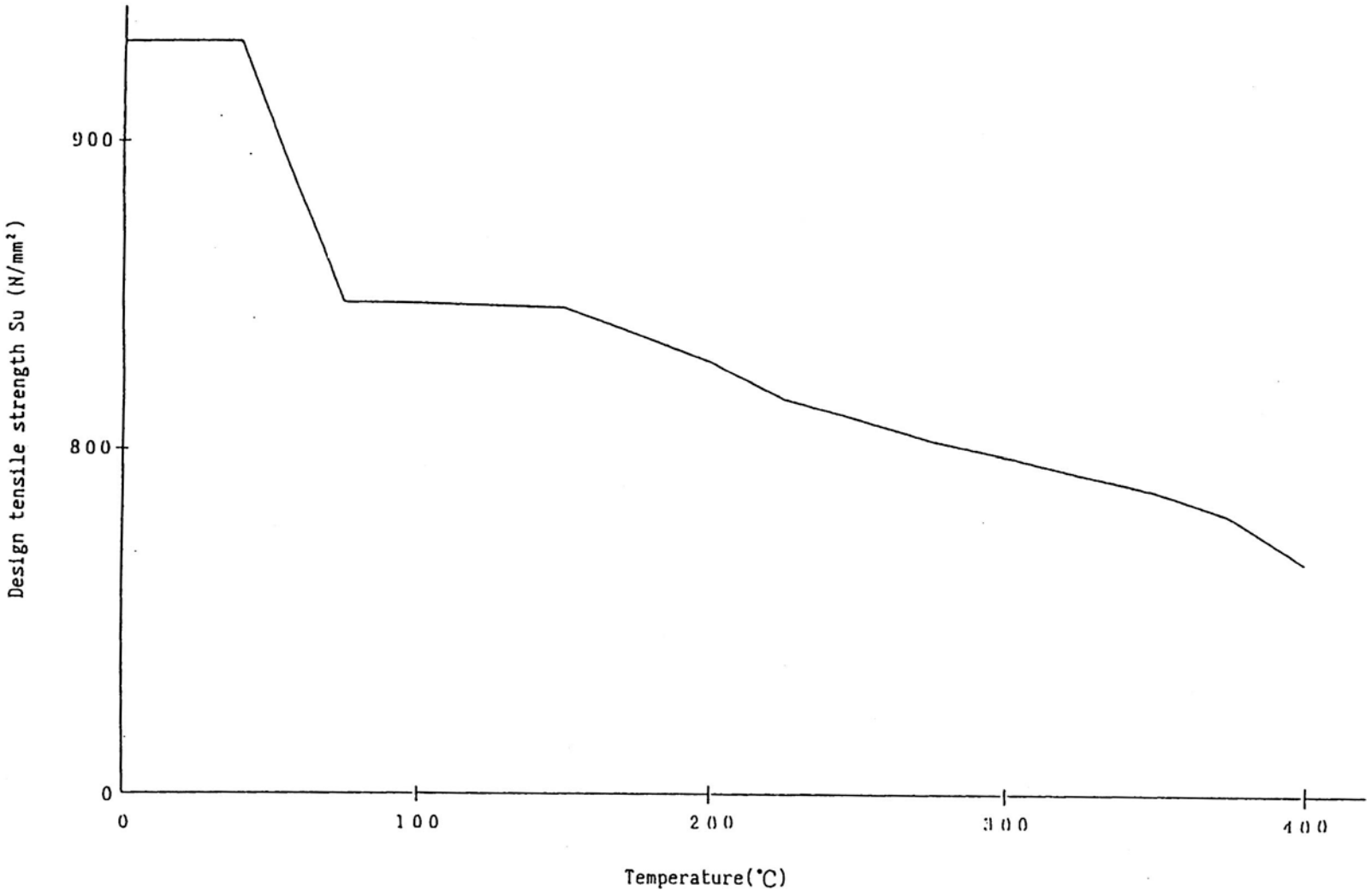

(Ⅱ)-Fig.A.3 Variations in mechanical properties of SUS630 according to changes in temperature (bolt material) (1/4)

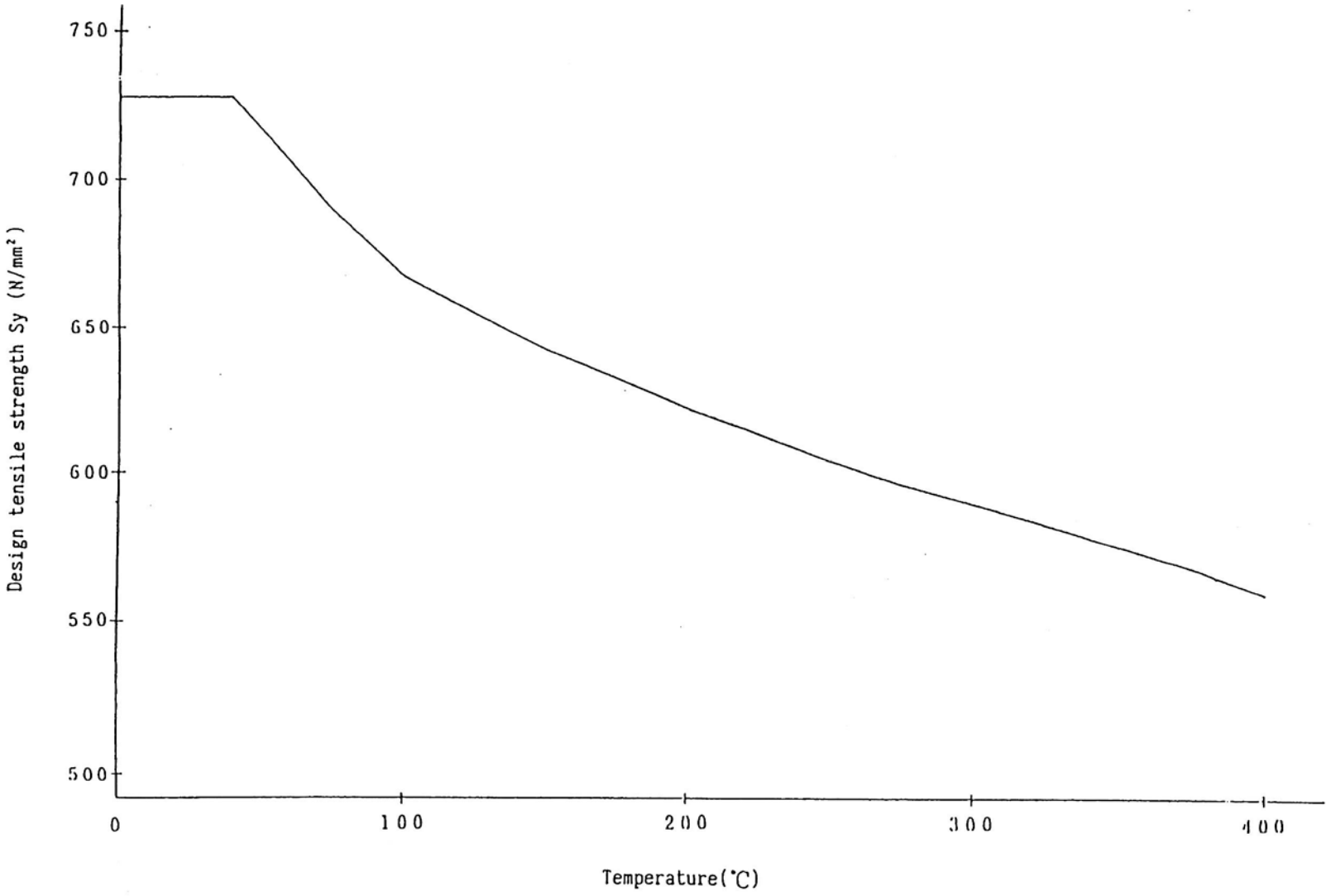

(Ⅱ)-Fig.A.3 Variations in mechanical properties of SUS630 according to changes in temperature (bolt material) (2/4)

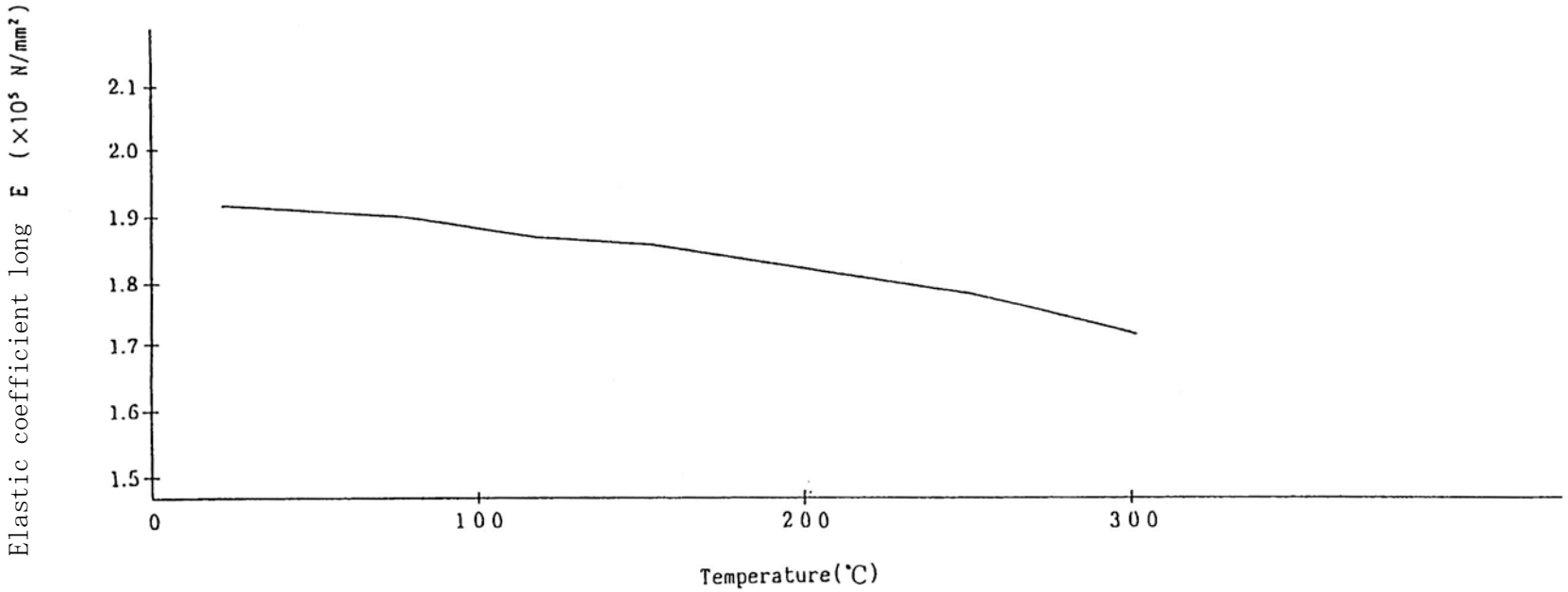

(Ⅱ)-Fig.A.3 Variations in mechanical properties of SUS630 according to changes in temperature (bolt material) (3/4)

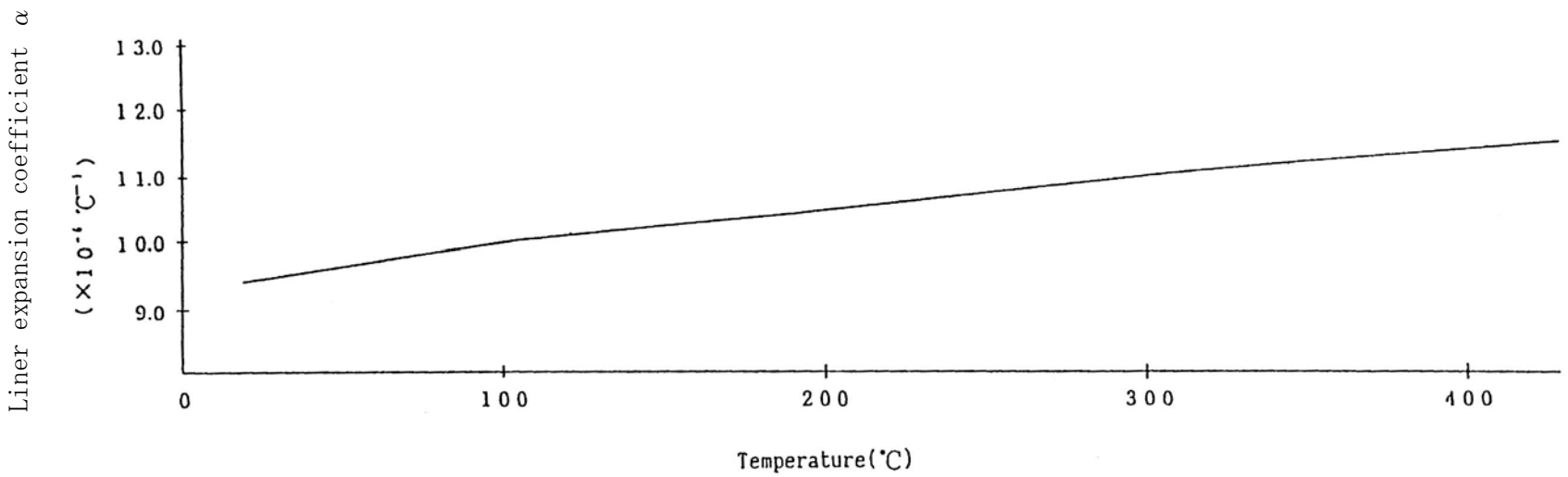

(Ⅱ)-Fig.A.3 Variations in mechanical properties of SUS630 according to changes in temperature (bolt material) (4/4)

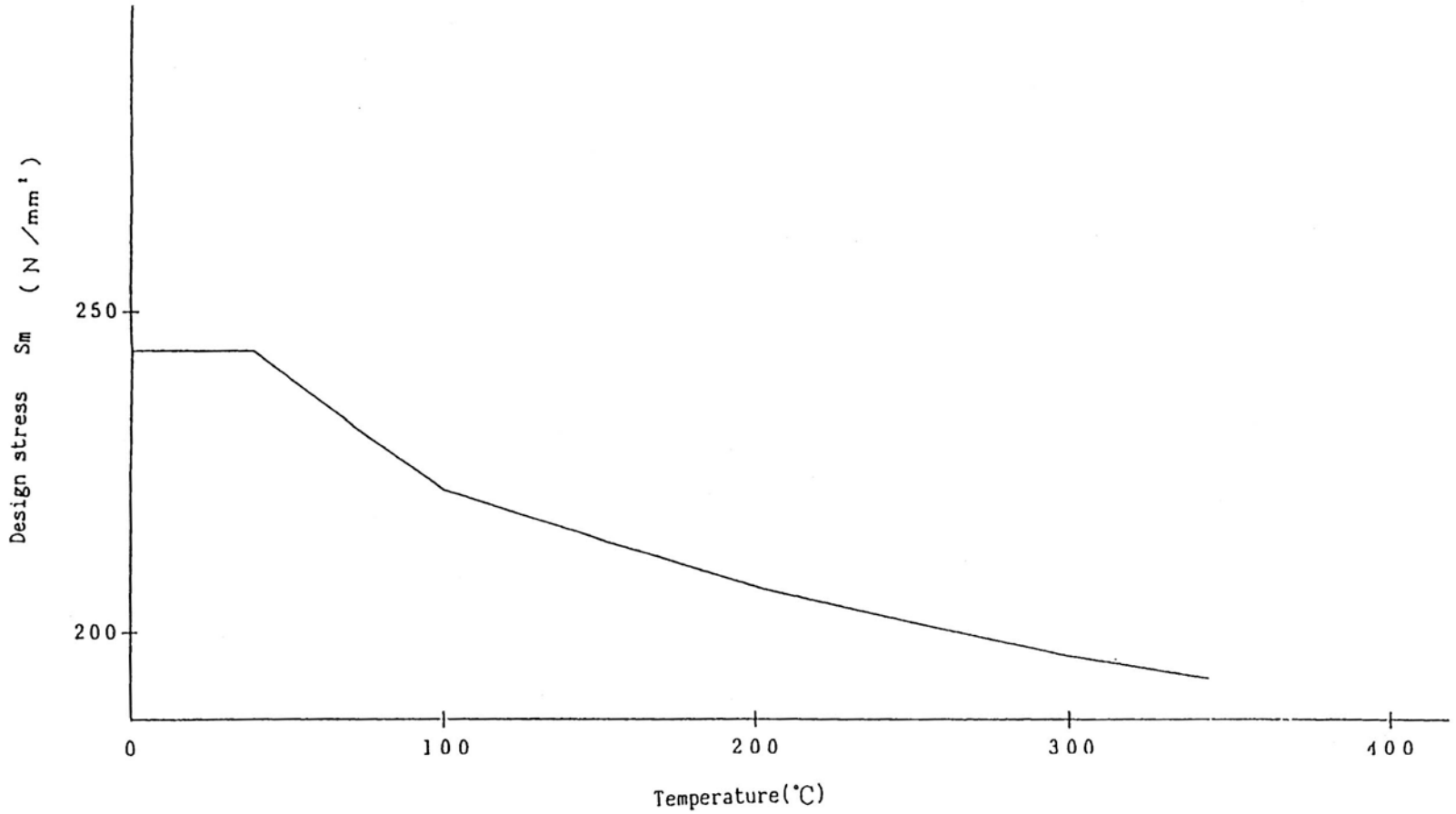

(Ⅱ)-Fig.A.4 Variations in mechanical properties of SUS630 according to changes in temperature (1/1)

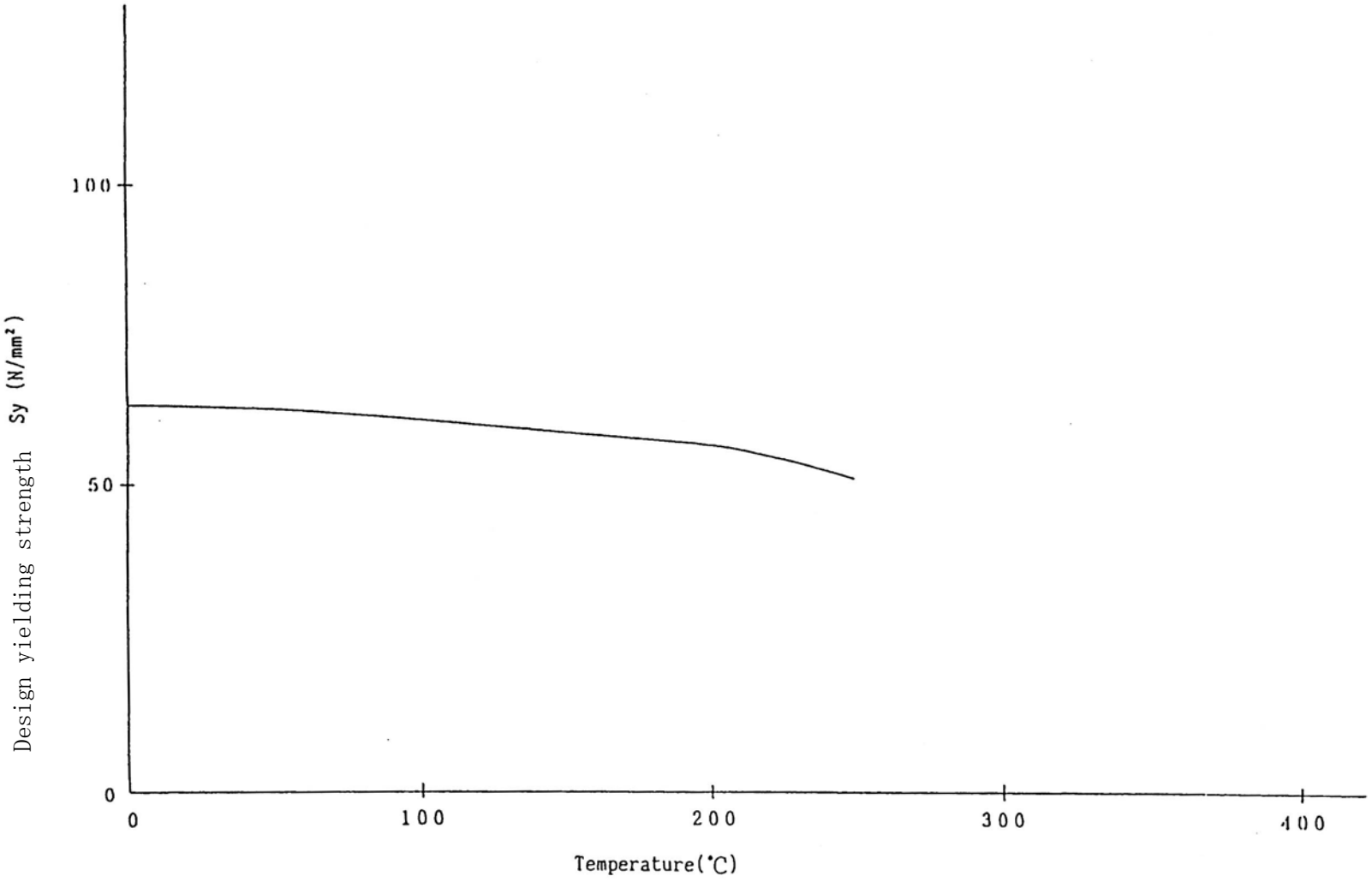

(Ⅱ)-Fig.A.5 Variations in mechanical properties of AG3NE according to changes in temperature (1/1)

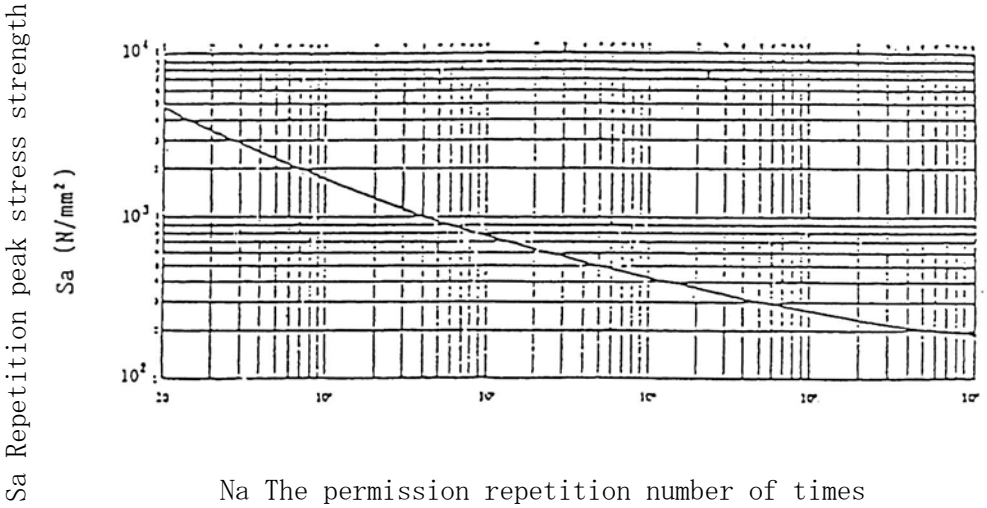

(Ⅱ)-Fig.A.6 Design fatigue curve (austenitic type stainless steel and high nickel alloy)[2]

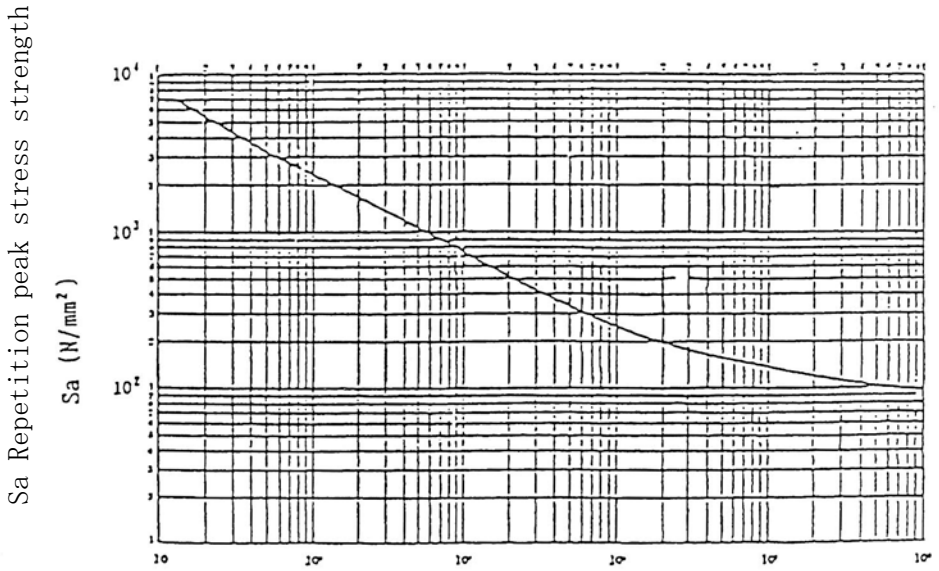

(Ⅱ)-Fig.A.7 Design fatigue curve (high tensile strength bolt)[2]

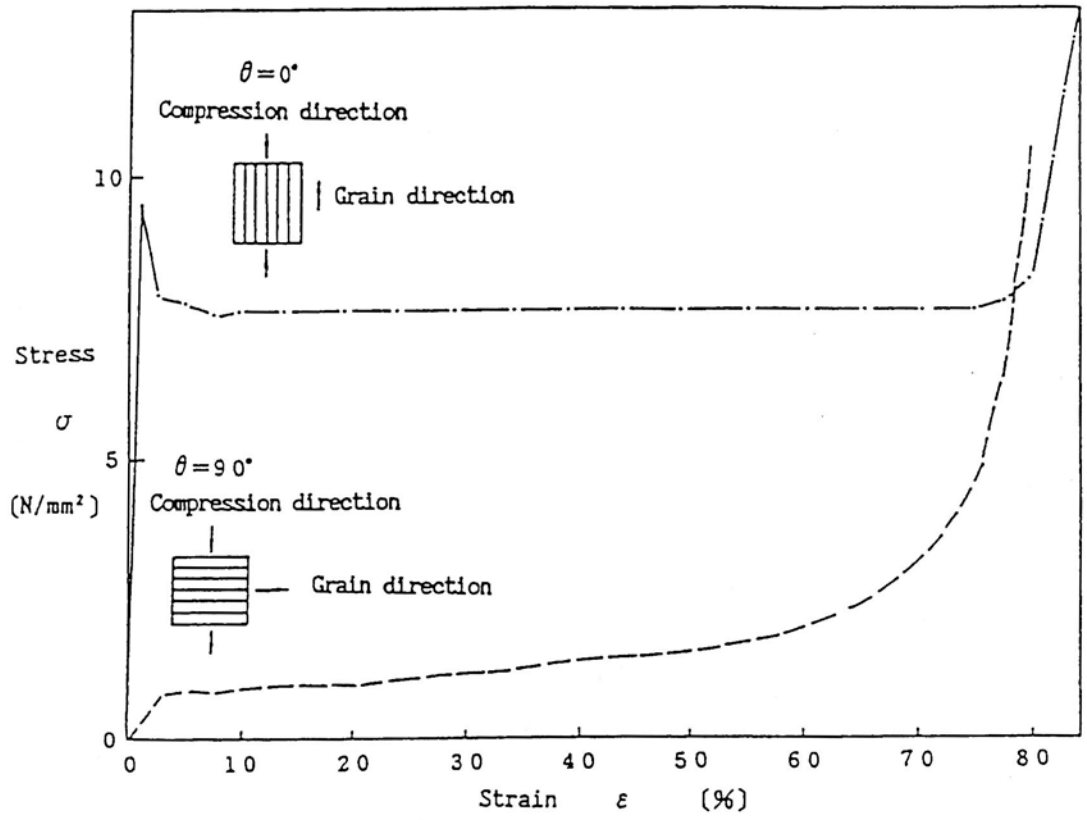

(Ⅱ)-Fig.A.8 Stress-strain curve of shock absorber[4]

A.4 Requirements of the package

A.4.1 Chemical and electrical reactions

(Ⅱ)-Table A.7 is a list of the different materials that come in contact with each other in this package. The materials used in this package, being chemically stable in air, will not trigger any chemical or electrical reaction when coming in contact with one another.

(Ⅱ)-Table A.7 List of different materials contacted

Positions			Materials
Inner shell Outer shell	—	Shock absorber	Stainless steel — Timber
Inner shell Outer shell	—	Heat insulator	Stainless steel — Hardened polyurethane
Inner shell main body Inner lid	—	O-ring	Stainless steel — Silicone rubber
Fuel basket Inner lid	—	Spacer	Stainless steel — Silicone rubber
Protective sheets	—	Spacer	Polyethylene — Silicone rubber
Protective sheets	—	Fuel basket	Polyethylene — Stainless steel
Protective sheets	—	Peripheral shock absorber	Polyethylene — Polyurethane foam
Protective sheets	—	Fuel element	Polyethylene — Aluminum alloy
Peripheral shock absorber	—	Fuel element	Polyurethane foam — Aluminum alloy
Cushion rubber	—	Lower part of the fuel basket	Silicone rubber — Stainless steel
Inner shell Outer shell	—	Gasket	Stainless steel — Ethylene propylene rubber
Fitting bracket	—	Fusible plug	Stainless steel — Solder

A.4.2 Low temperature strength

This package is a BU type package, as is indicated in (Ⅰ)-B. This section will demonstrate the reliability of the packaging in ambient conditions of -40℃.

The minimum temperatures of each part of the package and the materials involved are shown in (Ⅱ)-Table A.8.

(Ⅱ)-Table A.8 Minimum temperatures of parts of package

No.	Evaluated position	Material	Minimum temperature (℃)	Brittleness transition temp./min. service temperature (℃)	Citation, literatures and references
1	Content	Aluminum alloy	-40	No brittle fracture	Aluminum Hand Book [20]
2	Inner shell	Austenitic stainless steel	-40	No brittle fracture	JIS B 8270 Stainless Steel Manual [16]
3	Outer shell	Austenitic stainless steel	-40	No brittle fracture	
4	Inner lid	Precipitation hardened stainless steel	-40	Below -40	Stainless steel Heat Treatment [18]
5	Outer lid	Austenitic stainless steel	-40	No brittle fracture	JIS B 8270 Stainless Steel Manual [16]
6	Fuel basket	Austenitic stainless steel	-40	No brittle fracture	
7	Inner lid clamping bolt	Precipitation hardened stainless steel	-40	Below -40	Stainless steel Heat Treatment [18]
8	Outer lid clamping bolt	Precipitation hardened stainless steel	-40	Below -40	
9	Inner lid O-ring	Silicone rubber	-40	Below -40	Summary of technology for hybrid materials [21]
10	Shock absorber	Balsa	-40	Below -40	Appendices A.10.4
11	Heat insulator	Hardened polyurethane foam	-40	Below -40	Internal data of manufacturers [22]

The austenitic stainless steels of the inner and outer shells, as shown in (Ⅱ)-Fig.A.103 and the precipitation hardened stainless steels of the inner lid and bolts as shown in (Ⅱ)-Fig.A.104 can maintain adequate value of strength

endurable to impulse at the temperature -40℃, and also the Aluminum alloy used for fuel elements is free from any brittle fracture at the temperature -40℃, as show in (Ⅱ)-Table.A.8.

The tolerable temperature for the silicone rubber used for the O-ring is lower then -40℃. The O-ring preserves full sealing performance at -40℃.

The Balsa wood used for the shock absorber, as shown in (Ⅱ)-Fig.A.100, can maintain the function as the shock absorber sufficiently at the temperature -40℃, since the material properties are free of any significant error at each temperatures, at room temperature, -20℃ and -40℃.

Therefore, at -40℃, this package is completely functional.

A.4.3 Sealing device

After the fuel elements are stored in the main body of the inner shell, the inner lid is clamped with bolts and then secured with the outer lid. Thus, the inner lid cannot be opened inadvertently. Similarly, the outer lid cannot be easily opened as it is locked and sealed after being fixed to the main body of the outer shell.

If opened, it will easily be detected.

A.4.4 Hoisting accessory

The hoisting accessory described in this section is a hoisting eye-plate fixed to the side of the main body of the outer shell. For design standard of the stress generated at the hoisting accessory, the yield stress S_y at the temperature of 75℃ is employed with safety margin, in consideration of 65℃, the maximum temperature at the point of eye-plate on the outer surface of the packaging on normal transportation, obtained by (II) -B Thermal Analysis.

(Ⅱ)-Fig.A.9 shows an analytical model of an eye-plate of the hoisting accessory for the main body.

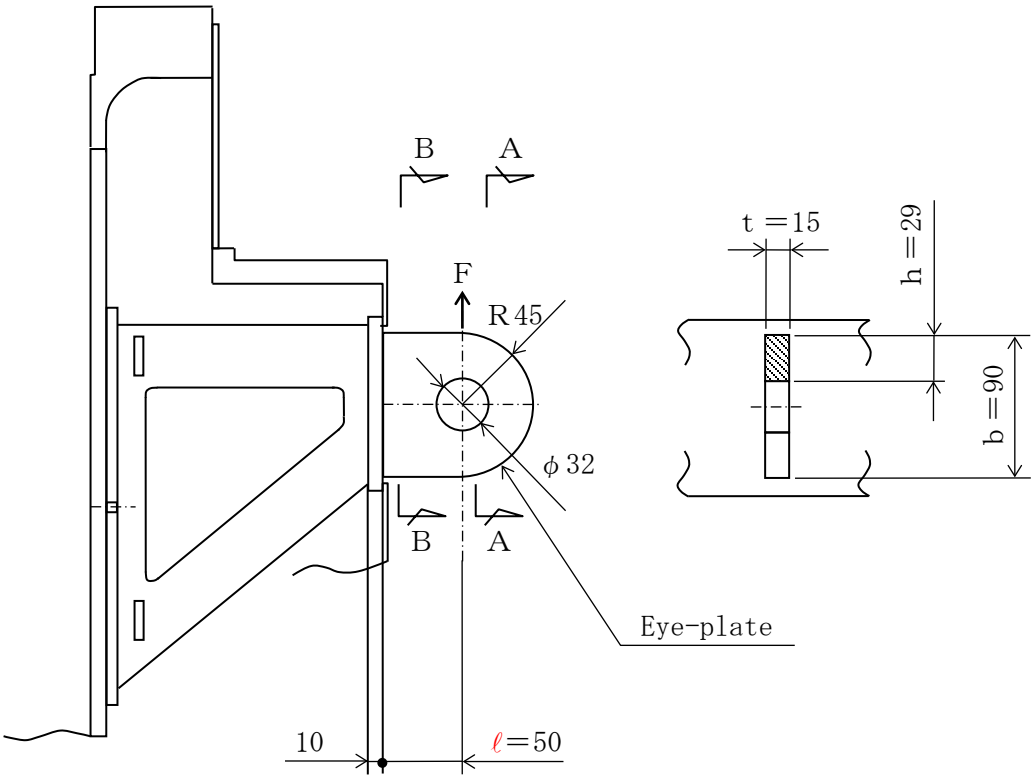

(Ⅱ)-Fig.A.9 Analytical model for eye-plate

The gross weight of a package lifted (mo) on a hoisting eye-plate of the main body is 950 kg at the maximum, as indicated in (Ⅱ)-Table C.3.

A maximum load F(N) applied on one of four eye-plates when lifting a package is given by the following equation, with the load factor of 3.

$$F=\frac{1}{n}(3\times g\times mo)=\frac{3}{4}\times 9.81\times 950=6.99\times 10^{3} \quad [N]$$

where

g: gravitational acceleration; g=9.81 [m/sec^2]

Therefore, when the upward vertical load , F=6.99×10^3 [N] as shown in (Ⅱ)-Fig.A.9 works on the eye-plate, stress on each cross section is analysed as follows.

(1) Section A-A

The shearing stress τ [N/mm^2] generated in the shaded portion (section A-A) of the eye-plate shown in (Ⅱ)-Fig.A.9 is given by the following equation.

$$\tau = \frac{F}{A} = \frac{F}{t \cdot h}$$

where

τ: Shearing stress [N/mm^2]

F: Maximum load, F=6.99×10^3 [N]

t: Plate thickness, t=15 [mm]

h: Height, h=29 [mm]

Therefore,

$$\tau = \frac{6.99 \times 10^3}{29 \times 15} = 16.1 \quad [N/mm^2]$$

So it is less than the design standard value allowable correspond to shearing stress on the eye-plate material (SUS 304) (0.6sy=108 N/mm^2). And the margin of safety (MS) is

$$MS = \frac{0.6Sy}{\tau} - 1 = \frac{108}{16.1} - 1 = 5.70$$

(2) Section B-B

The bending stress σb [N/mm2] generated at the fixing point of the eye-plate as indicated in (Ⅱ)-Fig.A.9 is given by the following equation.

$$\sigma_b = \frac{M}{Z} = \frac{F \cdot 1}{tb^2/6}$$

where

M: Bending moment [N/mm2]

Z: Section modulus [mm3]

l: Moment arm, l=50 [mm]

b: Width of eye-plate, b =90 [mm]

t: Plate thickness, t=15 [mm]

Therefore,

$$\sigma_b = \frac{6.99 \times 10^3 \times 50}{15 \times 90^2 / 6} = 17.3 \quad [N/mm^2]$$

and it is less than the design yield strength (Sy=180N/mm2) of the eye-plate material (SUS304).

The margin of safety (MS) turns out

$$MS = \frac{Sy}{\sigma_b} - 1 = \frac{180}{17.3} - 1 = 9.40$$

And the shearing stress τ generated in the section B-B is given by the following equation.

$$\tau = \frac{F}{A} = \frac{F}{t \times b} = \frac{6.99 \times 10^3}{15 \times 90} = 5.18 \quad [N/mm^2]$$

It is therefore less than the design standard value allowable correspond to shearing stress on the eye-plate material (SUS304).

The margin of safety (MS) is

$$MS = \frac{0.6Sy}{\tau} - 1 = \frac{108}{5.18} - 1 = 19.8$$

The composite stress σ [N/mm^2] of the above-mentioned bending stress σ_b and shearing stress τ is given by the following equation.

$$\sigma = \sqrt{\sigma_b^{\,2} + 4\tau^2} = \sqrt{17.3^2 + 4 \times 5.18^2} = 20.2 \quad [N/mm^2]$$

It is less than the yield point of the design of the eye-plate material (SUS304).

The margin of safety (MS) is

$$MS = \frac{Sy}{\sigma} - 1 = \frac{180}{20.2} - 1 = 7.91$$

(3) Welded part on the section B-B

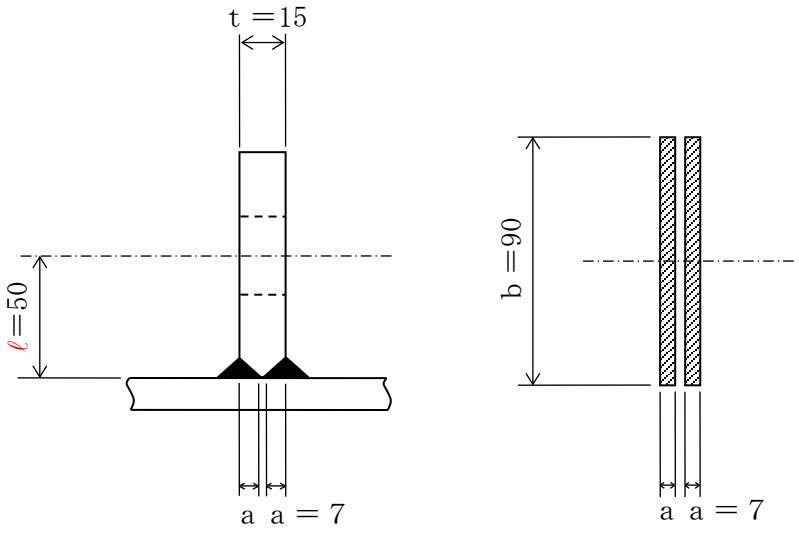

(Ⅱ)-Fig.A.10 Analytical model of welded part on eye-plate.

The bending stress σb [N/mm2] generated on the welded fixing part of the eye-plate shown in (Ⅱ)-Fig.A.10 is given by the following equation

$$\sigma_b = \frac{M}{Z} = \frac{F \cdot 1}{Z}$$

where

Z: Section modulus of the welded part [mm^3]

$$Z = \frac{1}{6} \cdot 2a \cdot b^2$$

a: Weld-throat thickness, a=7 [mm]

b: Width of a plate, b=90 [mm]

Therefore, σb will be

$$\sigma_b = \frac{6.99 \times 10^3 \times 50}{\frac{1}{6} \times 2 \times 7 \times 90^2} = 18.5 \quad [N/mm^2]$$

This is less than the design standard value on the welded part (0.45Sy=81.0N/mm^2).

The margin of safety (MS) is

$$MS = \frac{0.45Sy}{\sigma_b} - 1 = \frac{81.0}{18.5} - 1 = 3.37$$

The shearing stress τ generated on the welded part of the section B-B is given by the following equation.

$$\tau = \frac{F}{A} = \frac{F}{2a \cdot b} = \frac{6.99 \times 10^3}{2 \times 7 \times 90} = 5.55 \quad [N/mm^2]$$

This is less than the design standard value allowable correspond to shearing strength on the welded part (0.45×0.6×Sy=48.6 N/mm2).

The margin of safety (MS) is

$$MS = \frac{0.45 \times 0.6 \times Sy}{\tau} - 1 = \frac{0.45 \times 0.6 \times 180}{5.55} - 1 = 7.75$$

The composite stress σ [N/mm2] of the bending stress mentioned above σ_b and the shearing stress τ is given by the following equation

$$\sigma = \sqrt{\sigma_b^{\,2} + 4 \cdot \tau^2} = \sqrt{18.5^2 + 4 \times 5.55^2} = 21.6 \quad [N/mm^2]$$

It is less than the design standard value on the welded part (0.45Sy=81.0N/mm^2).

The margin of safety (MS) is,

$$MS = \frac{0.45Sy}{\sigma} - 1 = \frac{81.0}{21.6} - 1 = 2.75$$

The results of the analysis mentioned above is outlined in (Ⅱ)-Table A.9.

As indicated in (Ⅱ)-Table A.9, the margin of safety (MS) in every analysis is positive and the eye-plate is sound during hoisting.

If the expiration year of use is 40 years, the number of transport is 3 times per year and the number of times of handling per transport is 10 times, the number of times of lifting is 12,000 times. The maximum stress in the evaluations (1) to (3) above is 21.6 N/mm^2, and the repeated stress is 10.8 N/mm^2. This is lower than 4.0 × 10^2 N/mm^2 which is repeated peak pressure strength at 12000 times shown in (Ⅱ) -Fig.A.6, and the allowable number of repetitions is larger than the number of repetitions during the planned use period.

A.4.5 Tightening device

This packaging is transported after being tightened by a device, shown in (Ⅱ)-Fig.A.11.

The packaging and the tightening device are secured with an eye-plate and a turnbuckle.

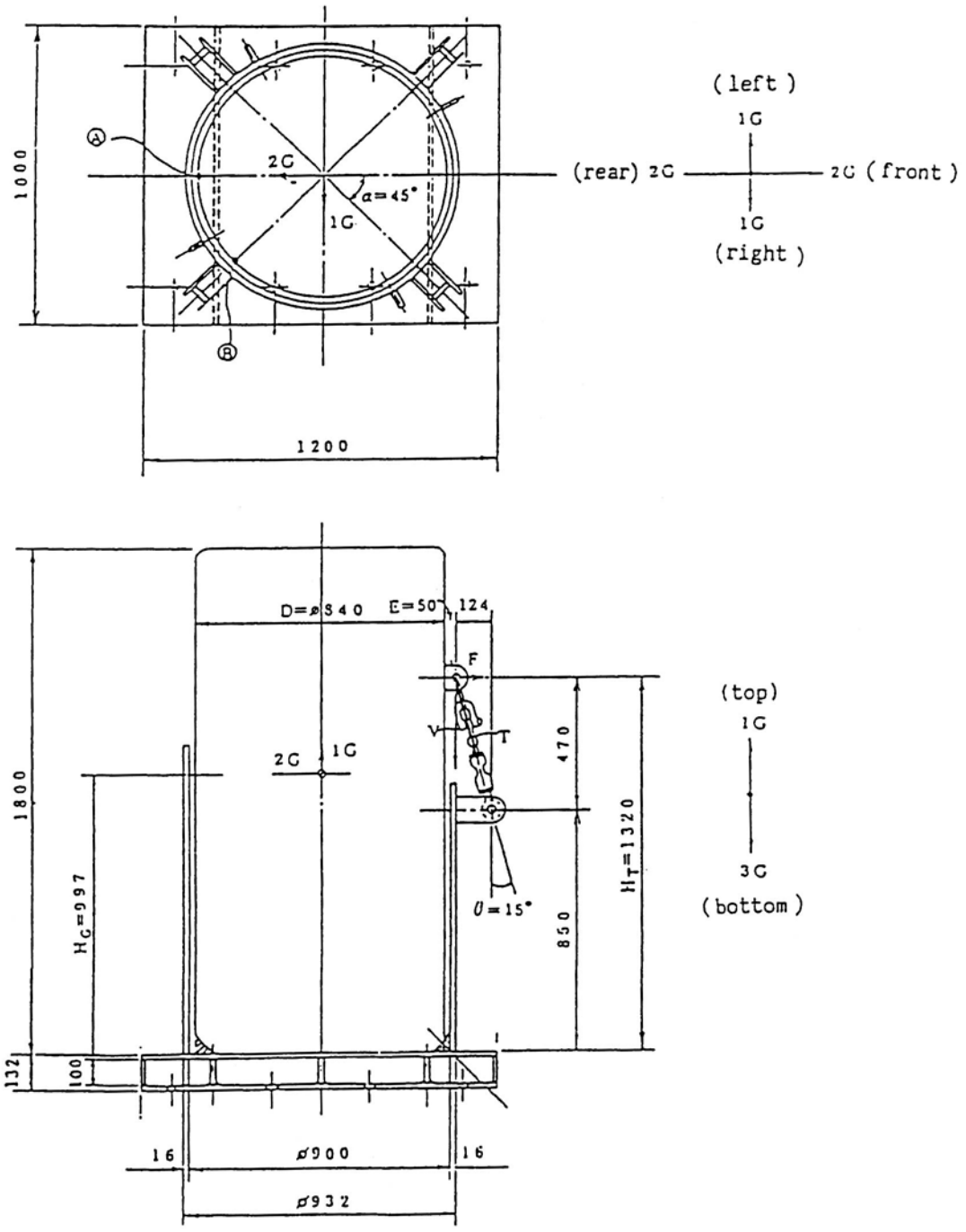

(Ⅱ)-Fig.A.11 Acceleration during transportation

The acceleration which occurs during transportation is 2G from front to rear, 1G from left to right, 1G towards the top and 3G towards the bottom, as indicated in (Ⅱ)-Fig.A.11.

After taking the combined force of these factors into consideration, the tensile strength applied to the turnbuckle due to the overturning moment around the supporting points Ⓐ and Ⓑ as indicated in (Ⅱ)-Fig.A.11 is as follows:

$$T_A=\frac{2\cdot H_G+R}{2H_T\sin\theta\cdot\sec\alpha+2\cos\theta\{R(1+\cos\alpha)+E\cos\alpha\}}\times m_o\times g \quad [N]$$

$$T_B=\frac{3\cdot H_G\cos\alpha+R}{H_T\sin\theta+(2R+E)\cos\theta}\times mo\times g \quad [N]$$

where

T_A : Tensile force of the turnbuckle taking Ⓐ as the supporting point.

T_B : Tensile force of the turnbuckle taking Ⓑ as the supporting point.

HG : Gravity height, HG= 997 [mm]

HT : Height to the center of the eye-plate, HT= 1320 [mm]

R: Outer radius of the packaging, R= 420 [mm]

E: Length where the eye-plate is fixed: E= 50 [mm]

θ: Angle of the turnbuckle, θ = 15°

α: Direction angle of the eye-plate, α = 45°

mo: Weight of the package, mo= 950 [kg]

g: Gravitational acceleration, g = 9.81 [m/s2]

The following equations are given,

$$T_A=\frac{2\times997+420}{2\times1320\times\sin15^\circ\cdot\sec45^\circ+2\cos15^\circ\{420(1+\cos45^\circ)+50\times\cos45^\circ\}}$$

$\times950\times9.81=9.30\times10^3$ [N]

$$T_B=\frac{3\times997\times\cos45^\circ+420}{1320\times\sin15^\circ+(2\times420+50)\cos15^\circ}\times950\times9.81=1.97\times10^4 \quad [N]$$

Therefore, the tensile force is greater when point Ⓑ is taken as the supporting point

$T=T_B=1.97\times10^4$ [N]

Thus, the stress analysis is conducted at this load level.

The following equations demonstrate the horizontal and the vertical components of force (F and V) when the eye-plate of the packaging receives the maximum tensile force T from the tie-down turnbuckle during transport.

T= 1.97×104 [N]

F= T･sin θ =1.97×104×sin15° =5.10×10^3 [N]

V= T･cos θ =1.97×104×cos15° =1.90×10^4 [N]

The analytical model for this case is displayed in (Ⅱ)-Fig.A.12

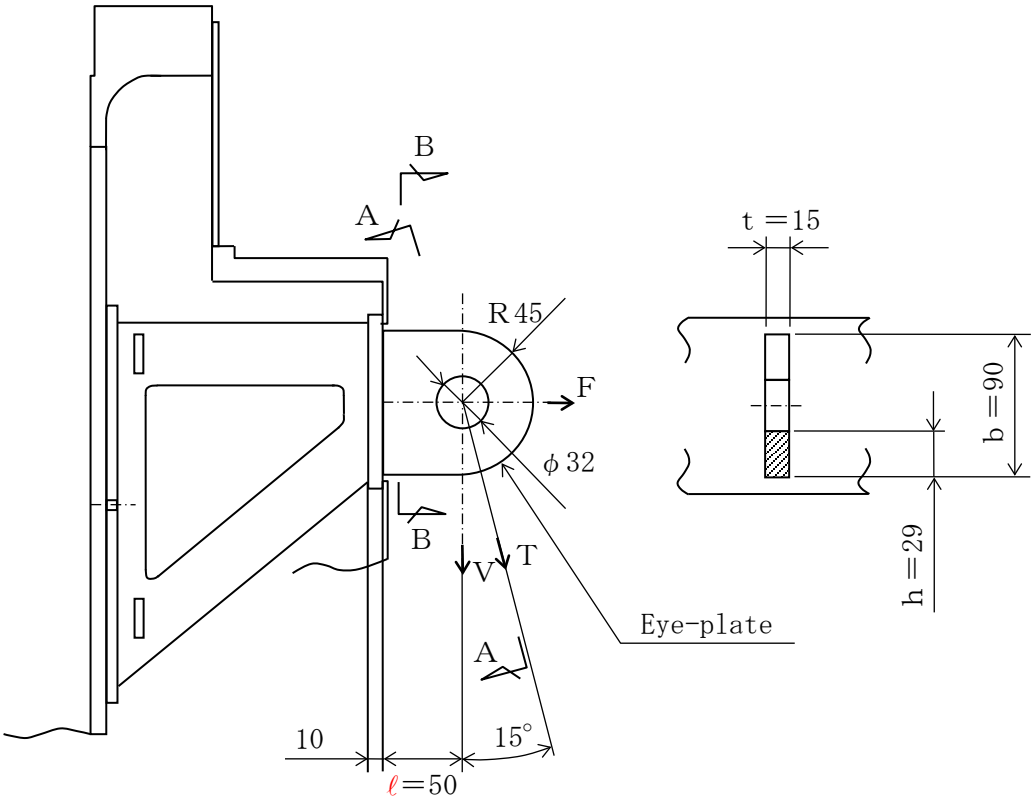

(Ⅱ)-Fig.A.12 Analytical model for eye-plate

The following is an analysis of the stress generated in each cross section when the directional load of the turnbuckle T =1.97×10^4 [N] is applied to the eye-plate as indicated in (Ⅱ)-Fig.A.12.

(1) A-A cross section

The following equation demonstrates the shearing stress τ (N/mm^2) generated in the shaded portion (A-A cross section) of the eye-plate shown in (Ⅱ)-Fig.A.12.

$$\tau = \frac{T}{A} = \frac{T}{t \cdot h}$$

where

τ : shearing stress [N/mm^2]

T: maximum load, T=1.97×10^4 [N]

t: board thickness, t =15 [mm]

h: height, h=29 [mm]

Therefore

$$\tau = \frac{1.97 \times 10^4}{29 \times 15} = 45.3 \quad [N/mm^2]$$

It is less than the design standard value allowable correspond to shearing strength (0.6Sy =108N/mm^2 of the eye-plate material (SUS 304).

The margin of safety MS is

$$MS = \frac{0.6Sy}{\tau} - 1 = \frac{108}{45.3} - 1 = 1.38$$

(2) B-B cross section

The following equation demonstrates the bending stress σ_b(N/mm^2) generated in the fixed part (B-B cross section) of the eye-plate shown in (Ⅱ)-Fig.A.12.

$$\sigma_b = \frac{M}{Z} = \frac{V \cdot 1}{tb^2/6}$$

where

M: bending moment [N·mm]

z: section modulus [mm^3]

V: vertical component force, V=1.90×10^4 [N]

t: eye-plate board thickness, t=15 [mm]

l: moment arm, l =50 [mm]

b: eye-plate width, b=90 [mm]

Therefore,

$$\sigma_b = \frac{1.90\times10^4\times50}{15\times90^2/6} = 46.9 \quad [N/mm^2]$$

is obtained, and it is less than Yield point of the design (Sy=180N/mm^2) of the eye-plate material (SUS 304).

The margin of safety MS is

$$MS = \frac{Sy}{\sigma_b} - 1 = \frac{180}{46.9} - 1 = 2.83$$

The shearing stress τ generated in the B-B cross section is given by the following equation:

$$\tau = \frac{V}{A} = \frac{V}{t\times b} = \frac{1.90\times10^4}{15\times90} = 14.1 \quad [N/mm^2]$$

It is less than the design standard value allowable correspond to shearing stress (0.6Sy=108N/mm^2) of the eye-plate material (SUS 304).

The margin of safety (MS) is

$$MS = \frac{0.6Sy}{\tau} - 1 = \frac{108}{14.1} - 1 = 6.65$$

The composite stress σ (N/mm^2) of the bending stress σ_b (N/mm^2) mentioned above and the shearing stress is given by the following equation

$$\sigma = \sqrt{\sigma_b{}^2 + 4\tau^2} = \sqrt{46.9^2 + 4\times14.1^2} = 54.7 \quad [N/mm^2]$$

It is less than Yield point of the design (Sy =180N/mm^2) of the eye-plate material (SUS 304).

The margin of safety (MS) is

$$MS = \frac{Sy}{\sigma} - 1 = \frac{180}{54.7} - 1 = 2.29$$

(3) Welded part of B-B cross section

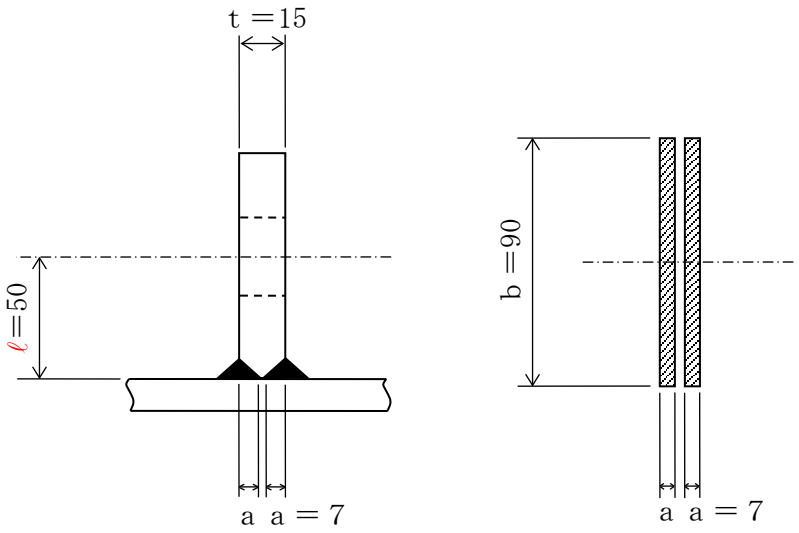

(Ⅱ)-Fig.A.13 Analytical model for welded part of eye-plate

The following equation demonstrates the bending stress σ_b(N/mm^2) generated in the welded part of the fixed part of the eye-plate shown in (Ⅱ)-Fig.A.13.

$$\sigma_b = \frac{M}{Z} = \frac{V \cdot 1}{Z}$$

where

Z: Section modulus of the welded part,

$$Z = \frac{1}{6} \cdot 2a \cdot b^2 \quad [mm^3]$$

a: Throat depth, a = 7 [mm]

b: Board width, b = 90 [mm]

Therefore, σ_b is

$$\sigma_b = \frac{1.90 \times 10^4 \times 50}{\frac{1}{6} \times 2 \times 7 \times 90^2} = 50.3 \quad [N/mm^2]$$

This is less than the design standard value (0.45Sy= 81.0N/mm^2) of the welded part.

The margin of safety (MS) is

$$MS=\frac{0.45Sy}{\sigma_b}-1=\frac{0.45\times180}{50.3}-1=0.61$$

The shearing stress τ generated at the welded part of the B-B cross section is given by the following equation

$$\tau=\frac{V}{A}=\frac{V}{2a\cdot b}=\frac{1.90\times10^4}{2\times7\times90}=15.1 \quad [N/mm^2]$$

This is less than the design standard value allowable correspond to shearing stress ($0.45\times0.6\times Sy=48.6N/mm^2$) of the welded part.

The margin of safety (MS) is

$$MS=\frac{0.45\times0.6\times S_y}{\tau}-1=\frac{0.45\times0.6\times180}{15.1}-1=2.21$$

The composite stress σ (N/mm^2) of the bending stress σ_b and the shearing stress τ is given by the following equation

$$\sigma=\sqrt{\sigma_b{}^2+4\cdot\tau^2}=\sqrt{50.3^2+4\times15.1^2}=58.7 \quad [N/mm^2]$$

This is less than the design standard value ($0.45Sy=81.0N/mm^2$) of the welded part.

The margin of safety (MS) is

$$MS=\frac{0.45Sy}{\sigma}-1=\frac{0.45\times180}{58.7}-1=0.37$$

A summary of the results of the above-mentioned analyses is given in (Ⅱ)-Table A.9.

As shown in (Ⅱ)-Table A.9, the margin of safety (MS) of the results of the analyses being positive in each case, the eye-plate is sound when tied down.

(Ⅱ)-Table.A.9 Summary of analyses under routine transport

Conditions	Analysis item		Type of load	Design standard	The design standard value [N/mm²]	Analysis result [N/mm²]	Margin of safety MS
Routine transport	Hoisting accessory 1.Eye-plate during hoisting A-A cross section	(1)Shearing stress	Weight of the package×3	0.6Sy	108	16.1	5.70
	B-B cross section	(1)Bending stress (2)Shearing stress (3)Composite stress		Sy 0.6Sy Sy	180 108 180	17.3 5.18 20.2	9.40 19.8 7.91
	B-B cross section (welded part)	(1)Bending stress (2)Shearing stress (3)Composite stress		0.45Sy 0.27Sy 0.45Sy	81.0 48.6 81.0	18.5 5.55 21.6	3.37 7.75 2.75
	Tightening device 2.Eye-plate in tie-down position A-A Cross section	(1)Shearing stress	Acceleration Left-right:1G Front-rear:2G Top :1G Bottom :3G	0.6Sy	108	45.3	1.38
	B-B cross section	(1)Bending stress (2)Shearing stress (3)Composite stress		Sy 0.6Sy Sy	180 108 180	46.9 14.1 54.7	2.83 6.65 2.29
	B-B cross section (welded part)	(1)Bending stress (2)Shearing stress (3)Composite stress		0.45Sy 0.27Sy 0.45Sy	81.0 48.6 81.0	50.3 15.1 58.7	0.61 2.21 0.37

A.4.6 Pressure

We shall analyze the soundness and sealing performance of the packaging in the case where external pressure would decrease to 60 kPa. The analysis is performed assuming that minimum temperature if the package components is -40 ℃ and the maximum temperature is 65 ℃.

When external pressure decreases to 60 kPa, the pressure in the inner shell is

$P_2 = P_0 - P_a = 0.1013 - 0.060 = 0.0413$ [MPa]

where

P_0 : Inner shell initial internal pressure (atmospheric pressure), $P_0 = 0.1013$ [MPa]

Pa : External pressure after pressure decrease, Pa= 0.060 [MPa]

For purposes of stress evaluation, in A.5.1.3 Stress Calculation, the internal pressure utilized in the packaging is 9.81×10^{-2}MPa. In this section, we will analyze the internal pressure, utilizing the total of differential pressure

$P = P_1 + P_2 = 0.0981 + 0.0413 \fallingdotseq 0.140$ [MPa]

The stress evaluation parts and the analysis method are the same as in section A.5.1.3 and the results of the stress evaluation are shown in (Ⅱ)-Table A.10.

Stress units ;N/mm²

(Ⅱ) -Table A.10 Stresses evaluation under changed pressure

No.	Position to be evaluated / Stress			Stress at initial clamping	Stress due to internal pressure	Stress due to thermal expansion	Primary stress						Primary+secondary stress			Fatigue					
							Pm(PL)	Sm	MS	PL+Pb	1.5Sm	MS	PL+Pb +Q	3Sm	MS	PL+Pb +Q+F	Sa	N	Na	DF	MS
1	Frame of Inner shell		σ_r	—	-0.070	—	3.36	137	39.7	—	—	—	3.36	411	121	3.36	1.68	500	min 10^6	5×10^{-4}	2×10^3
			σ_θ		3.29																
			σ_z		1.65																
2	Bottom plate of the inner shell	Inner Surface	σ_r	—	4.53	—	0.140	137	977	4.67	205	42.8	4.67	411	87.0	4.67	2.34	500	min 10^6	5×10^{-4}	2×10^3
			σ_θ		1.36																
			σ_z		-0.140																
		Outer Surface	σ_r	—	-4.53	—															
			σ_θ		-1.36																
			σ_z		0																
3	Inner shell lid	Inner Surface	σ_r	—	-4.66	—	0.140	2/3Sy 458	3270	4.66	Sy 687	146	4.66	Sy 687	146	4.66	2.33	500	min 10^6	5×10^{-4}	2×10^3
			σ_θ		-4.66																
			σ_z		-0.140																
		Outer Surface	σ_r	—	4.66	—															
			σ_θ		4.66																
			σ_z		0																
4	Inner shell lid clamping bolt		σ_t	174	4.59	—	180	Sy/1.5 459	1.55	—	—	—	180	Sy 688	2.82	720*	360	500	4000	0.125	7.0
5	Displacement of the inner lid O-ring	(1) Displacement $\mu = 1.72\times10^{-2}$mm (2) Initial clamping value of the O-ring $\delta \fallingdotseq 1.1$mm (3) Residual margin of tightening of O-ring $\Delta t = \delta - \mu \fallingdotseq 1.082$mm																				

Pm ; General primary membrane stress; PL ; Local primary membrane stress; Pb ; Primary bending stress; Q ; Secondary stress; F ; Peak stress; Sa ; Repeated peak stress; N ; Number of uses; σ_t; Ability of bolt stress; Na ; Permissible number of repetition; DF ; Cumulative fatigue coefficient; Sm ; Design stress intensity value; Sy ; Yield point of the design; MS ; Margin of safety; * ; Stress concentration factor = 4; σ_r; Diameter direction stress; σ_o;Periphery direction stress; σ_t; Axial stress;

A.4.7 Vibration

This package is secured with a turnbuckle on a tightening device, as indicated in (Ⅰ)-Fig.C.2. The turnbuckle is safely secured in order to avoid loosening due to vibration from the transport vehicle. Hence, we shall assume that no vibrations will be caused by this. Below, we shall calculate the natural frequency of the package itself, which will be compared to the vibration caused by the vehicle or ship of transport, and demonstrate that this will not cause the package to resonate during transport.

(1) Vibrations of the packaging

(Ⅱ)-Fig.A.14 shows an analytical model for the vibration of the packaging.

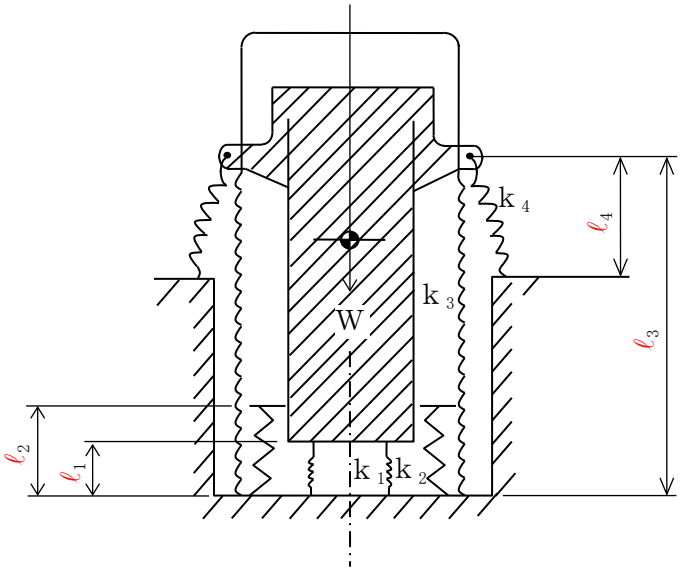

(Ⅱ)-Fig.A.14 Vibration analytical model of packaging

As is indicated in (Ⅱ)-Fig.A.14, by assuming that the packaging is a mass system supported by four types of parallel springs, the natural frequency at that time can be given by the following equation [8] :

$$\omega_0 = \sqrt{\frac{K}{m} \times 10^3} \qquad [\text{rad/sec}]$$

Therefore,

$$f_0 = \frac{\omega_0}{2\pi} = \frac{1}{2\pi}\sqrt{\frac{K \times 10^3}{m}} \qquad [\text{Hz}]$$

where

ω_0 : Natural angular frequency of the packaging [rad/sec]

f_0 : Natural frequency of the packaging [Hz]

m : Package mass, m=950 [kg]

K : Parallel spring constant[kg/mm]

$$K = \sum_{i=1}^{4} = ki = K_1 + K_2 + K_3 + K_4$$

$$= \sum_{i=1}^{4} \frac{A_i E_i}{1_i} = \frac{A_1 E_1}{1_1} + \frac{A_2 E_2}{1_2} + \frac{A_3 E_3}{1_3} + \frac{A_4 E_4}{1_4}$$

A_1 : Cross section of the reinforcement, A1 =2.83×10^3 [mm^2]

A2 : Cross section of the balsa, A2 =4.76×10^5 [mm^2]

A3 : Cross section of the outer shell board, A3 =7.92×10^3 [mm^2]

A4 : Cross section of the turnbuckle, A4 =2.83×10^3 [mm^2]

E1 : Modulus of longitudinal elasticity of the reinforcement;

E1 =1.92×10^5 [N/mm^2]

E2 : Modulus of longitudinal elasticity of the balsa, E2 =98.1 [N/mm^2]

E3 : Modulus of longitudinal elasticity of the outer shell board,

E3 =1.92×10^5 [N/mm^2]

E4 : Modulus of longitudinal elasticity of the turnbuckle,

E4 =2.04×10^5 [N/mm^2]

l1 : Length of the reinforcement, l1 =194 [mm]

l2 : Length of the balsa, l2 =341 [mm]

l3 : Length of the outer shell board, l3 =1320 [mm]

l4 : Length of turnbuckle, l4 =470 [mm]

Therefore,

k_1 : Spring constant of the reinforcement, k1 =2.79×10^6 [N/mm]

k2 : Spring constant of the balsa, k2 =0.137×10^6 [N/mm]

k3 : Spring constant of the inner shell board, k3 =1.15×10^6 [N/mm]

k4 : Spring constant of the turnbuckle, k4 =1.23×10^6 [N/mm]

K=(2.79+0.14+1.15+1.23)×10^6 =5.31×10^6

Therefore, the natural frequency is

$$f_0=\frac{1}{2\pi}\sqrt{\frac{5.31\times10^6\times10^3}{950}}=377 \quad [Hz]$$

This natural frequency of 377 Hz is outside the vibration range of 0 to 50 Hz which will present in the vehicle or ship during transport. Therefore, there is no possibility of coincidental vibration. In addition, the frequency expected during transportation is about 0 to 50 [Hz], which is different from the natural frequency, so that the input excitation force is not amplified. Therefore, since the acceleration generated by the main body during transportation is sufficiently included in the free fall under general test conditions, the package will not be cracked or damaged.

(2) Fuel basket

The fuel basket is supported by a spacer in the inner shell, and will not receive directly any external vibration.

The fuel element and so on is also protected at top and bottom by a silicone foam spacer, and will not receive any vibrations.

(3) Evaluation

The natural frequency of this packaging is higher than the vibration generated by the transport vehicle, and so, coincidental resonance will not occur.

Therefore, the inner lid clamping bolt and other clamping devices will

not loosen during transport, and sealing performance will be fully preserved.

In addition, the fuel basket and the fuel element are supported by rubber inside the inner shell, and soundness will be fully preserved despite the vibrations during transport.

A.5 Normal test conditions

This package is a BU type package. Therefore, the normal test conditions defined on the regulation are as follows.

(1) Water spray test

The following tests shall be performed after test (1).

(2) Free drop test

(3) Stacking test

(4) Penetration test

The following test shall be performed after tests (1) to (4).

(5) One week period placed in an environment of -40℃ to 38℃.

The following section will analyze the effect to the package caused by the tests mentioned above. The results of this analysis shall demonstrate that the design standards for normal test conditions are satisfied.

A.5.1 Thermal test

A.5.1.1 Outline of temperature and pressure

This section is a summary of the pressure and temperature used for design analysis under normal test conditions.

(1) Design temperature

As determined in (Ⅱ)-B.4.2 Maximum Temperature, the package temperature may rise to a maximum of 65℃ (minimum -40℃). Therefore, the design temperature under normal test conditions shall be conservatively determined to be 75℃, adopting a margin of safety, as indicated in (Ⅱ)-Table A.11, for both the inner and outer shells.

(Ⅱ)-Table A.11 Design temperature under normal test conditions

No.	Part	Design temperature(℃)
1	Fuel element	75
2	Fuel basket	75
3	Inner shell main body	75
4	Inner lid	75
5	Outer shell	75

(2) Design pressure

As determined in (Ⅱ)-B.4.4 Maximum Internal Pressure, the internal pressure of the inner shell may increase up to 0.016 MPa in gauge pressure. Even when the temperature changes from -40℃ to 65℃, the pressure inside the container is 0.046MPa [gauge]. Therefore, the design pressure in normal test conditions shall be conservatively determined as 0.0981 MPa, adopting a margin of safety, as indicated in (Ⅱ)-Table A.12.

(Ⅱ)-Table A.12 Design pressure under normal test conditions

No.	Portion	Design pressure
1	In the inner shell	9.81×10^{-2}MPa･G

A.5.1.2 Thermal expansion

This section will assess the stress generated when differential thermal expansion causes the inner shell and fuel basket to come into contact. The analytical model is shown in (Ⅱ)-Fig.A.15

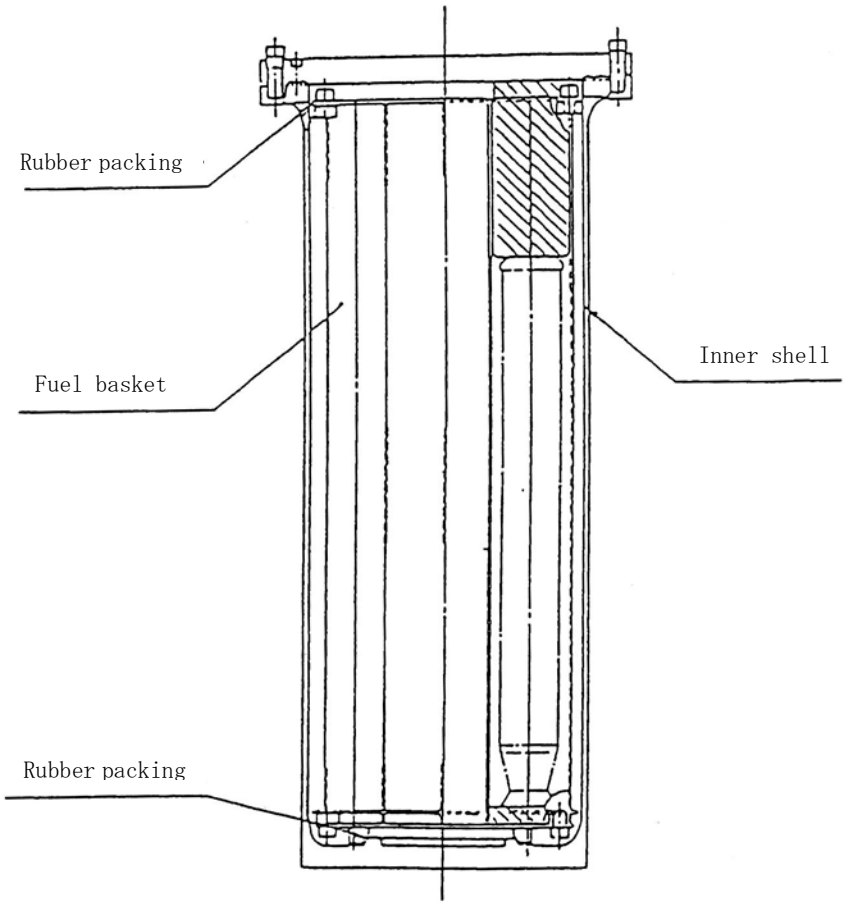

(Ⅱ)-Fig.A.15 Analytical model of thermal expansion

The increase in temperature in the fuel basket and the inner shell is 75℃, as indicated in (Ⅱ)-B Thermal Analysis. There is no temperature difference, where thermal expansion does not occur, since the two parts are made of the same material (SUS 304).

There is also practically no temperature difference between the outer and inner shells. The inner shell will not be influenced by thermal expansion of the outer shell.

Therefore, no stress will be generated by thermal expansion in the fuel basket and inner shell.

A.5.1.3 Stress calculation

Stress calculation shall be conducted in this section.

Temperature gradient, loads from the outside and pressure may generate stress in each part of the package.

The ratio of the inner shell's inner radius to the board thickness is higher than 10 and can be considered as a thin cylinder. Therefore, temperature differences will little occur inside the board thickness of the shell. Also, although the inner lid and the bottom plate of the inner shell are thicker than the other parts, temperature differences will have little possibility of occurring since these parts are protected by heat insulators and shock absorbers, as in the outer lid.

The same applies to the fuel basket, where the board thickness is 3 or 3.4mm. This thinness will make it improbable for temperature differences to occur.

Therefore, since the thermal stress due to temperature differences in the plate thickness of the parts of the packaging is minimal, this stress is not calculated in this section.

Next, we shall analyze the stress generated in each part by internal pressure, keeping in mind the fact that the internal pressure of the inner shell is the pressure used in the package.

We shall also analyze the inner lid clamping bolt, which is a crucial part in the sealing boundary, after taking into consideration the initial clamping strength and thermal expansion.

(1) Stress evaluation positions

The stress evaluation position of the inner shell under normal test conditions is shown in (Ⅱ)-Fig.A.16. In this section, the main stress shall be determined, the different types of stress being shown in (Ⅱ)-Table A.13.

A stress evaluation will be conducted in section A.5.1.4.

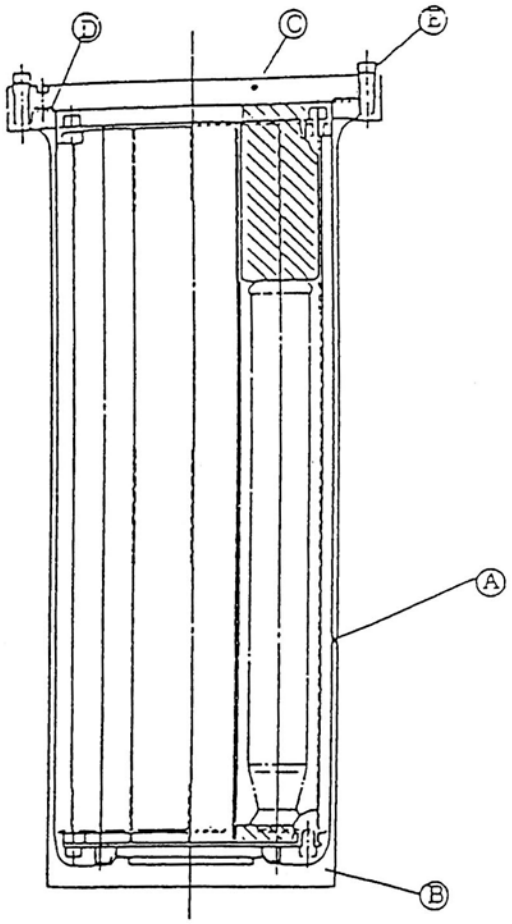

Code	Evaluation position
Ⓐ	Frame of inner shell
Ⓑ	Bottom plate of inner shell
Ⓒ	Inner lid
Ⓓ	Inner lid O-ring displacement
Ⓔ	Inner lid clamping bolt

(Ⅱ)-Fig.A.16 Stress evaluation position under normal test conditions

Ⓐ Inner shell

In the center of the inner shell, pressure inside the inner shell shall be utilized as internal pressure.

The analytical model of the stress generated in the center of the inner shell which subjected to internal pressure is shown in (Ⅱ)-Fig.A.17. The stress (σ_θ, σ_z, σ_r) generated in the center of the shell is given as a thin cylinder by the following equations [7]:

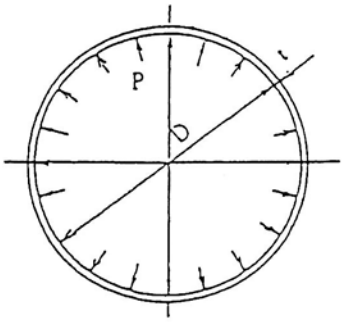

(Ⅱ)-Fig.A.17 Stress analysis model of inner shell center portion

$$\sigma_\theta = \frac{PD_m}{2t}$$

$$\sigma_z = \frac{PD_m}{4t}$$

$$\sigma_r = -\frac{P}{2}$$

where

σ_θ : Circumferential stress [N/mm^2]

σ_z : Axial stress [N/mm^2]

σ_r : Radial stress [N/mm^2]

P: Design pressure inside the inner shell, P =9.81×10^{-2} [MPa·gauge]

D_m: Frame of inner shell mean diameter, D_m =D + t =460 +10=470 [mm]

t: Frame of inner shell board thickness, t=10.0 [mm]

D: Frame of inner shell bore, D =460 [mm]

Thus, the stresses are

$$\sigma_\theta = \frac{9.81\times10^{-2}\times470}{2\times10} = 2.31 \quad [N/mm^2]$$

$$\sigma_z = \frac{9.81\times10^{-2}\times470}{4\times10} = 1.15 \quad [N/mm^2]$$

σ_r=-0.0491 [N/mm^2]

Ⓑ Bottom plate of the inner shell

(Ⅱ)-Fig.A.18 shows an analytical model for the stress on the bottom plate of the inner shell when receiving internal pressure.

The stress σ generated in the fixed part of the peripherally supported disc is,

$$\sigma_\theta = \pm 0.225 \frac{P \cdot a^2}{h^2}$$

$$\sigma_r = \pm 0.75 \frac{P \cdot a^2}{h^2}$$

σ_z=-P (Inner surface)

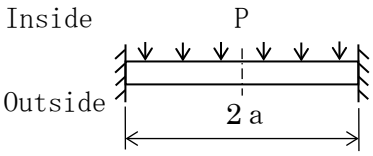

(Ⅱ)-Fig.A.18 Stress analysis model of inner shell bottom plate

where

σ_θ : Circumferential stress [N/mm^2]

σ_z : Axial stress [N/mm^2]

σ_r : Radial stress [N/mm^2]

P: Design pressure inside the inner shell,

P =9.81×10^{-2} [MPa･gauge]

a: Radius of inner shell bottom plate, a =230 [mm]

h: Wall thickness of inner shell bottom plate,

h =35 [mm]

Therefore, the stresses are

$$\sigma_\theta = \pm 0.225 \frac{9.81\times10^{-2}\times230^2}{35^2} = \pm 0.953 \quad [N/mm^2]$$

$$\sigma_r = \pm 0.75 \frac{9.81\times10^{-2}\times230^2}{35^2} = \pm 3.18 \quad [N/mm^2]$$

σ_z=-0.098 (Inner Surface) [N/mm^2]

The double signs of the stress values correspond to the inner and outer surface respectively.

Ⓒ Inner lid

(Ⅱ)-Fig.A.19 shows an analytical model of the stress on the inner lid when receiving internal pressure.

The stress σ (σ$_\theta$, σ$_r$, σ$_z$) generated in the peripherally simply supported disc is maximum at the center

$$\sigma_\theta = \sigma_r = \mp 1.24 \frac{P \cdot a^2}{h^2}$$

$$\sigma_z = -P \quad \text{(Inner surface)}$$

where

σ$_\theta$: Circumferential stress [N/mm^2]

σr : Radial stress [N/mm^2]

σz : Axial stress [N/mm^2]

P: Design pressure inside the inner shell,

P =9.81×10^{-2} [MPa･gauge]

a: Radius of inner shell bottom plate, a =285 [mm]

h: Wall thickness of inner shell bottom plate,

h =55 [mm]

Therefore, the following values are obtained,

$$\sigma_\theta = \sigma_r = \mp 1.24 \frac{9.81\times10^{-2}\times285^2}{55^2} = \mp 3.27 \quad [\mathrm{N/mm^2}]$$

$$\sigma_z = -0.098 \quad \text{(inner surface)} \quad [\mathrm{N/mm^2}]$$

The double sign indicates the inside for the top, the outside for the bottom.

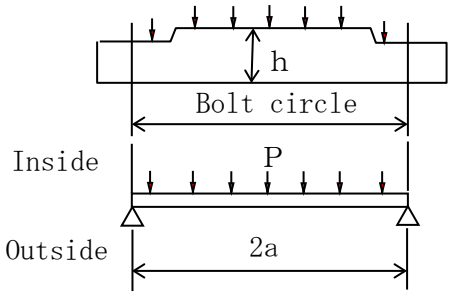

(Ⅱ)-Fig.A.19 Stress analysis model of inner lid center portion

Ⓓ Inner lid O-ring displacement

An analytical model of the inner lid O-ring displacement is shown in (Ⅱ)-Fig.A.20.

An displacement ω (mm) of the simply supported disc shown in (Ⅱ)-Fig.A.20 can be determined by the following equations [7] :

$$\omega = \frac{P \cdot a^4}{64D} \cdot \left(1 - \frac{r^2}{a^2}\right) \cdot \left(\frac{5+\nu}{1+\nu} - \frac{r^2}{a^2}\right)$$

where

P: Design pressure in the inner shell, P =9.81×10^{-2} [MPa･gauge]

ν : Poisson's ratio, ν =0.3

a: Radius of the support points circle of the inner lid, a =285 [mm]

r: Distance from the center to the evaluation point,

ri : radius of inner O-ring groove, ri =237.5 [mm]

D: Inner lid bending stiffness,

$$D = \frac{E \cdot h^3}{12(1-\nu^2)} \quad [N\cdot mm]$$

E: Modulus of longitudinal elasticity

E =1.99×10^5 [N/mm^2]

h: Minimum plate thickness of the inner lid, h=36.7 [mm]

Therefore, the displacement ω_i of the groove portion of the inner O-ring is

$$\omega_i = \frac{9.81\times10^{-2}\times285^4\times12\times(1-0.3^2)}{64\times1.99\times10^5\times36.7^3}\times\left(1-\frac{237.5^2}{285^2}\right)$$

$$\times\left(\frac{5+0.3}{1+0.3}-\frac{237.5^2}{285^2}\right)=1.16\times10^{-2} \quad [mm]$$

ω_i is sufficiently smaller than the initial clamping value $\delta \fallingdotseq 1.1$mm

(Difference of O-ring groove depth and O-ring diameter)

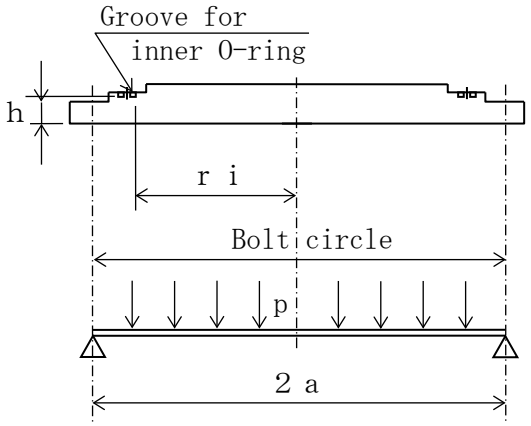

(Ⅱ)-Fig.A.20 Analytical model of inner lid O-ring displacement

Ⓔ Inner lid clamping bolt

The stress generated by initial clamping stress, internal pressure and thermal expansion shall be analyzed regarding the inner lid clamping bolt (hereinafter referred to as “bolt”).

(a) Initial clamping stress

The analytical model figure of the stress generated by the initial clamping force in the bolt is shown in (Ⅱ)-Fig.A.21.

The tensile stress σ_t generated in the bolt as shown in (Ⅱ)-Fig.A.21 is given by the equation

$$\sigma_t = \frac{F}{A_i}$$

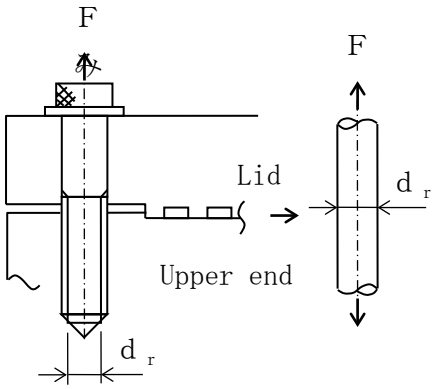

(Ⅱ)-Fig.A.21 Stress analysis model of bolt of inner lid (initial clamping stress)

Where

F : Initial clamping force of the bolt,

$$F = \frac{T}{k \cdot d} = \frac{2.825 \times 10^5}{0.2 \times 24} = 5.89 \times 10^4 \quad [N]$$

T : Initial clamping torque, $T = 2.825 \times 10^5$ [N·mm]

k : Torque coefficient, k=0.2

d : Nominal diameter of the bolt, d=24 [mm]

Ai: Cross section of the trough radius of the bolt (M24),

$$A_i = \frac{\pi}{4} \cdot d_i^2 = \frac{\pi}{4} \times 20.752^2 = 338.2 \quad [mm^2]$$

d_i: Minimum diameter of the bolt, $d_i = 20.752$ [mm]

Therefore, the following value is obtained

$$\sigma_t = \frac{5.89 \times 10^4}{338.2} = 174 \quad [N/mm^2]$$

(b) Stress due to internal pressure

The analytical model of the stress generated by the internal pressure in the bolt is shown in (Ⅱ)-Fig A.22.

The tensile stress σ_t generated in the bolt as shown in (Ⅱ)-Fig.A.22 is given by the following equation

$$\sigma_t = \frac{\pi \cdot r_i^2 \cdot P}{n \cdot Ar}$$

where

r_i : Radius of the surface receiving pressure, ri =237.5 [mm]

P : Design pressure in the inner shell, P =9.81×10^{-2} [MPa[gauge]]

Ar: Cross section of the minimum diameter of the bolt M24,

Ar=338.2 [mm^2]

n : Number of bolts, n =16

Therefore, the tensile stress is,

$$\sigma_t = \frac{\pi \times 237.5^2 \times 9.81\times10^{-2}}{16\times338.2} = 3.21 \quad [N/mm^2]$$

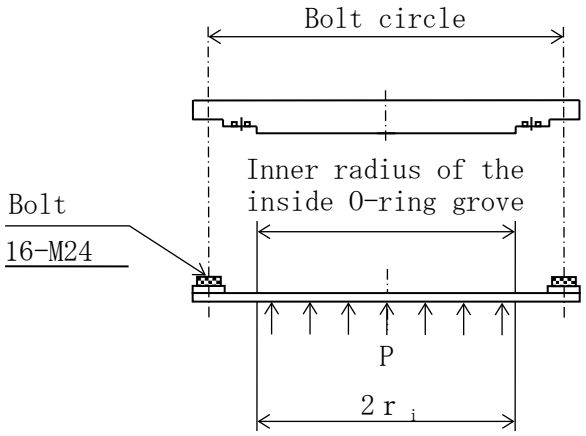

(Ⅱ)-Fig.A.22 Stress analysis model of bolt of inner lid (stress due to internal pressure)

(c) Stress due to thermal expansion

The analytical model of the stress generated by thermal expansion in the bolt is shown in (Ⅱ)-Fig.A.23.

The temperature of the bolt and of the inner lid is 75℃, in accordance with (Ⅱ)-B Thermal Analysis, and there is no temperature difference. The material also is the same, the SUS630, Stress due to thermal expansion is negligible.

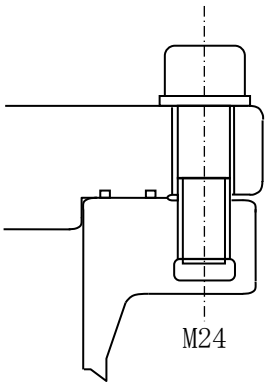

(Ⅱ)-Fig.A.23 Stress analysis model of bolt of inner lid (stress due to thermal expansion)

A.5.1.4 Comparison of allowable stress

The results of stress evaluation related to each of the analyses conducted in section (Ⅱ)-A.5.1.3 are summarized in (Ⅱ)-Table A.13.

As is shown in this table, the margin of safety against the design standard value allocated to each case, whether they are simple or multiple loads, is positive. Even when the ambient temperature changes from -40℃ to 38℃, there is no effect on thermal expansion and thermal stress.

Therefore, under normal test conditions (thermal test), the soundness of the package can be maintained. In addition, in the case where the number of usage of the package is set at 500*, the margin of safety in regard to allowable cycles is, as shown in (Ⅱ)-Table A.13, positive. Therefore, the soundness of the packaging will not be lost through repeated loads.

---

* Times of use N = 3/year×40 years×tolerance ratio ≒ 500 times

Stress units ;N/mm²

(Ⅱ) -Table A.13 Stress evaluation under normal test conditions (thermal test)

No.	Position to be evaluated / Stress			Stress at initial clamping	Stress due to internal pressure	Stress due to thermal expansion	Primary stress						Primary+secondary stress			Fatigue					
							Pm(PL)	Sm	MS	PL+Pb	1.5Sm	MS	PL+Pb +Q	3Sm	MS	PL+Pb +Q+F	Sa	N	Na	DF	MS
1	Frame of Inner shell		σ_r	—	-0.0491	—	2.36	137	57.0	—	—	—	2.36	411	173	2.36	1.18	500	min 10^6	5×10^{-4}	2×10^3
			σ_θ		2.31																
			σ_z		1.15																
2	Bottom plate of the inner shell	Inner Surface	σ_r	—	3.18	—	0.098	137	1396	3.28	205	61.5	3.28	411	124	3.28	1.64	500	min 10^6	5×10^{-4}	2×10^3
			σ_θ		0.953																
			σ_z		-0.098																
		Outer Surface	σ_r	—	-3.18	—															
			σ_θ		-0.953																
			σ_z		0																
3	Inner shell lid	Inner Surface	σ_r	—	-3.27	—	0.098	2/3Sy 458	4672	3.27	Sy 687	209	3.27	Sy 687	209	3.27	1.64	500	min 10^6	5×10^{-4}	2×10^3
			σ_θ		-3.27																
			σ_z		-0.098																
		Outer Surface	σ_r	—	3.27	—															
			σ_θ		3.27																
			σ_z		0																
4	Inner lid clamping bolt		σ_t	174	3.22	—	177	2/3Sy 458	1.58	—	—	—	177	Sy 687	2.89	708*	354	500	4000	0.125	7.0
5	Displacement of the inner shell lid O-ring	(1) Displacement $\mu = 1.16\times10^{-2}$mm (2) Initial clamping value of O-ring $\delta \fallingdotseq 1.1$mm (3) Compression dipth of O-ring $\Delta t = \delta - \mu \fallingdotseq 1.088$mm																			

Pm ; General primary membrane stress; PL ; Local primary membrane stress; Pb ; Primary bending stress; Q ; Secondary stress; F ; Peak stress; Sa ; Repeated peak stress; N ; Number of uses; σ_t; Ability of bolt stress Na ; Permissible number of repetition; DF ; Cumulative fatigue coefficient; Sm ; Design stress intensity value; Sy ; Yield point of deesign; MS ; Margin of safety; * ; Stress concentration factor = 4 σ_r ; Diameter direction stress σ_o ; Periphery direction stress

A.5.2 Water spray

The outside surface of this packaging is made of stainless steel, and there is no water absorption. Therefore, there is no possibility of degradation of the material due to the spraying of water.

In addition, the outer lid is secured to the main body with a outer lid clamping bolt using a washer. This is waterproof and presents no risks of water entering inside the packaging.

A.5.3 Free drop

The weight of this package is maximum 950 kg. Since it is below 5000 kg, the free drop height under normal test conditions is determined by regulation standards as 1.2 m.

The free drop posture is analyzed for the following four cases:

1) Horizontal drop

2) Vertical drop (lid side and bottom side)

3) Corner drop (lid side and bottom side)

4) Inclined drop (lid side and bottom side)

The purposes of this analysis are,

1) To demonstrate that the sealing performance of the inner shell is preserved by demonstrating that the deformation wrought by a free drop do not extend to the inner shell which is the sealing boundary.

2) The inner shell will not be damaged by the shock caused by the free drop, and will preserve full leak tightness.

3) There is no damage of the contained material.

(1) Analysis method

The following are the analysis conditions for the stress generated in the contained material, the fuel basket, the main body of the packaging and for the deformation of the transport packaging in the case where the package would

be subjected to a free drop test of 1.2m.

(a) Deformation

1) The drop energy of the package will be completely absorbed by the shock absorber in the case where the shock surface is a rigid body. Therefore, the deformation of the outer shell will be the deformation of the shock absorber.

This is conservative assumption ignoring absorption by the steel plate or the heat insulator.

2) The deformation and acceleration caused by the shock absorber shall be calculated on the basis of the shock absorbing function analysis program "CASH-Ⅱ" indicated in A.10.1.

(b) Stress

1) The drop energy of the package shall be absorbed by the deformation of the steel plate utilized in the shock absorber, the main body of the outer shell and the outer lid.

2) The acceleration utilized in the stress analysis (hereafter referred to as "design acceleration") shall be 1.2 times the calculation value (acceleration generated in the shock absorber) of "CASH-Ⅱ (this value was determined through comparison with test results as indicated in section A.10.1) plus the acceleration of the steel plate.

This is a safety evaluation since the shock strength present in the package will be combined to the acceleration of the shock absorber and the acceleration of the steel plate.

Design acceleration = calculation results of CASH-Ⅱ × 1.2
+ acceleration due to steel plate.

3) Generated acceleration of the steel plate will be determined using simplified calculations.

(2) Drop energy

The weight of the package utilized in the analysis is 960 kg as indicated in “A.2 Weight and Center of Gravity.” The drop energy is

$$Ea = Ev = m \cdot g \cdot h$$

where

Ea: Energy absorption of the shock absorber [J]

Ev: Drop energy of the package [J]

m: Package mass, m=950 [kg]

h: Drop height, h=1.20 [m]

g: Gravitational acceleration, g =9.81 [m/s2]

Therefore, the following value is obtained

$$Ea = Ev = 960 \times 9.81 \times 1.2 = 1.12 \times 10^4 \quad [J]$$
$$= 1.12 \times 10^7 \quad [N \cdot mm]$$

(3) Performance of the shock absorbers obtained by means of the CASH-Ⅱ analysis program

The results of the deformation in the shock absorber and of the acceleration through the shock absorbers performance analysis program CASH-Ⅱ are shown in (Ⅱ)-Table A.14.

The acceleration which is 1.2 times the results of the CASH-Ⅱ program utilized in the analysis is also shown in the above table.

(Ⅱ)-Table A.14 Deformation and acceleration of shock absorber under normal test conditions

Drop posture			Deformation (mm)	Acceleration (×g)	
				Calculation value	× 1.2
Horizontal			20.9	89.3	107.1
Vertical	Lid side		24.1	58.8	70.5
	Bottom side		18.2	78.9	94.6
Corner	Lid side	27.6° *	58.6	16.3	19.6
	Bottom side	22.8°	50.3	17.3	20.8
Inclined	Lid side	5°	21.5	14.1	16.9
		15°	41.5	13.0	15.6
		30°	60.8	17.1	20.5
		45°	65.8	21.7	26.0
		60°	59.3	25.7	30.8
		75°	46.9	34.5	41.4
		85°	27.4	36.5	43.8
	Bottom side	5°	22.2	5.96	7.15
		15°	40.1	16.8	20.2
		30°	56.2	19.5	23.4
		45°	60.4	22.5	27.0
		60°	61.4	24.9	29.9
		75°	44.4	29.0	34.8
		85°	25.0	30.2	36.2

*: This is the angle of the center line of the package to the drop direction. (same below)

where

g: Gravitational acceleration, g = 9.81 [m/s^2]

(4) Increase in acceleration caused by steel plate

(i) Horizontal drop

We will obtain the increase in acceleration caused by the steel plate during a horizontal drop.

The position of evaluation is shown in (Ⅱ)-Fig.A.24.

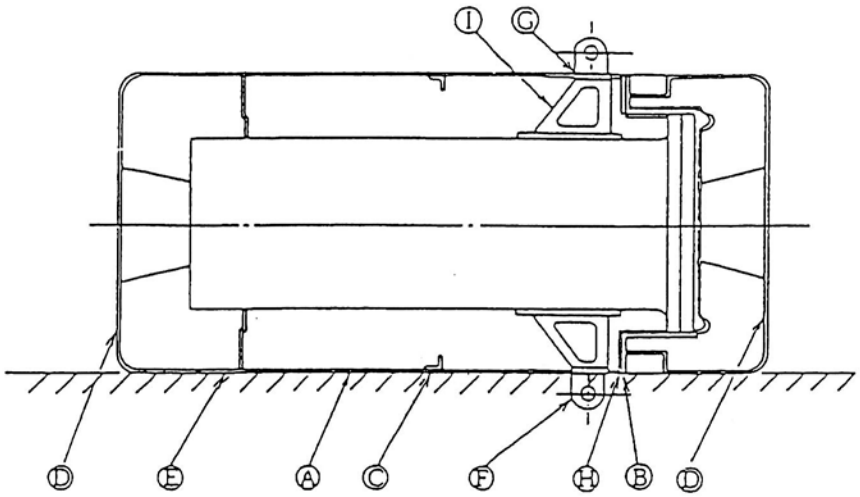

Code	Position of evaluation
Ⓐ	Outside cylinder steel plate
Ⓑ	Outer lid flange
Ⓒ	Stiffening ring
Ⓓ	Outer shell panel
Ⓔ	Partition
Ⓕ	Eye-plate
Ⓖ	Eye-plate fixation plate
Ⓗ	Flange of the main body of the outer shell
Ⓘ	Eye-plate fixation leg

(Ⅱ)-Fig.A.24 Acceleration evaluation position of steel plate for horizontal drop

Ⓐ Outside cylinder steel plate

An analytical model of the outside cylinder steel plate as an annulus ring on which the whole weight of the package rests uniformly is shown in (Ⅱ)-Fig.A.25.

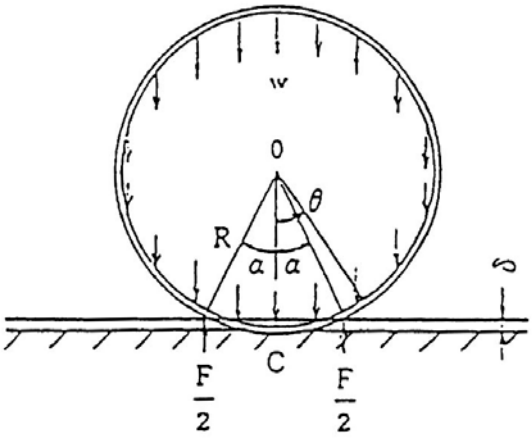

(Ⅱ)-Fig.A.25 Acceleration analysis model of outer shell plate for horizontal drop

As is indicated in (Ⅱ)-Fig.A.25, the bending moment of the annulus ring on which the uniform load w rests, can be given by the following equation.

$$M = wR^2 \left\{ \cos\alpha + \alpha\sin\alpha + \cos\alpha \cdot \sin^2\alpha + \frac{1}{2}\cos\theta + (\theta - \pi)\sin\theta \right\}$$

In the above equation, M is maximum at $\theta = \alpha$, and the following is obtained,

$$M = wR^2 \left\{ \left(\frac{3}{2} + \sin^2\alpha \right)\cos\alpha + (2\alpha - \pi)\sin\alpha \right\}$$

When the stress generated by the bending moment becomes equal to the deformation stress σ_s, the maximum resistance force F may be generated.

$$\sigma_s = \frac{M}{Z_p} = \frac{wR^2\left\{ \left(\frac{3}{2} + \sin^2\alpha \right)\cos\alpha + (2\alpha - \pi)\sin\alpha \right\}}{Z_p}$$

Therefore, the uniform load w at this time is given by the following

$$W = \frac{\sigma s \cdot Z_p}{R^2\left\{\left(\frac{3}{2}+\sin^2\alpha\right)\cos\alpha+(2\alpha-\pi)\sin\alpha\right\}}$$

Therefore, the maximum resistance force is the following

$$F = 2\pi wR = \frac{2\pi\sigma s \cdot Z_p}{R\left\{\left(\frac{3}{2}+\sin^2\alpha\right)\cos\alpha+(2\alpha-\pi)\sin\alpha\right\}}$$

where

M: Bending moment of the annulus ring [N·mm]

w: Uniform load [N/mm]

F: Maximum resistance force [N]

R: Radius of the annulus ring, R =420 [mm]

σ s: Deformation stress (at ordinary temperatures), σ s =520 [N/mm^2]

θ : Arbitrary angle based on OC [rad]

α : Radius of the deformed part,

$$\alpha = \cos^{-1}\left(\frac{R-\delta}{R}\right) = \cos^{-1}\left(\frac{420-20.9}{420}\right) = 18.15° = 0.317 \quad [\text{rad}]$$

δ : Deformation, δ =20.9 [mm]

Zp: Plasticity section modulus,

$$Z_p = \frac{1}{4}bh^2 = \frac{1500\times 3^2}{4} = 3375 \quad [\text{mm}^3]$$

b: Annulus ring width, b =1500 [mm]

h: Annulus ring thickness, h=3 [mm]

Therefore, the maximum resistance force is,

$$F = \frac{2\times\pi\times 520\times 3375}{420\times\left\{\left(\frac{3}{2}+\sin^2 18.15°\right)\cos 18.15° + (2\times 0.317-\pi)\sin 18.15°\right\}}$$

$= 3.57\times 10^4$ [N]

The equation of the increase in acceleration N_{H1} caused by the outside cylindrical steel plate is,

$$N_{H1}=\frac{F}{m}=\frac{3.57\times10^{4}}{950}=37.6=3.83\cdot g \quad [m/s^{2}]$$

where

m: Weight of the package, m=950 [kg]

Ⓑ Flange of the outer lid

The analytical model is shown in (Ⅱ)-Fig.A.25, as with section A.5.3 (4)(i) Ⓐ. But, since the deformation has not reached the annulus ring, the α in the moment equation is given as 0.

The cross section of the flange of the outer lid is given in (Ⅱ)-Fig.A.26.

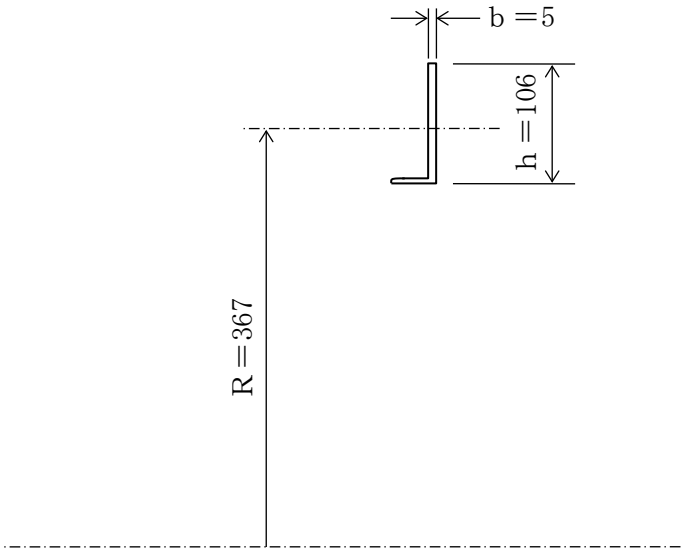

(Ⅱ)-Fig.A.26 Cross section of outer shell lid flange

The maximum resistance force is given by the following [10]

$$F=\frac{4\pi}{3R}\cdot\sigma s\cdot Zp=\frac{4\times\pi}{3\times367}\times520\times1.40\times10^{4}=8.31\times10^{4}\quad[N]$$

where

F: Maximum resistance force [N]

R: Radius of the annulus ring, R =367 [mm]

σs: Deformation stress (at ordinary temperatures), σs =520 [N/mm^2]

Zp: Section modulus of plasticity,

$$Zp=\frac{1}{4}bh^{2}=\frac{5\times106^{2}}{4}=1.40\times10^{4}\quad[mm^3]$$

b: Annulus ring width, b =5 [mm]

h: Annulus ring thickness, h =106 [mm]

Therefore, the increase in acceleration N_{H2} caused by the flange of the outer

lid is,

$$N_{H2}= \frac{F}{m}=\frac{8.31\times10^{4}}{950}=87.5=8.92\cdot g \quad [m/s^{2}]$$

Ⓒ Stiffening ring

The analytical model is shown in (Ⅱ)-Fig.A.25, as with section A.5.3(4)(i) Ⓐ. The maximum resistance force is given by the following equation [10]

$$F=\frac{2\pi\sigma_s\cdot Z_p}{R\left\{\left(\frac{3}{2}+\sin^2\alpha\right)\cos\alpha+(2\alpha-\pi)\sin\alpha\right\}}$$

where

F: Maximum resistance force [N]

R: Radius of the annulus ring, R =406 [mm]

σs: Deformation stress (ordinary temperature), σs =520 [N/mm^2]

δ: Deformation amount, δ =6.9 [mm]

α: Half angle of the deformed part,

$$\alpha=\cos^{-1}\left(\frac{R-\delta}{R}\right)=\cos^{-1}\left(\frac{406-6.9}{406}\right)=10.58^\circ=0.185 \text{ [rad]}$$

Zp: section modulus of plasticity [mm^3],

$$Zp=\frac{h}{4}\{(b-h)^2+h^2\}$$

$$=\frac{3}{4}\{(40-3)^2+3^2\}$$

$$=1.03\times10^3 \text{ [mm}^3\text{]}$$

b: Ring width, b=40 [mm]

h: Ring thickness, h=3 [mm]

Therefore, F is

$$F=\frac{2\times\pi\times520\times1.03\times10^3}{406\times\left\{\left(\frac{3}{2}+\sin^2 10.58^\circ\right)\cos10.58^\circ+(2\times0.187-\pi)\times\sin10.58^\circ\right\}}$$

$$=8.30\times10^3 \text{ [N]}$$

Therefore, the increase in acceleration N_{H3} due to the stiffening ring is

$$N_{H3}=\frac{F}{m}=\frac{8.30\times10^3}{950}=8.74=0.891\cdot g \text{ [m/s}^2\text{]}$$

Ⓓ Panel of the outer lid

The analytical model is shown in (Ⅱ)-Fig.A.27.

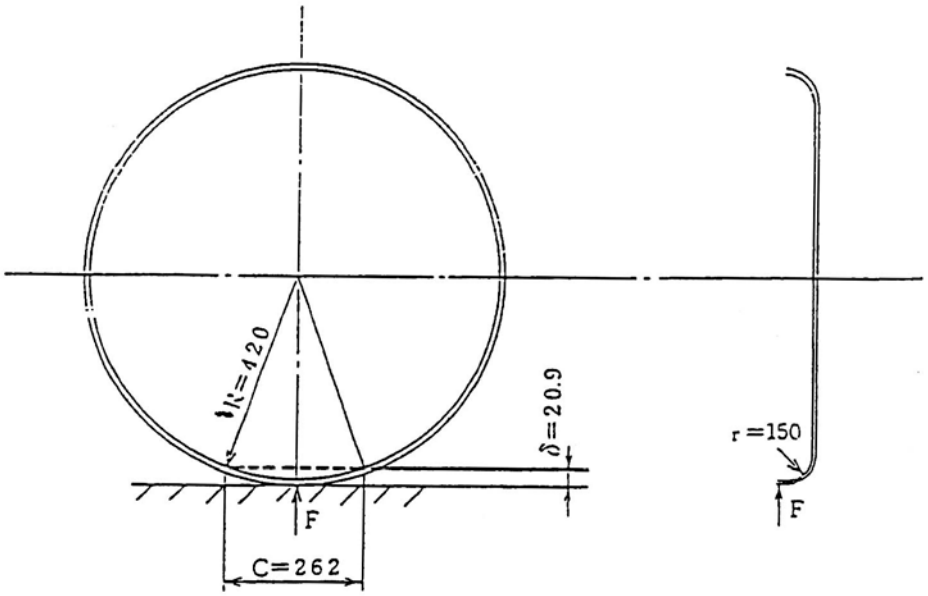

(Ⅱ)-Fig.A.27 Acceleration analysis model of outer shell head plate for horizontal drop

As indicated in (Ⅱ)-Fig.A.27, bending moment is generated by the reaction force of the drop in the outer lid panel at the curved point of the head. When the stress produced by this bending moment becomes equal to the deformation stress σs, the maximum resistance force F, assuming that it is generated, is given by the equation

$$F=\frac{\sigma s}{r}\cdot Zp=\frac{\sigma s}{r}\cdot\frac{C\cdot h^2}{4}$$

where

F: Maximum resistance force [N]

σs: Deformation stress (room temperature), σs =520 [N/mm^2]

Zp: Section modulus of plasticity,

$$Zp=\frac{C\cdot h^2}{4}\quad[mm^3]$$

C: Shock absorber deformation width, C =262 [mm]

h: Panel thickness, h=3 [mm]

r: Radius of the corner, r=150 [mm]

Therefore, the following equation is given.

$$F=\frac{520}{150}\times\frac{262\times3^2}{4}=2.04\times10^3 \quad [N]$$

Two panels are provided in the packaging, and the increase in acceleration N_{H4} caused by the outer lid panel is

$$N_{H4}=\frac{2\cdot F}{m}=\frac{2\times2.04\times10^3}{950}=4.29=0.437\cdot g \quad [m/s^2]$$

Ⓔ Partition

The analytical model is shown in (Ⅱ)-Fig.A.25, as with section A.5.3(4)(i) Ⓐ .But, since the deformation has not reached the annulus ring, α in the moment equation is given as 0.

The cross section of the partition is given in (Ⅱ)-Fig.A.28.

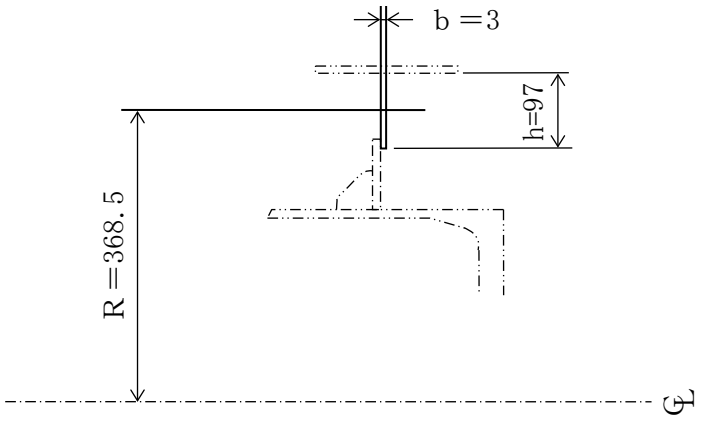

(Ⅱ)-Fig.A.28 Cross section of partition plate

The maximum resistance force is given by the following equation.

$$F=\frac{4\pi}{3R}\cdot\sigma_z\cdot Zp=\frac{4\times\pi}{3\times368.5}\times520\times7.06\times10^3$$

$$=4.17\times10^4 \quad [N]$$

where

F: Maximum resistance force [N]

R: Radius of the annulus ring, R =368.5 [mm]

σz : Deformation stress (at ordinary temperatures), σz =520 [N/mm^2]

Zp: Plasticity section modulus,

$$Zp=\frac{1}{4}b\cdot h^2=\frac{3\times97^2}{4}=7.06\times10^3 \quad [mm^3]$$

b: Annulus ring width, b=3 [mm]

h: Annulus ring thickness, h =97 [mm]

Therefore, the increase in acceleration N_{H5} caused by the partition is obtained by the following.

$$N_{H5}= \frac{F}{m}=\frac{4.17\times10^{4}}{950}=43.9=4.48\cdot g \quad [m/s^2]$$

Ⓕ Eye-plate

The analytical model is shown in (Ⅱ)-Fig.A.29.

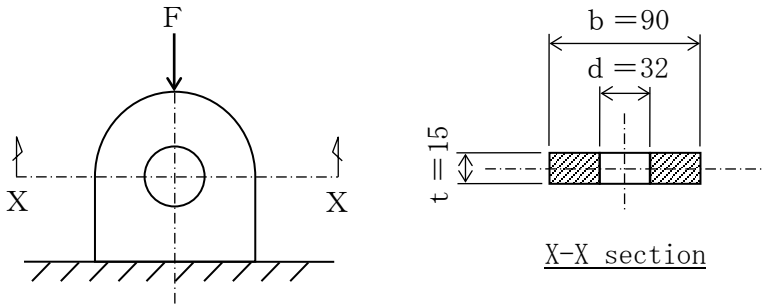

(Ⅱ)-Fig.A.29 Deformation analysis model of eye plate

As is indicated in (Ⅱ)-Fig.A.29, when the eye-plate is hit by a direct force, maximum compression stress is generated at the cross section X-X. When this stress is equal to the deformation stress σs, maximum resistance force F is generated, shown by the following equation

$$F=\sigma s \cdot A = \sigma s \cdot (b-d) \cdot t$$

where

F: Maximum resistance force [N]

σs: Deformation stress (at room temperatures), σs =520 [N/mm^2]

A: Evaluated cross sectional area [mm^2]

b: Eye-plate width, b=90 [mm]

t: Eve-plate board thickness, t=15 [mm]

d: Eye-plate hole radius, d=32 [mm]

Therefore,

$F=520\times(90-32)\times15=4.52\times10^5$ [N]

The increase in acceleration N_{H6} due to the eye-plate is obtained by the following equation.

$$N_{H6}=\frac{F}{m}=\frac{4.52\times10^5}{950}=476=48.5\cdot g \quad [m/s^2]$$

Ⓖ Eye-plate fixation plate

The analytical model is shown in (Ⅱ)-Fig.A.30.

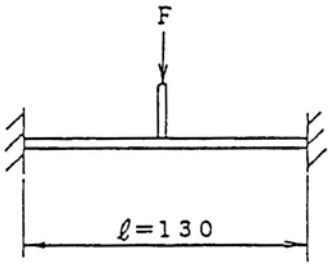

(Unit: mm)

(Ⅱ)-Fig.A.30 Analytical model of eye-plate fixing-plate

As is indicated in (Ⅱ)-Fig.A.30, the fixed bridge beams which receive the concentrated load in their center generate maximum bending moments on both extremities.

When this stress is equal to the deformation stress σs, maximum resistance force F is generated, shown by the following equation [7]

$$F = \frac{8}{1} \cdot \sigma s \cdot Zp$$

where

F: Maximum resistance force [N]

σs: Deformation stress (at ordinary temperatures), σs =520 [N/mm^2]

Zp: Plasticity section modulus,

$$Zp = \frac{1}{4} b \cdot h^2$$

b: Eye-plate width, b=110 [mm]

h: Eye-plate board thickness, h=10 [mm]

l: Distance between fixed points, l=130 [mm]

Therefore,

$$F = \frac{8}{130} \times 520 \times \frac{1}{4} \times 110 \times 10^2 = 8.80 \times 10^4 \quad [N]$$

The increase in acceleration N_{H7} due to the eye-plate fixation plate is obtained by the following equation

$$N_{H7}=\frac{F}{m}=\frac{8.80\times10^{4}}{950}=92.6\ [m/s^{2}]=9.44\cdot g$$

Ⓗ Flange of the outer shell

The analytical model is shown in (Ⅱ)-Fig.A.31.

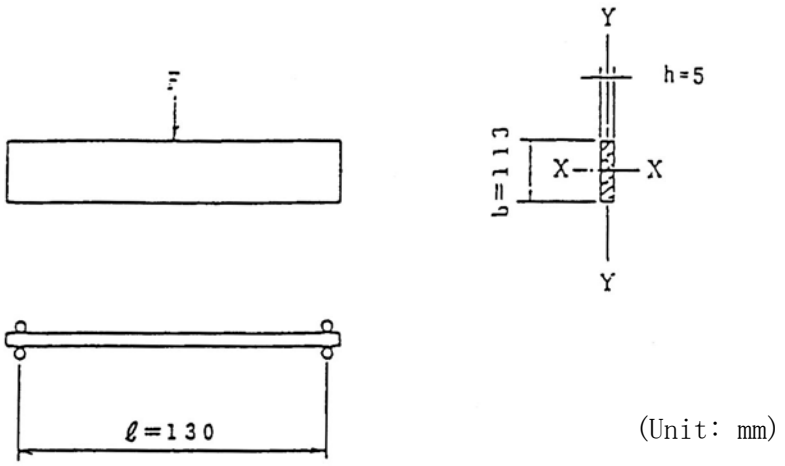

(Unit: mm)

(Ⅱ)-Fig.A.31 Analytical model of flange of outer shell

As indicated in (Ⅱ)-Fig.A.31, the fixed beam, having a long thin rectangular cross section, suffers side buckling when receiving the concentrated load on its center. If this buckling load is equal to the maximum resistance force F, it is given by the following equation[19]

$$F=\frac{16.93\sqrt{B_y C}}{\ell^2}$$

where

F: Maximum resistance force [N]

ℓ: Distance between supported points, ℓ=130 [mm]

By : Bending rigidity on Y axis,

$$B_y=\frac{1}{12}Ebh^3=\frac{1}{12}\times 1.95\times 10^5\times 113\times 5^3=2.30\times 10^8 \quad [N\cdot mm^2]$$

E: Modulus of longitudinal elasticity (at ordinary temperatures);

$E=1.95\times 10^5$ [N/mm^2]

h: Flange board thickness, h =5 [mm]

b: Flange point width, b =113 [mm]

C: Twisting rigidity,

$$C = \frac{bh^3}{3}\left(1 - 0.630\frac{h}{b}\right)G$$

$$= \frac{113 \times 5^3}{3}\left(1 - 0.630 \times \frac{5}{113}\right) \times 7.51 \times 10^4$$

$$= 3.44 \times 10^8 \quad [N/mm^2]$$

G: Modulus of transverse elasticity (at ordinary temperatures);

$$G = 7.51 \times 10^4 \quad [N/mm^2]$$

Therefore, F is

$$F = \frac{16.93\sqrt{2.30 \times 10^8 \times 3.44 \times 10^8}}{130^2} = 2.82 \times 10^5 \quad [N]$$

The increase in acceleration N_{H8} caused by the flange in the main body of the outer shell is

$$N_{H8} = \frac{F}{m} = \frac{2.82 \times 10^5}{950} = 297 \ [m/s^2] = 30.3 \cdot g \quad [m/s^2]$$

Ⅰ Eye-plate fixation lug

The analytical model is shown in (Ⅱ)-Fig.A.32.

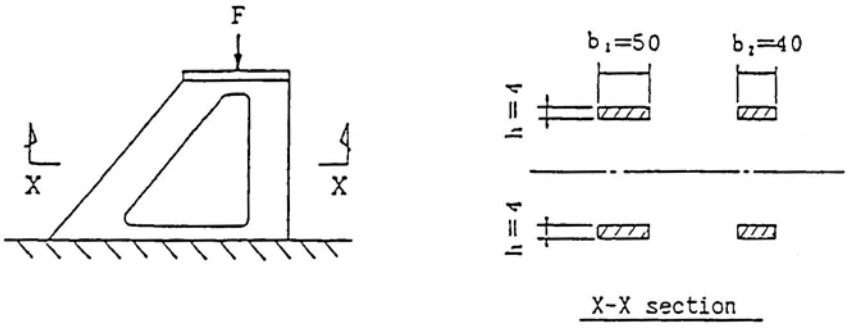

(Unit: mm)

(Ⅱ)-Fig.A.32 Analytical model of eye-plate fixing lug

As indicated in (Ⅱ)-Fig.A.32, when the compression stress at the X-X cross section is equal to the deformation stress σs, maximum resistance force F is generated and given by

$F = \sigma s \cdot A = \sigma s \cdot 2h \cdot (b_1 + b_2)$

where

F: Maximum resistance force [N]

σs: Deformation stress (at room temperatures); σs =520 [N/mm^2]

A: Evaluated cross sectional area [mm^2]

b1 : Plate width, b1 =50 [mm]

b2 : Plate width, b2 =40 [mm]

h: Plate thickness, h=4 [mm]

Therefore,

$F = 520 \times 2 \times 4 \times (50+40) = 3.74 \times 10^5$ [N]

The increase in acceleration N_{H9} due the eye-plate fixation leg is,

$$N_{H9} = \frac{F}{m} = \frac{3.74 \times 10^5}{950} = 394 = 40.2 \cdot g \quad [m/s^2]$$

Based on the results mentioned so far, the equation for the total increase in

acceleration caused by the steel plate during the horizontal drop is

$$N_H = N_{H1} + N_{H2} + N_{H3} + N_{H4} + N_{H5} + N_{H6} + N_{H7} + N_{H8} + N_{H9}$$

$$= (3.83+8.92+0.891+0.437+4.48+48.5+9.44+30.3+40.2) \times g$$

$$= 147.0 \cdot g \qquad [m/s^2]$$

(ii) Vertical drop

We shall obtain the increase in acceleration caused by the steel plate during a vertical drop. An analytical model is given in (Ⅱ)-Fig.A.33.

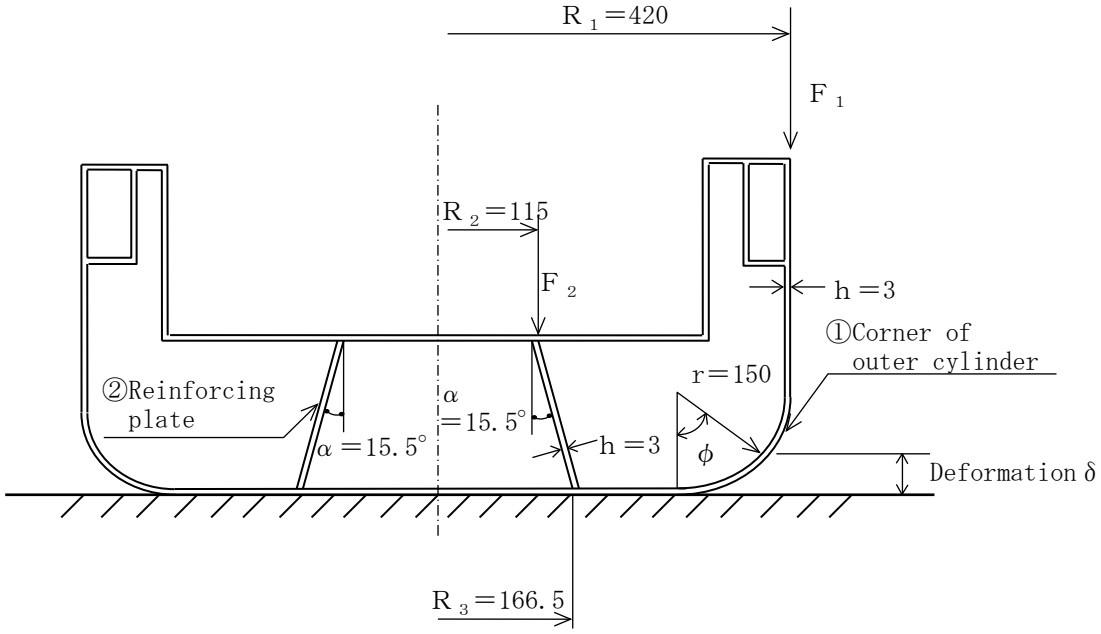

(Ⅱ)-Fig.A.33 Acceleration analysis model of steel plate for vertical drop

As indicated in (Ⅱ)-Fig.A.33, the resistance force is the addition of ① the strength F_1 which compresses the outside cylinder corner and ② the strength F_2 which compresses the conical reinforcement plate. The deformation δ of the steel plate is equal to the deformation of the shock absorber indicated in (Ⅱ)-Table A.14. The resistance forces F_1 and F_2, which arise when the stress is equal to the deformation stress, can be obtained by the following equations.[17]

$F_1=2\pi hr\sin 2\phi \cdot \sigma s$

$F2=2\pi h(R_2+\delta \tan\alpha)\cos\alpha \cdot \sigma s$

where

F_1 : Outside cylinder corner resistance force [N]

F2 : Conical reinforcement plate resistance force [N]

h : Board thickness, h =3 [mm]

r : Radius of the outside cylinder corner, r=150 [mm]

ϕ: Angle for deformation σ,

$$\phi = \cos^{-1}\left(1-\frac{\delta}{r}\right)$$

δ: deformation, Lid side vertical drop : δ_1 = 24.1 [mm]

Bottom side vertical drop : δ_2 = 18.2 [mm]

$$\phi_1 = \cos^{-1}\left(1-\frac{24.1}{150}\right)=32.9^\circ$$

$$\phi_2 = \cos^{-1}\left(1-\frac{18.2}{150}\right)=28.5^\circ$$

R_2 : Radius of the upper part of cone,

Lid side vertical drop : R2 = 115 [mm]

Bottom side vertical drop : R2 = 113 [mm]

α: Conical angle, α=15.5°

σs: Flow stress (at room temperatures), σs =Su=520 [N/mm^2]

Therefore, F_1 and F_2 in a lid side vertical drop are as follows,

$F_1 = 2\pi \times 3 \times 150 \times \sin^2 32.9^\circ \times 520 = 4.34 \times 10^5$ [N]

$F_2 = 2\pi \times 3 \times (115 + 24.1 \times \tan 15.5^\circ) \times \cos 15.5^\circ \times 520$

$= 11.49 \times 10^5$ [N]

and in a bottom side vertical drop,

$F_1 = 2\pi \times 3 \times 150 \times \sin^2 28.5^\circ \times 520 = 3.35 \times 10^5$ [N]

$F_2 = 2\pi \times 3 \times (113 + 18.2 \times \tan 15.5^\circ) \times \cos 15.5^\circ \times 520$

$= 11.15 \times 10^5$ [N]

Hence, the acceleration generated by these can be determined by the following equation,

$$N_V = \frac{F}{m} = \frac{F_1 + F_2}{m}$$

In a lid side vertical drop,

$$N_V = \frac{4.34 + 11.49}{950} \times 10^5 = 1.67 \times 10^3 \text{ [m/s}^2\text{]} = 170.2 \cdot g \text{ [m/s}^2\text{]}$$

In a bottom side vertical drop,

$$N_V = \frac{3.35 + 11.15}{950} \times 10^5 = 1.53 \times 10^3 \text{ [m/s}^2\text{]} = 156.0 \cdot g \text{ [m/s}^2\text{]}$$

where

g: Gravitational acceleration, g=9.81 [m/s^2]

(iii) Corner drop

We shall determine the increase in acceleration caused by the steel plate during a corner drop.

The analytical model is shown in (Ⅱ)-Fig.A.34.

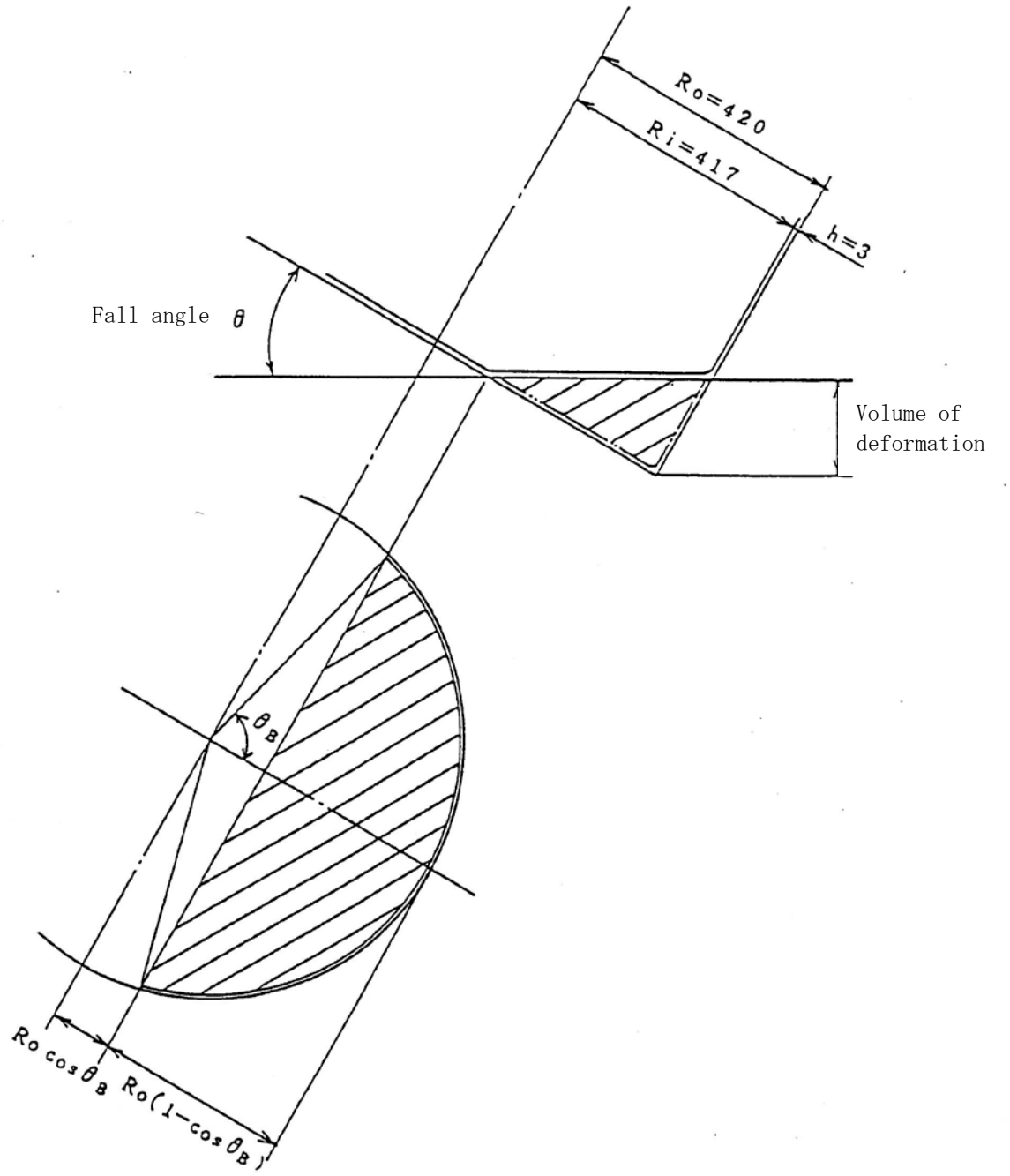

(Ⅱ)-Fig.A.34 Acceleration analysis model of steel plate for corner drop.

As indicated in (Ⅱ)-Fig.A.34, the maximum resistance force caused by the outer steel plate during a corner drop is given by the following[15]

$$F=\frac{(R_o{}^3-R_i{}^3)\times\tan\theta\times(\theta-\sin\theta_B\cdot\cos\theta_B)}{R_o\times\sin\theta}\times\sigma s$$

where

F : Maximum resistance force [N]

R_o: Cylindrical steel plate outer radius, R_o =420 [mm]

R_i: Cylindrical steel plate inner radius, R_i =417 [mm]

h : Cylindrical steel plate board thickness, h =3 [mm]

θ: Drop angle

Lid side corner drop: θ =27.6° =0.482 [rad]

Bottom side corner drop: θ =22.8° =0.398 [rad]

δ: Deformation

Lid side corner drop δ =58.6 [mm]

Bottom side corner drop δ =50.3 [mm]

θ_B : Angle

$$\theta_B=\cos^{-1}\left(1-\frac{\delta}{R_o\sin\theta}\right)$$

Lid side corner drop,

$$\theta_B=\cos^{-1}\left(1-\frac{58.6}{420\times\sin27.6°}\right)=45.7°=0.797\ [rad]$$

Bottom side corner drop,

$$\theta_B=\cos^{-1}\left(1-\frac{50.3}{420\times\sin22.8°}\right)=46.3°=0.808\ [rad]$$

σs: Deformation stress (at room temperatures), σs=520 [N/mm^2]

Therefore, F is

in the lid side corner drop,

$$F=\frac{(420^3-417^3)\times\tan27.6°\times(0.797-\sin45.7°\times\cos45.7°)}{420\times\sin27.6°}\times520$$

$$=6.55\times10^5\ [N]$$

and in the bottom side corner drop,

$$F=\frac{(420^3-417^3)\times\tan22.8°\times(0.808-\sin46.3°\times\cos46.3°)}{420\times\sin22.8°}\times520$$

$$=6.53\times10^5\ [N]$$

Therefore, the acceleration generated by these is given by the following equation.

$$N_c=\frac{F}{m}$$

In the lid side corner drop,

$$N_c=\frac{6.55\times10^5}{950}=689\ [m/s^2]=70.3\cdot g\ [m/s^2]$$

and in the bottom side corner drop,

$$N_c=\frac{6.53\times10^5}{950}=687\ [m/s^2]=70.0\cdot g\ [m/s^2]$$

(5) Design acceleration

As with the corner drop, we shall determine the acceleration during an inclined drop. This is shown in (Ⅱ)-Table A.15. In addition, we shall calculate the design acceleration utilized in the drop stress analysis which will be summarized in the same table.

Design acceleration = Calculation results of CASH-Ⅱ ×1.2＋Acceleration due to steel plate

(Ⅱ)-Table A.15 Design acceleration under normal test conditions

Drop posture			CASH-Ⅱ ×1.2	Acceleration due to steel plate (×g)	Design acceleration (×g)
Horizontal			107.1	147.0	254.1
Vertical	Lid side		70.5	170.2	240.7
	Bottom side		94.6	156.0	250.6
Corner	Lid side	27.6°	19.6	70.3	89.9
	Bottom side	22.8°	20.8	70.0	90.8
Inclined	Lid side	5°	16.9	161.7	178.6
		15°	15.6	90.7	106.3
		30°	20.5	67.9	88.4
		45°	26.0	56.3	82.3
		60°	30.8	50.7	81.5
		75°	41.4	58.9	100.3
		85°	43.8	75.6	119.4
	Bottom side	5°	7.15	169.2	176.4
		15°	20.2	86.4	106.6
		30°	23.4	60.5	83.9
		45°	27.0	49.6	76.6
		60°	29.9	53.3	83.2
		75°	34.8	54.3	89.1
		85°	36.2	65.9	101.8

where

g: Gravitational acceleration, g = 9.81 [m/s^2]

(6) Stress analysis of 1.2m horizontal drop

The stress analysis of the 1.2 m horizontal drop are conducted separately with the main body, the fuel basket and the fuel element. In addition, as for the stress analysis in each of these sections, the only principal stress will be determined, the evaluation of the stress intensity and the stress classification shall be conducted in section A.5.3(6)(d).

(a) Main body of the packaging

The stress evaluation positions of the main body of the packaging during the 1.2 m horizontal drop are determined as shown in (Ⅱ)-Fig.A.35 from a sealing performance preservation.

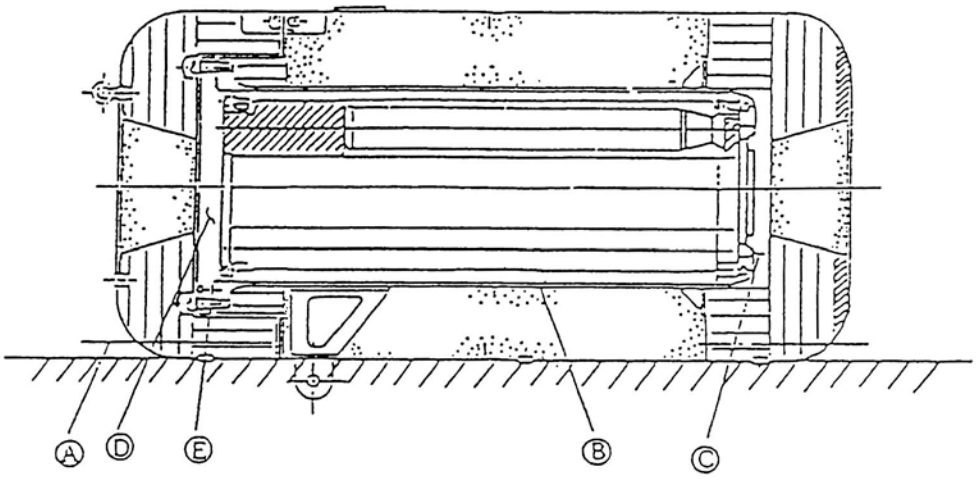

Symbol	Evaluation position
Ⓐ	Shock absorber (deformation quantity)
Ⓑ	Inner shell
Ⓒ	Bottom plate of the inner shell
Ⓓ	Top part of the inner shell (Inner lid)
Ⓔ	Inner lid clamping bolt

(Ⅱ)-Fig.A.35 Stress evaluation position for 1.2m horizontal drop (main body of inner shell)

Ⓐ Deformation of the shock absorber

We shall determine that even if the shock absorber is deformed by the 1.2 m horizontal drop, this deformation will not reach the inner shell nor to the inner lid.

The analytical model is shown in (Ⅱ)-Fig.A.36.

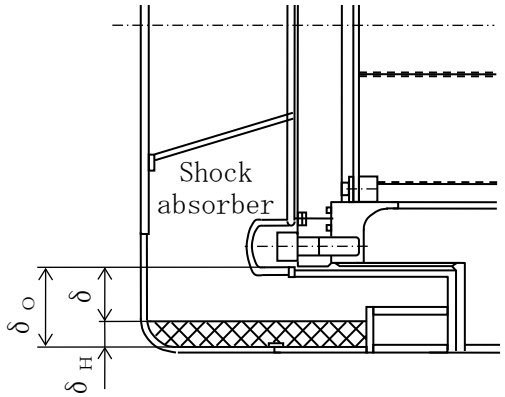

(Ⅱ)-Fig.A.36 Analytical model of interference to inner shell due to shock absorber deformation for 1.2 m horizontal drop

As is indicated in (Ⅱ)-Fig.A.36, the remaining thickness δ (mm) of the shock absorber after the 1.2 m horizontal drop can be given by the following equation

$$\delta = \delta_0 - \delta_H$$

where

δ_0 : Minimum thickness of the shock absorber before the test,

$\delta_0 = 104$ [mm]

δ_H : Deformation of the shock absorber, $\delta_H = 20.9$ [mm]

Therefore, the remaining thickness is

$$\delta = 104 - 20.9 = 83.1 \text{ [mm]}$$

This determines that the deformation caused by the 1.2 m horizontal drop will concern the shock absorber only, and will not reach the main body of the inner shell nor to the inner lid.

Ⓑ Inner shell

(Ⅱ)-Fig.A.37 shows an analytical model of the stress on the inner shell for the 1.2 horizontal drop.

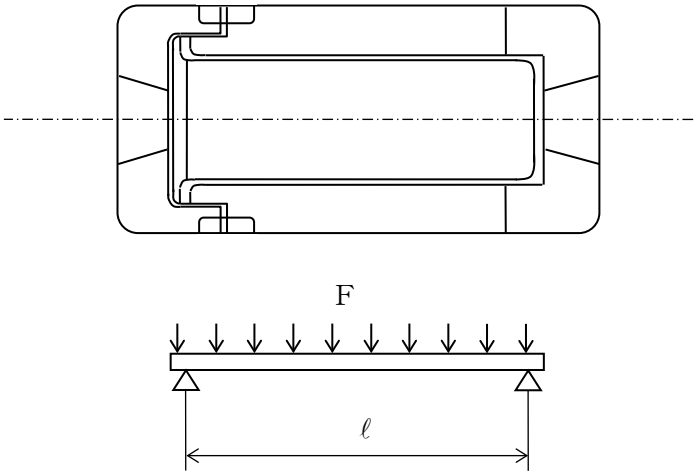

(Ⅱ)-Fig.A.37 Stress analysis model of inner shell for 1.2m horizontal drop

As is indicated in (Ⅱ)-Fig.A.37, the inner shell is supported at both ends, the beam is assumed to support the uniform load, the bending stress σ_b is at its maximum in the center of the supporting points and can be given by the following equation

$$\sigma_b = \frac{M}{Z}$$

where

M: Bending moment,

$$M = \frac{F \cdot 1}{8} = \frac{1}{8} \cdot m \cdot N \cdot l \quad [N \cdot mm]$$

F: Impact load, F= m・N [N]

m: Load between the supporting points of the package, m=700 [kg]

N: Design acceleration, N =254.1・g [m/s^2]

l: Length between the supporting points, l =1359 [mm]

$$M = \frac{1}{8} \times 700 \times 254.1 \times 9.81 \times 1359 = 2.96 \times 108 \quad [N \cdot mm]$$

Z: section modulus,

$$Z = \frac{\pi}{32} \times \frac{d_2^{\,4} \cdot d_{\cdot}^{\,4}}{d_2} \qquad [mm^3]$$

d_2: Outside diameter of the inner shell, d2 ＝480 [mm]

d1: Inside diameter of the inner shell, d_1 ＝460 [mm]

$$Z = \frac{\pi}{32} \times \frac{480^4 \square 460^4}{480} = 1.70 \times 10^6 \quad [mm^3]$$

Therefore, the bending stress is given by the following equation.

$$\sigma_b = \frac{2.96 \times 10^8}{1.70 \times 10^6} = 174 \quad [N/mm^2]$$

Ⓒ Bottom plate of the inner shell

An analytical model of the stress on the bottom plate of the inner shell for the 1.2 horizontal drop is shown in (Ⅱ)-Fig.A.38.

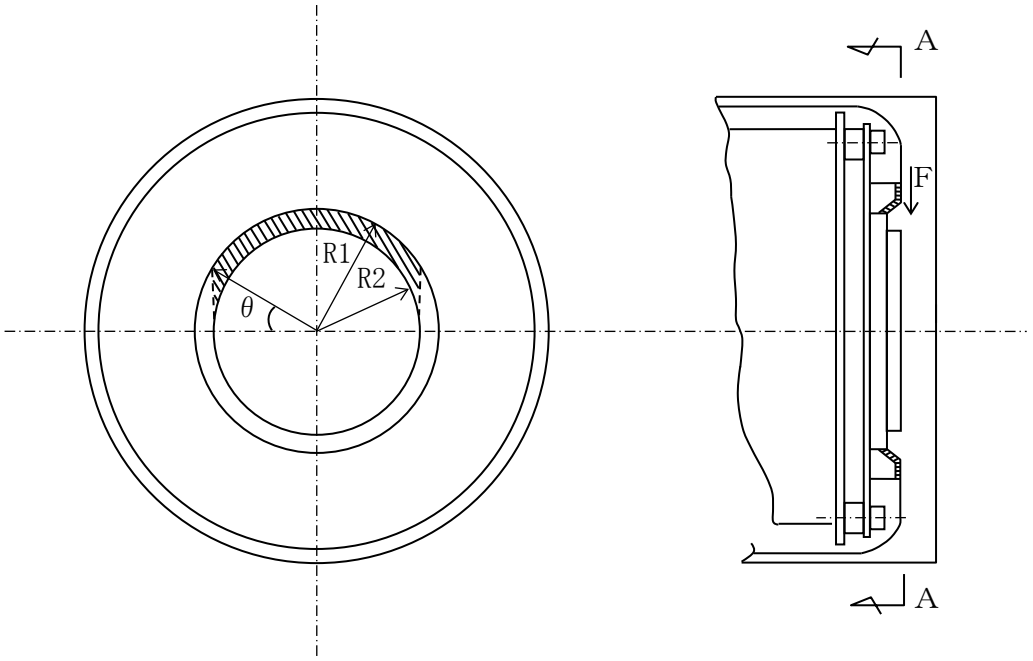

(Ⅱ)-Fig.A.38 Stress analysis model of inner shell bottom plate for 1.2m horizontal drop

As is indicated in (Ⅱ)-Fig.A.38, the A-A cross section of the inner shell's bottom plate receives the drop force of the fuel basket for horizontal drop. The stress generated at this time is,

$$\tau = \frac{F}{A}$$

where

F: Impact force,

$$F = \frac{1}{2} (m_B + m_F) \times N \quad [kg]$$

m_B : Mass of fuel basket, mB =138 [kg]

mF : Mass of contents, mF =92 [kg]

N: Design acceleration, N=254.1 ・ g [m/s^2]

$$F=\frac{1}{2}\ (138+92)\ \times 254.1\ \times 9.81=2.87\times 10^5\ \ [N]$$

A: Cross sectional area of the inner shell's bottom plate (shaded portion in (Ⅱ)-Fig.A.38)

$$A\ =\ R_1{}^2\left(\frac{\pi}{2}-\theta\right)-R_2{}^2\left(\frac{\pi}{2}-\tan\theta\right)$$

R_1: Outside radius of inner shell's bottom plate outside the protruding section, R1=130 [mm]

R_2: Inside radius of inner shell's bottom plate inside the protruding section, R2=105 [mm]

θ :Angle, $\theta=\cos^{-1}\frac{R_2}{R_1}=36.1^\circ=0.631$ [rad]

$$A\ =130^2\times\left(\frac{\pi}{2}-0.631\right)-105^2\times\left(\frac{\pi}{2}-\tan 36.1^\circ\right)$$

$$=6.60\times 10^3\ \ [mm^2]$$

Therefore, the shearing stress τ is,

$$\tau=\frac{2.87\times 10^5}{6.60\times 10^3}=43.5\ \ [N/mm^2]$$

Ⓓ Upper part of the inner shell

An analytical model of the stress on the upper part of the inner shell for the 1.2 horizontal drop is shown in (Ⅱ)-Fig.A.39.

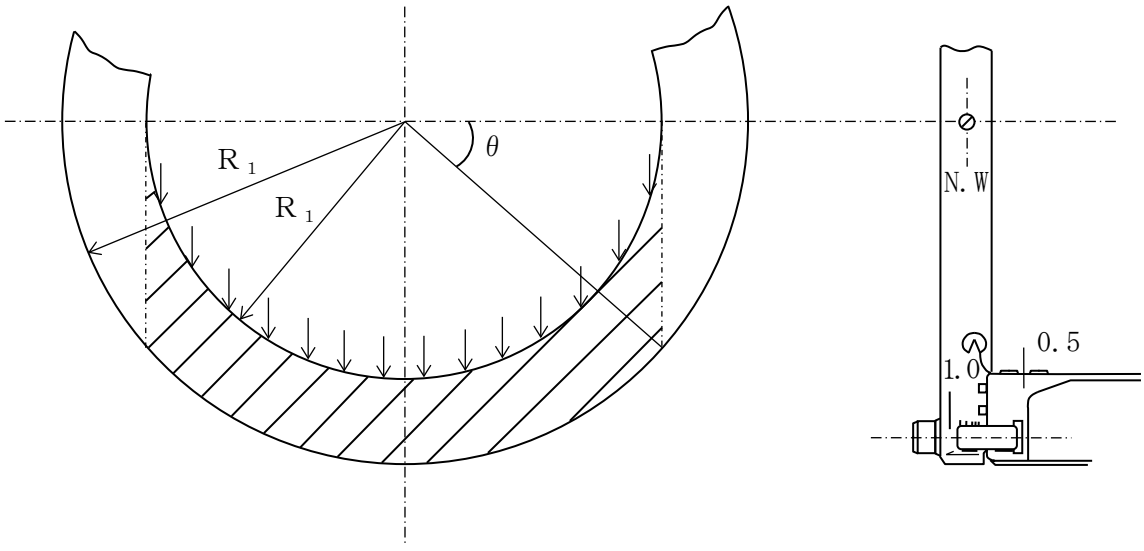

(Ⅱ)-Fig.A.39 Stress analysis model of inner shell upper part

of 1.2m horizontal drop

As indicated in (Ⅱ)-Fig.A.39, the inner lid slides to the drop direction and comes in contact with the upper part of the inner shell at point Ⓐ.

Shearing stress is generated in the inner lid,

$$\tau = \frac{F}{A}$$

where,

F: Impact strength, F=N・m [N]

m: Weight of the inner lid, m=120 [kg]

N: Design acceleration, N=254.1･g [m/s^2]

F =254.1×9.81×120 =2.99×10^5 [N]

A: Cross sectional area of the inner shell's upper part (shaded portion in (Ⅱ)-Fig.A.39),

$$A = R_1^{\,2}\left(\frac{\pi}{2} - \theta\right) - R_2^{\,2}\left(\frac{\pi}{2} - \tan\theta\right)$$

R_1: Outside radius of the inner shell flange, R1=307 [mm]

R_2: Inside radius of the inner shell, R2=230 [mm]

θ: Angle,

$$\theta = \cos^{-1}\frac{R_2}{R_1} = 41.5^\circ = 0.724 \quad [\text{rad}]$$

$$A = 307^2 \times \left(\frac{\pi}{2} - 0.724\right) - 230^2 \times \left(\frac{\pi}{2} - \tan 41.5\right)$$

$$= 4.35 \times 10^4 \quad [\text{mm}^2]$$

Therefore, the shearing stress τ is,

$$\tau = \frac{2.99 \times 10^5}{4.35 \times 10^4} = 6.87 \quad [\text{N/mm}^2]$$

Ⓔ Inner lid clamping bolt

An analytical model of the stress on the inner lid clamping bolt for the 1.2 m horizontal drop is shown in (Ⅱ)-Fig.A.40.

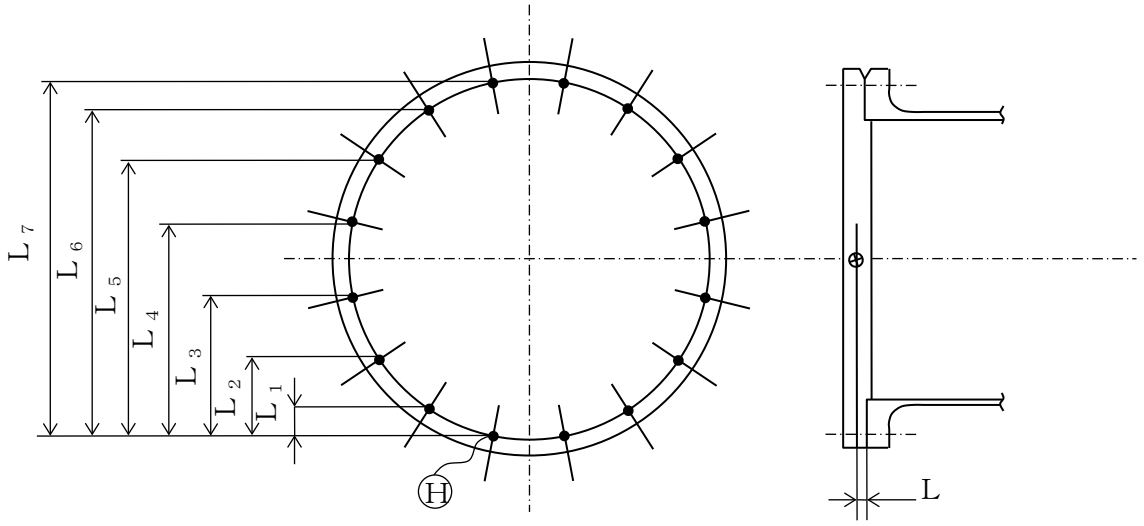

(Ⅱ)-Fig.A.40 Stress analysis model for inner lid clamping bolt for 1.2m horizontal drop

As indicated in (Ⅱ)-Fig.A.40, the momentum of the inner lid acts on the clamping bolts of the inner lid for the 1.2m horizontal drop.

Bending stress σ_b [N/mm^2] is thus generated in the clamping bolt, and this is given by the following equation

$$\sigma_b = \frac{M \cdot L_{max}}{I} = \frac{N \cdot m \cdot L \cdot L_{max}}{\sum L_i^2 \cdot Ar}$$

where

M: Angular momentum
M = N・m・L [N·mm]
N: Design acceleration, N=254.1・g [m/s^2]
m: Weight of the inner lid, m=120 [kg]
L: Moment arm, L =18.0 [mm]
L_i: Distance from each bolt to the overturning point Ⓗ [mm]

L_1 = 42.5	L_5 =437.8
L_2 =121.2	L_6 =516.5
L_3 =223.9	L_7 =559.0
L_4 =335.1	

L_{max}: Distance from the overturning point to the farthest bolt,
$L_{max} = L_7 = 559$
Ar: Cross section of the groove of the inner lid clamping bolt (M24),

$$Ar = \frac{\pi}{4} \cdot dr^2 = \frac{\pi}{4} \times 20.752^2 = 338.2 [mm^2]$$

Therefore, the stress is,

$$\sigma_b = \frac{254.1 \times 9.81 \times 120 \times 18.0 \times 559}{2 \times (42.5^2 + 121.2^2 + 223.9^2 + 335.1^2 + 437.8^2 + 516.5^2 + 559^2) \times 338.2}$$

$$= 4.68 \ [N/mm^2]$$

(b) Fuel basket

In this section, we shall analyze the stress generated in the fuel basket at the 1.2m horizontal drop. The fuel basket is the rectangular type. We shall determine the section modulus for this type.

The stress shall be evaluated according to the axial strength of the pipe.

(1) Section modulus of square fuel basket

We shall determine the section modulus of the square fuel basket.

The analytical model is shown in (Ⅱ)-Fig.A.41.

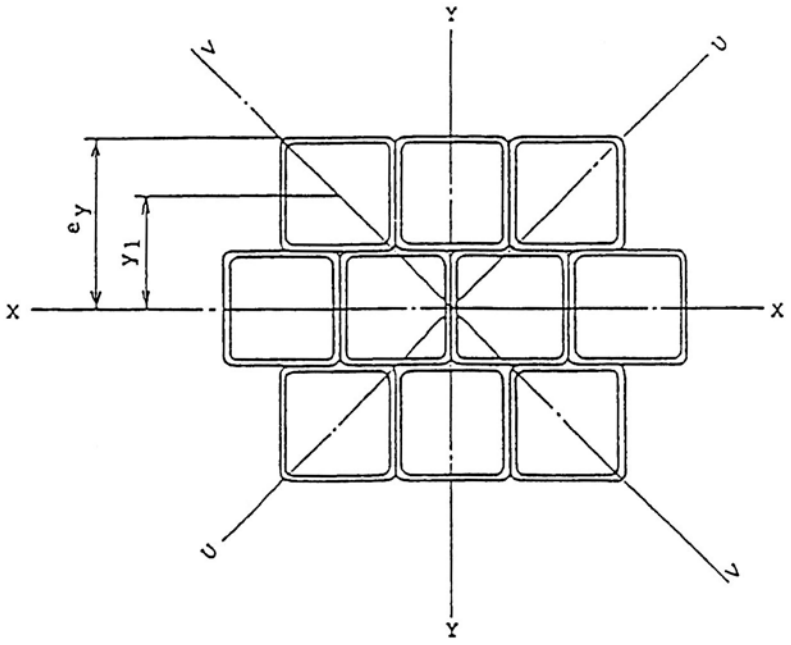

(Ⅱ)-Fig.A.41 Analytical model of section modulus of rectangular fuel basket

(i) Section modulus regarding X-X axis

As indicated in (Ⅱ)-Fig.A.41, the section modulus regarding the X-X axis is given by the following equation,

$$Z_x = \frac{10 \cdot I_o + 6A \cdot y_1^2}{e_y}$$

where

Z_x : Section modulus regarding the X-X axis [mm^3]

I_o : Second moment of area of a single square pipe,

$$I_o = \frac{1}{12}(h_2^4 - h_1^4) = \frac{1}{12}(100^4 - 94^4) = 1.83 \times 10^6 \quad [mm^4]$$

h_1 : Outside dimension of the square pipe, $h_1 = 100$ [mm]

h_2 : Inside dimension of the square pipe, $h_2 = 94$ [mm]

A : Cross sectional area of the square pipe,
$A = h_1^2 - h_2^2 = 100^2 - 94^2 = 1.16 \times 10^3$ [mm^2]

y_1 : Distance to the center of the square pipe, $y_1 = 100$ [mm]

e_y : Distance to the top surface of the fuel basket, $e_y = 150$ [mm]

Therefore, the section modulus is

$$Z_x = \frac{10 \times 1.83 \times 10^6 + 6 \times 1.16 \times 10^3 \times 100^2}{150} = 5.86 \times 10^5 \quad [mm^3]$$

(ii) Section modulus regarding Y-Y axis

As indicated in (Ⅱ)-Fig.A.41, the section modulus regarding the Y-Y axis is given by the following equation

$$Z_y = \frac{10 \cdot I_o + 2A \cdot (x_1^2 + 2x_2^2 + x_3^2)}{e_x}$$

where

Zy : Section modulus regarding the Y-Y axis [mm^3]

Io : Secondary moment of the cross section of a single square pipe,
$I_o = 1.83 \times 10^6$ [mm^4]

A: Cross sectional area of the square pipe, A=1.16×103 [mm^2]

X1 : Distance to the center of the pipe, x1 = 50 [mm]

X2 : Distance to the center of the pipe, x2 =100 [mm]

X3 : Distance to the center or the pipe, x3 ＝150 [mm]

ex : Distance to the top part of the fuel basket, e_x＝200 [mm]

Therefore, the following equation is obtained.

$$Z_y = \frac{10\times1.83\times10^6+2\times1.16\times10^3\times(50^2+2\times100^2\times150^2)}{200}$$

$$=6.14\times10^5 \quad [mm^3]$$

(iii) Section modulus regarding U-U axis

As indicated in (Ⅱ)-Fig.A.41, the section modulus regarding the U-U axis is given by the following equation.

$$Z_u = \frac{10\cdot I_o + 2A\cdot(v_1^2+v_2^2+v_3^2+v_4^2)}{e_v}$$

where

Z_u : Section modulus regarding the U-U axis [mm^3]

Io : Second moment of area for a single square pipe,
I_o ＝1.83×10^6 [mm^4]

A : Cross sectional area of the square pipe, A＝1.16×103 [mm^2]

V1 : Distance to the center of the pipe, v1 ＝$25\sqrt{2}$ ＝35.4 [mm]

V2 : Distance to the center of the pipe, v2 ＝$50\sqrt{2}$ ＝70.7 [mm]

V3 : Distance to the center of the pipe, v3 ＝$75\sqrt{2}$ ＝106 [mm]

V4 : Distance to the center of the pipe, v4 ＝$100\sqrt{2}$ ＝141 [mm]

ev : Distance to the top of the fuel basket, e_v＝$150\sqrt{2}$ ＝212 [mm]

Therefore, the sectional modulus is

$$Z_u = \frac{10\times1.83\times10^6+2\times1.16\times10^3\times(35.4^2+70.7^2+106^2+141^2)}{212}$$

$$=4.95\times10^5 \quad [mm^3]$$

Of the values mentioned above, the smallest shall be adopted

$Z=_{min}\{Z_x, Z_y, Z_u\}$ ＝4.95×10^5 [mm^3]

(2) Axial strength of square fuel basket

The analytical model is the same as in (Ⅱ)-Fig.A.41.

The bending stress generated in the fuel basket reaches its maximum in the center and is given by the following equation.

$$\sigma_b = \frac{M}{Z} = \frac{(W_f + W_p) \cdot N \cdot L^2}{8Z}$$

where

σ_b : Bending stress [N/mm^2]

M: Maximum bending moment [N·mm]

$$M = \frac{(W_f + W_p) \cdot N \cdot L^2}{8}$$

W_f : Uniform weight due to the fuel element
(This uniform load should be of the maximum weight per unit length among all square fuel elements (JRR-3 Standard type))

$$W_f = \frac{m_f}{l} = \frac{92}{1150} = 0.08 \quad [kg/mm]$$

mf : Weight of the fuel element, mf＝92 [kg]

l: Length of the fuel element, l＝1150 [mm]

Wp : Uniform weight due to the individual weight of the fuel basket,

$$W_p = \frac{m_p}{L} = \frac{138}{1200} = 0.115 \quad [kg/mm]$$

m_p : Weight of the fuel basket, mp＝138 [kg]

L: Length of the supporting point, L＝1200 [mm]

N: Acceleration, N＝254.1· g [m/s^2]

Z: Section modulus of the fuel basket, Z＝4.95×10^5 [mm^3]

Therefore, the bending stress is,

$$\sigma_b = \frac{(0.08+0.115) \times 254.1 \times 9.81 \times 1200^2}{8 \times 4.95 \times 10^5} = 177 \quad [N/mm^2]$$

(c) Fuel elements and fuel plate (Non-irradiated fresh fuels for research reactor)

(c)-1. Fuel elements

In this paragraph, an analysis of stress is performed on fuel elements for the 1.2 m horizontal drop. As indicated in (I)-D, specifications of the rectangular fuel elements.

(1) Evaluation of the fuel elements for a drop case

Fuel elements are evaluated for two cases of horizontal drop as shown in (Ⅱ)-Fig.A.42.

① Horizontal drop to the direction perpendicular to the fuel plate

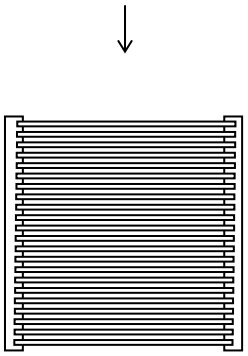

Rectangular fuel elements

② Horizontal drop to the direction parallel to the fuel plate

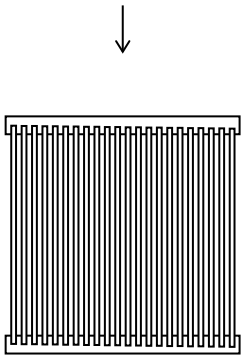

Rectangular fuel elements

(Ⅱ)-Fig.A.42 Evaluation of fuel elements for 1.2 m horizontal drop

(2) Fuel elements

(i) Fuel plate

As shown in (Ⅰ)-D with regard to the rectangular fuel element, there are 11 types of fresh fuel elements including 3 KUR fuel elements, and there are 9 types of lowly irradiated fuel elements. In this section, horizontal drop to the direction perpendicular to fuel plate and to the direction parallel to the fuel plate are treated separately. Furthermore, it is assumed that uranium aluminum alloy has the same strength as the covering material.

① Horizontal drop to the direction perpendicular to fuel plate

In this section, the analysis method for JRR-3 standard type is shown and the analysis result for the other 19 types, using the same analysis method, is shown in (Ⅱ)-Table A.16.

The analytical model is shown in (Ⅱ)-Fig.A.43.

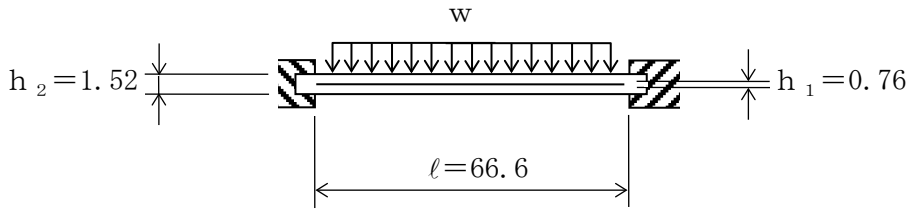

(Ⅱ)-Fig.A.43 Analytical model of rectangular fuel elements for 1.2 m horizontal drop perpendicular to fuel plate.

As indicated in (Ⅱ)-Fig.A.43, a beam with both ends fixed and receiving uniform load due to dead load will receive maximum bending moment at its fixed end. The bending stress σ_b is,

$$\sigma_b = \frac{M}{Z}$$

where M: Bending moment per unit [N·mm/mm]

$$M = \frac{w \cdot l^2}{12}$$

w: Uniform load [N/mm^2]

$$w = \frac{m}{b \cdot a} \cdot N = \frac{0.279}{66.6 \times 770} \times 254.1 \times 9.81 = 1.36 \times 10^{-2}$$

m: Weight of the fuel plate, m＝0.279 [kg]

N: Design acceleration, N＝254.1 ・ g [m/s^2]
a: Length of the fuel plate, a＝770 [mm]
l: Distance between fixed points, l＝66.6 [mm]
Z: Cross sectional area per unit width,

$$Z=\frac{1}{6}\cdot\frac{h_2{}^3-h_1{}^3}{h_2}=\frac{1}{6}\times\frac{1.27^3-0.51^3}{1.27}=0.251 \quad [mm^3/mm]$$

h_2 : Fuel plate thickness, h2 ＝1.27 [mm]
h1 . Fuel plate core thickness, h1 ＝0.51 [mm]

Therefore, the bending stress is,

$$\sigma_b=\frac{1.36\times10^{-2}\times66.6^2}{12\times0.251}=20.0 \quad [N/mm^2]$$

② Horizontal drop to the direction parallel to the fuel plate

As shown in (Ⅰ)-D with regard to the fuel elements, the KUR fuel elements consists of curved fuel plates, so the inertial force of the fuel plates and side plates may cause both compressive and buckling stress. Therefore, buckling stress analysis is performed for KUR fuel elements.

For the KUR special fuel element, the two middle plates of 3.1mm thickness placed in parallel to the fuel plates receive the inertial force of the side plates. Therefore, for the fuel plates of the KUR special element, stress analysis of the middle plates will be perfomed, followed by stress analysis of the fuel plates.

For the fuel elements of other reactor types, the analysis method for JRR-3 standard type is shown in the following and the analysis result for the other 16 types, using the same analysis method, is shown in (Ⅱ)-Table A.16.

The analytical model is shown in (Ⅱ)-Fig.A.44.

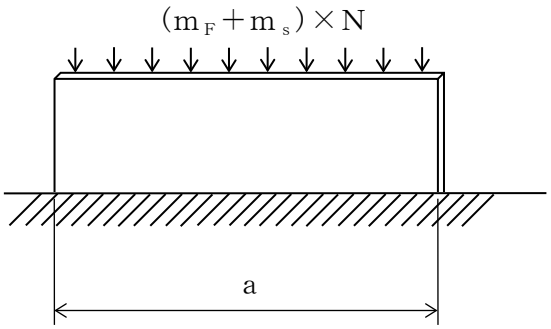

(Ⅱ)-Fig.A.44 Analytical model of rectangular fuel element for 1.2m horizontal drop parallel to fuel plate

As indicated in (Ⅱ)-Fig.A.44, the rectangular plate which receives its dead load and the partial weight of the side plate generates compressive stress σ_c.

$$\sigma_c = \frac{W}{A} = \frac{(m_F + m_S) \times N}{a\ (h_2 - h_1)} \quad [N/mm^2]$$

where

N: Design acceleration, N=254.1·g [m/s^2]
mF: Weight of the fuel plate, mF =0.279 [kg]
ms: Partial weight of the side plate, ms =0.038 [kg]
a: Length of the fuel plate, a=770 [mm]
h2: Fuel plate thickness, h2= 1.27 [mm]
h1: Fuel plate core thickness, h_1=0.51 [mm]

Therefore, the compressive stress is,

$$\sigma_c = \frac{(0.279+0.038) \times 254.1 \times 9.81}{770 \times (1.27-0.51)} = 1.35 \quad [N/mm^2]$$

Next, the analysis for the KUR fuel elements are summarized as following.

Firstly, KUR standard and half-loaded fuel elements are analyzed. Here, the analysis method for KUR standard type is shown, and the half-loaded fuel elements are analyzed using the same method.

For a curved beam subject to compressive axial load, the maximum bending moment occurs at the concave surface of the beam. Here, the buckling stress is analyzed based on the following formula by Southwell [23], where the combined compressive stress and yield stress are correlated;

$$\sigma_y = \sigma_{cr} \left(1 + \frac{e}{r} \sec \frac{L}{2k} \sqrt{\frac{\sigma_{cr}}{E}} \right) \text{---------- ①}$$

where

σ_{cr}:bucking stress of the beam (averaged axial compressive stress), $\frac{P}{A}$ [N/mm^2]

P : compressive load of the beam [N]
A : cross section of the beam [mm^2]
σ_y : yield stress [N/mm^2]
E : modulus of direct elasticity [N/mm^2]
L : beam length [mm]
e : eccentricity of the beam [mm]
k : radius-of-gyration of area $\sqrt{\frac{I}{A}}$ [mm]
I : geometrical moment of inertia [mm^4]
Z : modulus of section [mm^3]

$$r : \frac{Z}{A} \quad [mm]$$

The corresponding values for KUR standard elements are as follows;

modulus of direct elasticity at 75℃ : $E = 6.97 \times 10^4$ $[N/mm^2]$

yield stress at 75℃ : $\sigma_y = 63.7$ $[N/mm^2]$

cross section per fuel plate unit width :

$A = (1.52 - 0.5) \times 1 = 1.02$ $[mm^2 / mm]$

geometrical moment of inertia per fuel plate unit width :

$I = 0.282$ $[mm^4 / mm]$

modulus of section per fuel plate unit width :

$Z = 0.371$ $[mm^3 / mm]$

eccentricity : $e = 4$ [mm]

width : $L = 66$ [mm]

Then we obtain;

$$k = \sqrt{\frac{I}{A}}$$

$$= \sqrt{\frac{0.282}{1.02}}$$

$$= 0.526 \quad [mm]$$

$$r = \frac{Z}{A}$$

$$= \frac{0.371}{1.02}$$

$$= 0.364 \quad [mm].$$

By substituting the above values to RHS of Eq.①, σ_{cr} could be obtained as

$$\sigma_{cr} = 4.67 \quad [N/mm^2].$$

The compressive stress σ_c is obtained using the following formula as in the case of JRR-3 standard fuel element;

$$\sigma_c = \frac{W}{A} = \frac{(m_f + m_s) \cdot N}{a \cdot (h_2 - h_1)} \quad [N/mm^2]$$

where

N : Design acceleration, $N = 254.1 \cdot g$ $[m/s^2]$

m_f : Weight of the fuel plate, $m_f = 0.235$ [kg]

m_s : Partial weight of the side plate, $m_s = \frac{M_s}{n}$

M_s : weight of side plate 0.650 [kg]

n : number of fuel plates 18 [plates]

$$m_s = \frac{0.650}{18} = 0.036 \quad [kg]$$

a : Length of the fuel plate a = 625 [mm]
h_2 : Fuel plate thickness h_2 = 1.52 [mm]
h_1 : Fuel plate core thickness h_1 = 0.50 [mm]

Therefore, compressive stress is

$$\sigma_c = \frac{(0.235+0.036)\times 254.1\times 9.81}{625\times(1.52 - 0.50)}$$
$$= 1.07 \quad [N/mm^2].$$

This gives

$$\sigma_c = 1.07\ [N/mm^2] < \sigma_{cr} = 4.67\ [N/mm^2],$$

which shows that the integrity of fuel plates of KUR standard fuel elements are maintained under the horizontal drop condition to the direction perpendicular to the fuel plate.

Next, the KUR special elements will be analyzed as follows.

The KUR special fuel elements have two middle plates (thickness 3.18mm) placed in parallel to the fuel plates. In the analysis, we first assume that the inertial force of the side plates are totally received by these two middle plates and verify the integrity of the middle plates. Then, the integrity of the fuel plates will be analyzed.

The compressive stress of the middle plates σ_c are given as follows;

$$\sigma_c = \frac{W}{A} = \frac{(m_m+m_s)\cdot N}{a\cdot t} \quad [N/mm^2]$$

where

N : Design acceleration, N = 254.1・g [m/s^2]
m_m : weight of middle plate, m_m= a・t・ℓ・ρ [kg]
a : length of middle plate, a = 721 [mm]
t : thickness of middle plate, t= 3.18 [mm]
ℓ : distance between fixed edge, ℓ = 66 [mm]
ρ : density, $\rho = 2.7\times10^{-6}$ [kg/mm^3]
$m_m = 721\times3.18\times66\times2.7\times10^{-6}$
$= 0.409$ [kg]

m_s : weight of side plate section, $m_s = \frac{Ms}{n}$
M_s : weight of side plate, 0.650 [kg]
n : number of middle plates, 2 [plates]

$$m_s = \frac{0.650}{2} = 0.325 \quad [kg]$$

Therefore, the compressive stress is

$$\sigma_c = \frac{(0.409+0.325)\times 254.1\times 9.81}{721\times 3.18}$$

$$= 0.80 \quad [N/mm^2],$$

which is less than the design yield strength of the material at 75℃ (63.7 (N/mm^2)). Thus the integrity of the middle plates are maintained.

The integrity of the fuel plates are analyzed as follows. As the fuel plates of the KUR special type elements are identical to those of the KUR standard fuel elements, the buckling stress σ_{cr} is identical to that of KUR standard fuel element, i.e.

$$\sigma_{cr} = 4.67 \quad [N/mm^2].$$

The compressive stress σ_c is given as follows;

$$\sigma_c = \frac{W}{A} = \frac{m_f \cdot N}{a \cdot (h_2 - h_1)} \quad [N/mm^2]$$

where,

N : Design acceleration, $N = 254.1 \cdot g$ $[m/s^2]$
m_f : Weight of the fuel plate, $m_f = 0.235$ [kg]
a : Length of the fuel plate $a = 625$ [mm]
h_2 : Fuel plate thickness $h_2 = 1.52$ [mm]
h_1 : Fuel plate core thickness $h_1 = 0.50$ [mm].

Therefore,

$$\sigma_c = \frac{0.235\times 254.1\times 9.81}{625\times (1.52 - 0.5)}$$

$$= 0.92 \quad [N/mm^2],$$

This gives

$$\sigma_c = 0.92 \ [N/mm^2] < \sigma_{cr} = 4.67 \ [N/mm^2],$$

which shows that the integrity of fuel plates of KUR special fuel elements are maintained under the horizontal drop condition to the direction perpendicular to the fuel plate.

(ii) Fuel element hold down part

The lowly irradiated fuel element, as shown in section I-D, is cut at the portion of the lower adapter and the upper holder in order to reduce the weight. Therefore, since the total length becomes short, a hold-down part is provided to adjust the length. In this section, the stress analysis method and the stress generated at the hold-down. part are shown, the result is described in (Ⅱ)-Table A.16, and the stress analysis model is described in (Ⅱ)-Fig.A.45.

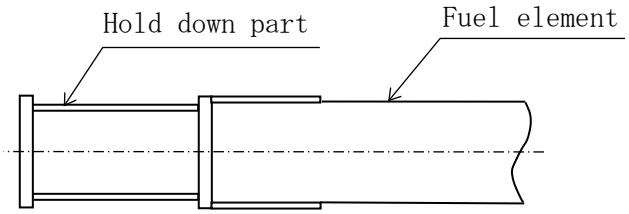

(Ⅱ)-Fig.A.45 Analytical model of holder

As shown (Ⅱ)-Fig.A.45, the hold-down part is considered to be a beam supported at the both end, subjected to the uniform load of its own weight, the maximum bending moment occurs at the center of the beam, and the stress is given as follows.

$$\sigma_b = \frac{M}{Z}$$

where M: Bending moment per unit length [N·mm]

$$M = \frac{w \cdot l^2}{8}$$

w: Uniform load [N/mm^2]

$$w = \frac{m_z}{l} \times N$$

$$= \frac{1.4}{204} \times 254.1 \times 9.81 = 17.1$$

$$M = \frac{1}{8} \times 17.1 \times 204^2 = 8.90 \times 10^4 \ [N \cdot mm]$$

m_z: Mass of the hold down part, mz＝1.4 [kg]

N : Design acceleration, N=254.1·g [m/s^2]

l : Length of hold down part, l=204 [mm]

z : Modulus of elasticity

$$Z = \frac{\pi}{32} \cdot \frac{h_o^4 h_i^4}{h_o}$$

$$= 9.242 \times 10^3 \ [mm^3]$$

ho: Outside diameter of hold down part; ho＝60 [mm]

hi: Inside diameter of hold down part; h_i＝52 [mm]

Therefore,

$$\sigma_b = \frac{8.90 \times 10^4}{9.242 \times 10^3} = 9.63 \ [N/mm^2]$$

(c)-2. Fuel plate (for Critical Assembly fuel (KUCA fuel))

In this paragraph, an analysis of stress is performed on KUCA fuel for the 1.2 m horizontal drop. As indicated in (I)-D, specifications of the rectangular fuel plate.

The analytical model is shown in (Ⅱ)-Fig.A.46.

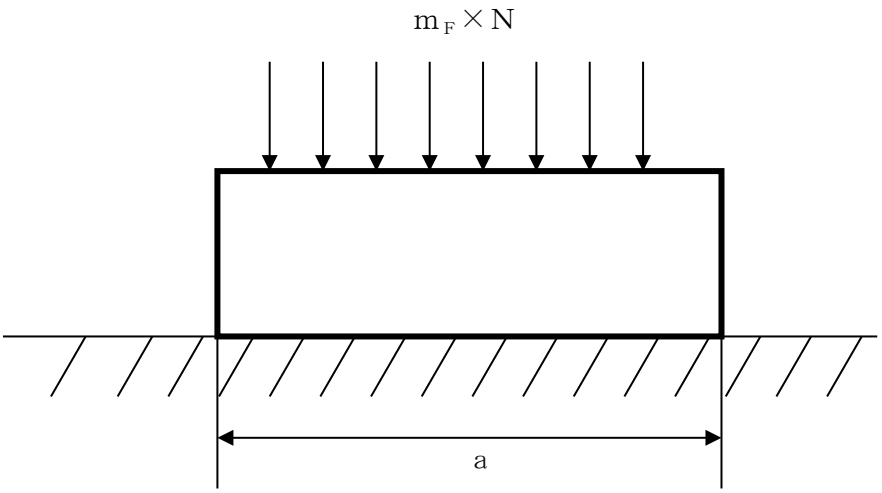

(Ⅱ)-Fig.A.46 Analytical model of the fuel plate for 1.2m horizontal drop parallel to fuel plate

As indicated in (Ⅱ)-Fig.A.46, the fuel plate which receives its dead load generates compressive stress σ_c.

$$\sigma_c = \frac{W}{A} = \frac{(m_F + m_S) \times N}{a\ (h_2 - h_1)} \quad [N/mm^2]$$

where

m_F: Weight of the fuel plate [kg]

a: Length of the fuel plate [mm]

h_2: Fuel plate thickness [mm]

h_1: Fuel plate core thickness [mm]

h_2-h_1:Cladding thickness [mm]

N: Design acceleration [m/s^2]

In the case of horizontal drop, the design acceleration is applied to coupon fuel in the direction shown in (Ⅱ)-Fig.A.47

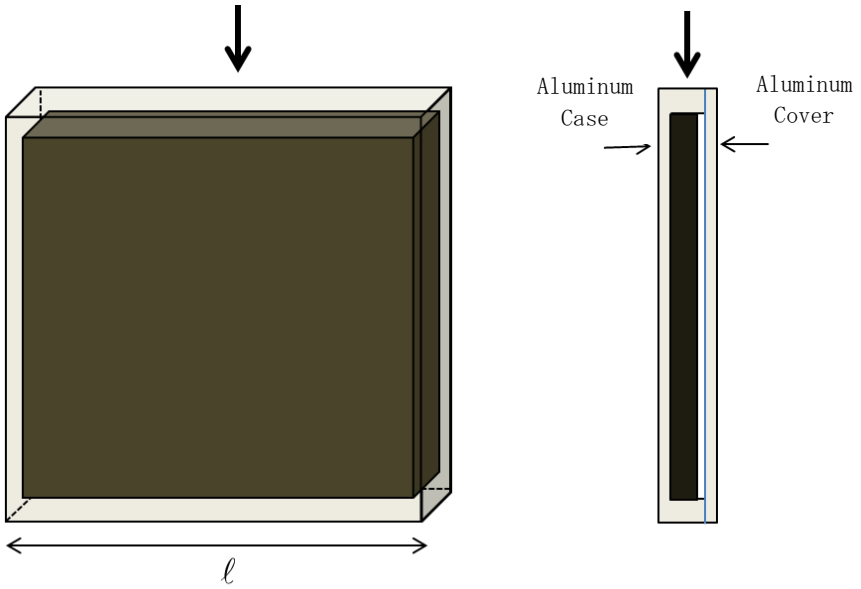

(Ⅱ)-Fig.A.47 Analytical model of the coupon fuel for 1.2m horizontal drop

In this case, the total thickness of cladding is 0.8 mm, which is the total of the bottom plate of aluminum case (thickness 0.4 mm) and the aluminum cover (thickness 0.4mm).

m_F: Weight of the fuel plate	m_f=0.036 [kg]
l: Length of the fuel plate	l=50.8 [mm]
h_2-h_1:Cladding thickness	h_2-h_1= 0.8 [mm]
N: Design acceleration	N=254.1・g [m/s^2]

Therefore, the compressive stress σ_c are given as follows.

$$\sigma_c = (0.036\times254.1\times g)/(50.8\times0.8)$$
$$= 2.21 \quad [N/mm^2]$$

Regarding flat fuel plate, two cases are conceivable: one is horizontal drop in the plane direction of the fuel plate and the other horizontal drop in the

direction parallel to the fuel plate.

In the case of horizontal drop in the plane direction of the fuel plate ((Ⅱ)-Fig.A.48), the compressive stress σ_c is obtained by the fuel plate width (62 mm), fuel core width (56 mm) and as follows.

m_F: Weight of the fuel plate m_f=0.23 [kg]

l: Length of the fuel plate l=600 [mm]

h_2: Fuel plate thickness h_2 =62 [mm]

h_1: Fuel plate core thickness h_1= 56 [mm]

N: Design acceleration N=254.1・g [m/s^2]

Therefore, the compressive stress σ_c are given as follows.

$$\sigma_c = (0.23 \times 254.1 \times g)/(600 \times (62-56))$$
$$= 0.16 \quad [N/mm^2]$$

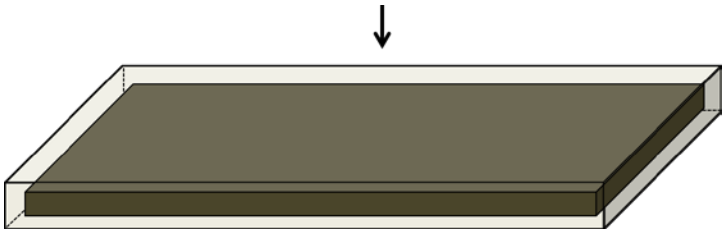

(Ⅱ)-Fig.A.48 Analytical model of the flat fuel plate for 1.2m horizontal drop in the plane direction of the fuel plate

In the case of horizontal drop in the direction parallel to the fuel plate ((Ⅱ)-Fig.A.49),

m_F: Weight of the fuel plate m_f=0.23 [kg]

l: Length of the fuel plate l=600 [mm]

h_2: Fuel plate thickness h_2 =1.5 [mm]

h_1: Fuel plate core thickness h_1= 0.5 [mm]

N: Design acceleration N=254.1・g [m/s^2]

Therefore, the compressive stress σ_c are given as follows.

$$\sigma_c = (0.23 \times 254.1 \times g)/(600 \times (1.5-0.5))$$

$$= 0.96 \quad [N/mm^2]$$

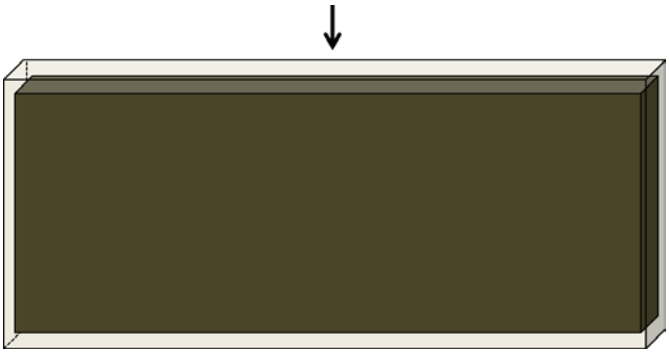

(Ⅱ)-Fig.A.49 Analytical model of the flat fuel plate for 1.2m horizontal drop in the direction parallel to the fuel plate

(c)-3. Fuel plate (for Spectrum Converter)

In this paragraph, an analysis of stress is performed on Spectrum converter for the 1.2 m horizontal drop. As indicated in (I)-D, the specifications of it is the disk-shaped fuel plate.

The analytical model is shown in (Ⅱ)-Fig.A.50.

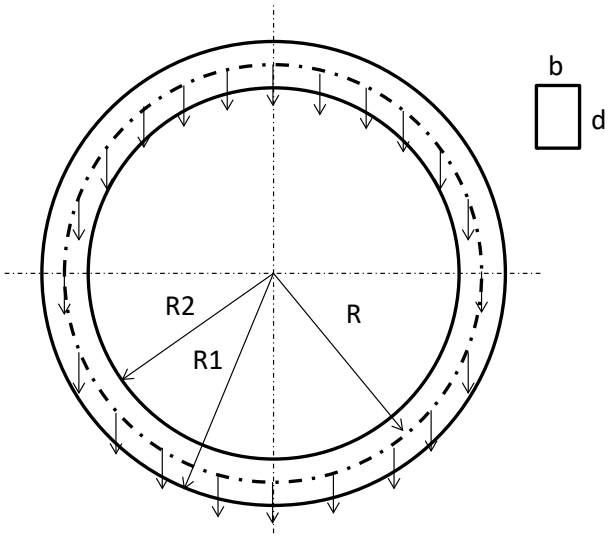

(Ⅱ)-Fig.A.50 Analytical model of the spectrum converter for 1.2m horizontal drop parallel to disk face

As indicated in (Ⅱ)-Fig.A.46, the torus which receives its dead load receives the maximum bending moment at the bottom surface, and the bending stress σ_b generated is given by the following equation.

$$\sigma_b = \frac{M}{Z} = \frac{6M}{bd^2}$$

where

M: Bending moment

$M = 1.5 \cdot w \cdot R^2$ 〔N・mm〕

w : Equally distributed load

$w = m_F \times N \times g / 2\pi R$

m_F : mass of spectrum converter (excluding top and bottom aluminum plate

m_F＝2.293 〔kg〕

R ：Average radius of the inner and outer diameters of the spectrum converter case 〔mm〕

R_1：Spectrum converter outer diameter 〔mm〕

R_2：Spectrum converter inner diameter 〔mm〕

R＝ $((R_1-R_2)/2+R_2)/2=((310-254)/2+254)/2$

＝ 141 〔mm〕

N ：Design acceleration N＝254.1・g 〔m／s^2〕

$M = 1.5 \times 2.293 \times 254.1 \times 9.81 \times 141/2\pi$

＝192.4 kNmm

b ：thickness of the spectrum converter 10.62 〔mm〕

d ：Width of the outer ring aluminum part of the spectrum converter

d＝ $(R_1 - R_2)/2$＝ $(310-254)/2$＝28 〔mm〕

Therefore,

σ_b ＝ $(6\times192.4\times10^3) / (10.62\times28^2)$

＝138.6 〔N／mm^2〕

(d) Comparison of the allowable stress

A summary of the stress evaluation results obtained for each analysis in section (Ⅱ)-A.5.3(6) is given in (Ⅱ)-Table A.16.

As demonstrated in this table, the margin of safety in regard to the design standard value is positive for individual or multiple loads.

Therefore, the soundness of this package is maintained under test conditions of the 1.2m horizontal drop.

Stress units ;N/mm²

(Ⅱ) -Table A.16 Stress evaluation for 1.2 m horizontal drop (1/6)

No.	Position to be evaluated \ Stress		Stress at initial clamping	Stress due to internal pressure	Stress due to thermal expansion	Impact stress	Primary stress						Primary+secondary stress			Fatigue					
							Pm(PL)	Sm	MS	PL+Pb	1.5Sm	MS	PL+Pb +Q	3Sm	MS	PL+Pb +Q+F	Sa	N	Na	DF	MS
1	Frame of Inner shell	σ_r	—	-0.0491	—	—	2.36	137	57.0	175	205	0.171	—	—	—	—	—	—	—	—	—
		σ_θ		2.31		—															
		σ_z		1.15		174															
2	Bottom plate of the inner shell	σ_r	—	3.18	—	—	0.098	137	1396	87.1	205	1.35	—	—	—	—	—	—	—	—	—
		σ_θ		0.953		—															
		σ_z		-0.098		—															
		τ		—		43.5															
3	Upper part of the inner shell (Inner lid)	σ_r	—	-0.0491	—	—	2.36	137	57.0	13.9	205	13.7	—	—	—	—	—	—	—	—	—
		σ_θ		2.31		—															
		σ_z		1.15		—															
		τ		—		6.87															
4	Inner shell lid clamping bolt	σ_t	174	3.20	—	—	177	2/3Sy 458	1.58	182	Sy 687	2.77	182	Sy 687	2.77	—	—	—	—	—	—
		σ_b	—	—	—	4.68															
		τ	—	—	—	—															
5	Square fuel basket	σ_b	—	—	—	177	—	—	—	177	205	0.158	—	—	—	—	—	—	—	—	—

Pm ; General primary membrane stress; PL ; Local primary membrane stress; Pb ; Primary bending stress; Q ; Secondary stress; F ; Peak stress;
Sa ; Repeated peak stress; N ; Number of uses; Na ; Permissible number of repetition; DF ; Cumulative fatigue coefficient;
Sm ; Design stress intensity value; Sy ; Yield point of the design; MS; Margin of safety σ_r; Diameter direction stress σ_o; Periphery direction stress σ_2; Axial stress σ_b; Bending stress τ ; Shear stress σ_t ; Ability of bolt stress

Stress units ;N/mm²

(Ⅱ) -Table A.16 Stress evaluation for 1.2 m horizontal drop (2/6)

No.	Position to be evaluated \ Stress			Stress at initial clamping	Stress due to internal pressure	Stress due to thermal expansion	Impact stress	Primary stress						Primary+secondary stress			Fatigue					
								Pm(PL)	2/3Sy	MS	PL+Pb	Sy	MS	PL+Pb +Q	Sy	MS	PL+Pb +Q+F	Sa	N	Na	DF	MS
1	JRR-3 standard element (Uranium silicon aluminum dispersion alloy)	Surface direction	σ	—	—	—	20.0	—	—	—	20.0	63.8	2.19	—	—	—	—	—	—	—	—	—
		Axial direction	σ	—	—	—	1.35	—	—	—	1.35	63.8	46.2	—	—	—	—	—	—	—	—	—
2	JRR-3 follower element (Uranium silicon aluminum dispersion alloy)	Surface direction	σ	—	—	—	13.2	—	—	—	13.2	63.8	3.83	—	—	—	—	—	—	—	—	—
		Axial direction	σ	—	—	—	1.13	—	—	—	1.13	63.8	55.4	—	—	—	—	—	—	—	—	—
3	JRR-4 B type element	Surface direction	σ	—	—	—	16.0	—	—	—	16.0	63.8	2.98	—	—	—	—	—	—	—	—	—
		Axial direction	σ	—	—	—	1.17	—	—	—	1.17	63.8	53.5	—	—	—	—	—	—	—	—	—
4	JRR-4 L type element	Surface direction	σ	—	—	—	16.4	—	—	—	16.4	63.8	2.89	—	—	—	—	—	—	—	—	—
		Axial direction	σ	—	—	—	1.62	—	—	—	1.62	63.8	38.3	—	—	—	—	—	—	—	—	—
5	JRR-4 (Uranium silicon aluminum dispersion alloy)	Surface direction	σ	—	—	—	22.0	—	—	—	22.0	63.8	1.90	—	—	—	—	—	—	—	—	—
		Axial direction	σ	—	—	—	1.50	—	—	—	1.50	63.8	41.5	—	—	—	—	—	—	—	—	—
6	JMTR standard element	Surface direction	σ	—	—	—	20.3	—	—	—	20.3	63.8	2.14	—	—	—	—	—	—	—	—	—
		Axial direction	σ	—	—	—	1.37	—	—	—	1.37	63.8	45.5	—	—	—	—	—	—	—	—	—
7	JMTR follower element	Surface direction	σ	—	—	—	13.9	—	—	—	13.9	63.8	3.58	—	—	—	—	—	—	—	—	—
		Axial direction	σ	—	—	—	1.18	—	—	—	1.18	63.8	53.0	—	—	—	—	—	—	—	—	—

Pm ; General primary membrane stress; PL ; Local primary membrane stress; Pb ; Primary bending stress; Q ; Secondary stress; F ; Peak stress;
Sa ; Repeated peak stress; N ; Number of uses; Na ; Permissible number of repetition; DF ; Cumulative fatigue coefficient;
Sm ; Design stress intensity value; Sy ; Yield point of design; MS ; Margin of safety σ_b; Bending stress σ_c ; Compression stress

Stress units ;N/mm²

(Ⅱ) -Table A.16 Stress evaluation for 1.2 m horizontal drop (3／6)

No.	Position to be evaluated / Stress			Stress at initial clamping	Stress due to internal pressure	Stress due to thermal expansion	Impact stress	Primary stress						Primary+secondary stress			Fatigue					
								Pm(PL)	2/3Sy	MS	PL+Pb	Sy	MS	PL+Pb +Q	Sy	MS	PL+Pb +Q+F	Sa	N	Na	DF	MS
1	KUR standard element (Uranium silicon aluminum dispersion alloy)	Surface direction	σ	—	—	—	13.9	—	—	—	13.9	63.7	3.58	—	—	—	—	—	—	—	—	—
		Axial direction	σ	—	—	—	1.06*1	1.06	4.67	3.40	—	—	—	—	—	—	—	—	—	—	—	—
2	KUR Special element (Uranium silicon aluminum dispersion alloy)	Surface direction	σ	—	—	—	13.9	—	—	—	13.9	63.7	3.58	—	—	—	—	—	—	—	—	—
		Axial direction	σ	—	—	—	1.06*1	1.06	4.67	3.40	—	—	—	—	—	—	—	—	—	—	—	—
3	KUR half-loaded element (Uranium silicon aluminum dispersion alloy	Surface direction	σ	—	—	—	13.9	—	—	—	13.9	63.7	3.58	—	—	—	—	—	—	—	—	—
		Axial direction	σ_c	—	—	—	0.92*1	0.92	4.67	4.07	—	—	—	—	—	—	—	—	—	—	—	—

Pm ; General primary membrane stress; PL ; Local primary membrane stress; Pb ; Primary bending stress; Q ; Secondary stress; F ; Peak stress;
Sa ; Repeated peak stress; N ; Number of uses; Na ; Permissible number of repetition; DF ; Cumulative fatigue coefficient;
Sm ; Design stress intensity value; Sy ; Yield point of design; MS ; Margin of safety σ_b; Bending stress σ_c ; Compression stress
*1 : axial compression stress

Stress units ;N/mm²

(Ⅱ) -Table A.16 Stress evaluation for 1.2 m horizontal drop (4/6)

No.	Position to be evaluated / Stress			Stress at initial clamping	Stress due to internal pressure	Stress due to thermal expansion	Impact stress	Primary stress						Primary+secondary stress			Fatigue					
								Pm(PL)	2/3Sy	MS	PL+Pb	Sy	MS	PL+Pb +Q	Sy	MS	PL+Pb +Q+F	Sa	N	Na	DF	MS
1	JMTRC Standard fuel element (A,B,C type)	Surface direction	σ	—	—	—	15.5	—	—	—	15.5	63.8	3.11	—	—	—	—	—	—	—	—	—
		Axial direction	σ	—	—	—	1.10	—	—	—	1.10	63.8	57.0	—	—	—	—	—	—	—	—	—
2	JMTRC Standard fuel element (φ2.2pin,fix type) (B,C type)	Surface direction	σ	—	—	—	15.4	—	—	—	15.4	63.8	3.14	—	—	—	—	—	—	—	—	—
		Axial direction	σ	—	—	—	1.09	—	—	—	1.09	63.8	57.5	—	—	—	—	—	—	—	—	—
3	JMTRC Special fuel element (Special A type)	Surface direction	σ	—	—	—	23.2	—	—	—	23.2	63.8	1.75	—	—	—	—	—	—	—	—	—
		Axial direction	σ	—	—	—	1.10	—	—	—	1.10	63.8	57.0	—	—	—	—	—	—	—	—	—
4	JMTRC Special fuel element (Special B type)	Surface direction	σ	—	—	—	15.9	—	—	—	15.9	63.8	3.01	—	—	—	—	—	—	—	—	—
		Axial direction	σ	—	—	—	1.37	—	—	—	1.37	63.8	45.5	—	—	—	—	—	—	—	—	—
5	JMTRC Special fuel element (Special C, Special D type)	Surface direction	σ	—	—	—	23.1	—	—	—	23.1	63.8	1.76	—	—	—	—	—	—	—	—	—
		Axial direction	σ	—	—	—	1.65	—	—	—	1.65	63.8	37.6	—	—	—	—	—	—	—	—	—
6	JMTRC fuel follower (HF type)	Surface direction	σ	—	—	—	9.92	—	—	—	9.92	63.8	5.43	—	—	—	—	—	—	—	—	—
		Axial direction	σ	—	—	—	0.89	—	—	—	0.89	63.8	70.6	—	—	—	—	—	—	—	—	—
7	JMTRC Standard fuel element (MA,MB,MC type)	Surface direction	σ	—	—	—	15.4	—	—	—	15.4	63.8	3.14	—	—	—	—	—	—	—	—	—
		Axial direction	σ	—	—	—	1.09	—	—	—	1.09	63.8	57.5	—	—	—	—	—	—	—	—	—
8	JMTRC Special fuel element (Special MB, Special MC type)	Surface direction	σ	—	—	—	23.0	—	—	—	23.0	63.8	1.77	—	—	—	—	—	—	—	—	—
		Axial direction	σ	—	—	—	1.08	—	—	—	1.08	63.8	58.0	—	—	—	—	—	—	—	—	—
9	JMTRC fuel follower (MF type)	Surface direction	σ	—	—	—	10.0	—	—	—	10.0	63.8	5.38	—	—	—	—	—	—	—	—	—
		Axial direction	σ	—	—	—	0.91	—	—	—	0.91	63.8	69.1	—	—	—	—	—	—	—	—	—

Pm ; General primary membrane stress; PL ; Local primary membrane stress; Pb ; Primary bending stress; Q ; Secondary stress; F ; Peak stress;
Sa ; Repeated peak stress; N ; Number of uses; Na ; Permissible number of repetition; DF ; Cumulative fatigue coefficient;
Sy ; Yield point of design; MS ; Margin of safety σ_b; Bending stress σ_c ; Compression stress

Stress units ;N/mm²

(Ⅱ) -Table A.16 Stress evaluation for 1.2 m horizontal drop (5/6)

No.	Position to be evaluated \ Stress		Stress at initial clamping	Stress due to internal pressure	Stress due to thermal expansion	Impact stress	Primary stress						Primary+secondary stress			Fatigue					
							Pm(PL)	2/3Sy	MS	PL+Pb	Sy	MS	PL+Pb +Q	Sy	MS	PL+Pb +Q+F	Sa	N	Na	DF	MS
1	JMTRC Special fuel element hold down part (Special A type)	σ_b	—	—	—	9.63	—	—	—	9.63	245	24.4	—	—	—	—	—	—	—	—	—
2	JMTRC Special fuel element hold down part (Special B type)	σ_c	—	—	—	15.6	—	—	—	15.6	245	14.7	—	—	—	—	—	—	—	—	—
3	JMTRC Special fuel element hold down part (Special C,Special D type)	σ_c	—	—	—	9.63	—	—	—	9.63	245	24.4	—	—	—	—	—	—	—	—	—
4	JMTRC Special fuel element hold down part (Special MB,Special MC type)	σ_c	—	—	—	9.63	—	—	—	9.63	245	24.4	—	—	—	—	—	—	—	—	—

Pm ; General primary membrane stress; PL ; Local primary membrane stress; Pb ; Primary bending stress; Q ; Secondary stress; F ; Peak stress;
Sa ; Repeated peak stress; N ; Number of uses; Na ; Permissible number of repetition; DF ; Cumulative fatigue coefficient;
Sy ; Yield point of design; MS ; Margin of safety σ_b; Bending stress σ_c ; Compression stress

Stress units ;N/mm²

(Ⅱ) -Table A.16 Stress evaluation for 1.2 m horizontal drop (6/6)

No.	Position to be evaluated \ Stress			Stress at initial clamping	Stress due to internal pressure	Stress due to thermal expansion	Impact stress	Primary stress						Primary+secondary stress			Fatigue					
								Pm(PL)	2/3Sy	MS	PL+Pb	Sy	MS	PL+Pb +Q	Sy	MS	PL+Pb +Q+F	Sa	N	Na	DF	MS
1	KUCA coupon		σ_c	—	—	—	2.21	—	—	—	2.21	63.7	28.8	—	—	—	—	—	—	—	—	—
2	KUCA flat plate	Surface direction	σ_b	—	—	—	0.16	—	—	—	0.16	63.7	398	—	—	—	—	—	—	—	—	—
		Axial direction	σ_c	—	—	—	0.96	—	—	—	0.96	63.7	66.4	—	—	—	—	—	—	—	—	—
3	Spectrum Converter		σ_b	—	—	—	138.6	—	—	—	138.6	245	0.77	—	—	—	—	—	—	—	—	—

Pm ; General primary membrane stress; PL ; Local primary membrane stress; Pb ; Primary bending stress; Q ; Secondary stress; F ; Peak stress;
Sa ; Repeated peak stress; N ; Number of uses; Na ; Permissible number of repetition; DF ; Cumulative fatigue coefficient;
Sy ; Yield point of design; MS ; Margin of safety σ_b; Bending stress σ_c ; Compression stress

(7) Analysis of stress for 1.2 m bottom side vertical drop

Analysis of stress for 1.2 m bottom side vertical drop is separately performed for the main body of the packaging and fuel elements. Stress analysis in each portion should be performed in order to determine the principal stress. Classification of stress and evaluation of stress intensity are conducted in A.5.3 (7)(c).

(a) Main body of the packaging

The positions for stress evaluation of the main body of the packaging for 1.2 m bottom side vertical drop are given as in (Ⅱ)-Fig.A.50 from the standpoint of maintaining sealing performance.

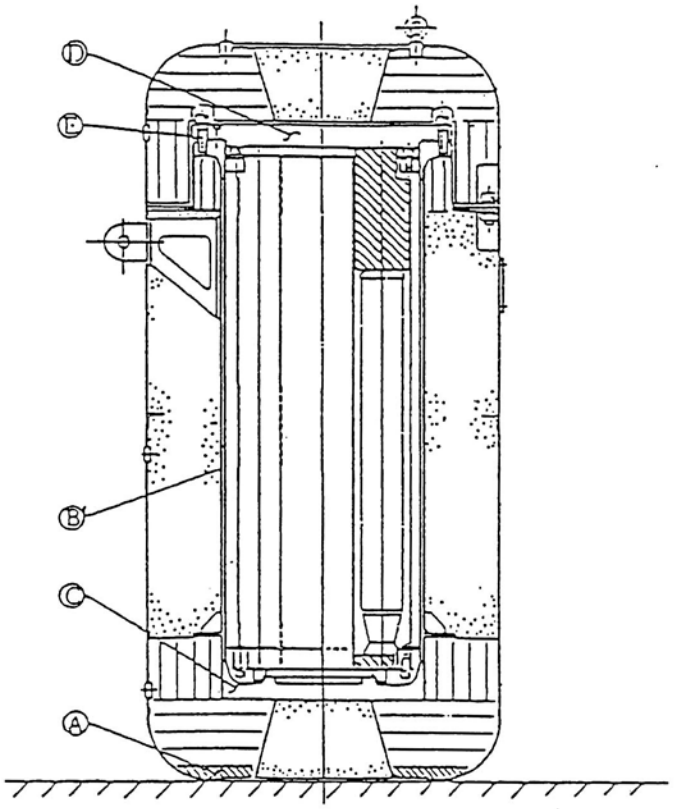

Symbol	Evaluation position
Ⓐ	Shock absorber (for quantity of deformation)
Ⓑ	Barrel of the inner shell
Ⓒ	Bottom plate of the inner shell
Ⓓ	Inner lid
Ⓔ	Inner lid clamping bolt

(Ⅱ)-Fig.A.50 Stress evaluation position for 1.2m lower side vertical drop (main body of packaging)

Ⓐ Deformation of the shock absorber

Even if the shock absorber is deformed for 1.2 m bottom side vertical drop, the deformation should not reach the bottom of the inner shell.

An analytical model is shown in (Ⅱ)-Fig.A.51.

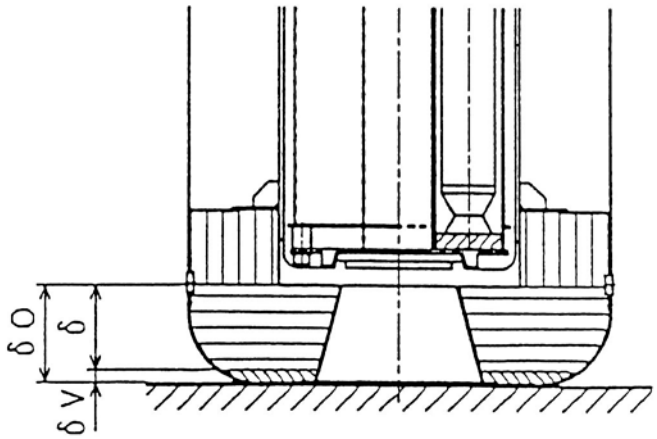

(Ⅱ)-Fig.A.51 Analytical model of interference to inner shell due to shock absorber deformation for 1.2 m lower side vertical drop

As is indicated in (Ⅱ)-Fig.A.51, residual quantity δ (mm) of the shock absorber for 1.2 m bottom side vertical drop is,

$$\delta = \delta_0 - \delta_v$$

where

δ_0 : Minimum thickness of the shock absorber before deformation,

$\delta_0 = 194$ [mm]

δ_v : Deformation of the shock absorber,

$\delta_v = 18.2$ [mm]

Therefore, the deformation is

$$\delta = 194 - 18.2 = 175.8 \text{ [mm]}$$

Thus, for 1.2 m bottom side vertical drop, deformation suffered by the shock absorber does not reach the bottom of the inner shell.

Ⓑ Frame of Inner shell

(Ⅱ)-Fig.A.52 shows an analytical model for the stress on the frame of inner shell for 1.2 m bottom side vertical drop.

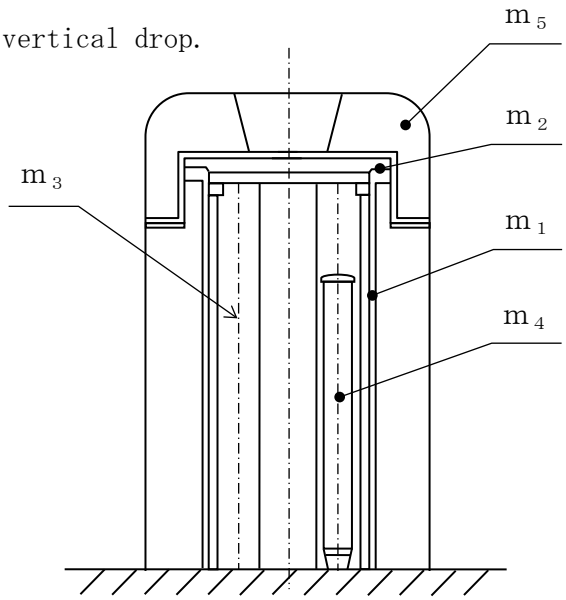

(Ⅱ)-Fig.A.52 Stress analysis model of inner shell for 1.2m lower side vertical drop

As shown in (Ⅱ)-Fig.A.52, compression force, due to dead weight and the weight of the peripheral part of the inner lid, acts on the inner shell.

The stress resulting from the compression is,

$$\sigma_c = \frac{F}{A}$$

where F: Compressive force acting on the side of inner shell,

$F = (m_1 + m_2 + m_3 + m_4 + m_5) \cdot N$ [N]

m_1 : Weight of the inner shell (side and flange), m1＝200 [kg]

m2 : Weight of the inner lid m2＝120 [kg]

m3 : Weight of the fuel basket m3＝138 [kg]

m4 : Weight of the content m4＝ 92 [kg]

m5 : Weight of the outer lid m5＝120 [kg]

N : Design acceleration, $N = 250.6 \cdot g\ [m/s^2]$

$F = (200 + 120 + 138 + 92 + 120) \times 250.6 \times 9.81 = 1.65 \times 10^6$ [N]

A: Cross sectional area of the inner shell

$$A=\frac{\pi}{4}\ (d_2{}^2-d_1{}^2) \quad [mm^2]$$

d_2 : Outer diameter of the inner shell, d2=480 [mm]

d1 : Inner diameter of the inner shell, d_1=460 [mm]

$$A=\frac{\pi}{4}\ (480^2-460^2) = 1.48\times10^4 \quad [mm^2]$$

Therefore, σc due to compression is,

$$\sigma c=\frac{1.65\times10^6}{1.48\times10^4}=111 \quad [N/mm^2]$$

Ⓒ Bottom plate of the inner shell

(Ⅱ)-Fig.A.53 shows the stress analysis model of the inner shell's bottom plate for 1.2 m bottom side vertical drop.

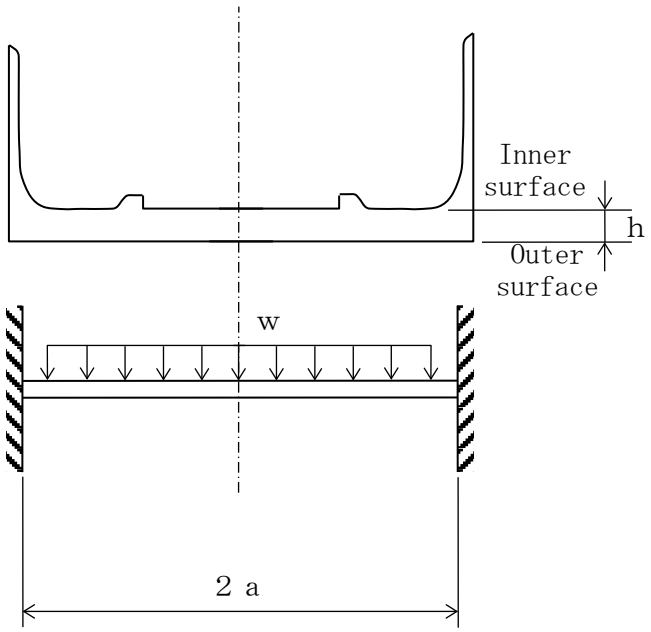

(Ⅱ)-Fig.A.53 Stress analysis model of inner shell bottom plate for 1.2m lower side vertical drop

As indicated in (Ⅱ)-Fig.A.53, the weight of the fuel baskets contents and the dead weight of the inner shell's bottom plate act uniformly on the bottom of the inner shell. The stress, generated on the disc which receives uniform load, reaches its maximum at the fixing point of the circumferentially fixed disc.

The stress is

$$\sigma_\theta = \pm 0.225 \frac{w \cdot a^2}{h^2}$$

$$\sigma_r = \pm 0.75 \frac{w \cdot a^2}{h^2}$$

$$\sigma_z = -w \text{ (inner surface)}$$

where

σ_θ: Circumferential stress [N/mm^2]

σ_r: Radial stress [N/mm^2]

σ_Z: Axial stress [N/mm^2]

a: Inner radius of inner shell's bottom plate, a=230 [mm]

h: Thickness of the inner shell's bottom plate, h= 35 [mm]

w: Uniform load,

$$w = \frac{\square m_3 \square \ \square_4 \square \ \square_7 \square\square \ N}{\pi a^2}$$

m3 :Weight of the fuel basket, m3 =138 [kg]

m4 :Weight of the content m4 = 92 [kg]

m7 :Weight of the inner shell's bottom plate, m7 =55 [kg]

N: Design acceleration, N=250.6 ・g [m/s^2]

$$w = \frac{(138+92+55) \times 250.6 \times 9.81}{\pi \times 230^2} = 4.22 \quad [N/mm^2]$$

Therefore,

$$\sigma_\theta = \pm 0.225 \times \frac{4.22 \times 230^2}{35^2} = \pm 41.0 \quad [N/mm^2]$$

$$\sigma_r = \pm 0.75 \times \frac{4.22 \times 230^2}{35^2} = \pm 137 \quad [N/mm^2]$$

$$\sigma_z = -4.22 \text{ (inner surface)} \quad [N/mm^2]$$

For the double signs of the stress values, the upper sign (+) corresponds to the inner surface and the lower sign (−) to the outer surface

Ⓓ Inner lid

(Ⅱ)-Fig.A.54 shows the stress analytical model of the inner lid for 1.2 m bottom side vertical drop.

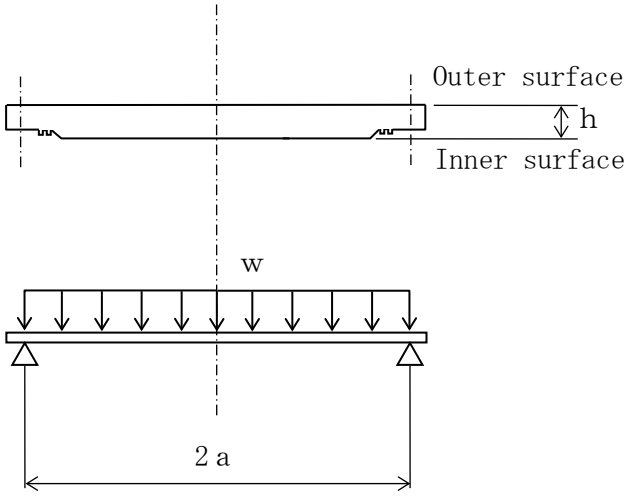

(Ⅱ)-Fig.A.54 Stress analysis model of inner lid for 1.2m lower side vertical drop

As indicated in (Ⅱ)-Fig.A.54, the dead weight acts uniformly on the inner lid. The stress, generated in the disc which receives uniform load, reaches its maximum in the center of the disc.

The stress is,

$$\sigma_r = \sigma_\theta = \mp 1.24 \frac{w \cdot a^2}{h^2}$$

$$\sigma_z = -w \text{ (outer surface)}$$

where

σ_r : Radial stress [N/mm^2]

σ_θ : Circumferential stress [N/mm^2]

σ_z : Axial stress [N/mm^2]

a: Radius of the circle of the inner lid supporting points,

a=285 [mm]

h: Thickness of the inner lid, h=55 [mm]

w: Uniform load resulting from dead weight of the lid,

$w = \gamma \cdot h \cdot N = 7.93 \times 10^{-6} \times 55 \times 250.6 \times 9.81 = 1.07$ [N/mm^2]

N: Design acceleration, N ＝250.6 ・ g [m/s^2]

γ: Density of the inner lid, $\gamma = 7.93 \times 10^{-6}$ [kg/mm^3]

Hence,

$$\sigma_r = \sigma_\theta = \mp 1.24 \frac{1.07 \times 285^2}{55^2} = \mp 35.6 \quad [\mathrm{N/mm^2}]$$

$\sigma_z = -1.07$ (outer surface) [N/mm^2]

For the double signs of the stress values, the upper sign (－) corresponds to the outer surface and the lower sign (＋) to the inner surface.

Ⓔ Inner lid clamping bolt

In a bottom side vertical drop, no load is received by the inner lid clamping bolt.

Therefore, no stress is generated.

(b) Fuel elements and fuel plate

(b)-1. Fuel elements (Non-irradiated fresh fuels for research reactor)

(1) Fuel plate

This section analyzes the stress generated on the rectangular fuel element for 1.2 m bottom side vertical drop.

(ⅰ) In case of calking both ends of fuel plate

With regard to the rectangular fuel element, there are 11 types of fresh fuel elements including the follower type, and there are 9 types of lowly irradiated fuel elements. In this section the analysis method is described for the JRR-3 standard, the same analysis was conducted for the other 11 types, and the result is shown in the (Ⅱ)-Table A.17.

However, analysis is performed on the assumption that uranium-aluminum alloy has the same strength as the covering material.

(Ⅱ)-Fig.A.55 shows an analytical model.

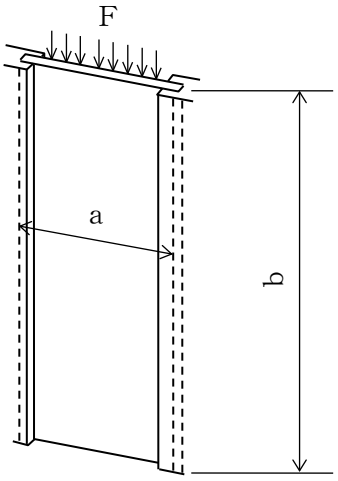

(Ⅱ)-Fig.A.55 Stress analysis model of rectangular fuel element for 1.2m lower side vertical drop.

As indicated in (Ⅱ)-Fig.A.55, the fuel plate is caulked and fixed at both extremities. Its sustaining force is,

$F_H = f \cdot 2b$

where

F_H : Strength to sustain the fuel plate [N]

f: Sustaining force per unit length; f=26.5 [N/mm]

b: Length of the fuel plate; b＝770 [mm]

Therefore,

F_H ＝26.5×2×770＝4.08×10^4 [N]

Thus, the force for dropping of the fuel plate is

F＝m・N

where

F: Force for dropping [N]

m: Weight of the fuel plate, m＝0.279 [kg]

N: Design acceleration, N＝250.6 ・ g [m/s^2]

Therefore,

F＝0.279×250.6×9.81＝686 [N]

Thus, the fuel plate does not slip down since the force to sustain the fuel plate exceeds the force for dropping of the plate.

As shown above, when a force for dropping due to the dead weight of the fuel plate which is fixed on its extremities acts on it, the shearing stress τ occurs. This stress is,

$$\tau = \frac{F}{2(h_2 - h_1)\ b}$$

where

τ: Shearing stress [N/mm^2]

F: Force for dropping of the fuel plate, F＝686 [N]

h2: Thickness of the fuel plate, h2＝1.27 [mm]

h1: Thickness of fuel plate core, h1＝0.51 [mm]

b: Length of the fuel plate, b＝770 [mm]

Thus, the shearing stress is

$$\tau = \frac{686}{2\times(1.27-0.51)\times 770} = 0.586 \quad [N/mm^2]$$

(ⅱ) In case of fuel plate fixed by pin

The stress of the pin fixing of the fuel plate of the lowly irradiated fuel element, generated at 1.2m vertical drop, is analyzed. There are 6 types of lowly irradiated fuel elements including follower types, in this section, the stress analysis method for the pin fixing type fuel element is described and its result is shown in the (Ⅱ)-Table A.17.

The uranium aluminum alloy is treated to have the same strength as the clad material in the analysis.

The analytical model is shown in (Ⅱ)-Fig.A.56.

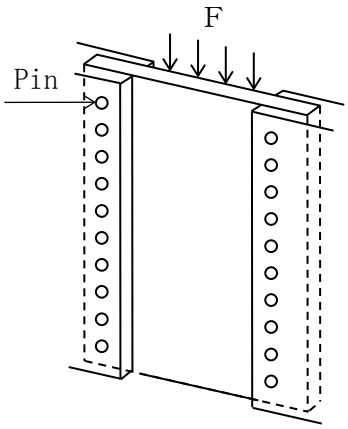

(Ⅱ)-Fig.A.56 Analytical model of 1.2m lower portion vertical drop of lowly irradiated fuel element

As shown in (Ⅱ)-Fig.A.56, the fuel plate is fixed with pin at the side plate.

This retaining force is given as follows.

$F_H = \tau_a \times A$ [N]

Where,

F_H : Force for retaining fuel plate [N]

τa : Allowable shear stress of pin = 36.8 [N/mm^2]

A : Sectional area of pin [mm^2]

$= \frac{\pi}{4} \times d^2 \times n$

d : Pin diameter = 2.2 [mm]

n : No. of pin = 62 [-]

$F_H = \tau_a \times \frac{\pi}{4} \times d^2 \times n$

$= 36.8 \times \frac{\pi}{4} \times 2.2^2 \times 62 = 8.67 \times 10^3$ [N]

The force acting on the fuel plate due to the acceleration is given as follows,

$F = m \cdot N$

Where,

F : Force acts on fuel plate when dropping [N]

m : Weight of the fuel plate = 0.217 [kg]

N : Design acceleration = 250.6 [m/s^2]

Therefore the following value is obtained.

$F = 0.217 \times 250.6 \times 9.81 = 533$ [N]

From the above, the retaining force of the pin is larger than the dropping force of the fuel plate by the acceleration. The fuel plate does not slide from fixing.

When the fuel plate, fixed with pin at the both ends, is freely dropped, the tensile force occurs at the pin portion of the fuel plate and is given as follows,

$$\sigma_t = \frac{W_o}{A}$$

Where,

$$W_o = \frac{W \times N}{n/2}$$

$$W_o = \frac{0.217 \times 250.6 \times 9.81}{62/2} = 17.2$$

σ_t : Stress of fuel plate pin [N/mm^2]

Wo : Load acting on fuel pin portion [kg]

n : No. of pin, n = 62

N : Design acceleration, N = 250.6g [m/sec^2]

A : Effective sectional area of pin [mm^2]

$$A = ((L_1 - L_2)/2 - d) \times t_1$$

L_1 : Width of fuel plate, L_1 =70.6 [mm]

L2 : Width of fuel plate core, L2 =61.8 [mm]

t1 : Thickness of fuel plate, t =1.27 [mm]

d : Pin diameter, d =2.35 [mm]

$$A = ((70.8 - 60.4)/2 - 2.35) \times 1.27 = 2.60 \ [mm^2]$$

Therefor the following value of stress is obtained.

$$\sigma_t = \frac{17.2}{2.60} = 6.61 \ [N/mm^2]$$

(iii) In case of fuel plate not fixed by the side plate

The stress of the lowly irradiated fuel element, when dropped vertically from 1.2m height, is analyzed. There are five types of lowly irradiated fuel elements including follower types, in this section. The fuel element not fixed by the side plate is analyzed and the result is shown in (Ⅱ)-Table A.17.

The uranium aluminum alloy is treated to have the same strength as the clad material in this analysis. The analytical model is shown in (Ⅱ)-Fig.A.57.

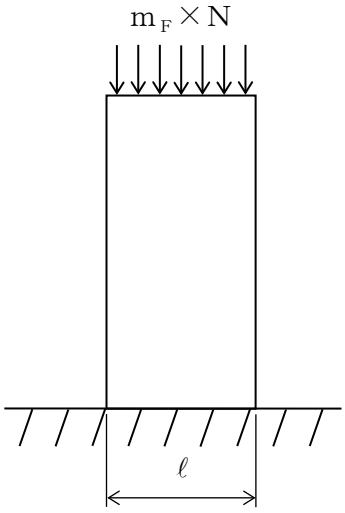

(Ⅱ)-Fig.A.57 Analytical model of 1.2m lower portion vertical drop of lowly irradiated fuel element

As shown in (Ⅱ)-Fig.A.57, the compressive stress is generated in the rectangular plate subjected to its own weight of the fuel element, and is given as follows,

$$\sigma_c = \frac{W}{A} = \frac{m_F \times N}{l\,(h_2 - h_1)}$$

Where,

m_F : Fuel plate mass, m_F = 0.223 [kg]

l : Width of fuel plate, l =66.6 [mm]

h2 : Thickness of fuel plate, h2 =1.27 [mm]

h1 : Thickness of fuel plate core, h1 =0.51 [mm]

N : Design acceleration, N =250.6g [m/s^2]

Therefore, the following value of stress is obtained.

$$\sigma_c = \frac{0.223 \times 250.6g}{66.6 \times (1.27 - 0.51)} = 10.8 \quad [N/mm^2]$$

(2) Fuel element hold-down part

As shown in (Ⅰ)-D section, the lowly irradiated fuel elements are cut at the lower adapter portion and the upper holder portion in order to reduce the weight, therefore the total length becomes short, A hold-down part is provided to adjust the length. In this section, the stress analysis method for the stress occurs in the hold down part is shown and the result is summarized in (Ⅱ)-Table A.17.

The analysis model is shown in (Ⅱ)-Fig.A.58.

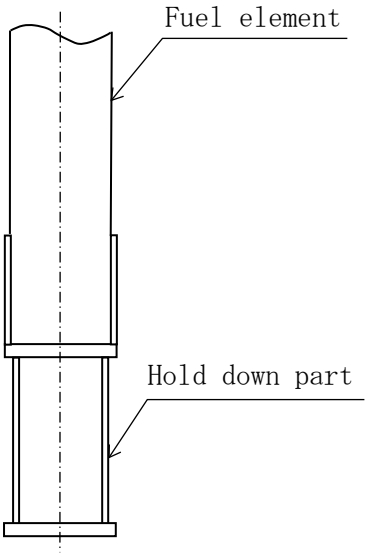

(Ⅱ)-Fig.A.58 Analytical model of hold down part

As shown in (Ⅱ)-Fig.A.58, the hold-down part is subjected to the own weight and the fuel element weight, and the compressive stress σ_c is generated as follows,

$$\sigma_c = \frac{W}{A} = \frac{(m_z + m_f) \times N}{\frac{1}{4}(h_o^2 - h_i^2)}$$

Where,

m_z : Mass of hold down part, mz = 1.3×2 [kg]

mf : Mass of hold element, mf = 2.0 [mm]

N : Design acceleration, N =250.6g [m/s^2]

ho : Outside diameter of hold down part, ho =60 [mm]

hi : Inside diameter of hold down part, h_i =52 [mm]

Therefore, following is obtained.

$$\sigma_c = \frac{(2.6+2.0)\times 250.6\cdot g}{\frac{1}{4}\times(60^2-52^2)} = 16.1 \quad [N/mm^2]$$

(b)-2. Fuel plate for the critical assembly fuel (KUCA fuel)

This section analyzes the stress generated in the fuel plate for the critical assembly at the time of 1.2 m vertical drop. The analysis model is the same as the lowly irradiated fuel elements shown in (Ⅱ)-Fig.A.57 (when the fuel plate and side plate are not fixed).

For the coupon fuel in vertical drop, the design acceleration is applied to the perpendicular direction to the plane of the fuel as shown in (Ⅱ)-Fig.A.59.

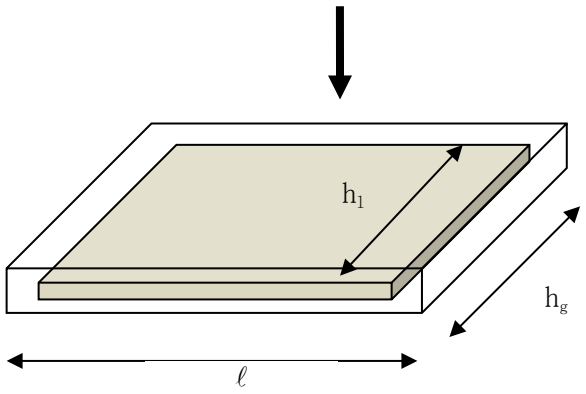

(Ⅱ)-Fig.A.59 Analytical model of 1.2m vertical drop: coupon fuel

In the case, the total thickness of cladding is 6 mm, which is the twice width of aluminum case.

m_F: Weight of the fuel plate	m_f=0.036 [kg]
l: Length of the fuel plate	l=50.8 [mm]
h_2-h_1:Cladding thickness	h_2-h_1= 6 [mm]
N: Design acceleration	N=250.6・g [m/s^2]

Therefore, the compressive stress σ_c are given as follows.

$$\sigma_c = (0.036 \times 250.6 \times g)/(50.8 \times 6)$$
$$= 0.30 \quad [N/mm^2]$$

For the flat fuel in vertical drop, the design acceleration is applied to the parallel direction to the plane of the fuel plate as shown in (Ⅱ)-Fig.A.60.

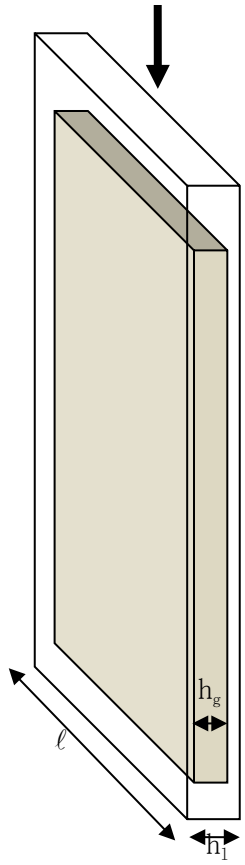

(Ⅱ)-Fig.A.60 Analytical model of 1.2m vertical drop: flat fuel

In the case,

m_F: Weight of the fuel plate	m_f=0.23 [kg]
l: Length of the fuel plate	l=62 [mm]
h_2: Fuel plate thickness	h_2 =1.5 [mm]
h_1: Fuel plate core thickness	h_1= 0.5 [mm]
N: Design acceleration	N=250.6・g [m/s^2]

Therefore, the compressive stress σ_c are given as follows.

$$\sigma_c = (0.23 \times 250.6 \times g)/(62 \times (1.5-0.5))$$
$$= 9.12 \quad [N/mm^2]$$

(b)-3. Fuel plate for Spectrum converter

This section analyzes the stress generated in the spectrum converter at the time of 1.2 m vertical drop. For the spectrum converter in vertical drop, the design acceleration is applied to the perpendicular direction to the plane of the fuel as shown in (Ⅱ)-Fig.A.62.

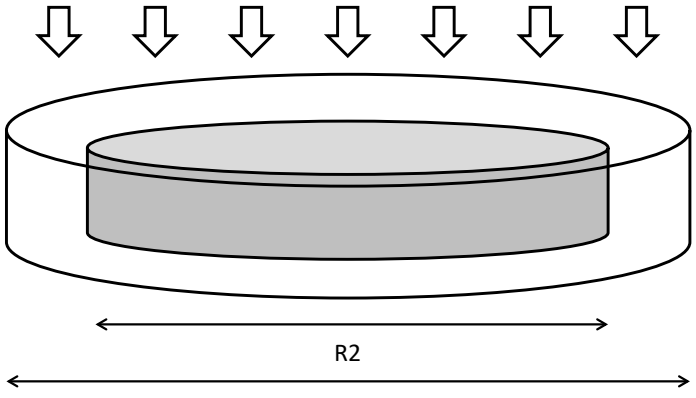

(Ⅱ)-Fig.A.62 Analytical model of 1.2m vertical drop: Spectrum converter

In the case, the spectrum converter receives its own weight, and the compressive stress σ_c generated at that time is given by the following equation.

$$\sigma_c = \frac{W}{A} = m_F \times N \Big/ \frac{\pi}{4}(R_1{}^2 - R_2{}^2)$$

where、

m_F : mass of spectrum converter	m_F=2.49	〔kg〕
R_1 : Spectrum converter outer diameter	R_1=310	〔mm〕
R_2 : Spectrum converter inner diameter	R_2=254	〔mm〕
N : Design acceleration	N=250.6・g	〔m／s^2〕

Therefore, the compressive stress is the following values.

σ_c = (2.49×250.6×9.81) /(π/4× (310^2−254^2))

=0.24 〔N／mm^2〕

(c) Comparison of allowable stress

Results of the stress evaluation in each analysis item in (Ⅱ)-5.3 (7) are shown together in (Ⅱ)-Table A.17.

As shown in this table, the margin of safety in regard to analysis reference is positive even if each or combined load is applied.

Therefore, the integrity of this package is maintained under the condition of the 1.2 m bottom side vertical drop test.

(Ⅱ) -Table A.17 Stress evaluation for 1.2 m bottom side vertical drop (1/6)

Stress units ;N/mm²

No.	Position to be evaluated \ Stress			Stress at initial clamping	Stress due to internal pressure	Stress due to thermal expansion	Impact stress	Primary stress						Primary+secondary stress			Fatigue					
								Pm(PL)	Sm	MS	PL+Pb	1.5Sm	MS	PL+Pb +Q	3Sm	MS	PL+Pb +Q+F	Sa	N	Na	DF	MS
1	Frame of Inner shell		σ_r	—	-0.0491	—	—	112	137	0.223	—	—	—	—	—	—	—	—	—	—	—	—
			σ_θ		2.31		—															
			σ_z		1.15		-111															
2	Bottom plate of the inner shell	Inner Surface	σ_r	—	3.18	—	137	4.32	137	30.7	144.5	205	0.418	—	—	—	—	—	—	—	—	—
			σ_θ		0.953		41.0															
			σ_z		-0.098		-4.22															
		Outer Surface	σ_r	—	-3.18	—	-137	0	137	—	140	205	0.464	—	—	—	—	—	—	—	—	—
			σ_θ		-0.953		-41.0															
			σ_z		0		0															
3	Upper part of the inner shell (Inner lid)	Inner Surface	σ_r	—	-3.27	—	35.6	0.098	2/3Sy 458	4672	32.4	Sy 687	20.2	—	—	—	—	—	—	—	—	—
			σ_θ		-3.27		35.6															
			σ_z		-0.098		0															
		Outer Surface	σ_r	—	3.27	—	-35.6	1.07	2/3Sy 458	427	31.3	Sy 687	20.9	—	—	—	—	—	—	—	—	—
			σ_θ		3.27		-35.6															
			σ_z		0		-1.07															
4	Inner shell lid clamping bolt		σ_t	174	3.20	—	—	177	2/3Sy 458	1.58	—	—	—	—	—	—	—	—	—	—	—	—
			σ_b	—	—	—	—															
			τ				—															

Pm ; General primary membrane stress; PL ; Local primary membrane stress; Pb ; Primary bending stress; Q ; Secondary stress; F ; Peak stress;
Sa ; Repeated peak stress; N ; Number of uses; Na ; Permissible number of repetition; DF ; Cumulative fatigue coefficient;
Sm ; Design stress intensity value; Sy ; Yeild point of the design; MS ; Margin of safety σ_r ; Diameter direction stress σ_o ; Periphery direction stress σ_2 ; Axial stress
σ_b ; Bending stress τ ; Shear stress σ_t ; Ability of bolt stress

Stress units ;N/mm²

(Ⅱ) -Table A.17 Stress evaluation for 1.2 m bottom side vertical drop (2/6)

No.	Position to be evaluated \ Stress		Stress at initial clamping	Stress due to internal pressure	Stress due to thermal expansion	Impact stress	Primary stress						Primary+secondary stress			Fatigue					
							Pm(PL)	2/3Sy	MS	PL+Pb	Sy	MS	PL+Pb +Q	Sy	MS	PL+Pb +Q+F	Sa	N	Na	DF	MS
1	JRR-3 standard (Uranium silicon aluminum dispersion alloy)	τ	—	—	—	0.586	—	—	—	0.586	63.8	107	—	—	—	—	—	—	—	—	—
2	JRR-3 follower element (Uranium silicon aluminum dispersion alloy)	τ	—	—	—	0.479	—	—	—	0.479	63.8	132	—	—	—	—	—	—	—	—	—
3	JRR-4 B type element	τ	—	—	—	0.439	—	—	—	0.439	63.8	144	—	—	—	—	—	—	—	—	—
4	JRR-4 L type element	τ	—	—	—	0.693	—	—	—	0.693	63.8	91.0	—	—	—	—	—	—	—	—	—
5	JRR-4 (Uranium silicon aluminum dispersion alloy)	τ	—	—	—	0.603	—	—	—	0.603	63.8	104	—	—	—	—	—	—	—	—	—
6	JMTR standard element	τ	—	—	—	0.595	—	—	—	0.595	63.8	106	—	—	—	—	—	—	—	—	—
7	JMTR follower element	τ	—	—	—	0.498	—	—	—	0.498	63.8	127	—	—	—	—	—	—	—	—	—

Pm ; General primary membrane stress; PL ; Local primary membrane stress; Pb ; Primary bending stress; Q ; Secondary stress; F ; Peak stress;
Sa ; Repeated peak stress; N ; Number of uses; Na ; Permissible number of repetition; DF ; Cumulative fatigue coefficient;
Sy ; Yield point of design; MS ; Margin of safety τ ; Shear stress

Stress units
;N/mm²

(Ⅱ) -Table A.17 Stress evaluation for 1.2 m bottom side vertical drop (3/6)

No.	Position to be evaluated \ Stress		Stress at initial clamping	Stress due to internal pressure	Stress due to thermal expansion	Impact stress	Primary stress						Primary+secondary stress			Fatigue					
							Pm(PL)	2/3Sy	MS	PL+Pb	Sy	MS	PL+Pb +Q	Sy	MS	PL+Pb +Q+F	Sa	N	Na	DF	MS
1	KUR standard (Uranium silicon aluminum dispersion alloy)	τ	—	—	—	0.454	—	—	—	0.454	63.7	139	—	—	—	—	—	—	—	—	—
2	KUR Special element (Uranium silicon aluminum dispersion alloy)	τ	—	—	—	0.454	—	—	—	0.454	63.7	139	—	—	—	—	—	—	—	—	—
3	KUR half-loaded element (Uranium silicon aluminum dispersion alloy)	τ	—	—	—	0.454	—	—	—	0.454	63.7	139	—	—	—	—	—	—	—	—	—

Pm ; General primary membrane stress; PL ; Local primary membrane stress; Pb ; Primary bending stress; Q ; Secondary stress; F ; Peak stress;
Sa ; Repeated peak stress; N ; Number of uses; Na ; Permissible number of repetition; DF ; Cumulative fatigue coefficient;
Sy ; Yield point of design; MS ; Margin of safety τ ; Shear stress

(Ⅱ) -Table A.17 Stress evaluation for 1.2 m bottom side vertical drop (4/6)

No.	Position to be evaluated / Stress		Stress at initial clamping	Stress due to internal pressure	Stress due to thermal expansion	Impact stress	Primary stress						Primary+secondary stress			Fatigue					
							Pm(PL)	2/3Sy	MS	PL+Pb	Sy	MS	PL+Pb +Q	Sy	MS	PL+Pb +Q+F	Sa	N	Na	DF	MS
1	JMTRC Standard fuel element (A,B,C type)	τ	—	—	—	0.45	—	—	—	0.45	63.8	140	—	—	—	—	—	—	—	—	—
2	JMTRC Standard fuel element (φ2.2pin,fix type) (B,C type)	σ_t	—	—	—	6.61	—	—	—	6.61	63.8	8.65	—	—	—	—	—	—	—	—	—
3	JMTRC Special fuel element (Special A type)	σ_c	—	—	—	10.8	—	—	—	10.8	63.8	4.90	—	—	—	—	—	—	—	—	—
4	JMTRC Special fuel element (Special B type)	σ_c	—	—	—	0.38	—	—	—	0.38	63.8	166	—	—	—	—	—	—	—	—	—
5	JMTRC Special fuel element (Special C,Special D type)	σ_c	—	—	—	11.0	—	—	—	11.0	63.8	4.80	—	—	—	—	—	—	—	—	—
6	JMTRC fuel follower (HF type)	τ	—	—	—	0.36	—	—	—	0.36	63.8	176	—	—	—	—	—	—	—	—	—
7	JMTRC Standard fuel element (MA,MB,MC type)	τ	—	—	—	0.45	—	—	—	0.45	63.8	140	—	—	—	—	—	—	—	—	—
8	JMTRC Special fuel element (Special MB,Special MC type)	σ_c	—	—	—	10.7	—	—	—	10.7	63.8	4.96	—	—	—	—	—	—	—	—	—
9	JMTRC fuel follower (MF type)	τ	—	—	—	0.36	—	—	—	0.36	63.8	176	—	—	—	—	—	—	—	—	—

Pm ; General primary membrane stress; PL ; Local primary membrane stress; Pb ; Primary bending stress; Q ; Secondary stress; F ; Peak stress;
Sa ; Repeated peak stress; N ; Number of uses; Na ; Permissible number of repetition; DF ; Cumulative fatigue coefficient;
Sy ; Yield point of the design; MS ; Margin of safety σ_c ; Compression stress τ ; Shear stress σ_t ; Stress of the part of fuel plate pin

(Ⅱ) -Table A.17 Stress evaluation for 1.2 m bottom side vertical drop (5/6)

No.	Position to be evaluated \ Stress		Stress at initial clamping	Stress due to internal pressure	Stress due to thermal expansion	Impact stress	Primary stress						Primary+secondary stress			Fatigue					
							Pm(PL)	2/3Sy	MS	PL+Pb	Sy	MS	PL+Pb +Q	Sy	MS	PL+Pb +Q+F	Sa	N	Na	DF	MS
1	JMTRC Special fuel element hold down part (Special B type)	σ_c	—	—	—	16.1	—	—	—	16.1	245	14.2	—	—	—	—	—	—	—	—	—

Pm ; General primary membrane stress; PL ; Local primary membrane stress; Pb ; Primary bending stress; Q ; Secondary stress; F ; Peak stress;
Sa ; Repeated peak stress; N ; Number of uses; Na ; Permissible number of repetition; DF ; Fatigue accumulation coefficient;
Sy ; Yield point of the design; MS ; Margin of safety σ_c ; Compression stress

(Ⅱ) -Table A.17 Stress evaluation for 1.2 m bottom side vertical drop (6/6)

No.	Position to be evaluated \ Stress		Stress at initial clamping	Stress due to internal pressure	Stress due to thermal expansion	Impact stress	Primary stress						Primary+secondary stress			Fatigue					
							Pm(PL)	2/3Sy	MS	PL+Pb	Sy	MS	PL+Pb +Q	Sy	MS	PL+Pb +Q+F	Sa	N	Na	DF	MS
1	KUCA Coupon type	σ_b	—	—	—	0.30	—	—	—	0.30	63.7	212	—	—	—	—	—	—	—	—	—
2	KUCA Flat type	σ_b	—	—	—	9.12	—	—	—	9.12	63.7	7.0	—	—	—	—	—	—	—	—	—
3	Spectrum converter	σ_c	—	—	—	0.24	—	—	—	0.24	245	1020	—	—	—	—	—	—	—	—	—

Pm ; General primary membrane stress; PL ; Local primary membrane stress; Pb ; Primary bending stress; Q ; Secondary stress; F ; Peak stress;
Sa ; Repeated peak stress; N ; Number of uses; Na ; Permissible number of repetition; DF ; Fatigue accumulation coefficient;
Sy ; Yield point of the design; MS ; Margin of safety σ_b ; Bending stress σ_c ; Compression stress

(8) Stress analysis for 1.2m lid side vertical drop

This section analyzes the stress for 1.2 m lid side vertical drop separately for the main body of the packaging and fuel basket. Stress analysis in each item is performed for the purpose of determining the principal stress. Classification of stress and evaluation of stress intensity are conducted in A.5.3(8)(c).

(a) Main body of the packaging

Stress evaluation positions of the main body of the packaging for 1.2 m lid side vertical drop are determined as shown in (Ⅱ)-Fig.A.61 from the viewpoint of maintaining the containment.

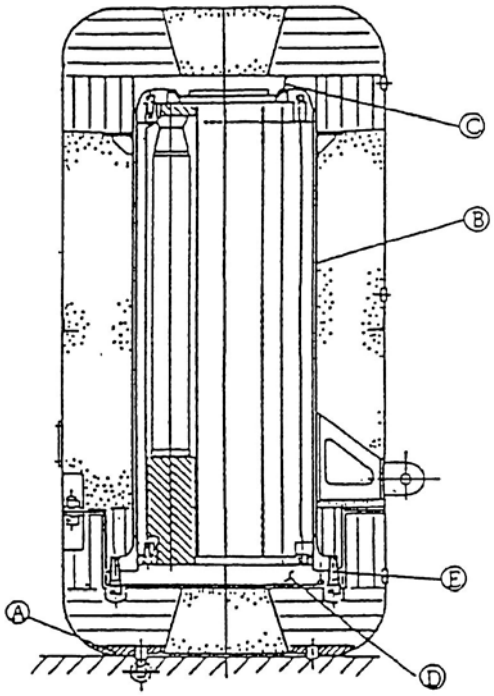

Symbol	Evaluation position
Ⓐ	Shock absorber (Quantity of deformation)
Ⓑ	Barrel of an inner shell
Ⓒ	Bottom plate of an inner shell
Ⓓ	Inner lid
Ⓔ	Inner lid clamping bolt

(Ⅱ)-Fig.A.61 Stress evaluation position for 1.2m lid side vertical drop (main body of a packaging)

Ⓐ Deformation of the shock absorber

Even if the shock absorber is deformed for 1.2 m lid side vertical drop, the deformation should not reach the bottom of the inner shell.

An analytical model is shown in (Ⅱ)-Fig.A.62.

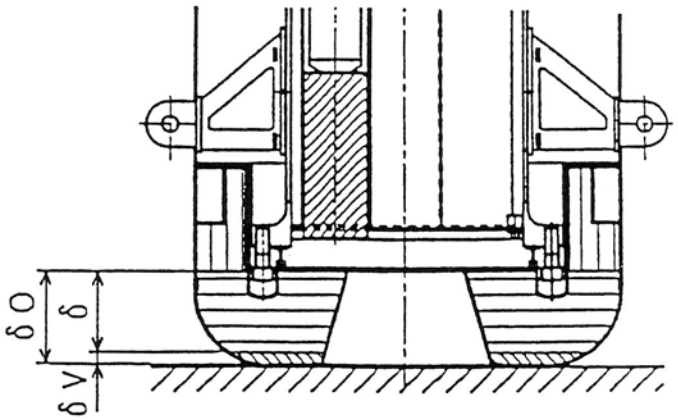

(Ⅱ)-Fig.A.62 Analytical model of interference to inner shell due to shock absorber deformation for 1.2m lid side vertical drop

As is indicated in (Ⅱ)-Fig.A.62, the remaining quantity δ (mm) of the shock absorber in the 1.2 m lid side vertical drop is,

$$\delta = \delta_0 - \delta_v$$

where

δ_0: Minimum thickness of shock absorber before deformation,

$\delta 0 = 186$ [mm]

δv: Deformation of the shock absorber, $\delta_v = 24.1$ [mm]

Hence, the remaining thickness is,

$\delta = 186 - 24.1 = 161.9$ [mm]

Therefore, for 1.2 m lid side vertical drop, it is only the shock absorber that suffers deformation and the deformation does not attain the inner lid.

Ⓑ Frame of Inner shell

(Ⅱ)-Fig.A.63 is a stress analysis model of the frame of inner shell for 1.2 m lid side vertical drop.

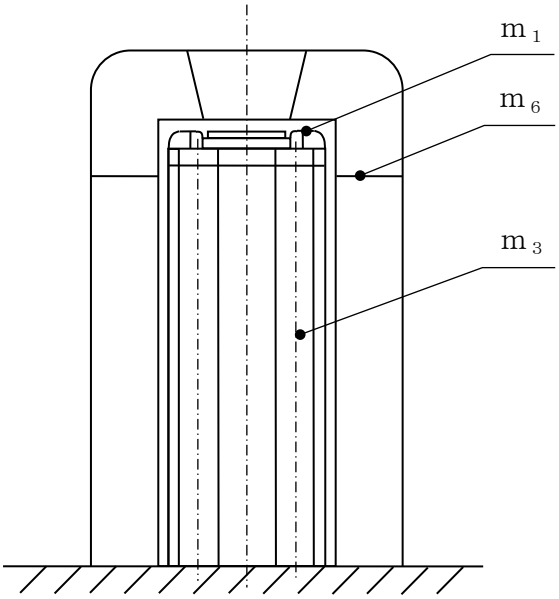

(Ⅱ)-Fig.A.63 Stress analysis model of inner shell for 1.2m lid side vertical drop

As shown in (Ⅱ)-Fig.A.63, compression, due to dead weight and the weight of the peripheral part of the inner lid, acts on the frame of inner shell.

The stress generated from the compression is given by the following equation.

$$\sigma_c = \frac{F}{A}$$

where

F: Compression force acting on the inner shell

F= (m1+m3+m6) ・N [N]

m1 : Weight of the inner shell (side and flange), m1=210 [kg]

m3 : Weight of the fuel basket, m3=138 [kg]

m6 : Weight of the outer shell, m6=225 [kg]

N : Acceleration, N=240.7・g [m/s2]

$F=(210+138+225)\times 240.7\times 9.81=1.35\times 10^6$ [N]

A: Cross sectional area of the frame of inner shell,

$$A = \frac{\pi}{4}(d_2^2 - d_1^2) \quad [mm^2]$$

d_2 : Outer diameter of the inner shell, d2 = 480 [mm]

d1 : Inner diameter of the inner shell, d_1 = 460 [mm]

$$A = \frac{\pi}{4}\ (480^2 - 460^2) = 1.48 \times 10^4 \quad [mm^2]$$

Therefore,

$$\sigma_c = \frac{1.35 \times 10^6}{1.48 \times 10^4} = 91.2 \quad [N/mm^2]$$

Ⓒ Bottom plate of the inner shell

(Ⅱ)-Fig.A.64 shows the stress analysis model of the inner shell's bottom plate for 1.2 m lid side vertical drop.

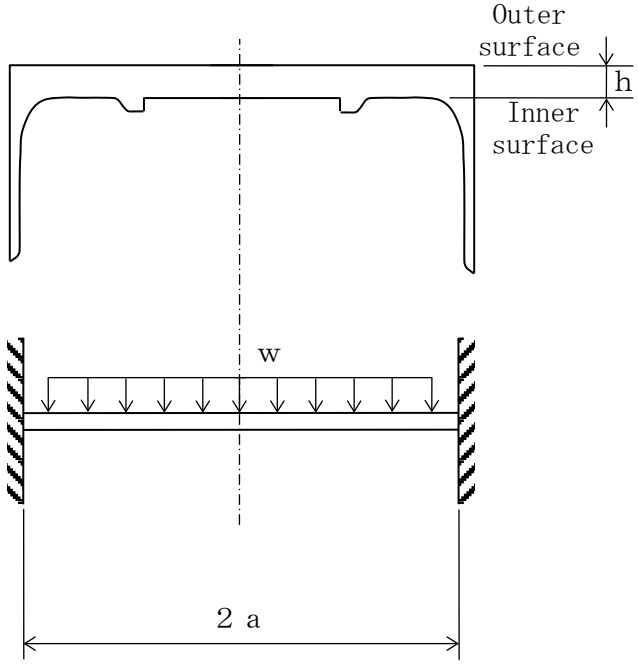

(Ⅱ)-Fig.A.64 Stress analysis model of inner shell bottom plate for 1.2m lid side vertical drop

As indicated in (Ⅱ)-Fig.A.64, the dead weight of both the bottom of the outer shell and the bottom plate of the inner shell act uniformly on the bottom of the inner shell. Stress generated in the disc which receives the uniform load reaches its maximum at the fixed end.

The stress is

$$\sigma\theta = \pm 0.225\ \frac{w \cdot a^2}{h^2}$$

$\sigma_r = \pm 0.75 \dfrac{w \cdot a^2}{h^2}$

$\sigma_z = -w$ (Outer surface)

where

$\sigma\theta$: Circumferential stress [N/mm^2]

σr: Radial stress [N/mm^2]

σz: Axial stress [N/mm^2]

a: Inner radius of the inner shell's bottom plate, a= 230 [mm]

h: Plate thickness of the inner shell's bottom plate, h=35 [mm]

w: Uniform load,

$w = \dfrac{(m_7 + m_8) \cdot N}{\pi a^2}$

m_7 : Weight of the inner shell's bottom plate, m7 = 55 [kg]

m_8 : Weight of the bottom of the outer shell, m8 =120 [kg]

N: Acceleration, N=240.7・g [m/s^2]

$w = \dfrac{(55+120) \times 240.7 \times 9.81}{\pi \times 230^2} = 2.49$ [N/mm^2]

Therefore,

$\sigma\theta = \pm 0.225 \times \dfrac{2.49 \times 230^2}{35^2} = \pm 24.2$ [N/mm^2]

$\sigma_r = \pm 0.75 \times \dfrac{2.49 \times 230^2}{35^2} = \pm 80.6$ [N/mm^2]

$\sigma_z = -2.49$ (outer surface)

For the double signs of the stress values, the plus sign corresponds to the outer surface and the minus sign to the inner surface.

Ⓓ Inner lid

(Ⅱ)-Fig.A.65 shows a stress analysis model of the inner lid for 1.2 m lid side vertical drop.

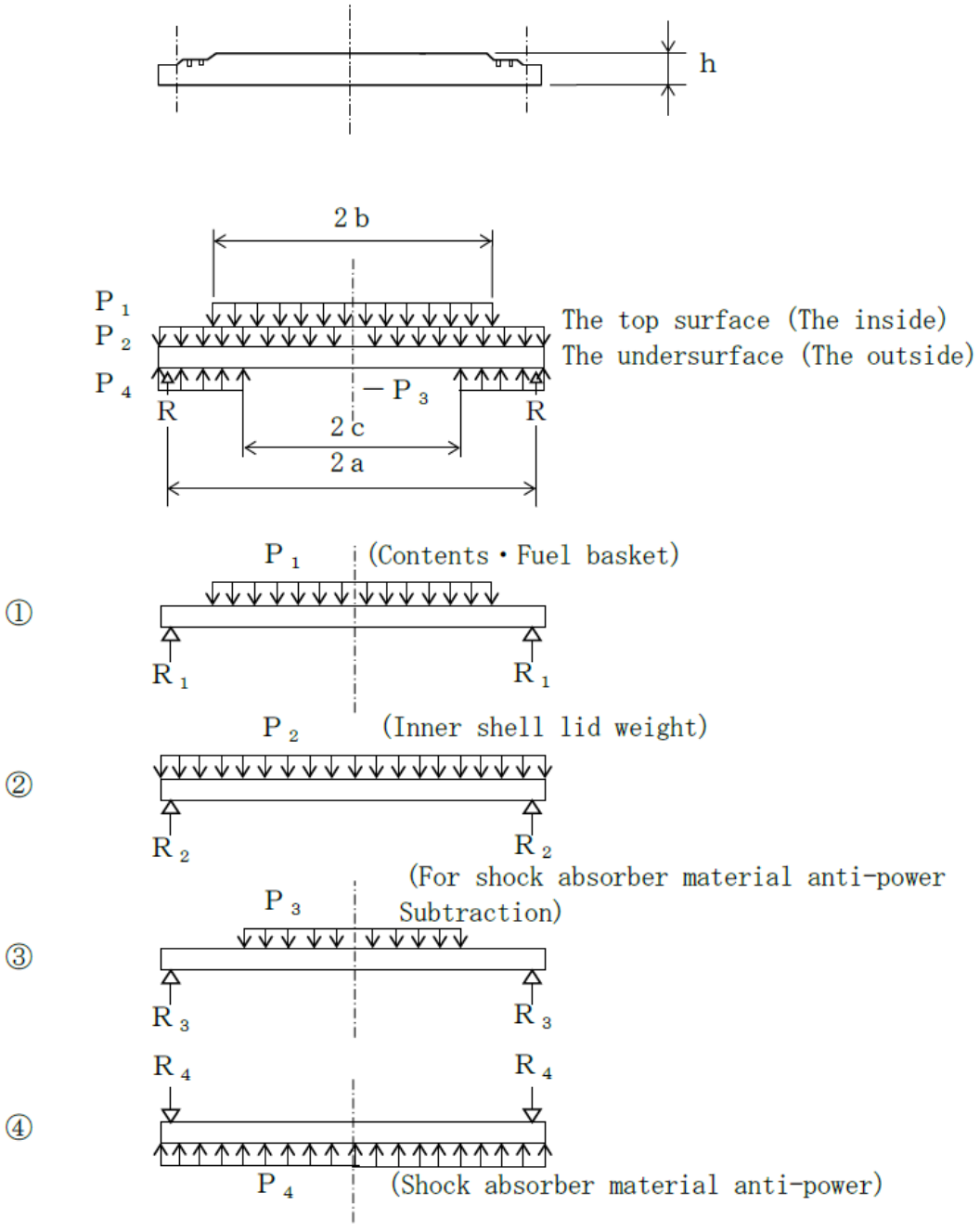

(Ⅱ)-Fig.A.65 Stress analysis model of inner lid for 1.2m lid side vertical drop

As indicated in (Ⅱ)-Fig.A.65, the weight of the contents and the fuel basket act uniformly on the center of the inner lid, and the dead weight of the inner lid also acts uniformly, while the latter is being supported by the circular reaction of the shock absorber and the inner lid clamping bolt.

The stress, generated on the circumferentially supported disc under these loads, reaches its maximum in the disc center. It can be given by superposing the analysis results of each of the models (1),(2),(3) and (4) shown in (Ⅱ)-Fig.A.65.

① Contents and fuel basket

As shown in (Ⅱ)-Fig.A.65-(1), the stress, generated within the concentric circle of the circumferentially supported disc under uniform load, reaches its maximum in the disc center. It is given by the following equation[7]

$$\sigma_r = \sigma_\theta = \mp \frac{3P_1 \cdot b^2}{8h^2}\left\{4(1+\nu)\ln\frac{a}{b} + 4 - (1-\nu)\frac{b^2}{a^2}\right\}$$

$$\sigma_z = -P_1 \quad \text{(inner surface)}$$

where

σ_r: Radial stress [N/mm^2]

σ_θ: Circumferential stress [N/mm^2]

σ_z: Axial stress [N/mm^2]

a: Radius of supporting points circle on inner lid, a=285 [mm]

b: Radius of load, b=230 [mm]

h: Plate thickness of the inner lid, h=55 [mm]

P1: Uniform load resulting from content and fuel basket,

$$P_1 = \frac{(m_3+m_4)}{\pi b^2} \cdot N \qquad [N/mm^2]$$

m_3 : Weight of the fuel basket, m3=138 [kg]

m4 : Weight of the bottom of the outer shell, m4=92 [kg]

N: Acceleration, N=240.7・g [m/s^2]

$$P_1 = \frac{(138+92)}{\pi \times 230^2} \times 240.7 \times 9.81 = 3.27 \quad [N/mm^2]$$

ν: Poisson's ratio, $\nu = 0.3$

Therefore,

$$\sigma_r = \sigma_\theta = \mp \frac{3 \times 3.27 \times 230^2}{8 \times 55^2}\left\{4(1+0.3)\ \ln\frac{285}{230} + 4 - (1-0.3)\frac{230^2}{285^2}\right\}$$

$= \mp 99.9$ [N/mm^2]

$\sigma_z = -3.27$ (inner surface)

For the double sign of the stress value, the upper sign (−) corresponds to the inner surface and the lower sign (+) to the outer surface.

The supporting point reaction R_1 in this case is,

$$R_1 = (m_3 + m_4) \cdot N$$
$$= (138 + 92) \times 240.7 \times 9.81 = 5.43 \times 10^5 \text{ [N]}$$

② Dead weight of inner lid

As indicated in (Ⅱ)-Fig.A.65-(2), the stress, generated on the circumferentially supported disc under the uniform load resulting from the disc's dead weight, reaches its maximum at the disc center. It is given by the following equation

$$\sigma_r = \sigma_\theta = \mp 1.24 \frac{P_2 \cdot a^2}{h^2}$$

$\sigma_z = -P_2$ (inner surface)

where

σ_r : Radial stress [N/mm^2]

σ_θ : Circumferential stress [N/mm^2]

σ_z : Axial stress [N/mm^2]

a: Radius of supporting points circle on inner lid, a = 285 [mm]

h: Plate thickness of the inner lid, h = 55 [mm]

N: Acceleration, N = 240.7 · g [m/s2]

γ: Density of the inner lid, $\gamma = 7.93 \times 10^{-6}$ [kg/mm^3]

P2 : Uniform load resulting from the lid's dead weight,

$P2 = \gamma \cdot h \cdot N = 7.93 \times 10^{-6} \times 55 \times 240.7 \times 9.81 = 1.03$ [N/mm^2]

Hence, the stress on the lid is

$$\sigma_r = \sigma_\theta = \mp 1.24 \frac{1.03 \times 285^2}{55^2} = \mp 34.3 \text{ [N/mm}^2\text{]}$$

$\sigma_z = -1.03$ (inner surface)

The upper sign (−) of the stress value corresponds to the inner surface and the lower sign (+) to the outer surface.

The supporting points' reaction force R_2 in this case is as follows.

$R_2 = P_2 \cdot \pi \cdot a^2 = 1.03 \times \pi \times 285^2 = 2.63 \times 10^5$ [N]

③ Deduction of the shock absorber's reaction

As shown in (Ⅱ)-Fig.A.65-(3), the stress, generated within the concentric circle of the circumferentially supported disc under uniform load, reaches its maximum at the disc center. It is given by the following equation[7]

$$\sigma_r = \sigma_\theta = \mp \frac{3P_3 \cdot c^2}{8h^2} \left\{ 4(1+\nu) \ln\frac{a}{c} + 4 - (1-\nu)\frac{c^2}{a^2} \right\}$$

$\sigma_z = -P_3$ (inner surface)

where

σ_r : Radial stress [N/mm^2]

σ_θ : Circumferential stress [N/mm^2]

σ_z : Axial stress [N/mm^2]

a: Radius of supporting points circle on inner lid, a =285 [mm]

c: Radius of load;

$c = c0 + \delta \cdot \tan\alpha = 115 + 24.1 \times \tan 15.5^\circ = 122$ [mm]

c0: Upper radius of the circular cone, c0 =115 [mm]

α: Circular cone angle, $\alpha = 15.5^\circ$

δ: Deformation thickness in the shock absorber, $\delta = 24.1$ [mm]

h: Plate thickness of the inner lid, h =55 [mm]

ν: Poisson's ratio, $\nu = 0.3$

P3 : Compressive stress on the shock absorber, $P_3 = 0.932$ [N/mm^2]

Therefore,

$$\sigma_r = \sigma_\theta = \mp \frac{3 \times 0.932 \times 122^2}{8 \times 55^2} \left\{ 4(1+0.3) \ln\frac{285}{122} + 4 - (1-0.3)\frac{122^2}{285^2} \right\}$$

$= \mp 14.2$ [N/mm^2]

$\sigma_z = -0.932$ (inner surface) [N/mm^2]

For the double sign of the stress value, the upper sign (−) corresponds to the inner surface and the lower sign (+) to the outer surface.

The supporting points' reaction in this case is

$R_3 = P_3 \pi c^2 = 0.932 \times \pi \times 122^2 = 4.36 \times 10^4$ [N]

④ Reaction of the shock absorber

As shown in (Ⅱ)-Fig.A.65-(4), the stress, generated in the circumferentially supported disc under uniform load of the shock absorber's reaction, reaches its maximum at the disc center, and it is given by the following equation.

$$\sigma_r = \sigma_\theta = \mp 1.24 \frac{P_4 \cdot a^2}{h^2}$$

$$\sigma_z = -P_4 \quad \text{(outer surface)}$$

where

σ_r : Radial stress [N/mm^2]

σ_θ : Circumferential stress [N/mm^2]

σ_z : Axial stress [N/mm^2]

a: Radius of supporting points circle on inner lid, a=285 [mm]

h: Plate thickness of the inner lid, h=55 [mm]

P4 : Compressive stress on the shock absorber, P_4=0.932 [N/mm^2]

Hence, the stress on the lid is

$$\sigma_r = \sigma_\theta = \mp 1.24 \frac{0.932 \times 285^2}{55^2} = \mp 31.0 \quad [\text{N/mm}^2]$$

$$\sigma_z = -0.932 \quad \text{(outer surface)} \quad [\text{N/mm}^2]$$

For the double sign of the stress value, the upper sign (+) corresponds to the inner surface and the lower sign (−) to the outer surface.

The supporting points' reaction force R_4 in this case is,

$$R_4 = P_4 \cdot \pi \cdot a^2 = -0.932 \times \pi \times 285^2 = -2.38 \times 10^5 \quad [\text{N}]$$

On the basis of the results mentioned above, the superposed reaction is,

$$\sigma_r = \sigma_\theta = \mp 99.9 \mp 34.3 \mp 14.2 \pm 31.0 = \mp 117 \quad [\text{N/mm}^2]$$

$$\sigma_z = -3.27 - 1.03 - 0.932 = -5.23 \quad \text{(inner surface)} \quad [\text{N/mm}^2]$$

The upper signs of these terms correspond to the inner surface and the lower signs to the outer surface.

The combined reaction of the supporting points is,

$$R = (5.43 + 2.63 + 0.44 - 2.38) \times 10^5 = 6.12 \times 10^5 \quad [\text{N}]$$

Ⓔ Inner lid clamping bolt

As indicated in A.5.3 (8)(a)(D), the dead weight of the contents, the fuel basket and the inner lid act on the inner lid. On the other hand, the inner lid is supported by the reaction of the shock absorber, the reaction of the conical reinforcing plate and the inner lid clamping bolt.

The supporting point reaction R works on the inner lid clamping bolts.

Therefore, the tensile stress arising in these bolts is,

$$\sigma_t = \frac{R}{n \cdot A_r}$$

where

σ_t : Tensile stress [N/mm^2]

R: Supporting points reaction, R $=6.12\times10^5$ [N]

n: Number of inner lid clamping bolts, n $=16$

Ar: Root thread area of the clamping bolt M 24,

$$A_r = \frac{\pi}{4} \cdot d_r^{\,2} = \frac{\pi}{4} \times 20.752^2 = 338.2 \quad [mm^2]$$

d_r: Minimum diameter of the clamping bolt, $d_r = 20.752$ [mm]

Therefore,

$$\sigma_t = \frac{6.12\times10^5}{16\times338.2} = 113 \quad [N/mm^2]$$

(b) Fuel elements, fuel plate

(b)-1. Fuel element

(Ⅰ) Fuel plate

In this section, the stresses of the rectangular fuel elements are analyzed for 1.2 m lid side vertical drop.

(i) In case of calking both ends of fuel plate

With regard to the rectangular fuel element, there are 7 types of fresh fuel elements including the follower type, and there are 9 types of lowly irradiated fuel elements. In this section, the analysis method is described for the JRR-3 standard, the same analysis was conducted for the other 8 types and the result is shown in the (Ⅱ)-Table A.18.

However, the analysis is performed on the assumption that uranium-aluminum alloy has the same strength as the covering material.

(Ⅱ)-Fig.A.66 shows an analytical model.

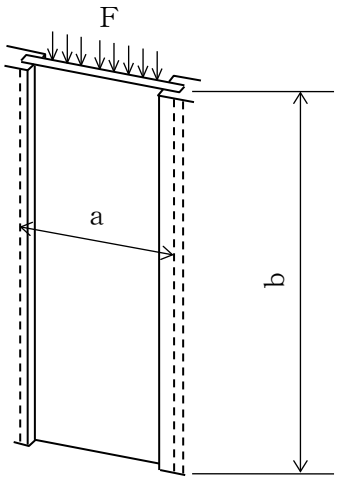

(Ⅱ)-Fig.A.66 Stress analysis model of rectangular fuel element for 1.2m lid side vertical drop

As indicated in (Ⅱ)-Fig.A.66, the fuel plate is caulked and fixed at both ends and its retaining strength is,

$F_H = f \cdot 2\ b$

where

F_H : Strength to sustain the fuel plate [N]

f: Sustaining strength per unit length, f＝26.5 [N/mm]

b: Length of the fuel plate, b＝770 [mm]

Therefore,

$F_H = 26.5 \times 2 \times 770 = 4.08 \times 10^4$ [N]

On the other hand, the force for dropping of the fuel plate is

F＝m・N

where

F: Dropping force of the fuel plate [N]

m: Weight of the fuel plate, m＝0.279 [kg]

N: Design acceleration, N＝240.7・g [m/s^2]

Therefore,

F ＝0.279×240.7×9.81＝659 [N]

Thus, the fuel plate does not slip down since the strength to sustain the fuel plate exceeds the dropping force.

As shown above, when the fuel plate which is fixed at its both ends suffers a dropping force due to its own dead weight, a shearing stress τ arises.

$$\tau = \frac{F}{2(h_2 - h_1)\ b}$$

where

τ :Shearing stress [N/mm^2]

F: Dropping force of the fuel plate, F＝659 [N]

h2: Thickness of the fuel plate, h2＝1.27 [mm]

h1: Thickness of the core of the fuel plate, h1＝0.51 [mm]

b: Length of the fuel plate, b＝770 [mm]

Therefore, the shearing stress is,

$$\tau = \frac{659}{2 \times (1.27 - 0.51) \times 770} = 0.563 \quad [N/mm^2]$$

(ⅱ) In case of fuel plate fixed by pin

The stress of the pin-fixing the fuel plate of the lowly irradiated fuel element, generated at 1.2m vertical drop, is analyzed.

There are 6 types of lowly irradiated fuel elements including follower types, in this section, the stress analysis method for the pin fixing type fuel element is shown and it's result is shown in (Ⅱ)-Table A.18.

The uranium aluminum alloy is treated to have the same strength as the clad material in the analysis.

The analytical model is shown in (Ⅱ)-Fig.A.67.

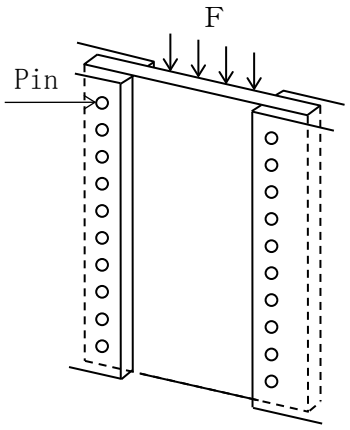

(Ⅱ)-Fig.A.67 Analytical model of 1.2m upper portion vertical drop of lowly irradiated fuel element

As shown in (Ⅱ)-Fig.A.67, the fuel plate is fixed with pin at the side plate.

This retaining force is given as follows.

$F_H = \tau_a \times A$ [N]

Where,

F_H : Force for retaining fuel plate [N]

τa : Allowable shear stress of pin = 36.8 [N/mm^2]

A : Sectional area of pin [mm^2]

$$= \frac{\pi}{4} \times d^2 \times n$$

d : Pin diameter = 2.2 [mm]

n : No. of pin = 62

Therefore, the following value is obtained.

$$F_H = \tau_a \times \frac{\pi}{4} \times d^2 \times n$$

$$= 36.8 \times \frac{\pi}{4} \times 2.2^2 \times 62 = 8.67 \times 10^3 \quad [N]$$

The force acting on the fuel plate due to the acceleration is given as follows,

$$F = mN$$

Where,

F : Force acts on fuel plate when dropping [N]

m : Weight of the fuel plate = 0.217 [kg]

N : Design acceleration = 240.7g [m/s^2]

Therefore the following value is obtained.

$$F = 0.217 \times 240.7 \times 9.81 = 512 \quad [N]$$

From the above, the retaining force of the pin is larger than the dropping force of the fuel plate by the acceleration, the fuel plate does not slide from fixing.

When the fuel plate, fixed with pin at the both ends, is freely dropped, the tensile force occurs at the pin portion of the fuel plate and is given as follows,

$$\sigma_t = \frac{W_o}{A}$$

Where,

$$W_o = \frac{W \times N}{n/2}$$

$$W_o = \frac{0.217 \times 240.7 \times 9.81}{62/2} = 16.5 \quad [N]$$

σ_t : Stress of fuel plate pin [N/mm^2]

Wo : Load acting on fuel pin portion [kg]

n : No. of pin, n = 62

N : Design acceleration, N = 240.7g [m/sec^2]

A : Effective sectional area of pin [mm^2]

$$A = ((L1 - L2)/2 - d) \times t1$$

L1 : Width of fuel plate, L1 =70.6 [mm]

L2 : Width of fuel plate core, L2 =61.8 [mm]

t1 : Thickness of fuel plate, t =1.27 [mm]

d : Pin diameter, d =2.35 [mm]

$$A = ((70.6 - 61.8)/2 - 2.35) \times 1.27 = 2.60 \ [mm^2]$$

Therefore, the following value of stress is obtained.

$$\sigma_t = \frac{16.5}{2.60} = 6.35 \ [N/mm^2]$$

(iii) In case of fuel plate not fixed by the side plate

The stress of the lowly irradiated fuel element, when dropped vertically from 1.2m height, is analyzed. Among five types of lowly irradiated fuel element including follower types, in this section, the fuel element not fixed by the side plate is analyzed and the result is shown in (Ⅱ)-Table A.18.

The uranium aluminum alloy is treated to have the same strength as the clad material in this analysis. The analytical model is shown in (Ⅱ)-Fig.A.68.

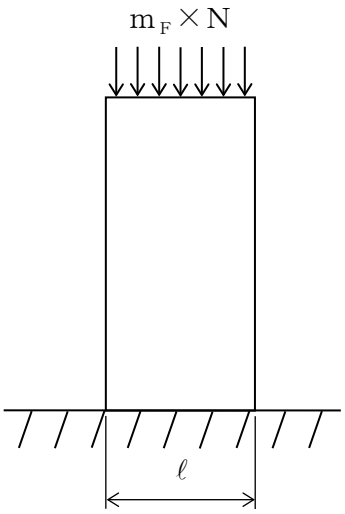

(Ⅱ)-Fig.A.68 Analytical model for 1.2m upper portion vertical drop of lowly irradiated fuel element

As shown in (Ⅱ)-Fig.A.68, the compressive stress is generated in the rectangular plate subjected to the fuel element own weight, and is shown as follows,

$$\sigma_c = \frac{W}{A} = \frac{m_F \times N}{l\,(h_2 - h_1)}$$

Where,

m_F : Fuel plate mass, mF = 0.223 [kg]

l : Width of fuel plate, l =66.6 [mm]

h2 : Thickness of fuel plate, h2 =1.27 [mm]

h1 : Thickness of fuel plate core, h1 =0.51 [mm]

N : Design acceleration, N =240.7g [m/s^2]

Therefore, the following value of stress is obtained.

$$\sigma_c = \frac{0.223 \times 240.7g}{66.6 \times (1.27 - 0.51)} = 10.4 \quad [N/mm^2]$$

(ⅱ) Fuel element hold down part

As shown in (Ⅰ)-D section, the lowly irradiated fuel elements are cut at the lower adapter portion and the upper holder portion in order to reduce the weight, Therefore the total length becomes short. A hold-down part is provided to adjust the length. In this section, the stress analysis method for the stress occurs in the hold-down part is shown and the result is summarized in (Ⅱ)-Table A.18.

The analysis model is shown in (Ⅱ)-Fig.A.69.

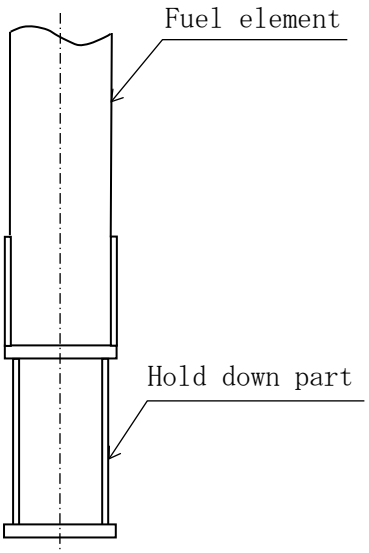

(Ⅱ)-Fig.A.69 Analytical model of hold down part

As shown in (Ⅱ)-Fig.A.69, the hold down part is subjected to the own weight and the fuel element weight, and the following compressive stress is generated.

$$\sigma_c = \frac{W}{A} = \frac{(m_z + m_f) \times N}{\frac{\pi}{4}(h_o^2 - h_i^2)}$$

Where,

m_z : Weight of the hold down part = 1.4 [kg]

mf : Weight of the fuel element = 6.6 [kg]

N : Design acceleration = 240.7g [m/sec^2]

ho : Outer diameter of the hold down part = 60 [mm]

hi : Inner diameter of the hold down part = 52 [mm]

Therefore,

$$\sigma_c = \frac{(1.4 + 6.6) \times 240.7g}{\frac{\pi}{4}(60^2 - 52^2)} = 26.8 \quad [N/mm^2]$$

(b)-2. Fuel plate for the critical assembly fuel (KUCA fuel)

This section analyzes the stress generated in the fuel plate for the critical assembly at the time of 1.2 m vertical drop. The analysis model is the same as the lowly irradiated fuel elements shown in (Ⅱ)-Fig.A.68 (when the fuel plate and side plate are not fixed).

For the coupon fuel in vertical drop, the design acceleration is applied to the perpendicular direction to the plane of the fuel as shown in (Ⅱ)-Fig.A.59 and the total thickness of cladding is 6 mm, which is the twice width of aluminum case.

m_F: Weight of the fuel plate	m_f=0.036 [kg]
l: Length of the fuel plate	l=50.8 [mm]
h_2-h_1:Cladding thickness	h_2-h_1= 6 [mm]
N: Design acceleration	N=240.7・g [m/s^2]

Therefore, the compressive stress σ_c are given as follows.

$$\sigma_c = (0.036 \times 240.7 \times g)/(50.8 \times 6)$$
$$= 0.28 \quad [N/mm^2]$$

For the flat fuel in vertical drop, the design acceleration is applied to the parallel direction to the plane of the fuel plate as shown in (Ⅱ)-Fig.A.60.

In the case,

m_F: Weight of the fuel plate	m_f=0.23 [kg]
l: Length of the fuel plate	l=62 [mm]
h_2: Fuel plate thickness	h_2 =1.5 [mm]
h_1: Fuel plate core thickness	h_1= 0.5 [mm]
N: Design acceleration	N=240.7・g [m/s^2]

Therefore, the compressive stress σ_c are given as follows.

$$\sigma_c = (0.23 \times 240.7 \times g) / (62 \times (1.5-0.5))$$

$$= 8.76 \quad [N/mm^2]$$

(b)-3. Fuel plate for the critical assembly fuel (KUCA fuel)

This section analyzes the stress generated in the spectrum converter at the time of 1.2 m vertical drop. The analysis model is the same as the model shown in (Ⅱ)-Fig.A.62.

m_F : mass of spectrum converter	$m_F = 2.49$	[kg]
R_1 : Spectrum converter outer diameter	$R_1 = 310$	[mm]
R_2 : Spectrum converter inner diameter	$R_2 = 254$	[mm]
N : Design acceleration	$N = 240.7 \cdot g$	[m／s^2]

Therefore, the compressive stress is the following values.

$$\sigma_c = (2.49 \times 240.7 \times 9.81) / (\pi/4 \times (310^2 - 254^2))$$

$$= 0.23 \quad [N/mm^2]$$

(c) Comparison of the allowable stresses

The results of the stress evaluation concerning each analyzed item in(Ⅱ)-5.3(8) are shown together in (Ⅱ)-Table A.18.

As shown in this table, the margin of safety in regard to the analysis reference is positive for individual and combined loads.

Therefore, the integrity of this package is maintained under the 1.2 m lid side vertical drop test conditions.

Stress units ;N/mm²

(Ⅱ) -Table A.18 Stress evaluation for 1.2 m lid side vertical drop (1/6)

No.	Position to be evaluated \ Stress			Stress at initial clamping	Stress due to internal pressure	Stress due to thermal expansion	Impact stress	Primary stress						Primary+secondary stress			Fatigue					
								Pm(PL)	Sm	MS	PL+Pb	1.5Sm	MS	PL+Pb +Q	3Sm	MS	PL+Pb +Q+F	Sa	N	Na	DF	MS
1	Frame of Inner shell		σ_r	—	-0.0491	—	—	92.4	137	0.482	—	—	—	—	—	—	—	—	—	—	—	—
			σ_θ		2.31		—															
			σ_z		1.15		-91.2															
2	Bottom plate of inner shell	Inner Surface	σ_r	—	3.18	—	-80.6	0.098	137	1396	77.3	205	1.65	—	—	—	—	—	—	—	—	—
			σ_θ		0.953		-24.2															
			σ_z		-0.098		0															
		Outer Surface	σ_r	—	-3.18	—	80.6	2.49	137	54.0	79.9	205	1.56	—	—	—	—	—	—	—	—	—
			σ_θ		-0.953		24.2															
			σ_z		0		-2.49															
3	Inner shell lid	Inner Surface	σ_r	—	-3.27	—	-117	5.33	2/3Sy 458	84.9	115	Sy 687	4.97	—	—	—	—	—	—	—	—	—
			σ_θ		-3.27		-117															
			σ_z		-0.098		-5.23															
		Outer Surface	σ_r		3.27		117	0.932	2/3Sy 458	490	121	Sy 687	4.67	—	—	—	—	—	—	—	—	—
			σ_θ		3.27		117															
			σ_z		0		-0.932															
4	Clamping bolt of inner shell lid		σ_r	174	3.20		113	290	2/3Sy 458	0.579	—	—	—	—	—	—	—	—	—	—	—	—
			σ_θ	—		—	—															
			σ_z				—															

Pm ; General primary membrane stress; PL ; Local primary membrane stress; Pb ; Primary bending stress; Q ; Secondary stress; F ; Peak stress;
Sa ; Repeated peak stress; N ; Number of uses; Na ; Permissible number of repetition; DF ; Cumulative fatigue coefficient;
Sm ; Design stress intensity value; Sy ; Yield point of the design; MS ; Margin of safety σ_t ; Ability of bolt stress σ_r ; Diameter direction stress σ_o ;Periphery direction stress σ_2 ; Axial stress σ_b ;Bending stress τ ; Shear stress

Stress units ;N/mm²

(Ⅱ) -Table A.18 Stress evaluation for 1.2 m lid side vertical drop (2/6)

No.	Position to be evaluated \ Stress		Stress at initial clamping	Stress due to internal pressure	Stress due to thermal expansion	Impact stress	Primary stress						Primary+secondary stress			Fatigue					
							Pm(PL)	2/3Sy	MS	PL+Pb	Sy	MS	PL+Pb +Q	Sy	MS	PL+Pb +Q+F	Sa	N	Na	DF	MS
1	JRR-3 standard element (Uranium silicon aluminum dispersion alloy)	τ	—	—	—	0.563	—	—	—	0.563	63.8	112		—	—	—	—	—	—	—	—
2	JRR-3 follower element (Uranium silicon aluminum dispersion alloy)	τ	—	—	—	0.460	—	—	—	0.460	63.8	137		—	—	—	—	—	—	—	—
3	JRR-4 B type element	τ	—	—	—	0.422	—	—	—	0.422	63.8	150	—	—	—	—	—	—	—	—	—
4	JRR-4 L type element	τ	—	—	—	0.666	—	—	—	0.666	63.8	94.7	—	—	—	—	—	—	—	—	—
5	JRR-4 (Uranium silicon aluminum dispersion alloy)	τ	—	—	—	0.579	—	—	—	0.579	63.8	109		—	—	—	—	—	—	—	—
6	JMTR standard element	τ	—	—	—	0.572	—	—	—	0.572	63.8	110	—	—	—	—	—	—	—	—	—
7	JMTR follower element	τ	—	—	—	0.479	—	—	—	0.479	63.8	132	—	—	—	—	—	—	—	—	—

Pm ; General primary membrane stress; PL ; Local primary membrane stress; Pb ; Primary bending stress; Q ; Secondary stress; F ; Peak stress;
Sa ; Repeated peak stress; N ; Number of uses; Na ; Permissible number of repetition; DF ; Cumulative fatigue coefficient;
Sy ; Yield point of the design; MS ; Margin of safety τ ; Shear stress

Stress units
;N/mm^2

(Ⅱ) -Table A.18 Stress evaluation for 1.2 m lid side vertical drop (3/6)

No.	Position to be evaluated \ Stress		Stress at initial clamping	Stress due to internal pressure	Stress due to thermal expansion	Impact stress	Primary stress						Primary+secondary stress			Fatigue					
							Pm(PL)	2/3Sy	MS	PL+Pb	Sy	MS	PL+Pb +Q	Sy	MS	PL+Pb +Q+F	Sa	N	Na	DF	MS
1	KUR standard (Uranium silicon aluminum dispersion alloy)	τ	—	—	—	0.436	—	—	—	0.436	63.7	145		—	—	—	—	—	—	—	—
2	KUR Special element (Uranium silicon aluminum dispersion alloy)	τ	—	—	—	0.436	—	—	—	0.436	63.7	145		—	—	—	—	—	—	—	—
3	KUR half-loaded element (Uranium silicon aluminum dispersion alloy)	τ	—	—	—	0.436	—	—	—	0.436	63.7	145	—	—	—	—	—	—	—	—	—

Pm ; General primary membrane stress; PL ; Local primary membrane stress; Pb ; Primary bending stress; Q ; Secondary stress; F ; Peak stress;
Sa ; Repeated peak stress; N ; Number of uses; Na ; Permissible number of repetition; DF ; Cumulative fatigue coefficient;
Sy ; Yield point of the design; MS ; Margin of safety τ ; Shear stress

(Ⅱ) -Table A.18 Stress evaluation for 1.2 m lid side vertical drop (4/6)

No.	Position to be evaluated \ Stress		Stress at initial clamping	Stress due to internal pressure	Stress due to thermal expansion	Impact stress	Primary stress						Primary+secondary stress			Fatigue					
							Pm(PL)	2/3Sy	MS	PL+Pb	Sy	MS	PL+Pb +Q	Sy	MS	PL+Pb +Q+F	Sa	N	Na	DF	MS
1	JMTRC Standard fuel element (A,B,C type)	τ	—	—	—	0.44	—	—	—	0.44	63.8	144	—	—	—	—	—	—	—	—	—
2	JMTRC Standard fuel element (ϕ2.2pin,fix type) (B,C type)	σ_t	—	—	—	6.35	—	—	—	6.35	63.8	9.04	—	—	—	—	—	—	—	—	—
3	JMTRC Special fuel element (Special A type)	σ_c	—	—	—	10.4	—	—	—	10.4	63.8	5.13	—	—	—	—	—	—	—	—	—
4	JMTRC Special fuel element (Special B type)	σ_c	—	—	—	0.37	—	—	—	0.37	63.8	171	—	—	—	—	—	—	—	—	—
5	JMTRC Special fuel element (Special C,Special D type)	σ_c	—	—	—	10.4	—	—	—	10.4	63.8	5.13	—	—	—	—	—	—	—	—	—
6	JMTRC fuel follower (HF type)	τ	—	—	—	0.34	—	—	—	0.34	63.8	186	—	—	—	—	—	—	—	—	—
7	JMTRC Standard fuel element (MA,MB,MC type)	τ	—	—	—	0.43	—	—	—	0.43	63.8	147	—	—	—	—	—	—	—	—	—
8	JMTRC Special fuel element (Special MB,Special MC type)	σ_c	—	—	—	10.3	—	—	—	10.3	63.8	5.19	—	—	—	—	—	—	—	—	—
9	JMTRC fuel follower (MF type)	τ	—	—	—	0.35	—	—	—	0.35	63.8	181	—	—	—	—	—	—	—	—	—

Pm ; General primary membrane stress; PL ; Local primary membrane stress; Pb ; Primary bending stress; Q ; Secondary stress; F ; Peak stress;
Sa ; Repeated peak stress; N ; Number of uses; Na ; Permissible number of repetition; DF ; Cumulative fatigue coefficient;
Sy ; Yield point of the design; MS ; Margin of safety τ ; Shear stress σ_c ; Compression stress σ_t ; Stress of the part of fuel pin

(Ⅱ) -Table A.18 Stress evaluation for 1.2 m lid side vertical drop (5/6)

No.	Position to be evaluated \ Stress		Stress at initial clamping	Stress due to internal pressure	Stress due to thermal expansion	Impact stress	Primary stress						Primary+secondary stress			Fatigue					
							Pm(PL)	2/3Sy	MS	PL+Pb	Sy	MS	PL+Pb +Q	Sy	MS	PL+Pb +Q+F	Sa	N	Na	DF	MS
1	JMTRC Special fuel element hold down part (Special A type)	σ_c	—	—	—	26.8	—	—	—	26.8	245	8.14	—	—	—	—	—	—	—	—	—
2	JMTRC Special fuel element hold down part (Special B type)	σ_c	—	—	—	15.4	—	—	—	15.4	245	14.9	—	—	—	—	—	—	—	—	—
3	JMTRC Special fuel element hold down part (Special C,Special D type)	σ_c	—	—	—	27.9	—	—	—	27.9	245	7.78	—	—	—	—	—	—	—	—	—
4	JMTRC Special fuel element hold down part (Special MB,Special MC type)	σ_c	—	—	—	27.9	—	—	—	27.9	245	7.78	—	—	—	—	—	—	—	—	—

Pm ; General primary membrane stress; PL ; Local primary membrane stress; Pb ; Primary bending stress; Q ; Secondary stress; F ; Peak stress;
Sa ; Repeated peak stress; N ; Number of uses; Na ; Permissible number of repetition; DF ; Cumulative fatigue coefficient;
Sy ; Yield point of the design; MS ; Margin of safety σ_c ; Compression stress

(Ⅱ) -Table A.18 Stress evaluation for 1.2 m lid side vertical drop (6/6)

No.	Position to be evaluated \ Stress		Stress at initial clamping	Stress due to internal pressure	Stress due to thermal expansion	Impact stress	Primary stress						Primary+secondary stress			Fatigue					
							Pm(PL)	2/3Sy	MS	PL+Pb	Sy	MS	PL+Pb +Q	Sy	MS	PL+Pb +Q+F	Sa	N	Na	DF	MS
1	KUCA coupon type	σ_b	—	—	—	0.28	—	—	—	0.28	63.7	227	—	—	—	—	—	—	—	—	—
2	KUCA Flat type	σ_b	—	—	—	8.76	—	—	—	8.76	63.7	7.3	—	—	—	—	—	—	—	—	—
3	Spectrum converter	σ_c	—	—	—	0.23	—	—	—	0.23	245	1065	—	—	—	—	—	—	—	—	—

Pm ; General primary membrane stress; PL ; Local primary membrane stress; Pb ; Primary bending stress; Q ; Secondary stress; F ; Peak stress;
Sa ; Repeated peak stress; N ; Number of uses; Na ; Permissible number of repetition; DF ; Cumulative fatigue coefficient;
Sy ; Yield point of the design; MS ; Margin of safety σ_b ; Bending stress σ_c ; Compression stress

(9) Corner drop

A corner drop is a special case of inclining drops The package is made to drop with its corner directed downwards, as shown in (Ⅱ)-Fig.A.70, where the line drawn from the center of gravity to the point which first touches the ground meets at a right angle to the solid plane.

(a) Deformation of shock absorber

(Ⅱ)-Fig.A.70 shows the relationship between the deformation of the shock absorber and its remaining thickness.

This figure shows that deformation only occurs in parts of the shock absorber and does not reach the inner shell.

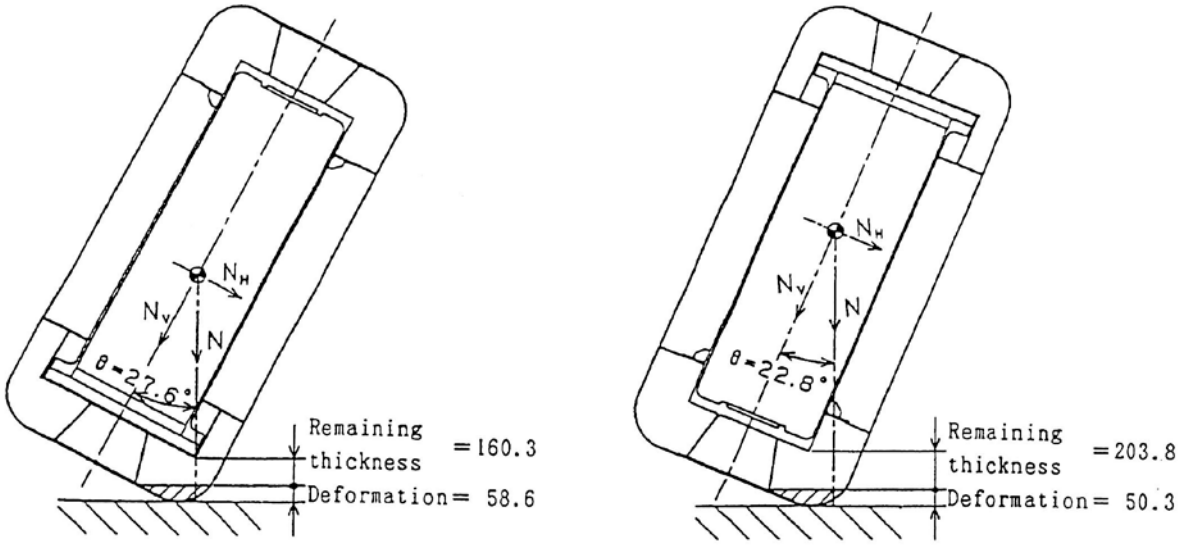

(Ⅱ)-Fig.A.70 Analytical model of interference to inner shell due to shock absorber deformation for 1.2 m corner drop

(b) Stresses on the packaging and content

(Ⅱ)-Table A.19 shows the horizontal and vertical components of the design acceleration for the corner drops (see (Ⅱ)-Table A.15).

(Ⅱ)-Table A.19 Design acceleration for corner drops

(×g)

Drop type for specimen		Total acceleration (N)	Vertical component ($N_V = N\cos\theta$)	Horizontal component ($N_H = N\sin\theta$)
Corner	Lid side	89.9	79.7	41.7
	Bottom side	90.8	83.7	35.2

(Ⅱ)-Table A.19 shows that each accelerating component is smaller than the acceleration recorded in the vertical and horizontal drop. Hence, stress is not analyzed here.

The analyses of the inner lid clamping bolts of different kinds other than those shown in section A.5.3(6) to (8) are described in the following paragraphs.

(c) Stress on the inner lid clamping bolts for corner drop

During the drop of the bottom side corner, the acceleration of the vertical component is far greater than that of the horizontal component. For this reason, the stress due to momentum on the bolts of the lid can be neglected.

During the drop of the upper corner, stress occurs on the bolts due to momentum of the inner lid. The stress is analyzed in this section.

(Ⅱ)-Fig.A.71 shows an analytical model of the stress.

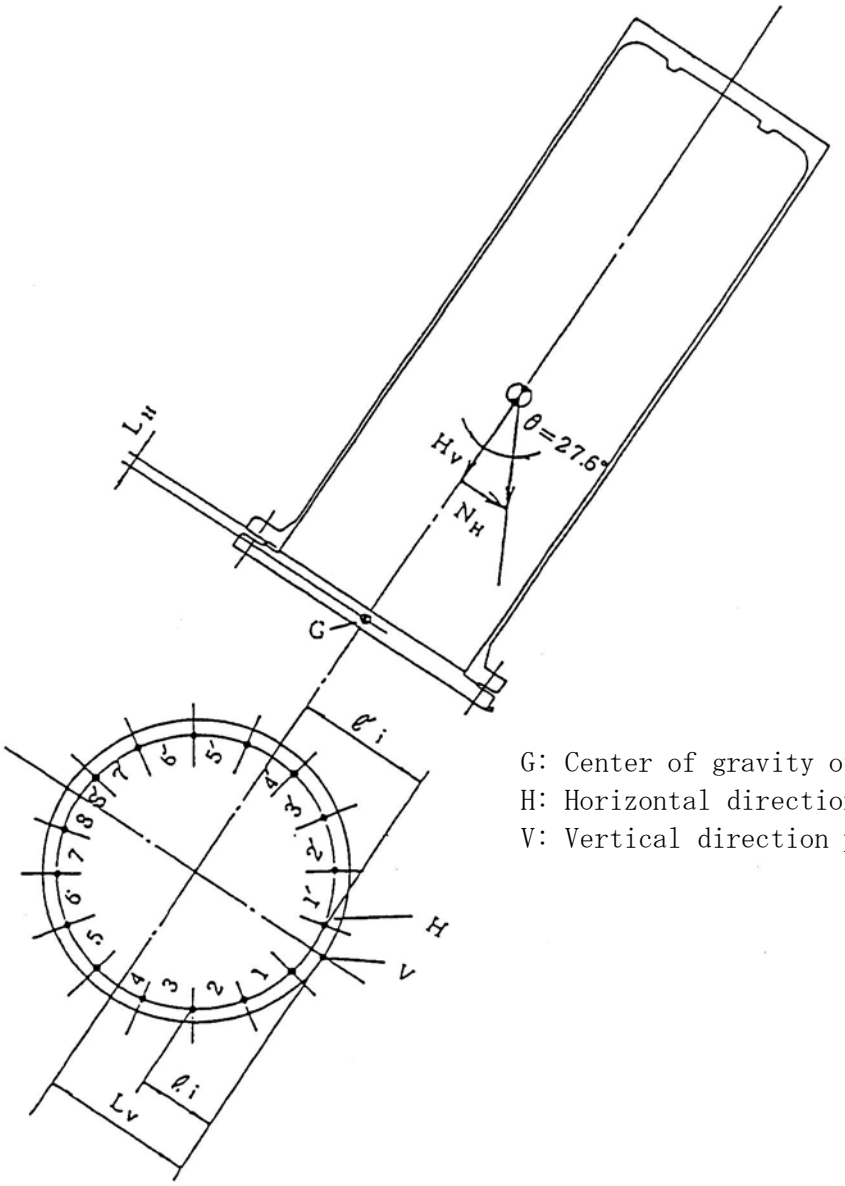

G: Center of gravity of the inner lid
H: Horizontal direction pivoting point
V: Vertical direction pivoting point

(Ⅱ)-Fig.A.71 Analytical model of stress on inner lid clamping bolts for lid side corner drop

Bending stress occurs on the inner lid clamping bolts due to the momentum of the inner lid when the package is made to fall with its lid side corner facing downwards (see (Ⅱ)-Fig.A.71).

The maximum bending stress that occurs on the bolt (8) and (8') during this drop is obtained as follows:

$$\sigma_{max} = \sigma_V + \sigma_H$$

$$\sigma_V = \frac{N_V \cdot m \cdot L_V \cdot l_8}{2 \times (l_1^2 + l_2^2 + l_3^2 + l_4^2 + l_5^2 + l_6^2 + l_7^2 + l_8^2) \cdot Ar}$$

$$\sigma_H = \frac{N_H \cdot m \cdot L_H \cdot l'_8}{2 \times (l'^2_2 + l'^2_3 + l'^2_4 + l'^2_5 + l'^2_6 + l'^2_7 + l'^2_8) \cdot Ar}$$

where

σ_{max} : Maximum bending stress on bolts 8 and 8' [N/mm2]

σV : Stress due to vertical acceleration component [N/mm2]

σH : Stress due to horizontal acceleration component [N/mm2]

NV : Vertical acceleration component Nv = 79.7·g [m/s2]

NH : Horizontal acceleration component NH = 41.7·g [m/s2]

m : Load applied on the inner lid m = 350 [kg]

LV : Vertical momentum arm Lv = 310 [mm]

LH : Horizontal momentum arm LH = 18.6 [mm]

l i : Distance from pivoting point V to a bolt [mm]

l'i : Distance from pivoting point H to a bolt [mm]

l_1 = 30.5

l_2 = 73.0 l'_2 = 42.5

l_3 = 151.7 l'_3 = 121.2

l_4 = 254.4 l'_4 = 223.9

l_5 = 365.6 l'_5 = 335.1

l_6 = 468.3 l'_6 = 437.8

l_7 = 547.0 l'_7 = 516.5

l_8 = 589.5 l'_8 = 559.0

Ar: Area of core section of bolt(M24);

$$Ar = \frac{\pi}{4} \cdot dr^2 = \frac{\pi}{4} \times 20.752^2 = 338.2 \quad [mm^2]$$

Hence, the stresses are obtained as follows:

$$\sigma_V = \frac{79.7 \times 9.81 \times 350 \times 310 \times 589.5}{2 \times (30.5^2 + 73.0^2 + 151.7^2 + 254.4^2 + 365.6^2 + 468.3^2 + 547.0^2 + 589.5^2) \times 338.2}$$

$$= 67.6 \quad [N/mm^2]$$

$$\sigma_H = \frac{41.7 \times 9.81 \times 350 \times 18.6 \times 559.0}{2 \times (42.5^2 + 121.2^2 + 223.9^2 + 335.1^2 + 437.8^2 + 516.5^2 + 559^2) \times 338.2}$$

$$= 2.32 \ [N/mm^2]$$

(Ⅱ)-Table A.20 shows an evaluation of the stresses on the inner lid clamping bolts for lid side corner drop.

Stress units ;N/mm²

(Ⅱ) -Table A.20 Stress evaluation for 1.2 m lid side corner drop

No.	Position to be evaluated / Stress		Stress at initial clamping	Stress due to internal pressure	Stress due to thermal expansion	Impact stress		Primary stress						Primary+secondary stress			Fatigue					
						Horizontal Component	Vertical Component	Pm(PL)	Sm	MS	PL+Pb	1.5Sm	MS	PL+Pb +Q	3Sm	MS	PL+Pb +Q+F	Sa	N	Na	DF	MS
1	Inner lid clamping bolt	σ_t	174	3.20	—	—	—	177	2/3Sy 458	1.58	247	Sy 687	1.78	—	—	—	—	—	—	—	—	—
		σ_b	—	—	—	2.32	67.6															
		τ				—	—															

Pm ; General primary membrane stress; PL ; Local primary membrane stress; Pb ; Primary bending stress; Q ; Secondary stress; F ; Peak stress;
Sa ; Repeated peak stress; N ; Number of uses; Na ; Permissible number of repetition; DF ; Cumulative fatigue coefficient; Sm ; Design stress intensity value;
Sy ; Yield point of the design; σ_c ; Compression stress MS ; Margin of safety σ_t ; Ability of bolt stress σ_b ; Bending stress, τ ; Shear stress

(10) Bottom side inclined drop

(a) Deformation in shock absorber

(Ⅱ)-Fig.A.72 shows the relationship between the angle of dropping and the deformation for various types of bottom side inclined drop.

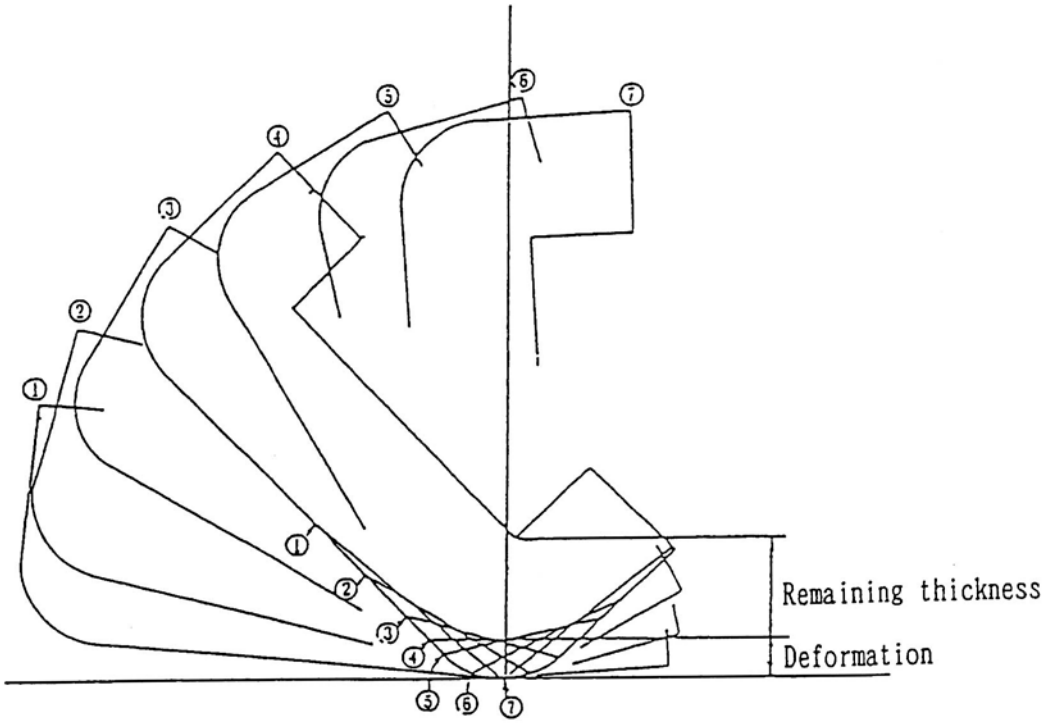

No.	Angle of dropping θ	Minimum thickness of shock absorber before deformation	Deformation of shock absorber	Remaining thickness of shock absorber
①	5°	211.9	22.2	189.7
②	15°	236.8	40.1	196.7
③	30°	260.2	56.2	204.0
④	45°	265.7	60.4	205.3
⑤	60°	252.9	61.4	191.5
⑥	75°	222.6	44.4	178.2
⑦	85°	193.7	25.0	168.7

(Ⅱ)-Fig.A.72 Analytical model of interference with inner shell due to shock absorber deformation for 1.2 m lower side inclined drop

(Ⅱ)-Fig.A.72 shows that at the drop, deformation only occurs in parts of the shock absorber and does not reach the inner shell.

(b) Stresses on packaging and content

(Ⅱ)-Table A.21 shows the horizontal and vertical components of the design acceleration at the bottom side inclined drop ((Ⅱ)-Table A.15).

(Ⅱ)-Fig.A.73 shows the relationships between the angle of dropping and the acceleration.

(Ⅱ)-Table A.21 Relationship between drop angle and acceleration

Angle at dropping θ (degrees)	Acceleration (G)		
	Acceleration (N)	Vertical component ($N \cdot \cos\theta$)	Horizontal component ($N \cdot \sin\theta$)
5	176.4	175.7	15.4
15	106.6	103.0	27.6
30	83.9	72.7	42.0
45	76.6	54.2	54.2
60	83.2	41.6	72.1
75	89.1	23.1	86.1
85	101.8	8.9	101.4

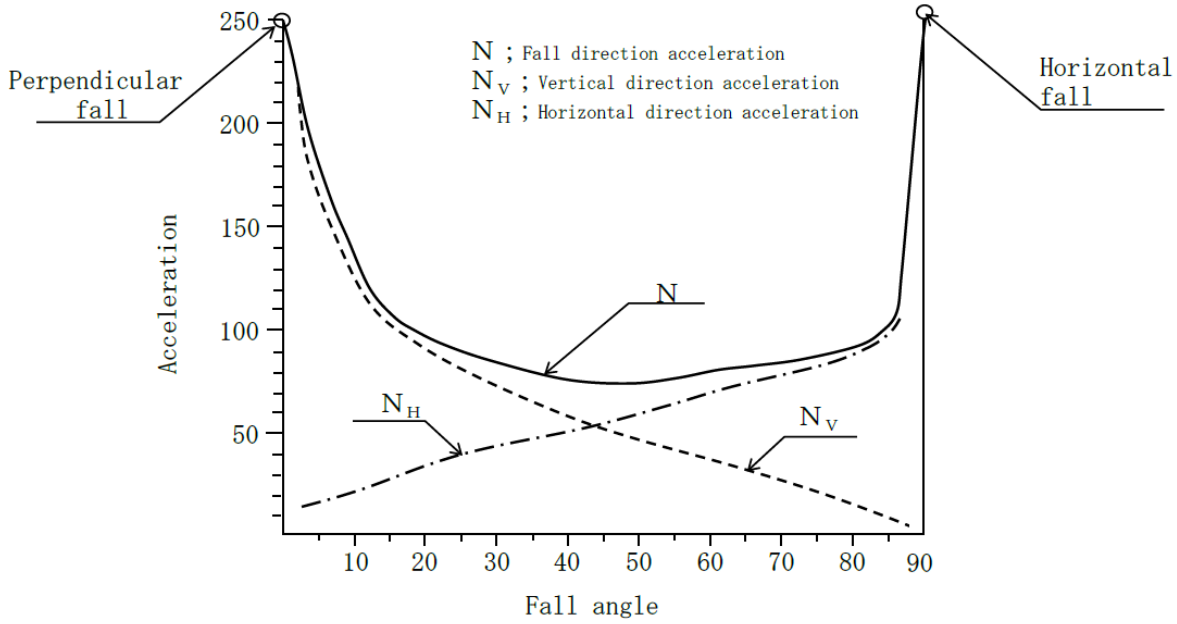

(Ⅱ)-Fig.A.73 Relationship between acceleration and drop angle for 1.2 m lower side inclined drop

(Ⅱ)-Table A.21 shows that each acceleration component is smaller than the acceleration recorded in the horizontal and vertical drop.

Hence, stress is not analyzed here.

(11) Lid side inclined drop

(a) Deformation of the shock absorber

(Ⅱ)-Fig.A.74 shows the relationship between the dropping angle and the deformation.

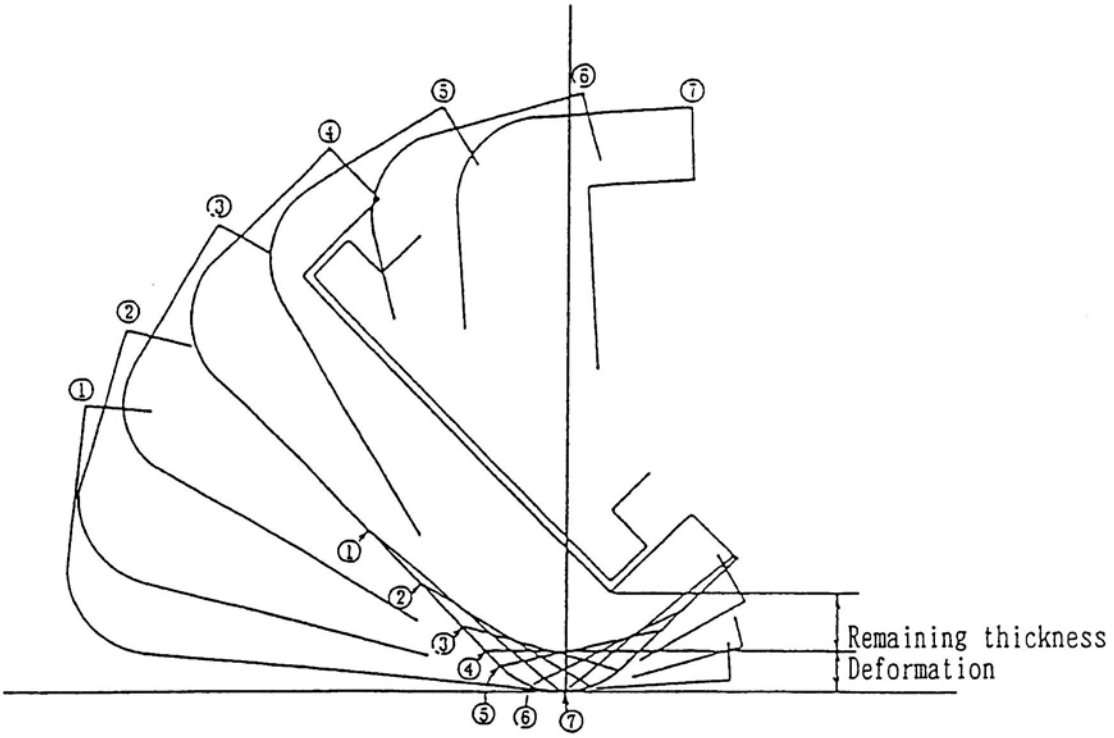

No.	Angle at dropping (θ)	Minimum thickness of shock absorber before deformation	Deformation in shock absorber	Remaining thickness of shock absorber
①	5°	201.1	21.5	179.6
②	15°	210.5	41.5	169.0
③	30°	212.2	60.8	151.4
④	45°	199.1	65.8	133.3
⑤	60°	171.9	59.3	112.6
⑥	75°	132.7	46.9	85.8
⑦	85°	101.1	27.4	73.7

(Ⅱ)-Fig.A.74 Analytical model of interference with inner shell due to shock absorber deformation for 1.2 m upper side inclined drop

(Ⅱ)-Fig.A.74 shows that deformation only occurs in parts of the shock absorber and does not reach the inner shell.

(b) Stresses on the packaging and content

(Ⅱ)-Table A.22 shows the vertical and horizontal components of the design acceleration for lid side inclined drop (see (Ⅱ)-Table A.15).

(Ⅱ)-Fig.A.75 shows the relationships between the angle of drop and the acceleration.

(Ⅱ)-Table A.22 Relationship between drop angle and acceleration

Angle at dropping θ (degrees)	Acceleration (G)		
	Acceleration (N)	Vertical component ($N \cdot \cos\theta$)	Horizontal component ($N \cdot \sin\theta$)
5	178.6	177.9	15.6
15	106.3	102.7	27.5
30	88.4	76.6	44.2
45	82.3	58.2	58.2
60	81.5	40.8	70.6
75	100.3	26.0	96.6
85	119.4	10.4	118.9

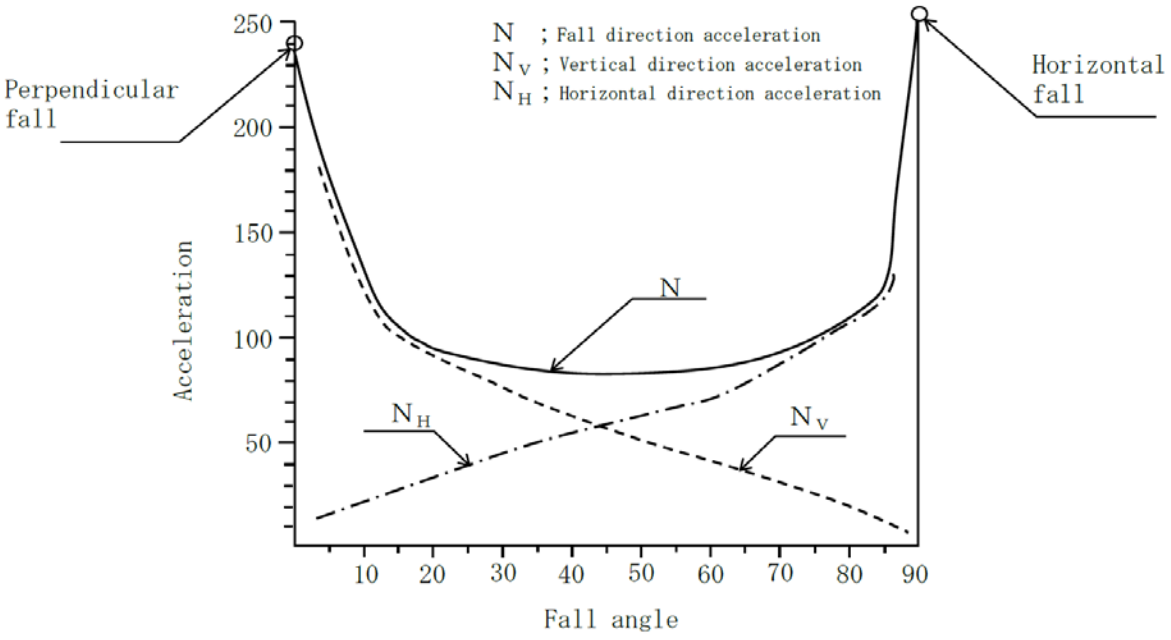

(Ⅱ)-Fig.A.75 Relationship between acceleration and drop angle for 1.2 m upper side inclined drop

(Ⅱ)-Table A.22 shows that each acceleration component is smaller than the acceleration recorded in the horizontal and vertical drop. Hence, stress is not analyzed here.

A.5.4 Stacking test

We will analyze here the stresses that may occur on the package when a compressive load on technical standards is applied on it.

In the analysis of the stresses, the principal stress is obtained. The stress classifications and stress intensity evaluations are shown in section A.5.4(3).

(1) Compressive load

The specified load to be applied to the specimen under the test condition is ; the greater of the two, the compressive load W_1 five times as high as the weight of the package, or the load W_2 obtained by multiplying the projected area A of the package by the pressure of 0.013 [MPa] (any which is larger).

For the package in question, these loads are respectively

$W1 = 5 \cdot m_o \cdot g$ [N]

$W2 = 0.013 \cdot A$ [N]

Where,

m_o: Weight of the package, mo = 950 [kg]

A: Projected area of the package,

$A = \frac{\pi}{4} \cdot D^2 = \frac{\pi}{4} \times 840^2 = 5.54 \times 10^5$ [mm^2]

D: Outer diameter of the package, D = 840 [mm]

g: Gravitational acceleration, g = 9.81 [m/s^2]

Thus,

$W_1 = 5 \times 950 \times 9.81 = 4.66 \times 10^4$ [N]

$W2 = 0.013 \times 5.54 \times 10^5 = 7.20 \times 10^3$ [N]

and $W_1 > W_2$.

The compressive load F is defined.

$F = W_1 = 4.66 \times 10^4$ [N]

(2) Analysis of the stresses

We will analyze stresses that may be generated when a compressive load is applied for a period of twenty-four hours to different parts of the packaging.

(Ⅱ)-Fig.A.76 shows the positions where stresses under the compressive load are to be evaluated.

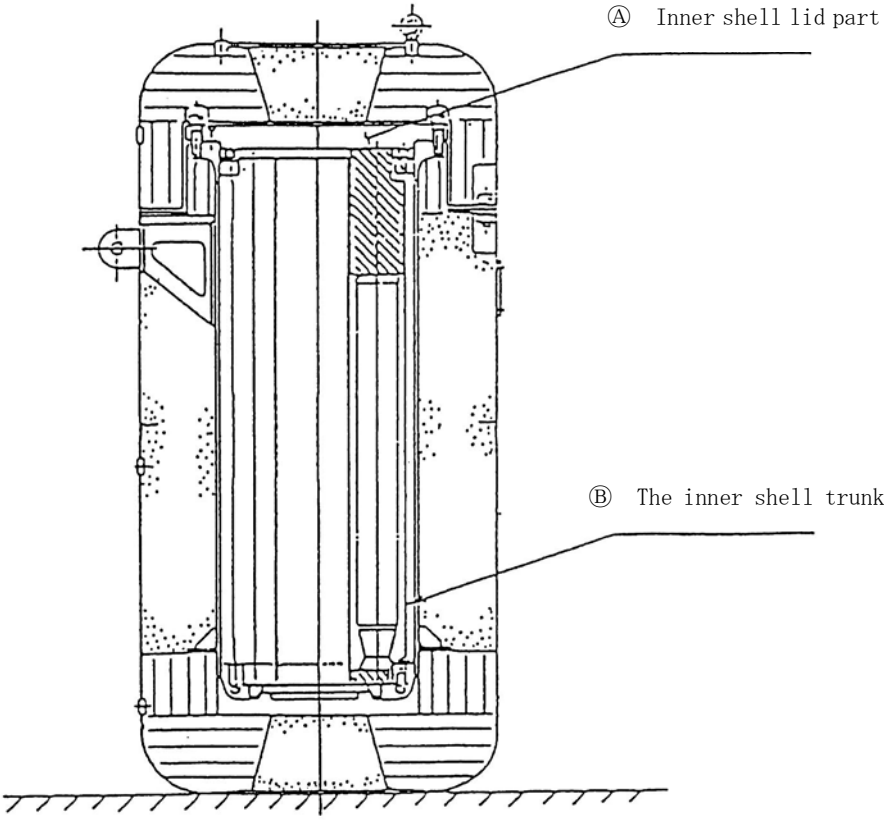

(Ⅱ)-Fig.A.76 Stress evaluation position for compressive load

(A) Inner lid

(Ⅱ)-Fig.A.77 shows an analytical model of the inner lid.

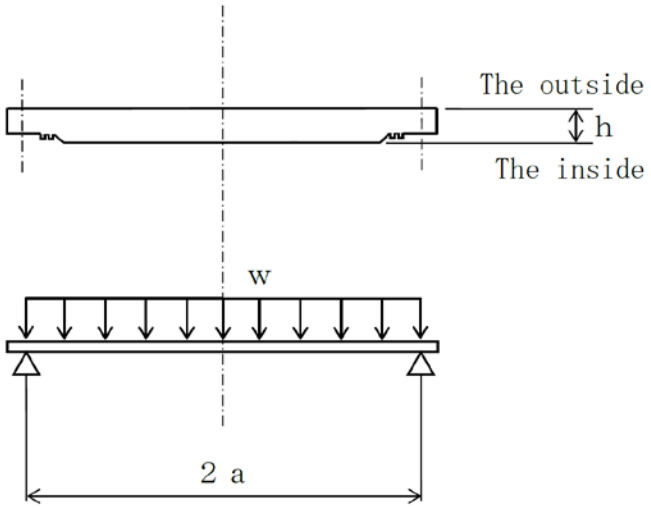

(Ⅱ)-Fig.A.77 Analytical model of inner lid under compressive load

(Ⅱ)-Fig.A.77 shows that both its own weight and the compressive load act uniformly on the inner lid which, supported on its circumference, suffers the maximum stress at the center. The stress results are as follows.

$$\sigma_r = \sigma\theta = \mp 1.24 \cdot \frac{w \cdot a^2}{h^2}$$

$$\sigma_z = -w \text{ (outer surface)}$$

where

σ_r : Radial stress [N/mm2]

$\sigma\theta$: Circumferential stress [N/mm2]

σz : Axial stress [N/mm2]

a: Diameter of inner lid supporting points, a = 285 [mm]

h: Thickness of inner lid, h = 55 [mm]

w: Uniform load,

$$w = \frac{(m_2 + m_5) \cdot g + F}{\pi a^2} \quad [N/mm^2]$$

m_2: Weight of inner lid, m2 = 120 [kg]

m5: Weight of outer lid, m5 = 120 [kg]

F : Compressive load, F = 4.66×10^4 [N/mm^2]

$$W = \frac{(120+120) \times 9.81 + 4.66 \times 10^4}{\pi \times 285^2} = 0.192 \quad [N/mm^2]$$

Thus, the stress to be obtained is,

$$\sigma_r = \sigma\theta = \mp 1.24 \times \frac{0.192 \times 285^2}{55^2} = \mp 6.39 \quad [N/mm^2]$$

$$\sigma_z = -0.192 \text{ (outer surface)} \quad [N/mm^2]$$

The upper and lower parts of the double sign correspond to the outer and inner surfaces respectively.

(B) Inner shell

(Ⅱ)-Fig.A.78 shows an analytical model of the inner shell.

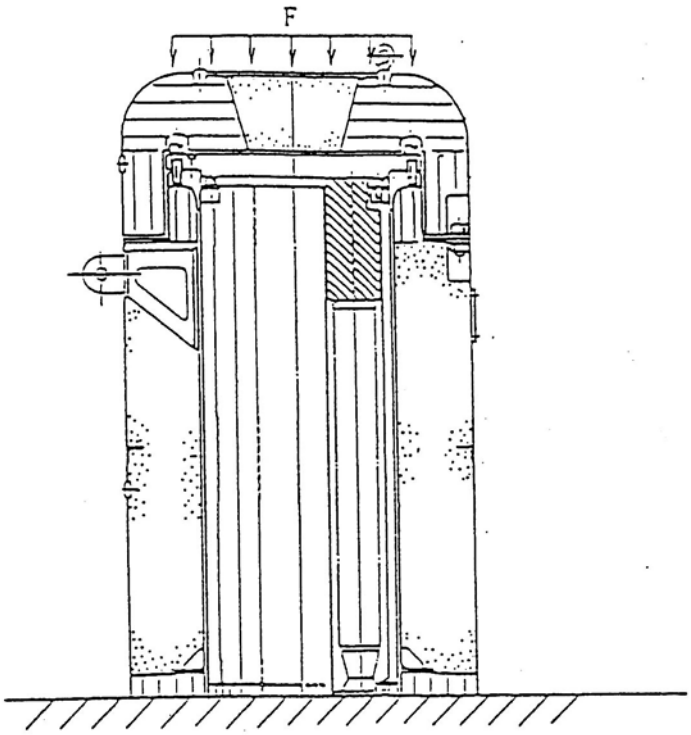

(Ⅱ)-Fig.A.78 Analytical model of inner shell under compressive load

(Ⅱ)-Fig.A.78 shows that both the weight of the inner shell and compressive load act on the inner shell. The stress σ_z which is generated by this compressive force is,

$$\sigma_z = \frac{F + m \cdot g}{A}$$

where

σ_z : Compressive load [N/mm^2]

F : Compressive force [N] F = 4.66×10^4 [N]

m : Weight of the inner shell

$m = m_1 + m_2 + m_3 + m_4 + m_5 + m_6$

m_1 : Weight of inner shell (barrel and flanges), m_1 = 200 [kg]

m_2 : Weight of inner lid, m_2 = 120 [kg]

m_3 : Weight of fuel basket, m_3 = 138 [kg]

m_4 : Weight of content, m_4 = 92 [kg]

m_5 : Weight of outer shell, m_5 = 120 [kg]

m_6 : Weight of outer lid, m_6 = 120 [kg]

m = 200 + 120 + 138 + 92 + 120 + 120 = 790 [kg]

g : Gravitational acceleration, g = 9.81 [m/s^2]

A : Cross section of inner shell,

$$A = \frac{\pi}{4} \cdot (d_2^2 - d_1^2)$$

d_2 : Outer diameter of inner shell, d2 = 480 [mm]

d1 : Inner diameter of inner shell, d_1 = 460 [mm]

$$A = \frac{\pi}{4}(480^2 - 460^2) = 1.48 \times 10^4 \ [mm^2]$$

Thus, the stress to be obtained is,

$$\sigma_z = \frac{4.66 \times 10^4 + 895 \times 9.81}{1.48 \times 10^4} = 3.74 \ [N/mm^2]$$

(3) Comparison of allowable stress

The results of the stress evaluation from the analyzed items defined in section A.5.4 are put together in (Ⅱ)-Table A.23.

This table shows that in relation to the reference values, a positive margin of safety can be achieved when single or superposed loads are generated.

Therefore, the soundness of the package can be maintained under normal test conditions (compression).

Stress units ;N/mm²

(Ⅱ) -Table A.23 Stress evaluation for stacking test

No.	Position to be evaluated / Stress			Stress at initial clamping	Stress due to internal pressure	Stress due to thermal expansion	Impact stress	Primary stress						Primary+secondary stress			Fatigue					
								Pm(PL)	Sm	MS	PL+Pb	1.5Sm	MS	PL+Pb +Q	3Sm	MS	PL+Pb +Q+F	Sa	N	Na	DF	MS
1	Inner shell lid	Inner Surface	σ_r	—	-3.27	—	6.39	0.098	2/3Sy 458	4672	3.22	Sy 687	212	—	—	—	—	—	—	—	—	—
			σ_θ		-3.27		6.39															
			σ_z		-0.098		0															
		Outer Surface	σ_r	—	3.27	—	-6.39	0.192	2/3Sy 458	2384	2.93	Sy 687	233	—	—	—	—	—	—	—	—	—
			σ_θ		3.27		-6.39															
			σ_z		0		-0.192															
2	Frame of Inner shell		σ_r	—	0.0491	—	—	4.83	137	27.3	—	—	—	—	—	—	—	—	—	—	—	—
			σ_θ		2.31		—															
			σ_z		1.15		-3.74															

Pm ; General primary membrane stress; PL ; Local primary membrane stress; Pb ; Primary bending stress; Q ; Secondary stress; F ; Peak stress;
Sa ; Repeated peak stress; N ; Number of uses; Na ; Permissible number of repetition; DF ; Cumulative fatigue coefficient;
Sm ; Design stress intensity value; Sy ; Yield point of the design; MS ; Margin of safety σ_r ; Diameter direction stress σ_θ ;Periphery direction stress σ_2 ;Axial stress

A.5.5 Penetration

The penetration test is carried out to demonstrate that a bar of 32 mm in diameter and 6kg in weight dropped vertically from a height of 1 meter with its hemispherical end downwards does not penetrate the weakest part of the package.

In the analyses, the contributions from the shock absorber and heat insulator under the outer shell is neglected on the assumption that the entire energy will be consumed in the deformation of the outer steel plate of the outer shell. Thus, the evaluation will ensure the maximum in safety.

The inner shell and lid that form the main structure of the containment system is covered with an outer shell and lid. The thickness of the outer steel sheet is 3 mm. (Ⅱ)-Fig.A.79 shows an analytical model of the package.

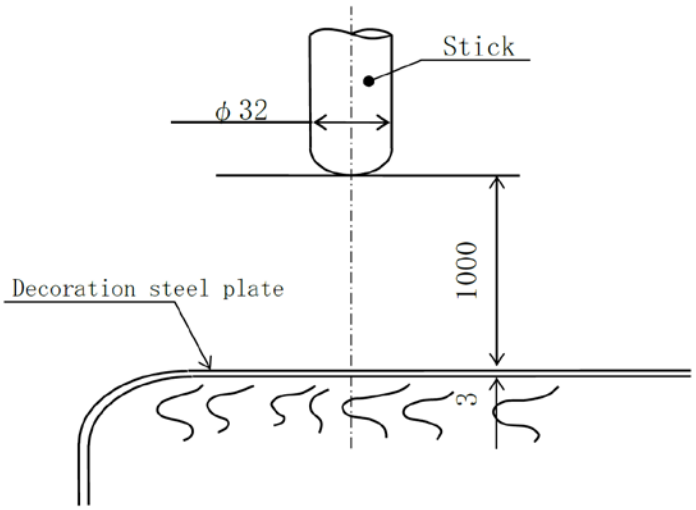

(Ⅱ)-Fig.A.79 Penetration model

We will describe below the case where the testing bar drops and reaches the object in such an orientation that the outer steel sheet is penetrated with the greatest of ease (see (Ⅱ)-Fig.A.79).

The potential energy E_1 [N·mm] of the bar before the drop is obtained as follows.

$E_1 = m \cdot g \cdot h$

where

m: Weight of the bar, m = 6 [kg]

h: Drop height, h = 1000 [mm]

g: Gravitational acceleration, g = 9.81 [m/s^2].

Thus,

$E_1 = 6 \times 9.81 \times 1000 = 5.89 \times 10^4$ [N·mm]

The energy E_2 which is necessary to permit the bar to penetrate the 3 mm steel sheet is obtained as follows.

$$E_2 = \int_0^t \tau_{cr} \cdot \pi \cdot d \cdot (t-y) \cdot dy$$

Where,

τ_{cr}: Shearing strength of the outer steel sheet,

$\tau_{cr} = 0.6 \times Su = 0.6 \times 466 = 280$ [N/mm^2]

Su: Design tensile strength, Su =466 [N/mm^2]

d: Diameter of the bar, d = 32 [mm]

t: Thickness of the outer steel sheet, t = 3 [mm].

When the equation is integrated with the above values,

$$E_2 = \tau_{cr} \cdot \pi \cdot d \times \frac{1}{2} \times t^2$$

$$= 280 \times \pi \times 32 \times \frac{1}{2} \times 3^2 = 1.27 \times 10^5 \text{ [N·mm]}$$

$E_1 = 5.89 \times 10^4$ [N·mm] $<$ $E_2 = 1.27 \times 10^5$ [N·mm]

Therefore, the dropping bar does not penetrate the outer steel sheet.

(Ⅱ)-Fig.A.80 shows an analytical model for this test.

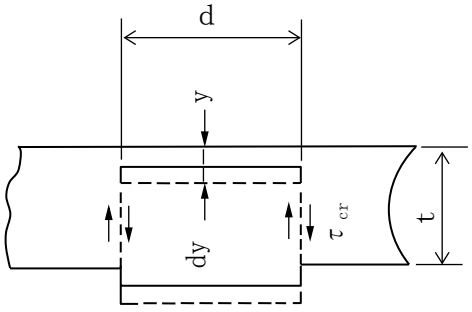

(Ⅱ)-Fig.A.80 Shearing model

This concludes that the dropping bar does not adversely affect the containment system or the soundness of the package.

A.5.6 Corner or edge drop

These requirements should be applied for the wooden or fiber plate made rectangular parallels piped shapes weighting less than 50kg and the cylindrical objects made of fiber plate weight less than 100kg. This packages, weighting 950kg, will be excluded from those requirements.

A.5.7 Summary of results and evaluation

An outline of the test results for the package under normal test conditions is given below.

(1) 1.2 m drop

As shown in section A.5.3, deformations in the shock absorber in different cases of 1.2 m drop come within the range from 18.2 mm (vertical drop) to 58.6 mm (corner drop). Hence, deformation in each orientation does not affect the inner shell.

The impact accelerations occurring come within the range from 89.9·G to 254.1·G. Stresses occurring are lower than the analytical reference values. Hence, the package retains its soundness and containment.

(2) Other analyses

The tests concerning the pressures at drop, vibration, water spraying, stacking test, and the analyses for penetration, prove that the inner shell constituting the containment barrier retains its sound containment and leaktightness.

(3) Comparison with the allowable stresses

The analyses conducted in consideration of the composite effect of different loads described in section A.1.2-(2) show that the package conforms with all the items of the design reference in section A.1.2-(1).

The package retains its sound containment and leaktightness.

A.6 Accident test conditions

This package is classified as B(U) type, and has the following test conditions set out in the relevant technical standards.

(1) Drop test Ⅰ

After the drop test I, package must be exposed to the following conditions.

(2) Drop test Ⅱ

(3) Thermal test

(4) Water immersion test

After these tests (1) to (4) the package must be exposed to the following test conditions.

This section analyzes the effects that the preceding test conditions have on the package and shows how test results satisfy the design standards for the accident test conditions.

A.6.1 Mechanical test - Drop test I (9 m drop) or mechanical test-Drop test Ⅲ (dynamic pressure pickles)

This section describes the effects at 9 m drop that has on the package and covers the following four types of drop, which shows this package can maintain its soundness at 9m drops.

1) Vertical drop (lid side, bottom side)

2) Horizontal drop

3) Corner drop (lid side, bottom side)

4) Inclined drop (lid side, bottom side)

(a) Analysis model

Analysis illustrates the stresses generated in these drop tests. The energy generated by a 9 m drop is absorbed by the deformation of the shock absorber installed at the top and bottom sections of the outer shell. This section evaluates the shock force applied to the package and analyzes its effects.

(b) Prototype test

The details are given in the accompanying document.

(c) Model test

Not applicable.

This analysis is intended to ensure ;

1) The deformation in outer shell, caused by the 9 m drop, is not transmitted to the sealed inner shell, thus precluding breaking of the containment

2) The impact of the 9 m drop does not damage the inner shell and break the seal.

3) No damage to package content.

(1) Analysis methods

The following characteristics of deformation and stress generated in the packaging, fuel baskets and content are analyzed when the 9 m drop tests performed on the package.

(a) Deformation

1) It is assumed that impact is with a rigid surface and the drop energy of the package is absorbed only by the shock absorber. This means the volume of outer shell deformation is equivalent to the extent of shock absorber deformation. It ignores absorption by the metal plating and heat insulator, and leads to the higher deformation values, safety evaluation.

2) The acceleration and volume of deformation caused by the shock absorbing material are calculated using the CASH-Ⅱ absorption performance program described in section A.10.1.

(b) Stress

1) The drop energy of the package is absorbed by the deformation of the shock absorber and the metal plating that constitutes the outer shell body and outer lid.

2) The design acceleration used for analyzing stress is a summation of the acceleration of the metal plating and the CASH-Ⅱ value

(acceleration generated in the external shock absorber) multiplied by 1.2 (factor established through comparisons with test results shown in section A.10.1.)

As this acceleration combines the acceleration factors of both the shock absorbing material and metal plating, it is used for safety evaluations of impact generated in the package.

Design accelerations = CASH-Ⅱ result×1.2 + metal plating acceleration

3) The acceleration generated in the metal plating is obtained by simple calculations.

(2) Drop force

As indicated in section「A.2 Weight and Center of Gravity」, the weight of the package used for analysis is 950kg and drop force is calculated using the following equation:

$Ua = Uv = m \cdot g \cdot h$

where

Ua: Energy absorbed by shock absorber [J]

Uv: Drop energy of the package [J]

m: Mass of transportation packaging, m = 950 [kg]

h: Height of drop, h = 9 [m]

g: Gravitational acceleration g = 9.81 [m/s^2]

And drop energy is、

$Ua = Uv = 950 \times 9.81 \times 9 = 8.39 \times 10^4$ [J]

$= 8.39 \times 10^7$ [N·mm]

(3) Results of CASH-Ⅱ shock absorber analysis program

(Ⅱ)-Table A.24 shows the results of CASH-Ⅱ program calculations of the values for acceleration and deformation generated in the shock absorbing material.

The table also lists the acceleration of the CASH-Ⅱ values multiplied by 1.2, which are used in stress analysis.

(4) Design acceleration

(Ⅱ)-Table A.25 lists the CASH-Ⅱ calculation code values multiplied by 1.2, shown in (Ⅱ)-Table A.24, and the acceleration factors for identical metal plating described in section A.5.3(4) and calculated using identical procedures.

The design acceleration factors, used for drop stress analysis, are calculated according to the following equation and are also listed in the table.

Design acceleration = CASH-Ⅱ result×1.2 + metal plating acceleration.

(Ⅱ)-Table A.24 Deformation and acceleration of shock absorber under accident test conditions

Drop posture			Volume of Deformation [mm]	Acceleration [×g]	
				Calculated value	×1.2
Horizontal			81.6	162.6	195.1
Vertical	Lid side		126.7	110.4	132.5
	Bottom side		106.3	102.4	122.9
Corner	Lid side	27.6°	128.6	61.8	74.2
	Bottom side	22.8°	111.3	65.1	78.1
Inclined	Lid side	5°	35.7	34.6	41.5
		15°	85.2	50.2	60.2
		30°	133.9	62.6	75.1
		45°	145.2	76.5	91.8
		60°	129.6	81.3	97.6
		75°	98.4	81.5	97.8
		85°	49.5	61.0	73.2
	Bottom side	5°	36.0	21.4	25.7
		15°	84.6	60.3	72.4
		30°	127.1	65.2	78.2
		45°	135.6	74.8	89.8
		60°	133.5	76.5	91.8
		75°	93.7	67.7	81.2
		85°	44.8	45.9	55.1

where

g: Gravitational acceleration, g=9.81 [m/s^2]

(Ⅱ)-Table A.25 Design acceleration under accident test conditions

Drop posture			CASH-Ⅱ ×1.2	Acceleration due to steel plate [×g]	Design acceleration [×g]
Horizontal			195.1	171.9	367.0
Vertical	Lid side		132.5	277.3	409.8
	Bottom side		122.9	265.5	388.4
Corner	Lid side	27.6°	74.2	225.6	299.8
	Bottom side	22.8°	78.1	232.8	310.9
Inclined	Lid side	5°	41.5	342.8	384.3
		15°	60.2	296.1	356.3
		30°	75.1	214.8	289.9
		45°	91.8	176.2	268.0
		60°	97.6	158.7	256.3
		75°	97.8	175.5	273.3
		85°	73.2	181.1	254.3
	Bottom side	5°	25.7	349.2	374.9
		15°	72.4	291.7	364.1
		30°	78.2	194.9	273.1
		45°	89.8	160.0	249.8
		60°	91.8	165.6	257.4
		75°	81.2	163.3	244.5
		85°	55.1	156.1	211.2

where

g: Gravitational acceleration, g=9.81 [m/s^2]

A.6.1.1 Vertical drop

(1) Bottom side vertical drop

Shock absorber deformation is 106.3 mm as shown in (Ⅱ)-Table A.24 and acceleration is 388.4·g as shown in (Ⅱ)-Table A.25 when package is dropped 9 m vertically onto its bottom.

(a) Deformation in shock absorber

This shows that deformation in the shock absorber caused by at 9 m vertical drop onto its bottom is not transmitted to the bottom of the inner shell. (Ⅱ)-Fig.A.81 shows an analytical model.

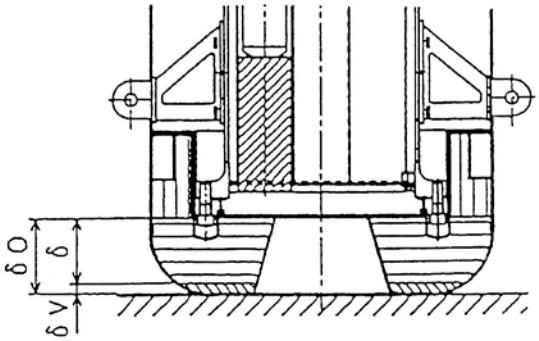

(Ⅱ)-Fig.A.81 Analytical model of interference to inner shell due to shock absorber deformation for 9 m lower side vertical drop

As shown in (Ⅱ)-Fig.A.81, the remaning δ mm of shock absorber after the package is dropped vertically 9 m onto its bottom is calculated using the following equation.

$\delta = \delta_o - \delta_v$

where

δ_o : Minimum thickness of shock absorber prior to deformation,

δ_o = 194 [mm]

δ_v : Deformation of shock absorber, δ_v = 106.3 [mm]

The remained thickness is,

$\delta = 194 - 106.3 = 87.7$ [mm]

The deformation produced by dropping the package vertically 9 m onto its bottom is limited to the shock absorber and is not transmitted to the bottom of the inner shell.

(b) Stress generated in various parts of package

The analysis procedures and evaluation positions described in section (Ⅱ) A.5.3 (7) are used and the analysis and evaluation results are both listed in (Ⅱ)-Table A.26.

(Ⅱ) -Table A.26 Stress evaluation for 9 m lower side vertical drop (1/6)

Stress units ;N/mm²

No.	Position to be evaluated / Stress			Stress at initial clamping	Stress due to internal pressure	Impact stress	Primary stress					
							Pm(PL)	2/3 Su	MS	PL＋Pb	Su	MS
1	Frame of Inner shell		σ_r	—	-0.0491	—	173	310	0.791	—	—	—
			σ_θ		2.31	—						
			σ_z		1.15	-172						
2	Bottom plate of inner shell	Inner Surface	σ_r	—	3.18	211	6.63	310	45.7	221	466	1.10
			σ_θ		0.953	63.4						
			σ_z		-0.098	-6.53						
		Outer Surface	σ_r	—	-3.18	-211	0	310	—	214	466	1.17
			σ_θ		-0.953	-63.4						
			σ_z		0	0						
3	Inner shell lid	Inner Surface	σ_r	—	-3.27	55.3	0.098	2/3 Sy 458	4672	52.1	Sy 687	12.1
			σ_θ		-3.27	55.3						
			σ_z		-0.098	0						
		Outer Surface	σ_r	—	3.27	-55.3	1.66	2/3 Sy 458	274	50.4	Sy 687	12.6
			σ_θ		3.27	-55.3						
			σ_z		0	-1.66						
4	Inner shell lid clamping bolt		σ_t	174	3.20	—	177	2/3 Sy 458	1.58	—	—	—
			σ_b	—	—	—						
			τ			—						

Pm ; General primary membrane stress; PL ; Local primary membrane stress; Pb ; Primary bending stress;
Sy ; Yield point of the design; Su ; Design tensile strength; MS ; Margin of safety σ_r; Diameter direction stress σ_o; Periphery direction stress σ_2;Axial stress σ_b; Bending stress τ; Shear stress σ_t; Ability of bolt stress

Stress units ;N/mm²

(Ⅱ) -Table A.26 Stress evaluation for 9 m lower side vertical drop (2/6)

No.	Position to be evaluated \ Stress		Stress at initial clamping	Stress due to internal pressure	Impact stress	Primary stress					
						Pm(PL)	2/3 Sy	MS	PL＋Pb	Sy	MS
1	JRR-3 standard element (Uranium silicon aluminum dispersion alloy)	τ	—	—	0.908	—	—	—	0.908	63.8	69.2
2	JRR-3 follower element (Uranium silicon aluminum dispersion alloy)	τ	—	—	0.742	—	—	—	0.742	63.8	84.9
3	JRR-4 B type element	τ	—	—	0.680	—	—	—	0.680	63.8	92.8
4	JRR-4 L type element	τ	—	—	1.074	—	—	—	1.074	63.8	58.4
5	JRR-4 (Uranium silicon aluminum dispersion alloy)	τ	—	—	0.935	—	—	—	0.935	63.8	67.2
6	JMTR standard element	τ	—	—	0.922	—	—	—	0.922	63.8	68.1
7	JMTR follower	τ	—	—	0.772	—	—	—	0.772	63.8	81.6

Pm ; General primary membrane stress; PL ; Local primary membrane stress; Pb ; Primary bending stress;
Sy ; Yield point of the design; MS ; Margin of safety τ ; Shear stress

Stress units ;N/mm²

(Ⅱ) -Table A.26 Stress evaluation for 9 m lower side vertical drop (3/6)

No.	Position to be evaluated / Stress		Stress at initial clamping	Stress due to internal pressure	Impact stress	Primary stress					
						Pm(PL)	2/3 Sy	MS	PL＋Pb	Sy	MS
1	KUR standard (Uranium silicon aluminum dispersion alloy)	τ	—	—	0.703	—	—	—	0.703	63.7	89.6
2	KUR Special element (Uranium silicon aluminum dispersion alloy)	τ	—	—	0.703	—	—	—	0.703	63.7	89.6
3	KUR half-loaded element (Uranium silicon aluminum dispersion alloy)	τ	—	—	0.703	—	—	—	0.703	63.7	89.6

Pm ; General primary membrane stress; PL ; Local primary membrane stress; Pb ; Primary bending stress;
Sy ; Yield point of the design; MS ; Margin of safety τ ; Shear stress

Stress units ;N/mm²

(Ⅱ) -Table A.26 Stress evaluation for 9 m lower side vertical drop (4/6)

No.	Position to be evaluated \ Stress		Stress at initial clamping	Stress due to internal pressure	Impact stress	Primary stress					
						Pm(PL)	2/3 Sy	MS	PL＋Pb	Sy	MS
1	JMTRC Standard fuel element (A,B,C type)	τ	—	—	0.71	—	—	—	0.71	63.8	88.8
2	JMTRC Standard fuel element (φ2.2pin,fix type) (B,C type)	σ_t	—	—	10.2	—	—	—	10.2	63.8	5.25
3	JMTRC Special fuel element (Special A type)	σ_c	—	—	16.8	—	—	—	16.8	63.8	2.79
4	JMTRC Special fuel element (Special B type)	σ_c	—	—	0.59	—	—	—	0.59	63.8	107
5	JMTRC Special fuel element (Special C,Special D type)	σ_c	—	—	17.1	—	—	—	17.1	63.8	2.73
6	JMTRC fuel follower (HF type)	τ	—	—	0.56	—	—	—	0.56	63.8	112
7	JMTRC Standard fuel element (MA,MB,MC type)	τ	—	—	0.70	—	—	—	0.70	63.8	90.1
8	JMTRC Special fuel element (Special MB,Special MC type)	σ_c	—	—	16.6	—	—	—	16.6	63.8	2.84
9	JMTRC fuel follower (MF type)	τ	—	—	0.56	—	—	—	0.56	63.8	112

Pm ; General primary membrane stress; PL ; Local primary membrane stress; Pb ; Primary bending stress;
Sy ; Yield point of the design; MS ; Margin of safety σ_t; Ability of bolt stress σ_c; Compression stress τ; Shear stress

Stress units ;N/mm^2

(Ⅱ) -Table A.26 Stress evaluation for 9 m lower side vertical drop (5/6)

No.	Position to be evaluated \ Stress		Stress at initial clamping	Stress due to internal pressure	Impact stress	Primary stress					
						Pm(PL)	2/3 Sy	MS	PL＋Pb	Sy	MS
1	JMTRC Special fuel element hold down part (Special B type)	σ_c	—	—	24.9	—	—	—	24.9	245	8.83

Pm ; General primary membrane stress; PL ; Local primary membrane stress; Pb ; Primary bending stress;
Sy ; Yield point of the design; MS ; Margin of safety σ_2;Axial stress

Stress units ;N/mm²

(Ⅱ) -Table A.26 Stress evaluation for 9 m lower side vertical drop (6/6)

No.	Position to be evaluated / Stress		Stress at initial clamping	Stress due to internal pressure	Impact stress	Primary stress					
						Pm(PL)	2/3 Sy	MS	PL＋Pb	Sy	MS
1	KUCA coupon type	τ	—	—	0.46	—	—	—	0.46	63.7	138
2	KUCA flat type	τ	—	—	14.2	—	—	—	14.2	63.7	4.5
3	Spectrum converter	σ_c	—	—	0.38	—	—	—	0.38	245	644

Pm ; General primary membrane stress; PL ; Local primary membrane stress; Pb ; Primary bending stress;
Sy ; Yield point of the design; MS ; Margin of safety τ; Shear stress

(2) Lid side vertical drop

Shock absorber deformation is 126.7 mm as shown in (Ⅱ)-Table A.24 and acceleration is 409.8·g as shown in (Ⅱ)-Table A.25 when the package is dropped 9 m vertically onto its top.

(a) Deformation in shock absorber

This shows that deformation in the shock absorber caused by a 9 m vertical drop onto its top is not transmitted to the top area of the inner shell. (Ⅱ)-Fig.A.82 shows an analytical model.

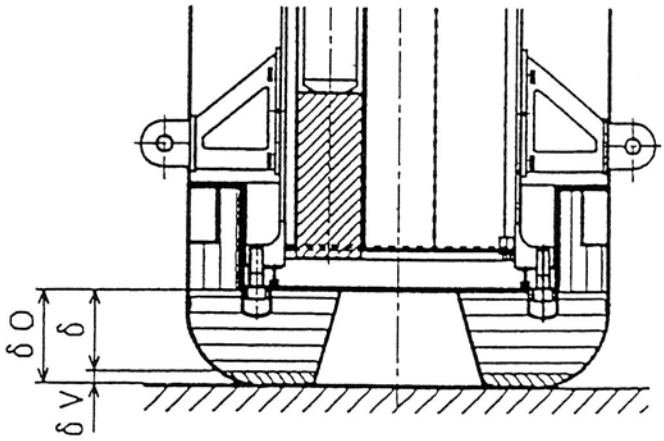

(Ⅱ)-Fig.A.82 Analytical model of interference to inner shell due to shock absorber deformation for 9 m upper side vertical drop

As shown in (Ⅱ)-Fig.A.82, the remaining δ mm of shock absorber after the package is dropped vertically 9 m onto its top is calculated using the following equation.

$\delta = \delta_o - \delta_v$

where

δ_o : Minimum thickness of shock absorber prior to deformation,

δ_o = 186 [mm]

δ_v : Deformation of shock absorber, δ_v = 126.7 [mm]

The remained thickness is,

δ = 186 - 126.7 = 59.3 [mm]

This shows that deformation in the shock absorber caused by a 9 m vertical drop onto its top is not transmitted to the inner shell lid.

(b) Stress generated in various parts of package

The analysis procedures and evaluation positions described in section (Ⅱ)A.5.3(8) are used and the analysis and evaluation results are both listed in (Ⅱ)-Table A.27.

Stress units ;N/mm²

(Ⅱ) -Table A.27 Stress evaluation for 9 m upper side vertical drop (1/6)

No.	Position to be evaluated / Stress			Stress at initial clamping	Stress due to internal pressure	Impact stress	Primary stress					
							Pm(PL)	2/3 Su	MS	PL+Pb	Su	MS
1	Frame of Inner shell		σ_r	—	-0.0491	—	156	310	0.987	—	—	—
			σ_θ		2.31	—						
			σ_z		1.15	-155						
2	Bottom plate of inner shell	Inner Surface	σ_r	—	3.18	-137	0.098	310	3162	134	466	2.47
			σ_θ		0.953	-41.1						
			σ_z		-0.098	0						
		Outer Surface	σ_r	—	-3.18	137	4.23	310	72.2	138	466	2.37
			σ_θ		-0.953	41.1						
			σ_z		0	-4.23						
3	Inner shell lid	Inner Surface	σ_r	—	-3.27	-193	10.1	2/3 Sy 458	44.3	186	Sy 687	2.69
			σ_θ		-3.27	-193						
			σ_z		-0.098	-10.0						
		Outer Surface	σ_r	—	3.27	193	—	—	—	196	Sy 687	2.50
			σ_θ		3.27	193						
			σ_z		0	0						
4	Inner shell lid clamping bolt		σ_t	174	3.20	150	327	2/3 Sy 458	0.400	—	—	—
			σ_b	—	—	—						
			τ			—						

Pm ; General primary membrane stress; PL ; Local primary membrane stress; Pb ; Primary bending stress; Sy ; Yield point of the design; Su ; Design tensile strength; MS ; Margin of safety σ_r; Diameter direction stress σ_o; Periphery direction stress σ_z; Axial stress σ_b; Bending stress σ_t; Stress of the part fuel plater pin

(Ⅱ) -Table A.27 Stress evaluation for 9 m upper side vertical drop (2/6)

Stress units ;N/mm²

No.	Position to be evaluated / Stress		Stress at initial clamping	Stress due to internal pressure	Impact stress	Primary stress					
						Pm(PL)	2/3 Sy	MS	PL＋Pb	Sy	MS
1	JRR-3 standard element (Uranium silicon aluminum dispersion alloy)	τ	—	—	0.958	—	—	—	0.958	63.8	65.5
2	JRR-3 follower element (Uranium silicon aluminum dispersion alloy)	τ	—	—	0.783	—	—	—	0.783	63.8	80.4
3	JRR-4 B type element	τ	—	—	0.718	—	—	—	0.718	63.8	87.9
4	JRR-4 L type element	τ	—	—	1.133	—	—	—	1.133	63.8	55.3
5	JRR-4 (Uranium silicon aluminum dispersion alloy)	τ	—	—	0.987	—	—	—	0.987	63.8	63.6
6	JMTR standard element	τ	—	—	0.973	—	—	—	0.973	63.8	64.5
7	JMTR follower	τ	—	—	0.815	—	—	—	0.815	63.8	77.2

Pm ; General primary membrane stress; PL ; Local primary membrane stress; Pb ; Primary bending stress;
Sy ; Yield point of the design; MS ; Margin of safety τ ; Shear stress

(Ⅱ) -Table A.27 Stress evaluation for 9 m upper side vertical drop (3/6)

Stress units ;N/mm²

No.	Position to be evaluated / Stress		Stress at initial clamping	Stress due to internal pressure	Impact stress	Primary stress					
						Pm(PL)	2/3 Sy	MS	PL＋Pb	Sy	MS
1	KUR standard (Uranium silicon aluminum dispersion alloy)	τ	—	—	0.741	—	—	—	0.741	63.7	84.9
2	KUR Special element (Uranium silicon aluminum dispersion alloy)	τ	—	—	0.741	—	—	—	0.741	63.7	84.9
3	KUR half-loaded element (Uranium silicon aluminum dispersion alloy)	τ	—	—	0.741	—	—	—	0.741	63.7	84.9

Pm ; General primary membrane stress; PL ; Local primary membrane stress; Pb ; Primary bending stress;
Sy ; Yield point of the design; MS ; Margin of safety τ ; Shear stress

Stress units ;N/mm^2

(Ⅱ) -Table A.27 Stress evaluation for 9 m upper side vertical drop (4/6)

No.	Position to be evaluated \ Stress		Stress at initial clamping	Stress due to internal pressure	Impact stress	Primary stress					
						Pm(PL)	2/3 Sy	MS	PL＋Pb	Sy	MS
1	JMTRC Standard fuel element (A,B,C type)	τ	—	—	0.74	—	—	—	0.74	63.8	85.2
2	JMTRC Standard fuel element (ϕ2.2pin,fix type) (B,C type)	σ_t	—	—	10.8	—	—	—	10.8	63.8	4.90
3	JMTRC Special fuel element (Special A type)	σ_c	—	—	17.7	—	—	—	17.7	63.8	2.60
4	JMTRC Special fuel element (Special B type)	σ_c	—	—	0.63	—	—	—	0.63	63.8	100
5	JMTRC Special fuel element (Special C,Special D type)	σ_c	—	—	18.1	—	—	—	18.1	63.8	2.52
6	JMTRC fuel follower (HF type)	τ	—	—	0.59	—	—	—	0.59	63.8	107
7	JMTRC Standard fuel element (MA,MB,MC type)	τ	—	—	0.73	—	—	—	0.73	63.8	86.3
8	JMTRC Special fuel element (Special MB,Special MC type)	σ_c	—	—	17.6	—	—	—	17.6	63.8	2.62
9	JMTRC fuel follower (MF type)	τ	—	—	0.59	—	—	—	0.59	63.8	107

Pm ; General primary membrane stress; PL ; Local primary membrane stress; Pb ; Primary bending stress;
Sy ; Yield point of the design; MS ; Margin of safety σ_t; Stress of the part fuel plater pin τ ; Shear stress σ_c; Compression stress

Stress units ;N/mm^2

(Ⅱ) -Table A.27 Stress evaluation for 9 m upper side vertical drop (5/6)

No.	Position to be evaluated / Stress		Stress at initial clamping	Stress due to internal pressure	Impact stress	Primary stress					
						Pm(PL)	2/3 Sy	MS	PL＋Pb	Sy	MS
1	JMTRC Special fuel element hold down part (Special A type)	σ_c	—	—	45.7	—	—	—	45.7	245	4.36
2	JMTRC Special fuel element hold down part (Special B type)	σ_c	—	—	26.3	—	—	—	26.3	245	8.31
3	JMTRC Special fuel element hold down part (Special C,Special D type)	σ_c	—	—	47.4	—	—	—	47.4	245	4.16
4	JMTRC Special fuel element hold down part (Special MB,Special MC type)	σ_c	—	—	47.4	—	—	—	47.4	245	4.16

Pm ; General primary membrane stress; PL ; Local primary membrane stress; Pb ; Primary bending stress;
Sy ; Yield point of the design; MS ; Margin of safety σ_t; Compression stress

Stress units ;N/mm^2

(Ⅱ) -Table A.27 Stress evaluation for 9 m upper side vertical drop (6/6)

No.	Position to be evaluated / Stress		Stress at initial clamping	Stress due to internal pressure	Impact stress	Primary stress					
						Pm(PL)	2/3 Sy	MS	PL＋Pb	Sy	MS
1	KUCA coupon type	τ	—	—	0.50	—	—	—	0.50	63.7	127
2	KUCA flat type	τ	—	—	15.0	—	—	—	15.0	63.7	4.2
3	Spectrum converter	σ_c	—	—	0.40	—	—	—	0.40	245	612

Pm ; General primary membrane stress; PL ; Local primary membrane stress; Pb ; Primary bending stress;
Sy ; Yield point of the design; MS ; Margin of safety τ ; Shear stress

A.6.1.2 Horizontal drop

The deformation of 81.6 mm as shown in (Ⅱ)-Table A.24 and acceleration of 367.0·g as shown in (Ⅱ)-Table A.25 are generated in the shock absorber when horizontal drop is 9 m.

(1) Deformation in shock absorber

This shows that the deformation generated in the shock absorber by a 9 m horizontal drop is not transmitted to the inner shell. (Ⅱ)-Fig.A.83 shows an analytical model.

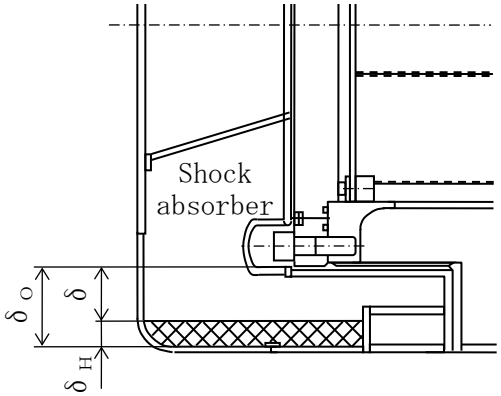

(Ⅱ)-Fig.A.83 Analytical model of interference to inner shell due to shock absorber deformation for 9 m horizontal drop

As shown in (Ⅱ)-Fig.A.83, the remaining δ mm of shock absorber after a 9 m horizontal drop is calculated by the following equation,

$$\delta = \delta_o - \delta_H$$

where

δ_o : Minimum thickness of shock absorber prior to deformation,

δ_o = 104 [mm]

δ_H : Deformation of shock absorber, δ_H = 81.6 [mm]

The remaining thickness is,

δ = 104 - 81.6 = 22.4 [mm]

The deformation produced by a 9 m horizontal drop is limited to the shock absorber and is not transmitted to the inner shell.

(2) Stress generated in package and content

The analysis procedures and evaluation positions described in section (Ⅱ) A.5.3(6) are used and both the analysis and evaluation results are listed in (Ⅱ)-Table A.28.

Stress units ;N/mm²

(Ⅱ) -Table A.28 Stress evaluation for 9 m horizontal drop (1/6)

No.	Position to be evaluated \ Stress		Stress at initial clamping	Stress due to internal pressure	Impact stress	Primary stress					
						Pm(PL)	2/3Su	MS	PL＋Pb	Su	MS
1	Frame of Inner shell	σ_r	—	-0.0491	—	2.36	310	130	253	466	0.841
		σ_θ		2.31	—						
		σ_z		1.15	252						
2	Bottom area of inner shell	σ_r	—	3.18	—	0.098	310	3162	125	466	2.72
		σ_θ		0.953	—						
		σ_z		-0.098	—						
		τ		—	62.6						
3	Top area of inner shell	σ_r	—	-0.0491	—	2.36	2/3 Sy 120	50.6	20.0	Sy 180	8.00
		σ_θ		2.31	—						
		σ_z		1.15	—						
		τ		—	9.93						
4	Inner shell lid clamping bolt	σ_t	174	3.20	—	177	2/3 Sy 458	1.58	184	Sy 687	2.73
		σ_b	—	—	6.78						
		τ	—	—	—						
5	Rectangular fuel basket	σ_x	—	—	255	—	—	—	255	466	0.827
		σ_y									
		σ_z									

Pm ; General primary membrane stress; PL ; Local primary membrane stress; Pb ; Primary bending stress;
Sy ; Yield point of the design; Su ; Design tensile strength; MS ; Margin of safety σ_r; Diameter direction stress σ_o; Periphery direction stress σ_2; Axial stress
σ_b; Bending stress σ_t; Stress of the part fuel plater pin τ ; Shear stress

Stress units ;N/mm²

(Ⅱ) -Table A.28 Stress evaluation for 9 m horizontal drop (2/6)

No.	Position to be evaluated / Stress			Stress at initial clamping	Stress due to internal pressure	Impact stress	Primary stress					
							Pm(PL)	2/3 Sy	MS	PL＋Pb	Sy	MS
1	JRR-3 standard element (Uranium silicon aluminum dispersion alloy)	Surface directio	σ_b	—	—	28.8	—	—	—	28.8	63.8	1.21
		Axial directio	σ_c	—	—	1.94	—	—	—	1.94	63.8	31.8
2	JRR-3 follower element (Uranium silicon aluminum dispersion alloy)	Surface directio	σ_b	—	—	19.0	—	—	—	19.0	63.8	2.35
		Axial directio	σ_c	—	—	1.63	—	—	—	1.63	63.8	38.1
3	JRR-4 B type element	Surface directio	σ_b	—	—	23.1	—	—	—	23.1	63.8	1.76
		Axial directio	σ_c	—	—	1.68	—	—	—	1.68	63.8	36.9
4	JRR-4 L type element	Surface directio	σ_b	—	—	24.6	—	—	—	24.6	63.8	1.59
		Axial directio	σ_c	—	—	2.34	—	—	—	2.34	63.8	26.2
5	JRR-4 (Uranium silicon aluminum dispersion alloy)	Surface directio	σ_b	—	—	31.8	—	—	—	31.8	63.8	1.00
		Axial directio	σ_c	—	—	2.17	—	—	—	2.17	63.8	28.4
6	JMTR standard element	Surface directio	σ_b	—	—	29.6	—	—	—	29.6	63.8	1.15
		Axial directio	σ_c	—	—	1.99	—	—	—	1.99	63.8	31.0
7	JMTR follower	Surface directio	σ_b	—	—	20.1	—	—	—	20.1	63.8	2.17
		Axial directio	σ_c	—	—	1.71	—	—	—	1.71	63.8	36.3

Pm ; General primary membrane stress; PL ; Local primary membrane stress; Pb ; Primary bending stress;
Sy ; Yield point of the design; MS ; Margin of safety σ_b; Bending stress σ_c; Compression stress

Stress units

(Ⅱ) -Table A.28 Stress evaluation for 9 m horizontal drop (3/6)

;N/mm^2

No.	Position to be evaluated / Stress			Stress at initial clamping	Stress due to internal pressure	Impact stress	Primary stress					
							Pm(PL)	2/3 Sy	MS	PL＋Pb	Sy	MS
1	KUR standard (Uranium silicon aluminum dispersion alloy)	Surface directio	σ_b	—	—	20.1	—	—	—	20.1	63.7	2.16
		Axial directio	σ_c	—	—	1.54 *1	1.54	4.67	2.03	—	—	—
2	KUR half-loaded element (Uranium silicon aluminum	Surface directio	σ_b	—	—	20.1	—	—	—	20.1	63.7	2.16
		Axial directio	σ_c	—	—	1.54 *1	1.54	4.67	2.03	—	—	—
3	KUR Special element (Uranium silicon aluminum dispersion alloy)	Surface directio	σ_b	—	—	20.1	—	—	—	20.1	63.7	2.16
		Axial directio	σ_c	—	—	1.33 *1	1.33	4.67	2.51	—	—	—

Pm ; General primary membrane stress; PL ; Local primary membrane stress; Pb ; Primary bending stress;

Sy ; Yield point of the design; Su ; Design tensile strength; MS ; Margin of safety σ_b; Bending stress σ_c; Compression stress

*1 ; axial compression stress

Stress units ;N/mm²

(Ⅱ) -Table A.28 Stress evaluation for 9 m horizontal drop (4/6)

No.	Position to be evaluated / Stress			Stress at initial clamping	Stress due to internal pressure	Impact stress	Primary stress					
							Pm(PL)	2/3 Sy	MS	PL＋Pb	Sy	MS
1	JMTRC Standard fuel element (A,B,C type)	Surface directio	σ_b	—	—	22.4	—	—	—	22.4	63.8	1.84
		Axial directio	σ_c	—	—	1.59	—	—	—	1.59	63.8	39.1
2	JMTRC Standard fuel element (φ2.2pin,fix type) (B,C type)	Surface directio	σ_b	—	—	22.2	—	—	—	22.2	63.8	1.87
		Axial directio	σ_c	—	—	1.58	—	—	—	1.58	63.8	39.3
3	JMTRC Special fuel element (Special A type)	Surface directio	σ_b	—	—	33.4	—	—	—	33.4	63.8	0.91
		Axial directio	σ_c	—	—	1.59	—	—	—	1.59	63.8	39.1
4	JMTRC Special fuel element (Special B type)	Surface directio	σ_b	—	—	22.9	—	—	—	22.9	63.8	1.78
		Axial directio	σ_c	—	—	1.98	—	—	—	1.98	63.8	31.2
5	JMTRC Special fuel element (Special C, Special D type)	Surface directio	σ_b	—	—	33.4	—	—	—	33.4	63.8	0.91
		Axial directio	σ_c	—	—	2.39	—	—	—	2.39	63.8	25.6
6	JMTRC fuel follower (HF type)	Surface directio	σ_b	—	—	14.3	—	—	—	14.3	63.8	3.46
		Axial directio	σ_c	—	—	1.29	—	—	—	1.29	63.8	48.4
7	JMTRC Standard fuel element (MA,MB,MC type)	Surface directio	σ_b	—	—	22.3	—	—	—	22.3	63.8	1.86
		Axial directio	σ_c	—	—	1.57	—	—	—	1.57	63.8	39.6
8	JMTRC Special fuel element (Special MB, Special MC type)	Surface directio	σ_b	—	—	33.2	—	—	—	33.2	63.8	0.92
		Axial directio	σ_c	—	—	1.56	—	—	—	1.56	63.8	39.8
9	JMTRC fuel follower (MF type)	Surface directio	σ_b	—	—	14.4	—	—	—	14.4	63.8	3.43
		Axial directio	σ_c	—	—	1.31	—	—	—	1.31	63.8	47.7

Pm ; General primary membrane stress; PL ; Local primary membrane stress; Pb ; Primary bending stress;

Sy ; Yield point of the design; MS ; Margin of safety σ_b; Bending stress σ_c; Compression stress

Stress units

(Ⅱ) -Table A.28 Stress evaluation for 9 m horizontal drop (5/6)

;N/mm^2

No.	Position to be evaluated \ Stress		Stress at initial clamping	Stress due to internal pressure	Impact stress	Primary stress					
						Pm(PL)	2/3 Sy	MS	PL＋Pb	Sy	MS
1	JMTRC Special fuel element hold down part (Special A type)	σ_b	—	—	13.9	—	—	—	13.9	245	16.6
2	JMTRC Special fuel element hold down part (Special B type)	σ_b	—	—	22.5	—	—	—	22.5	245	9.88
3	JMTRC Special fuel element hold down part (Special C,Special D type)	σ_b	—	—	13.9	—	—	—	13.9	245	16.6
4	JMTRC Special fuel element hold down part (Special MB, Special MC type)	σ_b	—	—	1.39	—	—	—	1.39	245	16.6

Pm ; General primary membrane stress; PL ; Local primary membrane stress; Pb ; Primary bending stress;

Sy ; Yield point of the design; MS ; Margin of safety σ_b; Bending stress

Stress units ;N/mm²

(Ⅱ) -Table A.28 Stress evaluation for 9 m horizontal drop (6/6)

No.	Position to be evaluated / Stress			Stress at initial clamping	Stress due to internal pressure	Impact stress	Primary stress					
							Pm(PL)	2/3 Sy	MS	PL＋Pb	Sy	MS
1	KUCA coupon type		σ_c	—	—	3.19	—	—	—	3.19	63.7	20.0
2	KUCA flat type	Surface direction	σ_b	—	—	0.24	—	—	—	0.24	63.7	265
		Axial direction	σ_c	—	—	1.39	—	—	—	1.39	63.7	45.8
3	Spectrum converter		σ_b	—	—	200.2	—	—	—	200.2	245	0.23

Pm ; General primary membrane stress; PL ; Local primary membrane stress; Pb ; Primary bending stress;
Sy ; Yield point of the design; MS ; Margin of safety σ_b; Bending stress σ_c; Compression stress

A.6.1.3 Corner drop

(1) Deformation of shock absorber

(Ⅱ)-Fig.A.84 shows the deformation and the remaining thickness of the shock absorber. Deformation affects only the external shock absorber and is not transmitted to the inner shell.

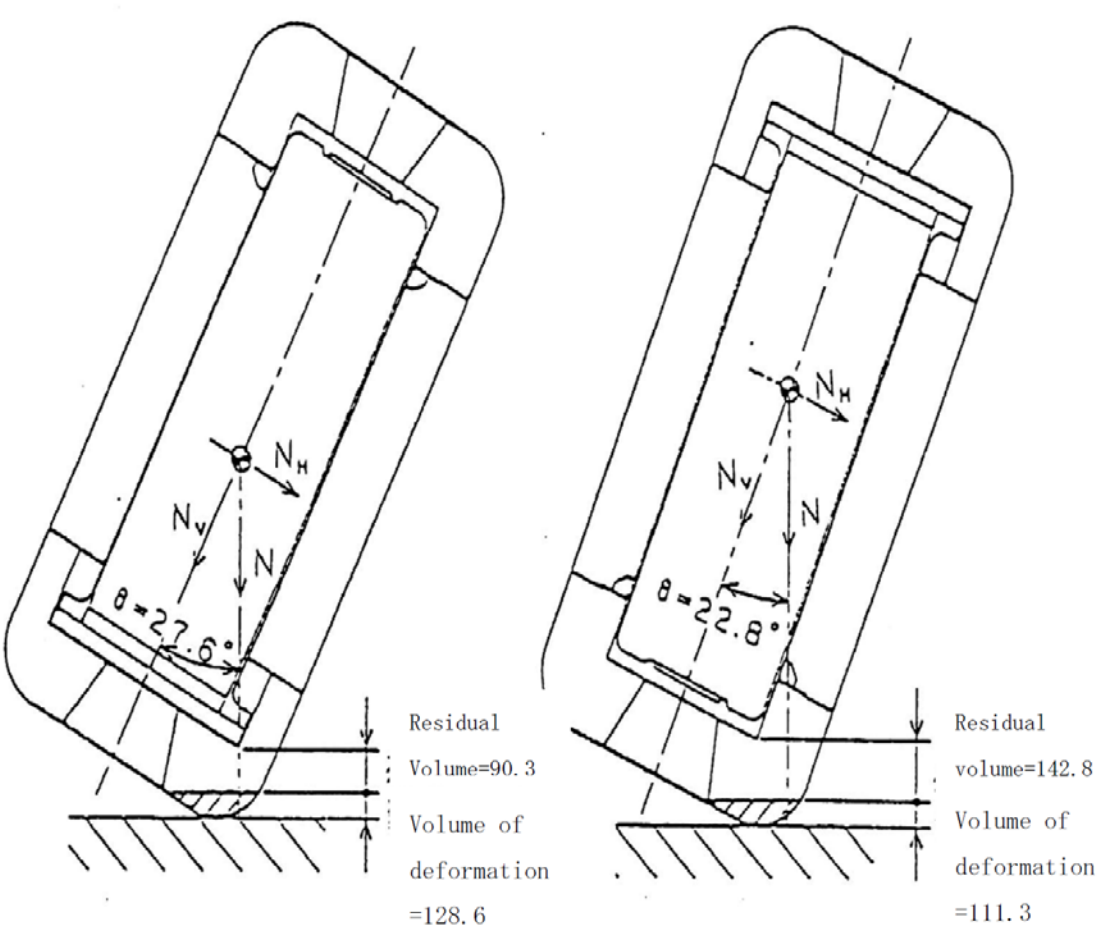

Lid side corner drop　　Bottom side corner drop

(Ⅱ)-Fig.A.84 Analytical model of interference to inner shell due to shock absorber deformation for 9m corner drop

(2) Stresses of packaging and content

(Ⅱ)-Table A.29 shows the design acceleration factors for the corner drop, listed in (Ⅱ)-Table A.25, separated into vertical and horizontal elements.

(Ⅱ)-Table A.29 Design acceleration for corner drop

(×g)

Drop type	Acceleration (N)	Vertical acceleration ($N_V = N\cos\theta$)	Horizontal acceleration ($N_H = N\sin\theta$)
Corner			
Lid side	299.8	265.7	138.9
Bottom side	310.9	286.6	120.5

As (Ⅱ)-Table A.29 shows, acceleration components for all directions are smaller than those for vertical and horizontal drop. For this reason stress analysis is omitted.

The procedures described in section (Ⅱ) A.5.3 (9) are used for the inner lid clamping bolts and the analysis and evaluation results are both listed in (Ⅱ)-Table A.30.

Stress units
;N/mm²

(Ⅱ) -Table A.30 Stress evaluation for 9 m upper corner drop

No.	Position to be evaluated / Stress		Stress at initial clamping	Stress due to internal pressure	Impact stress		Primary stress					
					Horizontal Component	Vertical Component	Pm(PL)	2/3 Sy	MS	PL＋Pb	Sy	MS
1	Inner lid clamping bolt	σ_t	174	3.20			177	459	1.58	411	687	0.671
		σ_b	—	—	7.73	226						
		τ										

Pm ; General primary membrane stress; PL ; Local primary membrane stress; Pb ; Primary bending stress;
Sy ; Yield point of the design; MS ; Margin of safety σ_t ; Ability of bolt stress σ_b ; Bending stress τ ; Shear stress

A.6.1.4 Inclined drop

(1) Bottom side inclined drop

(a) Deformation of shock absorber

(Ⅱ)-Fig.A.85 shows the relationship between the angle at dropping and the deformation.

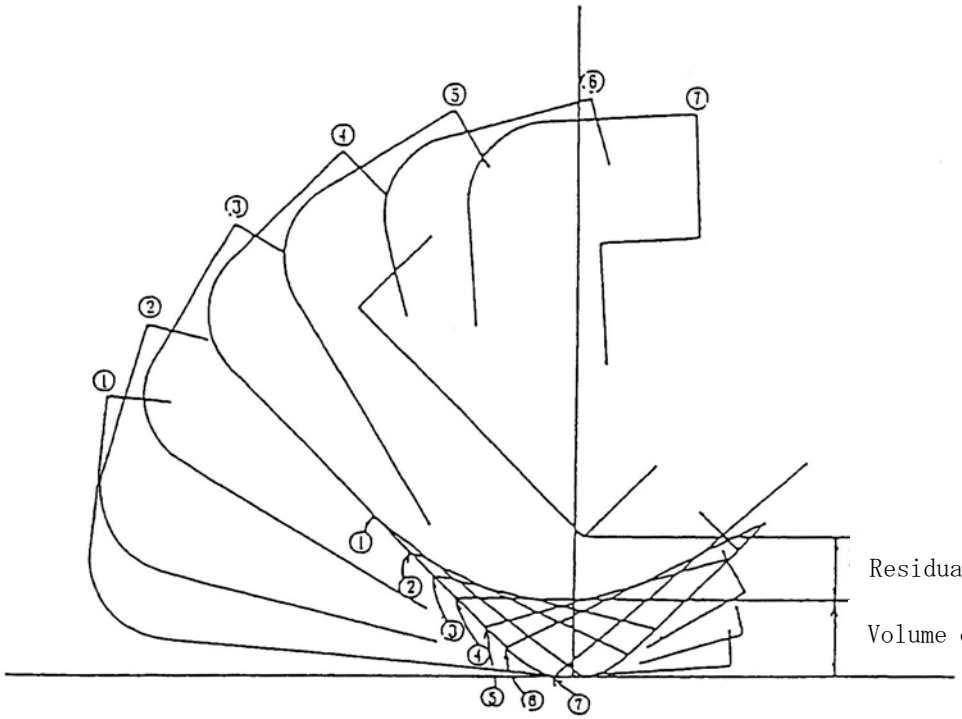

No.	Angle at dropping θ	Minimum thickness of shock absorber before deformation (mm)	Deformation of shock absorber (mm)	Remaining thickness of shock absorber (mm)
①	5°	211.9	36.0	175.9
②	15°	236.8	84.6	152.2
③	30°	260.2	127.1	133.1
④	45°	265.7	135.6	130.1
⑤	60°	252.9	133.5	119.4
⑥	75°	222.6	93.7	128.9
⑦	85°	193.7	44.8	148.9

(Ⅱ)-Fig.A.85 Analytical model of interference to inner shell due to shock absorber deformation for 9m lower side inclined drop

(Ⅱ)-Fig.A.85 shows that in the drop, deformation occurs only in parts of the shock absorber and does not reach the inner shell.

(b) Stresses of packaging and content

(Ⅱ)-Table A.31 shows the horizontal and vertical components of the design acceleration for the bottom side corner drop (Ⅱ)-Table A.25.

(Ⅱ)-Fig.A.86 shows the relationships between the angle of drop and the acceleration.

(Ⅱ)-Table A.31 Relationship between drop angle and acceleration

Angle at dropping θ	Acceleration (G)		
	Acceleration (N)	Vertical component ($N \cdot \cos\theta$)	Horizontal component ($N \cdot \sin\theta$)
5	374.9	373.5	32.7
15	364.1	351.7	94.2
30	273.1	236.5	136.6
45	249.8	176.6	176.6
60	257.4	128.7	222.9
75	244.5	63.3	236.2
85	211.2	18.4	210.4

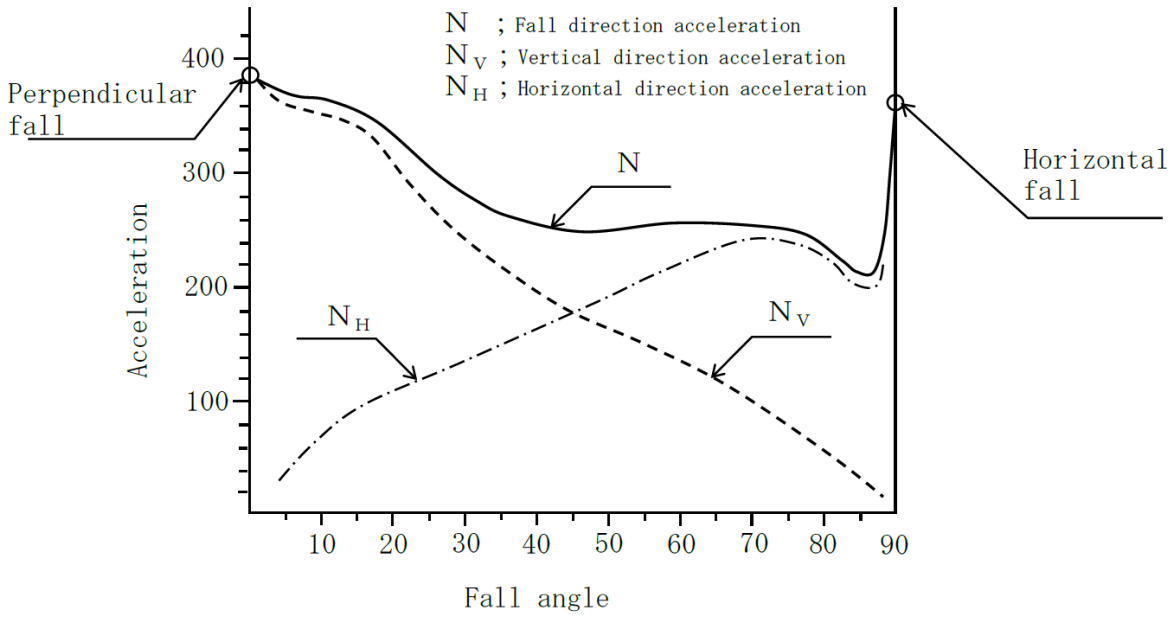

(Ⅱ)-Fig.A.86 Relationship between acceleration and drop angle for 9m lower side inclined drop

(Ⅱ)-Table A.31 shows that each accelerating component is smaller than the acceleration recorded for the vertical and horizontal drop. Hence, stress is not analyzed here.

(2) Lid side inclined drop

(a) Deformation of the shock absorber

(Ⅱ)-Fig.A.87 shows the relationship between the angle at dropping and the deformation.

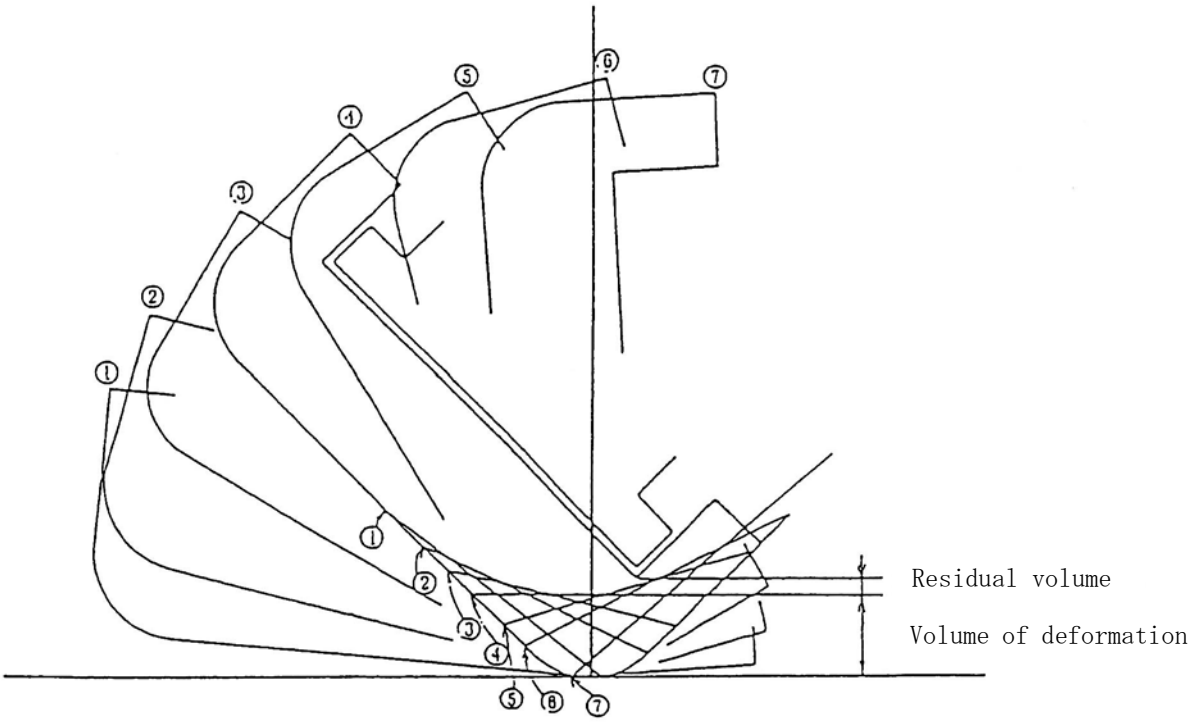

No.	Angle at dropping θ	Minimum thickness of shock absorber before deformation (mm)	Deformation in shock absorber (mm)	Remaining thickness of shock absorber (mm)
①	5°	201.1	35.7	165.4
②	15°	210.5	85.2	125.3
③	30°	212.2	133.9	78.3
④	45°	199.1	145.2	53.9
⑤	60°	171.9	129.6	42.3
⑥	75°	132.7	98.4	34.3
⑦	85°	101.1	49.5	51.6

(Ⅱ)-Fig.A.87 Analytical model of interference to inner shell due to shock absorber deformation for 9 m upper side inclined drop

(Ⅱ)-Fig.A.87 shows that deformation only occurs in parts of the shock absorber and does not reach the inner shell.

(b) Stresses on the packaging and content

(Ⅱ)-Table A.32 shows the horizontal and vertical components of the design acceleration when dropped on the lid side corner (Ⅱ)-Table A.25.

(Ⅱ)-Fig.A.88 shows the relationships between the angle of dropping and the acceleration.

(Ⅱ)-Table A.32 Relationship between drop angle and acceleration for drop test Ⅰ

Angle at dropping θ	Acceleration (G)		
	Acceleration (N)	Vertical component ($N \cdot \cos\theta$)	Horizontal component ($N \cdot \sin\theta$)
5	384.3	382.8	33.5
15	356.3	344.2	92.2
30	289.9	251.1	145.0
45	268.0	189.5	189.5
60	256.3	128.2	222.0
75	273.3	70.7	264.0
85	254.3	22.2	253.3

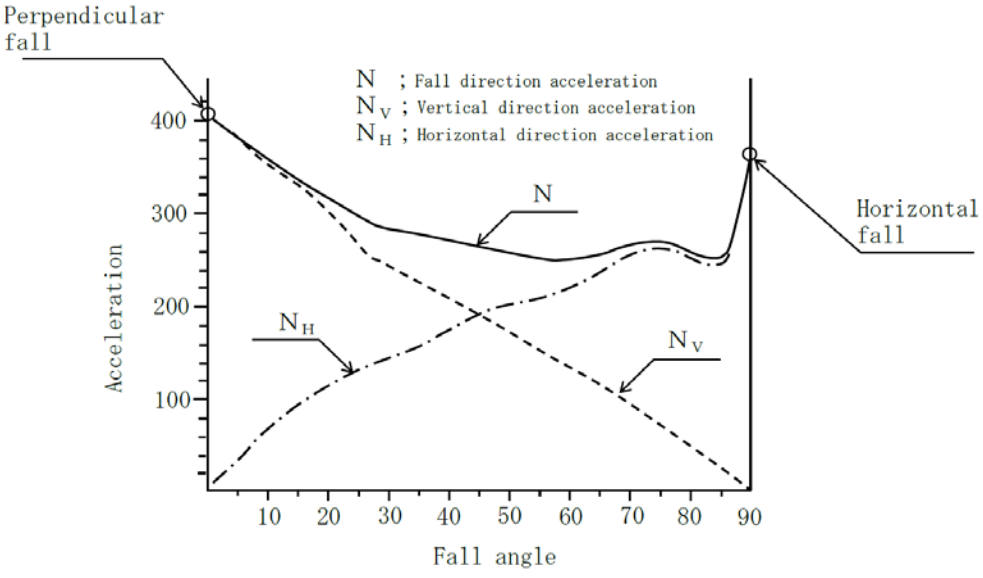

(Ⅱ)-Fig.A.88 Relationship between acceleration and drop angle for 9 m upper side inclined drop

(Ⅱ)-Table A.32 shows that each acceleration component is smaller than the acceleration recorded for the horizontal and vertical drop. Hence, stress is not analyzed here

A.6.1.5 Summary of the results

We will describe here what deformations occur on the package observed in the mechanical test (drop I). The analysis will evaluate the possibility of the inner shell being damaged.

(Ⅱ)-Table A.33 shows the deformations in various drop tests.

(Ⅱ)-Table A.33 Relationship between drop angle and acceleration for drop test Ⅱ

Item / Drop type		Analyzed part of shock absorber	Minimum thickness of shock absorber before deformation (mm)	Deformation in shock absorber (mm)	Remaining thickness of shock absorber (mm)	Design acceleration ×g(m/s^2)
Vertical drop		Lid side end	186	126.7	59.3	409.8
		Bottom side end	194	106.3	87.7	388.4
Horizontal drop		Cylindrical part	104	81.6	22.4	367.0
Corner drop		Lid side end	218.9	128.6	90.3	299.8
		Bottom side end	254.1	111.3	142.8	310.9
Inclined drop	5°	Lid side end	201.1	35.7	165.4	384.3
		Bottom side end	211.9	36.0	175.9	374.9
	15°	Lid side end	210.5	85.2	125.3	356.3
		Bottom side end	236.8	84.6	152.2	364.1
	30°	Lid side end	212.2	133.9	78.3	289.9
		Bottom side end	260.2	127.1	133.1	273.1
	45°	Lid side end	199.1	145.2	53.9	268.0
		Bottom side end	265.7	135.6	130.1	249.8
	60°	Lid side end	171.9	129.6	42.3	256.3
		Bottom side end	252.9	133.5	119.4	257.4
	75°	Lid side end	132.7	98.4	34.3	273.3
		Bottom side end	222.6	93.7	128.9	244.5
	85°	Lid side end	101.1	49.5	51.6	254.3
		Bottom side end	193.7	44.8	148.9	211.2

(Ⅱ)-Table A.33 shows that deformation occurs only in parts of the shock absorber and does not reach the inner shell in a bottom side corner drop.

(Ⅱ)-Tables A.26, A.27, A.28 and A.30 show that stress occurring on the packaging and content for each drop does not exceed the standard value, and therefore does not cause any damage to them.

Thus, the package do not affect the containments and shielding performance of the packaging.

A.6.2 Mechanical test --- Drop test Ⅱ (1 m drop)

In this section we will analyze the package on the assumption that drop test Ⅱ is carried out after drop test I.

We will examine here how the package is affected when it is dropped from the height of one meter onto a mild steel cylinder with a diameter of 150 mm.

(Ⅱ)-Fig.A.89 shows the package to be examined in this section for three different drops:

(a) Vertical lid side drop (direct hit on to the outer lid)

(b) Vertical bottom side drop (direct hit on to the outer shell bottom plate)

(c) Horizontal drop (direct hit on to the outer shell).

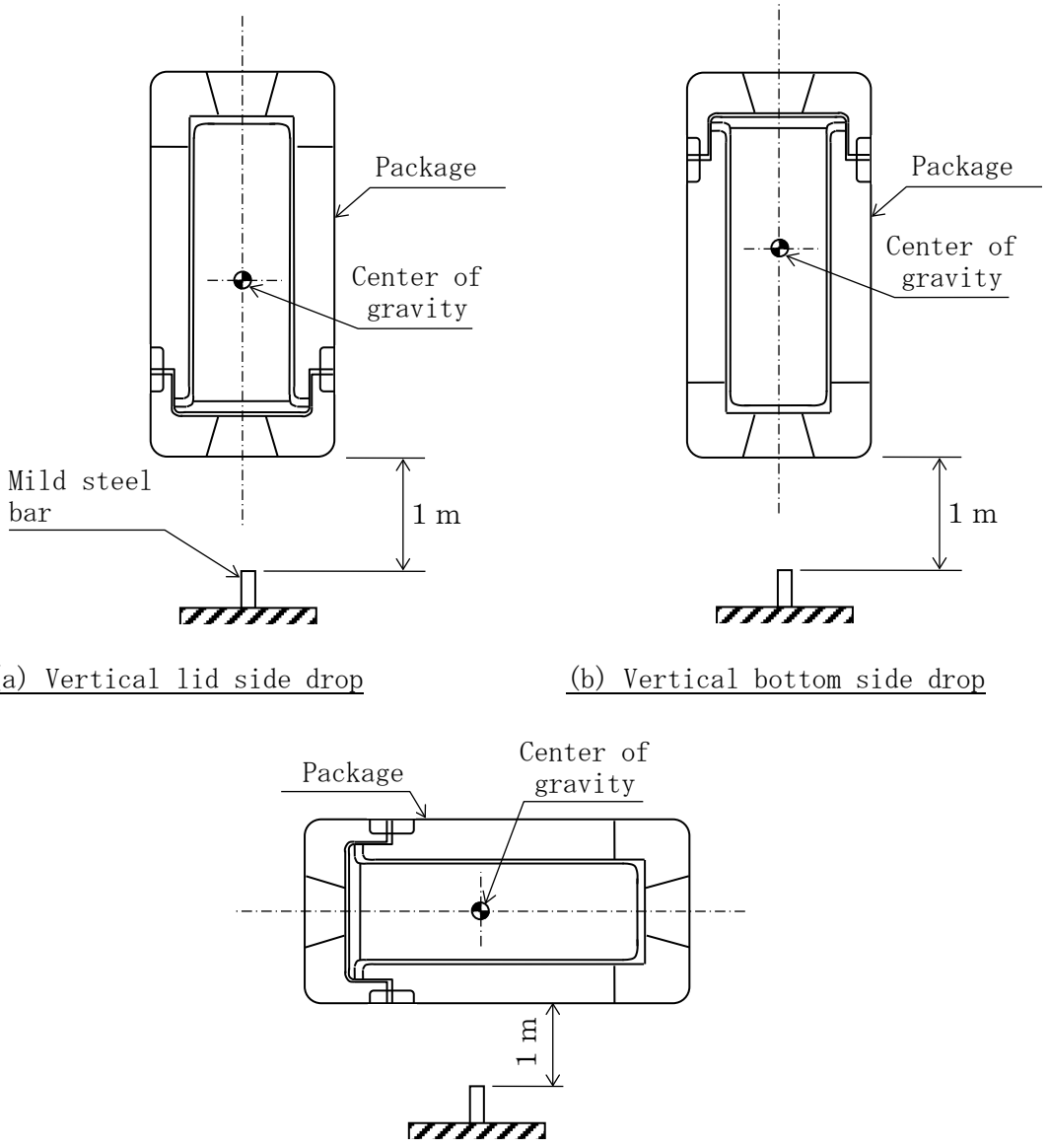

(a) Vertical lid side drop

(b) Vertical bottom side drop

(c) Horizontal drop (direct hit on to the outer shell)

(Ⅱ)-Fig.A.89 Analytical model for drop test Ⅱ

(1) Penetration

We will demonstrate in this section that the evaluated portions shown in (Ⅱ)-Fig.A.89 are not penetrated.

In the analyses, the contributions from the shock absorber and heat insulator under the outer shell is neglected on the assumption that the entire energy will be consumed in the transformation of the outer steel plate of the outer shell. Thus, the evaluation will ensure the maximum of safety.

(a) Direct hit of outer lid onto test cylinder (vertical drop) with the lid side end directed downwards.

(Ⅱ)-Fig.A.82(a) shows the case of a direct hit of the outer lid onto the mild steel test cylinder, the dropping energy Uo of the package is obtained by the equation.

$$Uo = m \cdot g \cdot H$$

where

m: Weight of the package, m = 950 [kg]

H: Height from which the package is dropped, H = 1000 [mm]

g: Gravitational acceleration, g = 9.81 [m/s^2]

Thus, Uo is,

$$Uo = 950 \times 9.81 \times 1000 = 9.32 \times 10^6 \ [N \cdot mm]$$

The deformation (U) is obtained on the assumption that the dropping energy Uo is equal to the deforming energy U.

$$U = \sigma_s \cdot V$$

where

σ_s: Stress on the panel, $\sigma s = 466 \ [N/mm^2]$

V: Volume of panel deformed,

$$V = \{\pi(d + t)t\} \ \delta \quad [mm^3]$$

d: Diameter of mild steel cylinder, d = 150 [mm]

t: Thickness of the panel, t = 6 [mm]

δ: Deformation [mm]

On the assumption that Uo is equal to U,

$$9.32 \times 106 = 466 \times \{\pi \cdot (150 + 6) \cdot 6\} \cdot \delta$$

Hence,

δ = 6.8 [mm]

When the deformation of 126.7 mm caused in drop test I is added to the above value, we obtain 133.5 mm. As the minimum thickness before deformation of the heat insulator is 186 mm, its remaining thickness after deformation is 52.5 mm. Therefore, deformation does not reach the inner shell.

The strength of the outer lid panel is evaluated on the assumption that the deformational strain is smaller than the specified elongation of the material. Drop test Ⅱ will not cause any penetration in the panel.

(Ⅱ)-Fig.A.90 shows an analytical model of the panel.

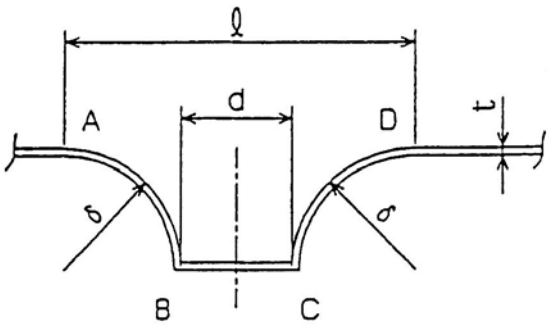

(Ⅱ)-Fig.A.90 Analytical model for penetration strength under conditions of drop test Ⅱ

As (Ⅱ)-Fig.A.90 shows, the elongation (Δ1) of the outer lid panel under the conditions of drop test Ⅱ is obtained by the equation

$\Delta 1 = 1' - 1$

where

1': Length of the panel after deformation,

$$1' = \left(2 \times \frac{\pi}{2}\delta + d\right) \text{ [mm]}$$

1: Length of the panel before deformation, 1 = 2 × δ + d [mm]

δ: Deformation, δ = 6.8 [mm]

d: Diameter of the mild steel bar, d = 150 [mm]

Therefore,

$$\Delta 1 = \left(2 \times \frac{\pi}{2} \cdot \delta + d\right) - (2 \cdot \delta + d) = 1.14 \cdot \delta$$

The strain ε in the case of such an elongation is

$$\varepsilon = \frac{\Delta 1}{1} = \frac{1.14\delta}{2\delta + d} = \frac{1.14 \times 6.8}{2 \times 6.8 + 150} = 0.047$$

The strain in head plate is 4.7 (%). Because the outer lid head plate of type SUS 304 has a specified elongation of more than 40 % before penetration, no real penetration can occur.

(b) Direct hit of the outer shell bottom plate onto the mild steel bar (Vertical drop, bottom side down)

As shown in (Ⅱ)-Fig.A.89 (b), the deformation δ produced when the bottom plate of the outer shell directly hits the mild steel bar, is 6.8mm because the thickness and materials of the bottom plate and head plate are the same as those described in the preceding section.

When the above value is added to the deformation value of 106.3 mm obtained in drop test I, 113.1 mm is obtained. As the minimum thickness of the heat insulator before deformation is 194 mm, its remaining thickness after deformation is 80.9 mm. Therefore, deformation does not reach the inner shell.

The strain is 4.7 %, the same as that described in the preceding section, and likewise, the elongation before penetration is 40 %. Therefore, no penetration occurs in the outer shell bottom plate.

(c) Direct hit of the outer shell on to mild steel bar (horizontal drop)

As (Ⅱ)-Fig.A.89(c) shows, the deformation δ which occurs when the outer shell directly hits the mild steel bar is obtained by the equation

$$Uo = \sigma_s \cdot \{\pi (d + t) \cdot t\} \delta$$

Where

Uo : Dropping energy, Uo = 9.32×106 [N/mm]

d: Diameter of the mild steel bar, d = 150 [mm]

t: Thickness of shell plate, t = 3 [mm]

σs: Deforming stress on the shell, σ_s = 466 [N/mm^2]

Hence,

$$9.32 \times 10^6 = 466 \times \{\pi (150 + 3) \times 3\} \times \delta$$

$$\delta = 13.9 \text{ [mm]}$$

When the above value is added to the value of deformation 81.6 mm obtained in drop test I, 95.5 mm is obtained. As the remaining thickness of the heat insulator before deformation is 177 mm, its remaining thickness after deformation is 81.5 mm. Therefore, deformation does not reach the inner shell.

As in the preceding cases, the strain ε is obtained by the following equation.

$$\varepsilon = \frac{\Delta 1}{1} = \frac{1.14\delta}{2\delta + d}$$

where

$\Delta 1$: Elongation [mm]

1: Length before deformation [mm]

δ: Deformation, δ = 13.9 [mm]

d: Diameter of the mild steel bar, d = 150 [mm]

Hence,

$$\varepsilon = \frac{1.14 \times 13.9}{2 \times 13.9 + 150} = 0.089$$

The strain in the shell sheet is 8.9 %. Because the outer lid head plate of type SUS304 has an elongation of more than 40 % before penetration, no real penetration can occur.

(2) Study of the packaging

The packages acceleration which occurs at the 1m drop will be obtained in this section.

(a) Lid side vertical drop

The acceleration, N, of the package which occurs when the outer lid directly hits the mild steel bar (see (Ⅱ)-Fig.A.89(a)) is obtained by using the analytical model (see (Ⅱ)-Fig.A.90) and the following equation,

$$N = \frac{F}{m} \quad [m/s^2]$$

where

F: Reaction force in the deformation of the panel,

$F = \sigma s \cdot \pi \cdot (d + t) \cdot t$ [N]

σs: Deforming stress in the panel, σs = 466 [N/mm^2]

d: Diameter of the mild steel bar, d = 150 [mm]

t: Thickness of the panel, t = 6 [mm]

m: Weight of the package, m = 950 [kg]

Therefore, N is,

$$N = \frac{466 \times \pi \times (150 + 6) \times 6}{950} = 1442 = 147.0 \cdot g \ [m/s^2]$$

(b) Bottom side vertical drop

The acceleration, N, of the package which occurs when the outer lids bottom plate directly hits the mild steel bar (see (Ⅱ)-Fig.A.89(b)) is 147.0·g because the thickness and material of the head plate is the same as those described in the preceding section.

(c) Horizontal drop

The acceleration, N, of the package which occurs when the outer shell directly hits the mild steel bar (see (Ⅱ)-Fig.A.89(c))is obtained by using the analytical model (see (Ⅱ)-Fig.A.90) and the following equation,

$$N = \frac{F}{m} \ [m/s^2]$$

where

F: Reaction force in the deformation of the panel,

$F = \sigma s \cdot \pi \cdot (d + t) \cdot t$ [N]

σs: Deforming stress in the panel, σs = 466 [N/mm^2]

d: Diameter of the mild steel bar, d = 150 [mm]

t: Thickness of the panel, t = 3 [mm]

m: Weight of the package, m = 950 [kg]

Hence, N is

$$N = \frac{466 \times \pi \times (150 + 3) \times 3}{950} = 707 = 72.1 \cdot g \ [m/s^2]$$

This result of the analysis is smaller than the design acceleration obtained in drop test I ((Ⅱ)-Table A.33 shows horizontal: 367.0·g, vertical/lid side end: 409.8·g; vertical/bottom side end: 388.4·g). For this reason, stresses are not analyzed in this section.

A.6.2.1 Summary of the results

(Ⅱ)-Table A.34 shows the results of the analyses and evaluation of drop test Ⅱ/mechanical test.

(Ⅱ)-Table A.34 Evaluation of penetration for drop test Ⅱ

(1) Deformation

No.	Evaluated position	Minimum insulator thickness before deformation (mm)	Deformation in drop test Ⅰ (mm)	Deformation in drop test Ⅱ (mm)	Remaining thickness (mm)
1	Outer shell lid	186	126.7	6.8	52.5
2	Outer shell bottom plate	194	106.3	6.8	80.9
3	Frame of outer shell	177	81.6	13.9	81.5

(2) Deformed strain

No.	Evaluated position	Reference in analysis	Reference value in analysis	Result	Margin of safety
1	Outer shell lid	Rupture strain	40 %	4.7 %	7.51
2	Outer shell bottom plate	Rupture strain	40 %	4.7 %	7.51
3	Frame of outer shell	Rupture strain	40 %	8.9 %	3.49

(3) Acceleration

No.	Evaluated position	Reference in analysis	Reference value in analysis	Result	Margin of safety
1	Outer shell lid	Acceleration in drop test Ⅰ	409.8・g	147.0・g	1.79
2	Outer shell bottom plate	Acceleration in drop test Ⅰ	388.4・g	147.0・g	1.64
3	Frame of outer shell	Acceleration in drop test Ⅰ	367.0・g	72.1・g	4.09

(Ⅱ)- of the packaging and contents are not damaged because the acceleration Table A.34 shows that the deformed strain of different parts observed in drop test Ⅱ is smaller than the reference elongation of SUS304. Therefore, no penetration occurs and the damage in this case does not reach the inner shell.

The acceleration occurring at drop test Ⅱ is lower than that which occurs at drop test Ⅰ.

Thus, dropping conditions that may cause maximum damage to the package do not affect the containment and shielding performance of the packaging.

The main body on is lower than that at drop test I.

A.6.3 Thermal test

A.6.3.1 Summary of temperatures and pressure

In this section, we will describe the outline of the temperatures and pressures to be used in the designing and analysis of the behavior of the package under accident test conditions.

(1) Design temperatures

The evaluation of (Ⅱ)-B.5.3 revealed that the temperature rises up to 209.9℃ in the fuel basket, 483.2℃ in the inner shell and 187.8℃ in the inner lid. Therefore, the design temperature under accident conditions is evaluated in the manner that contributes to ensuring the maximum safety as shown in (Ⅱ)-Table A.35.

(Ⅱ)-Table A.35 Design temperatures used for accident test condition

No.	Position	Temperature (℃)
1	Fuel basket	225
2	Inner shell	500
3	Inner lid	225

(2) Design pressure

As was evaluated in the section (Ⅱ)-B.5.4, the pressure in the inner shell can rise up to 0.065 MPa (measured at the gauge). Hence, the design pressure in the package under accident test conditions is evaluated to achieve maximum safety on the assumption that a pressure difference of 0.0981 MPa･G occurs (see (Ⅱ)-Table A.36).

(Ⅱ)-Table A.36 Design pressure of package under accident condition

No.	Position	Design pressure
1	Inner shell inside	9.81×10^{-2} MPa

A.6.3.2 Thermal expansion

Stress due to the difference of thermal expansion between the inner surface of the inner shell and the outer surface of the fuel basket will be described here.

The temperature of fuel basket and the inner shell may rise to 225℃ and 500℃ respectively (see (Ⅱ)-Table A.35).

However, stress is generated by difference of thermal expansion because the fuel basket is not fixed to the inner shell.

A.6.3.3 Comparison of allowable stresses

(1) Stress calculation

Stress generated on different parts of the package due to the design pressure will be analyzed for the same parts as those described in section A.5.1.3, using the same method.

In this analysis, the temperatures shown in (Ⅱ)-Table A.35 will be used on the parts of the package.

(2) Displacement of the O-rings of inner lid

Displacement that can be generated at the O-rings due to the design pressure will be analyzed for the same parts as those described in section A.5.1.3(1) Ｄ , using the same method.

(3) Stress analysis and evaluation

(Ⅱ)-Table A.37 shows the results of the stress analyses.

These results demonstrate that the integrity of the package can be maintained under accident test conditions (thermal test).

(Ⅱ) -Table A.37 Stress analysis and evaluation under accident test conditions (thermal test)

Stress units ;N/mm²

No.	Position to be evaluated / Stress			Stress at initial clamping	Stress due to internal pressure	Stress due to thermal expansion	Primary stress					
							Pm(PL)	2/3Su	MS	PL+Pb	Su	MS
1	Frame of Inner shell		σ_r	—	-0.0491	—	2.36	258	108	—	—	—
			σ_θ		2.31	—						
			σ_z		1.15	—						
2	Bottom plate of inner shell	Inner Surface	σ_r	—	3.18	—	0.098	258	2631	3.28	387	116
			σ_θ		0.953	—						
			σ_z		-0.098	—						
		Outer Surface	σ_r	—	-3.18	—	0	258	—	3.18	387	120
			σ_θ		-0.953	—						
			σ_z		0	—						
3	Inner shell lid	Inner Surface	σ_r	—	-3.27	—	0.098	2/3 Sy 408	4162	3.17	Sy 612	192
			σ_θ		-3.27	—						
			σ_z		-0.098	—						
		Outer Surface	σ_r	—	3.27	—	0	2/3 Sy 408	—	3.27	Sy 612	186
			σ_θ		3.27	—						
			σ_z		0	—						
4	Inner shell lid clamping bolt		σ_t	174	3.22		177	2/3 Sy 408	1.30	—	—	—
5	Displacement of the inner lid O-ring			Interior : 1) Displacement $\mu = 1.29\times10^{-2}$ mm 2) Initial clamping value of the O-ring $\delta = 1.1$ mm 3) Remaining height of O-rings $\Delta 1 = \delta - \mu \fallingdotseq 1.087$ mm								

Pm ; General primary membrane stress; PL ; Local primary membrane stress; Pb ; Primary bending stress;
Sy ; Yield point of the design; Su ; Design tensile strength; MS ; Margin of safety σ_r ; Diameter direction stress σ_o ;Periphery direction stress σ_2 ;Axial stress σ_t ; Ability of bolt stress

A.6.4 Water immersion

In this section we will demonstrate that when immersed 15 m under water, the package can sufficiently endure the external pressure of 147 kPa.

We supposed here that the inner shell is subjected to this pressure. (Ⅱ)-Fig A.91 shows the parts evaluated for stress.

Since the radioactivity of this package will not exceed 10^5 times A_2 , then water immersion test is not required.

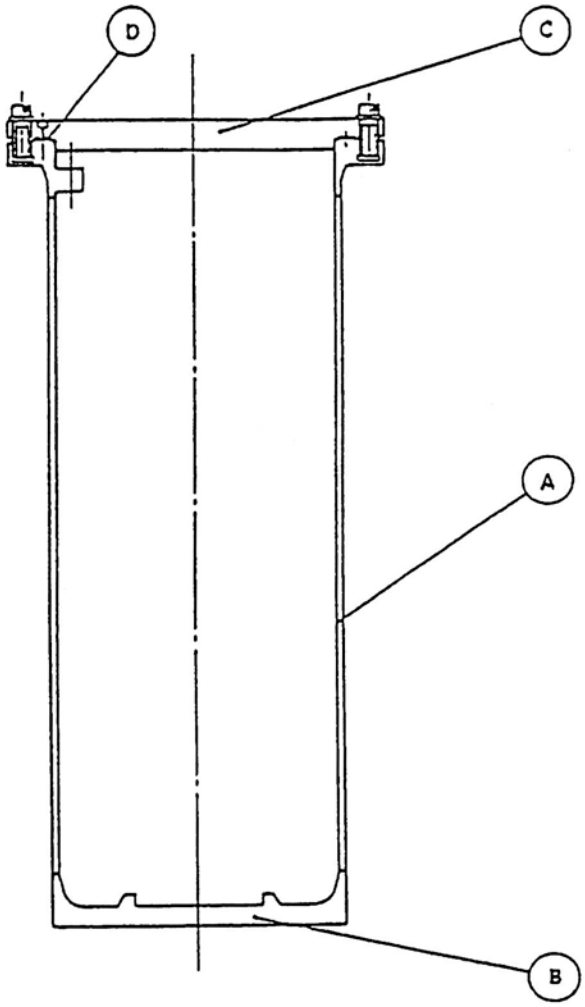

Symbol	Evaluated position
Ⓐ	Frame of inner shell
Ⓑ	Bottom plate of inner shell
Ⓒ	Inner shell lid
Ⓓ	Displacement of O-rings on inner shell lid

(Ⅱ)-Fig A.91 Stress evaluation position of inner shell for 15 m immersion test

Ⓐ Frame of inner shell

The frame of inner shell suffering external pressure is evaluated for its buckling and for the stress that may occur at its center.

(a) Buckling

(Ⅱ)-Fig.A.92 Analytical model shows the permissible buckling pressure for the frame of inner shell under external pressure.

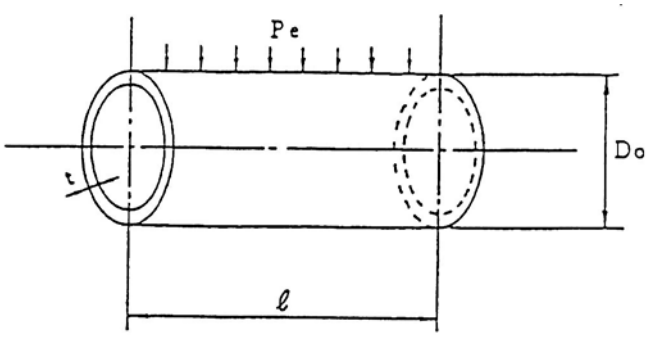

(Ⅱ)-Fig.A.92 Analytical model of allowable buckling pressure for frame of inner shell

The allowable buckling pressure Pe ((Ⅱ)-Fig.A.92) for the frame of inner shell is obtained by the following equation [1]

The formula and figure for finding the respective allowable bucking stress Pe are applied also to the current, appropriate source.

$$Pe = \frac{4B \cdot t}{2D_o}$$

where

P_e : Allowable buckling pressure [MPa]

Do : Outer diameter of inner shell, Do = 480 [mm]

t: Wall thickness of frame of inner shell, t = 10 [mm]

B: Factor obtained from (Ⅱ)-Fig.A.93, B = 650

1: Length of the inner shell, 1 = 1324 [mm]

Hence,

$$P_e = \frac{4 \times 650 \times 10 \times 9.81}{3 \times 480 \times 100} = 1.77 \text{ [MPa]}$$

Therefore, the margin of safety MS for the external pressure P = 0.147 MPa which the frame of inner shell suffers is,

$$MS = \frac{P_e}{P} - 1 = \frac{1.77}{0.147} - 1 = 11.0$$

Hence, the inner shell does not buckle under external pressure.

Stainless Steel (SUS304)

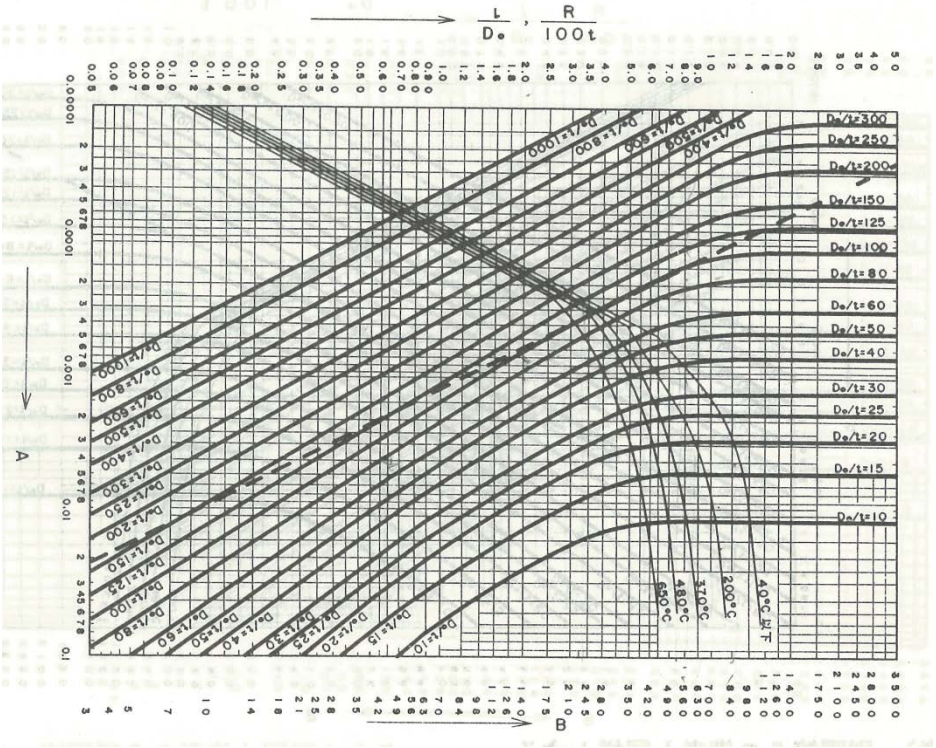

(Remarks)

1. The intermediate value shall be obtained by proportional calculation.

2. The way of application of this figure shall be given in the following,

《In case of the cylinder shape subjected to a pressure on the outer surface》

(1) Take a value, 1/Do, on the axis of ordinates.

(2) Calculate the value, Do/t, assuming the thickness, t, of the plate to be used.

(3) Draw a horizontal line from the point responding to 1/Do and obtain the crossing point of the horizontal line with the curve responding to Do/t.

(4) Draw a vertical line through the crossing point obtained in (c), and obtain the crossing point of the vertical line with the curve corresponding to the operating temperature.

(5) Draw a horizontal line from the crossing point obtain in (d), obtaining B which is the crossing point of the said horizontal line with the axis of ordinates.

(Ⅱ)-Fig.A.93 Curve representing backling behavior factor of inner shell under external pressure

(b) Center of inner shell

(Ⅱ)-Fig.A.94 shows an analytical model for the stresses occurring at the center of the inner shell under external pressure. The stress σ that may occur at the center of the inner shell is supposed to be a thin cylindrical wall and is obtained by the following equation.

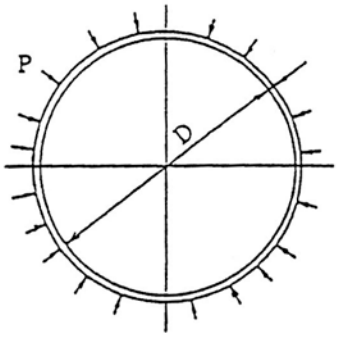

(Ⅱ)-Fig.A.94 Stress analysis model of center of inner shell

$$\sigma_\theta = -\frac{P \cdot D_m}{2t}$$

$$\sigma_z = -\frac{P \cdot D_m}{4t}$$

$$\sigma_r = -\frac{P}{2}$$

where

σ_θ: Circumferential stress [N/mm^2]

σ_z : Axial stress [N/mm^2]

σ_r : Radial stress [N/mm^2]

P: External pressure, P = 0.147 [MPa]

Dm: Average diameter of frame of inner shell,

Dm = D + t = 460 + 10 = 470 [mm]

t: Wall thickness of frame of inner shell, t = 10.0 [mm]

D: Inner diameter of frame of inner shell, D = 460 [mm]

Hence, the following values are obtained.

$$\sigma_\theta = -\frac{0.147 \times 470}{2 \times 10} = -3.45 \text{ [N/mm}^2\text{]}$$

$$\sigma_z = -\frac{0.147 \times 470}{4 \times 10} = -1.73 \text{ [N/mm}^2\text{]}$$

σ_r = − 0.0735 [N/mm²]

Ⓑ Bottom plate of inner shell

(Ⅱ)-Fig.A.95 Analytical model shows the stresses on the bottom plate of the inner shell under external pressure.

Assuming that the bottom plate of the inner shell is a disk fixed on its circumference, the stress σ on this fixed part is,

$$\sigma\theta = \pm 0.225 \frac{P \cdot a^2}{h^2}$$

$$\sigma_r = \pm 0.75 \frac{P \cdot a^2}{h^2}$$

σ_z = − P (outer surface)

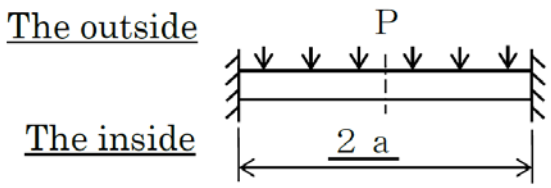

(Ⅱ)-Fig.A.95 Stress analysis model of bottom plate of inner shell

where

$\sigma\theta$: Circumferential stress [N/mm²]

σr : Radial stress [N/mm²]

σz : Axial stress [N/mm²]

P: External pressure, P = 0.147 [MPa]

a: Diameter of the bottom plate of inner shell, a = 230 [mm]

h: Wall thickness of the bottom plate of inner shell, h = 35 [mm]

Hence,

$$\sigma\theta = \pm 0.225 \frac{0.147 \times 230^2}{35^2} = \pm 1.428 \quad [N/mm^2]$$

$$\sigma_r = \pm 0.75 \frac{0.147 \times 230^2}{35^2} = \pm 4.76 \quad [N/mm^2]$$

σ_z = − 0.147 (outer surface) [N/mm²]

For the double sign of the stress value, the upper sign (−) corresponds to the inner surface and the lower sign (+) to the outer surface respectively.

Ⓒ Inner lid

(Ⅱ)-Fig.A.96 Analytical model shows the stresses that may occur on the inner lid under external pressure.

The stress σ [N/mm^2] that may occur on the disk supported on its circumference is at a maximum in the center (see (Ⅱ)-Fig.A.96) and is obtained as follows.

$$\sigma\theta = \sigma_r = \mp 1.24\frac{P\cdot a^2}{h^2}$$

$$\sigma_z = -P \text{ (outer surface)}$$

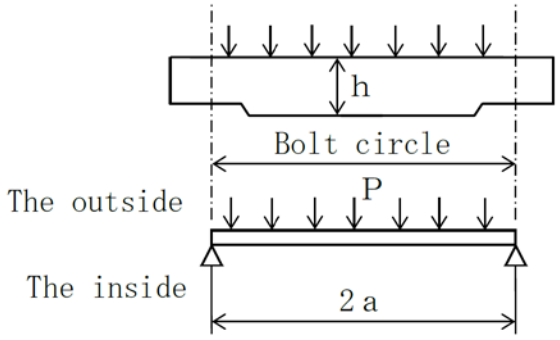

(Ⅱ)-Fig.A.96 Stress analysis model of center of inner lid

where

σθ: Circumferential stress [N/mm^2]

σr : Radial stress [N/mm^2]

σz : Axial stress [N/mm^2]

P: External pressure, P = 0.147 [MPa]

a: Diameter of the bottom plate of inner shell, a = 285 [mm]

h: Wall thickness of the bottom plate of inner shell, h = 55 [mm]

Hence,

$$\sigma\theta = \sigma_r = \mp 1.24\frac{0.147\times 285^2}{55^2} = \mp 4.89 \quad [\text{N/mm}^2]$$

$$\sigma_z = -0.147 \text{ (outer surface)} \quad [\text{N/mm}^2]$$

For the double sign of the stress value, the upper sign (-) corresponds to the inner surface and lower sign (+) to the outer surface respectively.

Ⓓ Displacement of the O-rings of inner lid

(Ⅱ)-Fig.A.97 Analytical model shows the displacement of the O-rings on the inner lid under external pressure.

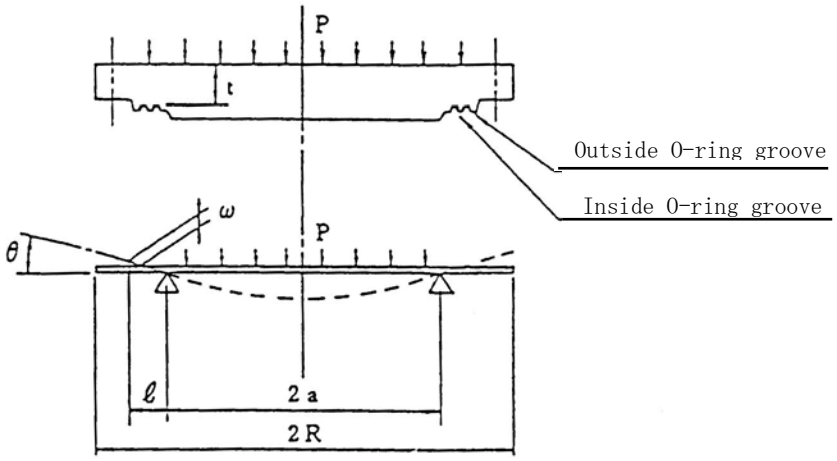

(Ⅱ)-Fig.A.97 Displacement analysis model of O-rings of inner lid under external pressure

The outer O-ring is at a distance of 1 from the supporting point of the disk suffering the uniform load. Its displacement ω is obtained as follows:

$$\omega = \theta \cdot 1 = \frac{P \cdot \alpha \cdot a^3}{8D \cdot (1+\nu)} \times 1 \qquad [mm]$$

where

ω : Displacement of the outer O-ring [mm]

θ : Angle of deflection at supporting point [rad];

$$\theta = \frac{P \cdot \alpha \cdot a^3}{8D \cdot (1+\nu)}$$

P: External pressure, P = 0.147 [MPa]

α: Factor of safety, $\alpha = (R/a)^2$

a : Distance from the center of inner lid to the supporting point,

a = 230 [mm]

R : Radius of the inner lid, R = 310 [mm]

D : Bending stiffness,

$$D = \frac{E \cdot t^3}{12(1-\nu^2)} \quad [N \cdot mm]$$

E : Longitudinal elastic modulus of the inner lid, $E = 1.92 \times 10^5$ [N/mm^2]

t : Minimum wall thickness of the inner lid, t = 36.7 [mm]

ν: Poisson's ratio, $\nu = 0.3$

1 : Distance from the supporting point to the outer O-ring, 1 =30.1 [mm]

Hence, the displacement of the outer O-ring is

$$\omega = \frac{0.147 \times (310/230)^2 \times 230^3 \times 12 \times (1-0.3^2)}{8 \times 1.99 \times 10^5 \times 36.7^3 \times (1+0.3)} \times 30.1$$

$$= 0.0104 \quad [\text{mm}]$$

This value is far smaller than the initial clamping value of the O-ring (δ = 1.1 mm). For this reason, the packaging cannot be adversely affected when exposed to external pressure.

(Ⅱ)-Table A.38 shows the test results of items Ⓐ to Ⓓ.

(Ⅱ)-Table A.38 Stresses evaluated for 15 m water immersion test

Position \ Stress		Stress	Stress	Primary stress					
				Pm (PL)	2/3 Su	Ms	Pl+Pb	Su	Ms
Center of inner shell		σ r	-0.0735	3.38	310	90.7	—	—	—
		σ θ	-3.45						
		σ z	-1.73						
Bottom plate of inner shell	Inner Surface	σ r	-4.76	0.147	310	2107	4.91	466	93.9
		σ θ	-1.428						
		σ z	0						
	Outer Surface	σ r	4.76						
		σ θ	1.428						
		σ z	-0.147						
Inner lid	Inner Surface	σ r	4.89	0.147	2/3 Sy 458	3114	4.89	Sy 687	139
		σ θ	4.89						
		σ z	0						
	Outer Surface	σ r	-4.89						
		σ θ	-4.89						
		σ z	-0.147						
Buckling of the inner shell			—	-External pressure P = 0.147 MPa -Allowable external pressure Pe = 1.77 MPa -Margin of safety MS = 11.0					
Displacement of O-rings on inner lid			—	-Displacement of outer O-ring ω = 0.0104 mm -Initial clamping value of O-rings δ = 1.1mm					

Note. Stress and stress intensity units: N/mm^2

These figures show that the package can maintain the integrity for its containment.

A.6.5 Summary of result and evaluation

The tests under accident conditions were examined by analytical methods. The results of the mechanical test (drop test Ⅰ) revealed that only the outer shell suffered deformation.

The results of the mechanical test (drop test Ⅱ) revealed that only the outer shell suffered local deformation.

In addition, the stress that occurs on each part of the inner shell does not exceed the allowable value, so the containment interface, suffering no damage, is not adversely affected.

In the thermal test, the stress that occurs on each part of the inner shell does not exceed the allowable value, so the containment interface, suffering no damage, is not adversely affected.

In the water immersion test, the inner shell can endure an external pressure of 147 KPa and maintain its soundness. Further, the fuel elements will never get fractured in the strength test, and the stress generated is not more than the allowable value.

The results of the evaluation of the outer shell, inner shell and content will be used for

(B) Thermal analysis, (C) Containment analysis, (D) Shielding analysis, and (E) Criticality analysis.

In the (B) Thermal analysis, (C) Containment analysis, (D) Shielding analysis, and (E) Criticality analysis, the results of the (A) Structural analysis were taken into consideration as follows.

(1) Thermal analysis

Those parts of the packaging which are essential to the thermal analysis are represented by the inner shell and inner lid.

The inner lid is covered with the outer lid.

In the structural analysis, the deformation of the lid side shock absorber is 126.7 mm at the vertical drop and 81.6 mm at the horizontal drop, while the thickness before deformation of the material is respectively 186 mm and 104 mm. So the deformation does not occur in the inner shell.

No penetration occurs in the outer shell at drop test Ⅱ.

The outer lid does not come off, sufficiently maintaining its functions as

a heat insulator.

We therefore suppose that in the thermal analysis, the inner shell is not damaged, and that the remaining thickness of the heat insulator and the shock absorber are determined to ensure the maximum in safety.

(2) Containment analysis

In the structural analysis, both the containment system of the packaging and the fuel elements suffer no damage and maintain their integrity.

In the containment analysis, the results are used to evaluate the leakage of radioactive material.

(3) Shielding analysis

In the shielding analysis, damage of either the outer shell, inner shell or fuel elements will influence the results.

In the structural analysis, the thickness of the lid side and bottom side shock absorber is 186 mm in the axial direction and 104 mm in the radial direction. Thus, deformation does not reach the inner shell and the packaging maintains its integrity.

In drop test Ⅱ, the outer shell is locally deformed, but the inner shell is not deformed.

Thus, in the shielding analysis we supposed that the inner shell would not be deformed, and, in order to ensure the maximum in safety, that the package has no outer shell, no heat insulator, and no shock absorbers.

(4) Criticality analysis

As in the case of the shielding analysis, we supposed here that the inner shell would not be deformed, and, in order to ensure the maximum in safety, that the package has no outer shell, no heat insulator, and no shock absorbers.

A.7 Reinforced immersion test

The maximum quantity of radioactivity of these transported articles is less than 100,000 times of the A2 level, which is not considered relevant.

A.8 Radioactive content

The fuel element, the radioactive content in the package consists of laminated fuel plates supported by the side plates on its ends (see (Ⅰ)-Fig.D.1). The fuel is located between aluminum alloy plates.

The specifications of the fuel element are shown in (Ⅰ)-Table D.

Structural analyses of the fuel elements are carried out under normal and accident test conditions on the assumption that they will suffer the same impact acceleration as that in the transport packaging. Therefore, the stress generated in any of the fuel elements is not more than the allowable stress under general and specific testing conditions, so that the fuel element are free from getting fractured.

A.9 Fissile package

This package, under the category of the fissile package in the Regulations, is used at an ambient temperature of more than -40℃. It is very unlikely that the package, as described in A.4.2, will be damaged or cracked at operating temperatures between -40℃ and 38℃.

Therefore, here is analyzed the damage of the package under the following test conditions, which is assumed for criticality analysis in (II)-E Criticality Analysis.

A.9.1 Normal test conditions

In consideration of (II) E Criticality Analysis, damage of the package is analyzed on the results of A.5 and A.9.2 as show in (Ⅱ)-Fig.A.98.

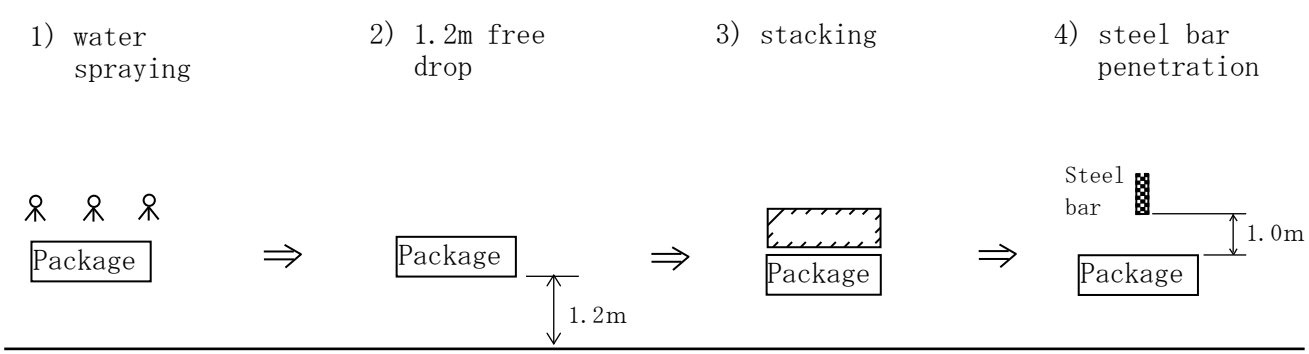

(Ⅱ)-Fig.A.98 Normal test conditions

A 9.1.1 Continuous test

(1) Water spray

The same as A 5.2, there is no damage to the package.

(2) 1.2m free drop(1.2m drop)

The same as the normal test conditions for the B(U) type package, there is no damage to the inner cell of criticality system as described in A 5.3

A 9.1.2 Stacking test

The same as A 5.4 there is no damage to the inner cell of criticality model.

A9.1.3 Penetration test

The same as A 5.5, there is no damage to the inner cell of criticality model. With the results above, the damages of the package are summarized as shown in (II)-Table A.39. This package, as shown in (II)-Table A40, meets the requirements for the fissile package under the normal tests conditions stipulated by the regulation and the notification.

(II)-Table A 39 Damages of the fissile package under the normal test conditions

Test conditions	Damage to the package	Note
Water spray	No damage	
1.2m drop	Deformation of outer shell, shock absorber and heat insulator	Outer shell, shock absorber and heat insulator are neglected in criticality analysis. Eye-plate has possibility to be deformed, but it is neglected in criticality analysis. Acceleration, stress at each part of the package, etc. do not exceed the value of 9m drop test respectively.
Stacking	No damage	
6kg penetration	No damage	

(II)-Table A40 Compliance with requirements for fissile package under normal test conditions

Requirements for fissile package	Evaluation
The structure should not be made a dent which contains a cube of 10cm.	The outer shell, shock absorber and heat insulator are deformed, but the deformation of inner shell, constituting criticality system, is not deformed with a dent which contains a cube of 10cm.
The package shall preserve the minimum overall outside dimensions of the package to at least 10cm.	The external dimensions of the inner shell, which is a system subject to criticality assessment, are 48 cm in outer diameter and 140 cm in length, and each side of the circumscribed rectangular solid is 10 cm or more.

A.9.2 Special test conditions for fissionable transported articles

The accident test conditions for the fissile packages are given as the testing procedures shown in (Ⅱ)-Fig.A.99, as A and B, i.e.,

A The damage incurred under normal test conditions and composite effect caused by the different tests including 9 m drop, 1 m penetration, fire test (800℃ for 30 minutes) and 0.9 m immersion.

B The damage incurred under normal test conditions and 15 m immersion test.

Among the above given A and B, the safety evaluation is to be executed under the condition A, in which the composite effect is taken into account considering 9 m drop test which is presumed having significant effect on the critical system and the fire test where the shock absorber burns out and adjacent packages come to be placed closer to each other.

[a]

1) Normal test conditions (A.9.1)　2) Drop test Ⅰ　3) Drop test Ⅱ　4) Fire test　5) Water immersion test

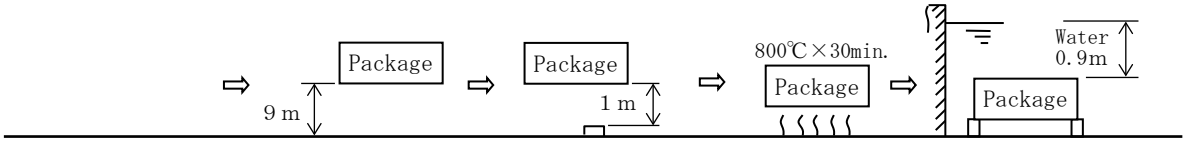

[b]

1) Normal test conditions (A.9.1)　2) Immersion test

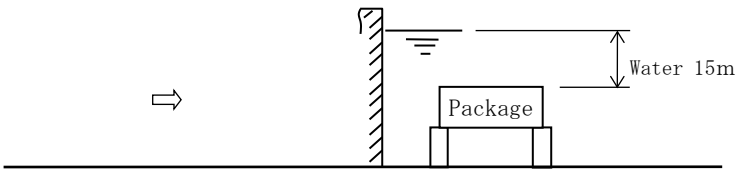

(Ⅱ)-Fig.A.99 Accident test condition

Here is employed as normal test conditions a continuous test accompanying damage, as shown in (II)-Table A 39.

In consideration of criticality analysis in (Ⅱ) E, damage affected package is evaluated as follows.

1. Continuous test of normal test conditions

Damage of the package under the mentioned test conditions is as shown in (Ⅱ)-Table 39.

2. drop test(9m)

(1)Dropping attitude and the order of the drop test

Dropping attitude and the order of the drop test are given in (Ⅱ)-Fig.A.100.

In case the dropping directions of 1.2m drop and 9m drop test are the same, deformation of the shock absorber will be considered the greatest, and thus here is considered that case.

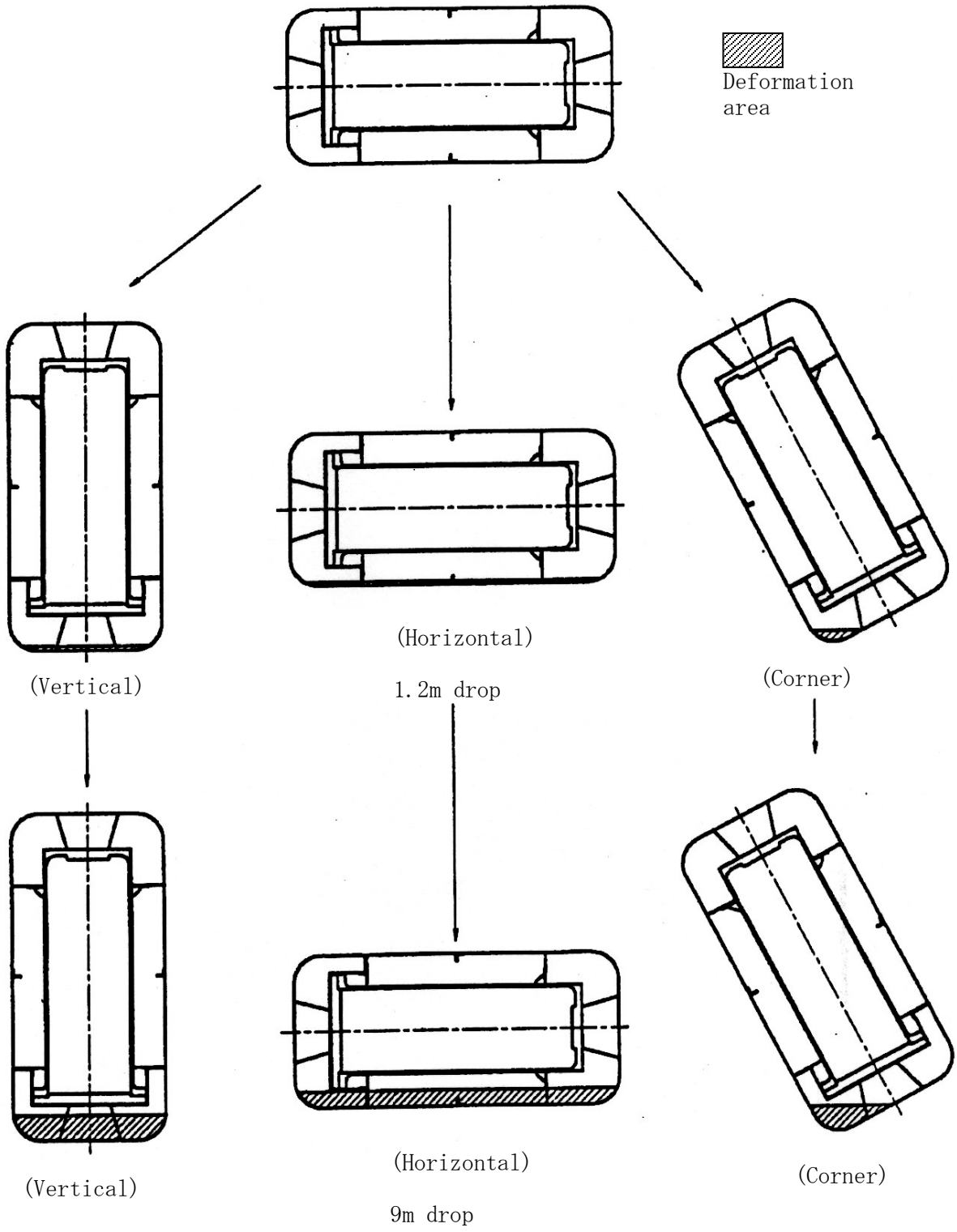

(Ⅱ)-Fig.A.100 Drop attitude and test order

(2)Deformations and design accelerations

Deformations and design accelerations of the fissile package produced in the drop test I (1.2m drop test and the consecutive 9m drop test) for fissile package are analyzed by the method described in section A.5.3.

(Ⅱ)-Table A.41 shows the results of the analyses.

(Ⅱ)-Table A.41 Deformations and design accelerations of shock absorber under accident test conditions (combined evaluation)

Drop height	Acceleration and Deformation / Drop attitude		Acceleration (g) CASH-Ⅱ ×1.2	Acceleration (g) Steel plate acceleration	Acceleration (g) Design acceleration	Deformation (mm)	Rate of acceleration to design acceleration due to drop test Ⅰ (9m drop only)
*9m	Horizontal		206.2	172.8	379.0	88.8	1.033
	Vertical	Upper Portion	161.8	284.4	446.2	136.6	1.089
		Lower portion	131.4	276.2	407.6	117.6	1.049
	Corner	Upper Portion	85.6	238.2	323.8	133.9	1.080
		Lower Portion	87.1	245.2	332.3	115.7	1.069

*1: 9 m drop is evaluated by considering the deformation by 1.2 m drop.

(3)Evaluation of damages of the package

Design acceleration of the drop test for the fissile package, as shown in (II)-Table A.41, increases by 9% at the maximum in comparison with that of the drop test 1 for the B(U) fissile package. Among the structural evaluation results of drop test 1 of the fissile package, the part of the smallest safety margin is the spectrum converter on the horizontal drop, as shown in (II)-Table A. 28. The safety margin is 0.23 or 23%.

In structural evaluation of the package, the increasing rate of acceleration is the same as that of the generated stress. Even when the design acceleration and the generated stress increases by 9%, the smallest safety margin is 0.19, which shows that the structural integrity of the packaging and its contents is maintained.

3. 1m penetration test

In the drop test of A 9.2.1 and A 9.2.2 above, the outer shell, shock absorber and heat insulator are deformed, but these are not related to evaluation of 1m penetration test, as shown in A 6.2. Therefore, the damage of the package on the present test will be the same as the results in A 6.2(See the summary A 6.2).

4. Thermal test

In the thermal test, deformation of outer shell, shock absorber and heat insulator is taken into account, but effect of their deformation is considered negligible. Thus, damage evaluation of the package under this test will be the same as A 6.3.3(3).

5. Immersion test(0.9m)

As proved by 15m immersion test, the package damage in 0.9m immersion test will not expand.

6. Summary of the package damage

Summary of damage to the package under special test conditions is described here.

(II)-Table A. 42 Damage of the fissile package under special test conditions

Conditions	Damage of the package	Notes
drop(9m)	Deformation of outer shell, shock absorber and heat insulator	Outer shell, shock absorber and heat insulator are neglected in criticality analysis.
Penetration(1m)	Deformation of outer shell, shock absorber and heat insulator	Outer shell, shock absorber and heat insulator are neglected in criticality analysis.
Thermal test(fire)	Partly damaged by a fire Rise in temperature for each part	In criticality analysis, heat insulator is neglected and water density is set at 1.0g/cm^3
Immersion(0.9m)	No damage	In criticality analysis, assessed for the package filled with water

A.10 Appendix

A.10.1 Analysis program for the absorbing performance of shock absorber : "CASH-Ⅱ"

(1) General

"CASH-Ⅱ" is a calculation code which is used to analyze the shock absorber by an uniaxial displacement method (U.D.M) when the package equipped with shock absorber on its top and bottom is dropped.

The deformation, the energy absorbed, and the impact force (acceleration and g value) occurring in the package when dropped with various postures (vertical, horizontal, and inclined).

As shown in (Ⅱ)-Fig.A.101, this code can be applied to shock absorbers consisting of areas (called "material areas") of different mechanical characteristics (stress/strain relationships).

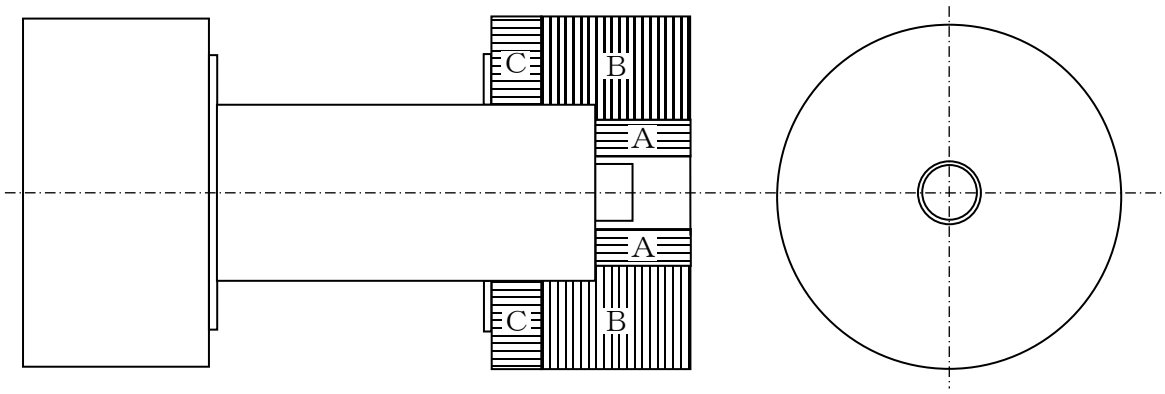

A, B, and C represent material areas.

(Ⅱ)-Fig.A.101 Analytical model of shock absorber

(2) Analysis theory

The "CASH-Ⅱ" code is a program for analyzing the impact performance of the packages shock absorber in various inclined drop tests (inclination θ = 0 degrees: vertical drop, inclination θ = 90 degrees: horizontal drop) in a uniaxial displacement method (U.D.M.) which is based on the following two basic principles.

a) Energy absorbing characteristics are analyzed by a U.D.M.;

b) Uniaxial bars with inclined orientation is replaced with an equivalent couple of uniaxial bars of horizontal and vertical orientation.

The analysis theory of the "CASH-Ⅱ" code based on these principles is described below.

a) Uniaxial displacement method (U.D.M.)

This is a theory which assumes that each area subject to deformation absorbs the deforming energy in a uniform and uniaxtial manner. Areas subject to deformation such as shock absorber are replaced with a number of uniaxial bars. The energy absorbing characteristics of the entire shock absorber is evaluated on the basis of the energy absorbing characteristics of the uniaxial bars.

We will consider here a case where a mass which weighs W and has an energy E_0 hits the structure shown in (Ⅱ)-Fig.A.102.

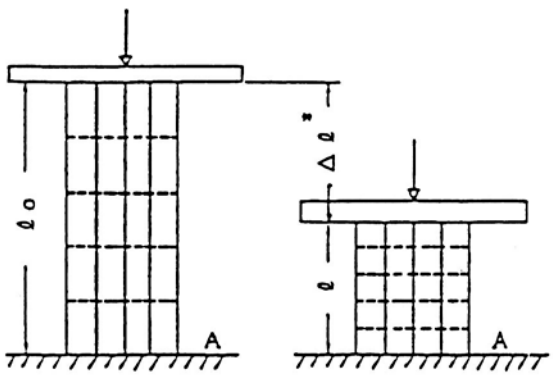

l_0 : Initial length
l : Final Leigh
Δl : Displacement
A : Cross section

Uniform deformation

Before deformation After deformation

(Ⅱ)-Fig.A.102 Analytical model by uniaxial displacement method

The compressive stress/strain relationship of the structure is supposed to appear as shown in (Ⅱ)-Fig.A.103

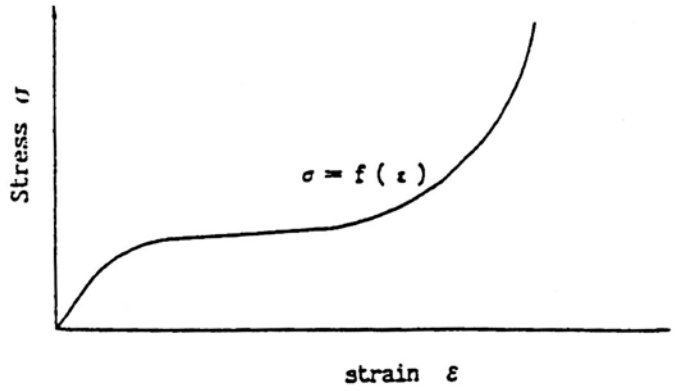

(Ⅱ)-Fig.A.103 Compressive stress/strain relationship of material

The deformation Δl of the structure and the acceleration a which occurs in the mass are obtained as follows.

The strain ε that is generated when a structure suffers a Δl deformation is,

$$\varepsilon = \Delta l / l_0 \qquad \text{(A.10-1)}$$

The stress σ is,

$$\sigma = f(\varepsilon) = f(\Delta l / l_0) \qquad \text{(A.10-2)}$$

Hence, the force F that occurs when the structure suffers a Δl deformation is,

$$F = A\sigma = A \times f(\Delta l / l_0) \qquad \text{(A.10-3)}$$

The energy E that is absorbed by the structure when it suffers a Δl deformation is,

$$E = \int_0^{\Delta \ell} F dl = l_0 \cdot \int_0^{\Delta \ell / \ell 0} A\sigma(\varepsilon) d\varepsilon \qquad \text{(A.10-4)}$$

When the energy E_0 that the structure has to absorb is given, the final deformation Δl^* is determined using formula A.10-4,

$$E_0 = l_0 \cdot \int_0^{\Delta \ell^* / \ell 0} A\sigma(\varepsilon) d\varepsilon \qquad \text{(A.10-5)}$$

When Δl* is substituted in formula(A.10-3), we obtain as follows,

$$F^* = Af(\Delta l^* / 10) \qquad \text{(A.10-6)}$$

Therefore, the acceleration a* is,

$$a^* = F^* / W \qquad \text{(A.10-7)}$$

b) Uniaxial bar with inclined orientation

We will describe in this section how to handle the uniaxial bars inclined orientation based on a uniaxial displacement method.

Calling θ the inclined drop angle, we suppose that the following equation is valid among the stresses with inclined direction $\sigma\theta$, vertical σz and horizontal direction σx for the same strain ε,

$$\sigma\theta(\varepsilon) = \sigma z(\varepsilon)\cos^m\theta + \sigma x(\varepsilon)\sin^m\theta \qquad \text{(A.10-8)}$$

Where m is the constant for inclination of the material.

In this case, there is approximately the following relationship between $E\theta$, Ez, and Ex,

$$E_\theta = Ez\cos^{m-2}\theta + Ex\sin^{m-2}\theta \qquad \text{(A.10-9)}$$

also, approximately the relationship between $F\theta$, Fz, and Fx,

$$F_\theta = Fz\cos^{m-1}\theta + Fx\sin^{m-1}\theta \qquad \text{(A.10-10)}$$

where E_θ and F_θ are respectively the energy and force generated when the uniaxial bars oriented to the inclination θ suffer ε, while the energy and force generated in Ez and Fz when the uniaxial bars are vertically oriented suffer ε, and the energy and force generated in Ex and Fx when the uniaxial bars are horizontally oriented suffer ε (see the following charts).

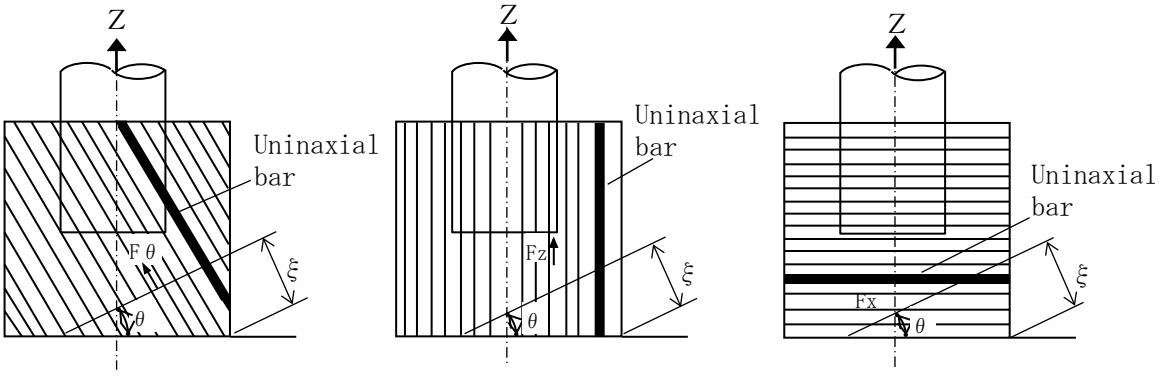

Uniaxial bars oriented to the inclination

Uniaxial bars vertically oriented

Uniaxial bars horizontally oriented

(3) Demonstration of "CASH-Ⅱ" code

To demonstrate the validity of the "CASH-Ⅱ", drop tests carried out for four kinds of casks were analyzed. The comparison of the analytical and experimental values are shown in (Ⅱ)-Table A.43.

(Ⅱ)-Table A.43 shows that,

a) The deformation of the shock absorber was found to be greater in the analytical values based on the "CASH-Ⅱ" code than in the experimental values, thus ensuring the maximum safety.

b) The design value of the acceleration based on the "CASH-Ⅱ" was found to be equal to, or greater than, the experimental value, thus ensuring valid results.

The weight of the package is 950 kg which remains within the weight range of the four different casks.

(Ⅱ)-Fig.A.104 shows that the shock absorber used in the package is in the same proportion as those of other packagings and cause no problems in applying the analysis code.

These results permit us to suppose that evaluation of the shock absorber performance based on the "CASH-Ⅱ" code will lead to justifiable results. However, in the designing of the shock absorber, the following points are taken into account,

i) A design acceleration + 20 % of the value based on the "CASH-Ⅱ" code is adopted as the acceleration that can occur.

ii) Calculated values are adopted as the deformation of the shock absorber because the "CASH-Ⅱ" code leads to higher values.

(Ⅱ)-Table A.43 Comparisons of analytical values by "CASH-Ⅱ" and experimental values

Type of cask		TYPE 1		TYPE 2			TYPE 3		TYPE 4		
Weight (kg)		62,000		43,500			710		9,600		
Outer dimensions (mm)		6,080× ϕ2,400		6,220× ϕ1,800			3,960× ϕ566		3,290× ϕ1,080		
Posture at droping		Verti-cal	Hori-zontal	Verti-cal	Hori-zontal	Corner	Verti-cal	Hori-zontal	Verti-cal	Hori-zontal	Corner
Acceleration	Analytical value (g)	78.2	90.8	95.4	112.4	115.4	131.4	274.9	167	128	73.3
	Design value (g)	93.8	109.0	115	135	138.4	158	330	201	152	88.0
	Experimental value (g)	70	67	114	117	73	135	320	200	150	51.5
Deformation	Analytical value (mm)	172	190.3	187	156	383	189.4	50.0	63.4	120	310.1
	Experimental value (mm)	131	117	88	73	155	68.5	16.3	50.0	73.7	22.4

*The design values which are equal to the values of the analytical value multiplied by a factor of 1.2 are used in the designing, taking possible variations of test results into account.

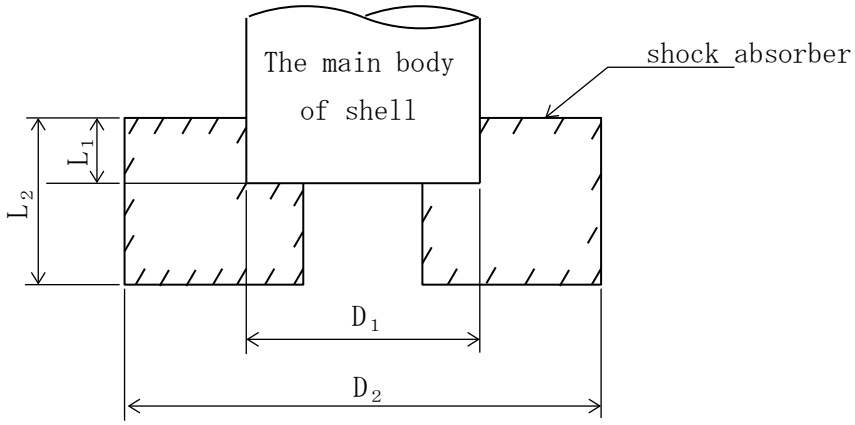

	TYPE 1	TYPE 2	TYPE 3	TYPE 4	Package
L_1/L_2	0.42	0.53	0.56	0.68	0.43
D_1/D_2	0.52	0.67	0.56	0.57	0.57
Shock absorber	Plywood	Plywood	Balsa	Balsa +Redwood	Balsa

(Ⅱ)-Fig A.104 Proportion of shock absorbers

A.10.2 Validity of the free drop analyses of the JRF-90Y-950K package

(Ⅱ)-Table A.44 compares the results of a drop tests and the analytical results obtained from a prototype packaging.

Generally, the analytical results were obtained so as to ensure the maximum in safety.

(Ⅱ)-Table A.44 Comparison of analytical and experimental results

Item		Analytical results	Test results	Ratio of analyses/ test	Remarks
Acceleration (G)	Drop test Ⅰ	367.0	366	1.003	
	Drop test Ⅱ	80.4	18.3	4.393	
Deformation (mm)	Drop test Ⅰ＋Ⅱ	94.0	46	2.043	

A.10.3 Displacement of inner lid O-rings

(Ⅱ)-Fig.A.105 shows an analytical model showing the displacement of the O-rings in the 1.2 m lid side vertical drop of the package.

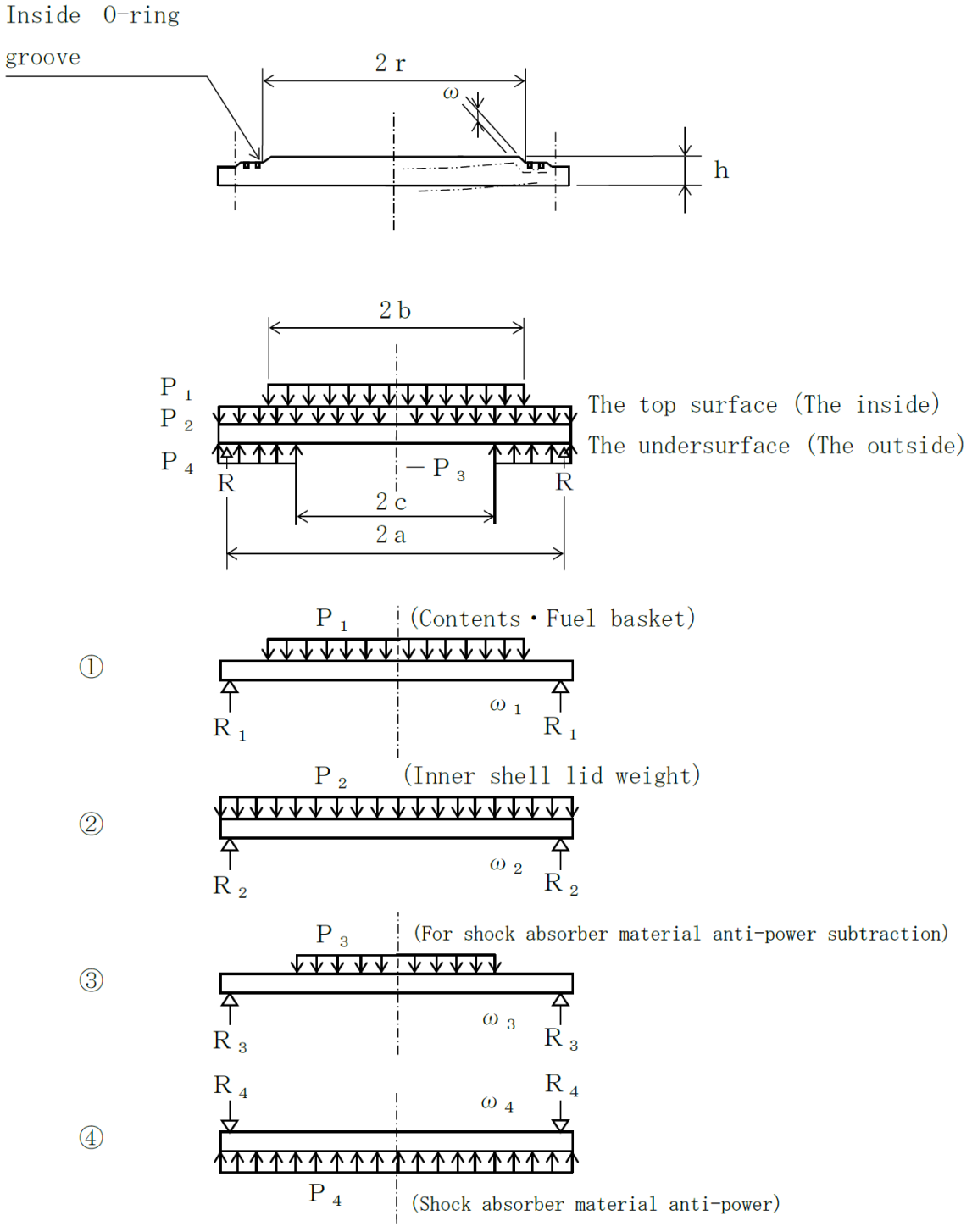

(Ⅱ)-Fig.A.105 Analytical model of inner lid for 1.2 m lid side vertical drop

(Ⅱ)-Fig.A.105 shows that the uniform load consisting of the weight of the content and that of the fuel basket act at the center of the inner lid, and that the uniform load due to the dead weight of the inner lid acts on the lid.

On the other hand, the inner lid is supported by inner lid clamping bolt and the shock absorber which has a circular reaction force.

Displacement of the O-rings fixed on the inner lid which suffer these loads can be calculated by combining the results of the analyses using the ①,②,③ and ④ models (see (Ⅱ)-Fig.A.99).

① Contents + fuel basket

The displacement that can occur in the disk suffering a uniform load on its concentric circle(see (Ⅱ)-Fig.A.105①) is,

$$\omega_1 = \frac{P_1 b^4}{16D}\left\{\frac{r^4}{4b^4} - \frac{4a^2-(1-\nu)b^2}{2(1+\nu)a^2}\cdot\frac{r^2}{b^2} - \left[2\cdot\frac{r^2}{b^2}+1\right]\cdot 1_n\frac{a}{b} + \frac{4(3+\nu)a^2-(7+3\nu)b^2}{4(1+\nu)b^2}\right\}$$

where

ω_1 : Displacement of the inner O-ring [mm]

ν : Poisson's ratio, ν =0.3

a: Radius of the supported points of the inner lid, a = 285 [mm]

b: Radius of the loads, b = 230 [mm]

r: Radius of the inner O-ring groove, r = 237.5 [mm]

m3 : Weight of the fuel basket, m3 = 138 [kg]

m4 : Weight of the content, m4 = 92 [kg]

N: Acceleration, N = 240.7·g [m/s^2]

h: Minimum wall thickness of the inner lid, h = 36.7 [mm]

E: Longitudinal modulus of elasticity, E = 1.99×10^5 [N/mm^2]

P1 : uniform load of the content/fuel basket,

$$P_1 = \frac{(m^3+m^4)}{\pi b^2}\cdot N = \frac{(138+92)}{\pi\times 230^2}\times 240.7\times 9.81 = 3.27 \text{ [N/mm}^2\text{]}$$

D: Bending stiffness of the inner lid,

$$D = \frac{E\cdot h^3}{12(1-\nu^2)} = \frac{1.99\times 10^5\times 36.7^3}{12(1-0.3^2)} = 9.01\times 10^8 \text{ [N・mm]}$$

Hence the displacement ω_1 due to the content + fuel basket is,

$$\omega_1 = \frac{3.27\times 230^4}{16\times 9.01\times 10^8}\left\{\frac{237.5^4}{4\times 230^4} - \frac{4\times 285^2-(1-0.3)\times 230^2}{2\times(1+0.3)285^2}\times\frac{237.5^2}{230^2} - \left[2\cdot\frac{237.5^2}{230^2}+1\right]\ell n\ \frac{285}{230} + \frac{4(3+0.3)285^2-(7+3\times 0.3)230^2}{4(1+0.3)230^2}\right\}$$

= 0.341 [mm]

② Weight of the inner lid

The displacement ω_2 (mm) that can occur in the disk suffering a uniform load (see (Ⅱ)-Fig.A.105 ②) is,

$$\omega_2 = \frac{P_2\, a^4}{64D}\left[1-\frac{r^2}{a^2}\right]\left[\frac{5+\nu}{1+\nu}-\frac{r^2}{a^2}\right]$$

where

ω_2 : Displacement of the inner O-ring [mm]

ν: Poisson's ratio, ν = 0.3

a: Radius of the supported points of the inner lid, a = 285 [mm]

r: Radius of the inner O-ring groove, r = 237.5 [mm]

h: Wall thickness of the inner O-ring groove, h = 55 [mm]

N: Acceleration, N = 240.7·g [m/s2]

γ: Density of the inner lid, γ = 7.93×10^{-6} [kg/mm^3]

D: Bending rigidity of the inner lid, D = 9.01×10^8 [N·mm]

P2 : Uniform load due to the dead weight of the inner lid,

P2 = γ hN = $7.93\times 10^{-6}\times 55\times 240.7\times 9.81$ = 1.03 [N/mm^2]

Hence the displacement ω_2 due to the weight of the inner lid is,

$$\omega_2 = \frac{1.03\times 285^4}{64\times 9.01\times 10^8}\left[1-\frac{237.5^2}{285^2}\right]\left[\frac{5+0.3}{1+0.3}-\frac{237.5^2}{285^2}\right] = 0.122\ [\text{mm}]$$

③ Reaction force of the shock absorber to be subtracted

The displacement ω_3 (mm) that can occur in the disk suffering a uniform load on its concentric circle (see (Ⅱ)-Fig.A.105 ③) is,

$$\omega_3 = \frac{P_3\, C^4}{16\, D}\left\{\frac{r^4}{4C^4} - \frac{4a^2-(1-\nu)C^2}{2(1+\nu)^2}\cdot\frac{r^2}{C^2} - \left[2\frac{r^2}{C^2}+1\right]1_n\frac{a}{C} + \frac{4(3+\nu)a^2-(7+3\nu)C^2}{4(1+\nu)C^2}\right\}$$

where

ω_3 : Displacement of the inner O-ring [mm]

ν: Poisson's ratio, ν = 0.3

a: Radius of the supported points of the inner lid, a = 285 [mm]

C: Radius of the load,

$C = C0 + \delta \tan\alpha = 115 + 24.1\tan 15.5^\circ = 122$ [mm]

C0: Upper radius of the circular cone, C0 = 115 [mm]

α: Circular cone angle, $\alpha = 15.5^\circ$ [degrees]

δ: Deformation of the shock absorber, $\delta = 24.1$ [mm]

D: Bending rigidity of the inner lid, $D = 9.01\times10^8$ [N・mm]

P3 : Compressive stress on the shock absorber, P3 = 0.932 [N/mm^2]

r: Radius of the inner O-ring groove, r = 237.5 [mm]

Hence, ω_3 is,

$$\omega_3 = \frac{0.932\times122^4}{16\times9.01\times10^8}\left\{\frac{237.5^4}{4\times122^4} - \frac{4\times285^2-(1-0.3)\times122^2}{2\times(1+0.3)285^2}\times\frac{237.5^2}{122^2} - \left[2\frac{237.5^2}{122^2}+1\right]\ell n\frac{285}{122} + \frac{4(3+0.3)285^2-(7+3\times0.3)122^2}{4(1+0.3)122^2}\right\}$$

$= 0.0370$ [mm]

④ Reaction force of the shock absorber

The displacement ω_4 (mm) that can occur in the disk which suffers a uniform load on its concentric circle (see (Ⅱ)-Fig.A.105 ④) is,

$$\omega_4 = \frac{P_4 a^4}{64D}\left[1-\frac{r^2}{a^2}\right]\left[\frac{5+\nu}{1+\nu}-\frac{r^2}{a^2}\right]$$

where,

ω_4 : Displacement in the inner O-ring [mm]

ν: Poisson's ratio, $\nu = 0.3$

a: Radius of the supported points of the inner lid, a = 285 [mm]

r: Radius of the inner O-ring groove, r = 237.5 [mm]

D: Bending rigidity of the inner lid, $D = 9.01\times10^8$ [N・mm]

P_4 : Compressive stress on the shock absorber, $P_4 = 0.932$ [N/mm^2]

Hence the displacement ω_4 due to the reaction force of the shock absorber is,

$$\omega_2 = \frac{0.932\times285^4}{64\times9.01\times10^8}\left[1-\frac{237.5^2}{285^2}\right]\left[\frac{5+0.3}{1+0.3}-\frac{237.5^2}{285^2}\right] = 0.110 \text{ [mm]}$$

Thus, the total displacement ω is,

$\omega = \omega_1 + \omega_2 + \omega_3 - \omega_4 = 0.341 + 0.122 + 0.0370 - 0.110 = 0.390$ [mm]

Incidentally, as for the 9 m lid side vertical drop test replacing the values of acceleration, (409.8g), compressive stress of shock absorber, (2.66N/mm^2) and displacement, (127mm), with the corresponding value for 1.2 m lid side vertical drop test, the same analysis is conducted and the results of evaluation are given in (Ⅱ)-Table A.45.

(Ⅱ)-Table A.45 Analysis results of displacement of inner O-rings of inner lid

No.	Analysis condition	Name of displacement	Displacement	Total displacement	Remaining height *
1	Normal condition (internal pressure)	ω_0	0.0116	0.402	0.698
	1.2 m lid side vertical drop	ω_1	0.341		
		ω_2	0.122		
		ω_3	0.0370		
		$-\omega_4$	-0.110		
2	Normal condition (internal pressure)	ω_0	0.0116	0.636	0.464
	9 m lid side vertical drop	ω_1	0.581		
		ω_2	0.207		
		ω_3	0.151		
		$-\omega_4$	-0.315		

*Note: Residual tightening interference = Initial clamping value (1.1 mm) - Total displacement

As shown in (Ⅱ)-Table A.45, remaining height of the inner O-ring in each of the cases of 1.2 m and 9 m lid side vertical drop tests is always positive so that it can be granted that the containment of packages will be duly maintained.

A.10.4 Stress/strain characteristics of the shock absorber at low temperatures

(Ⅱ)-Fig.A.106 shows the stress/strain characteristics of the shock absorber at low temperatures.

(1) Direction perpendicular to the wood grain of the shock absorber

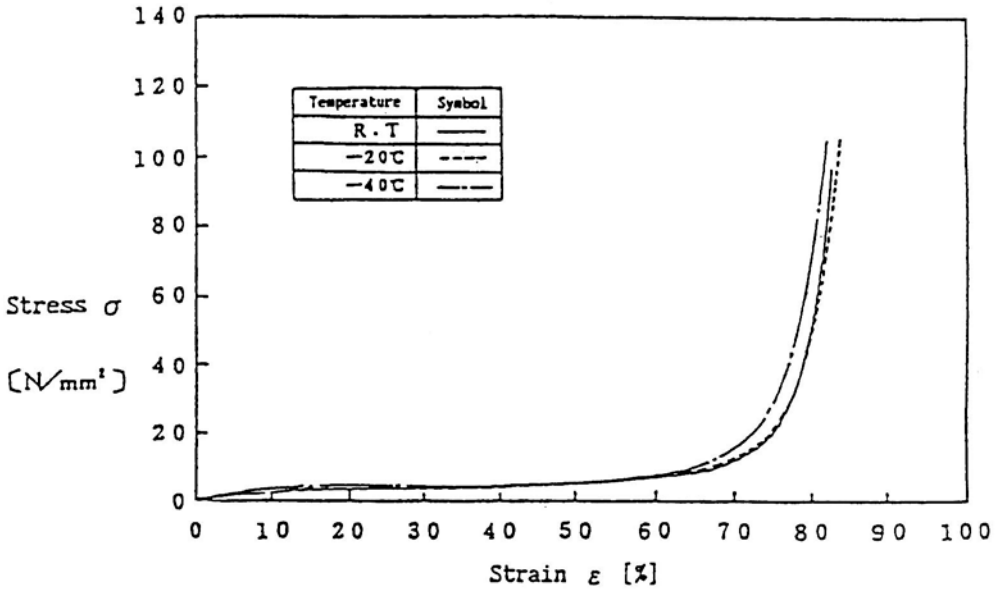

(2) Direction parallel to the wood grain of the shock absorber

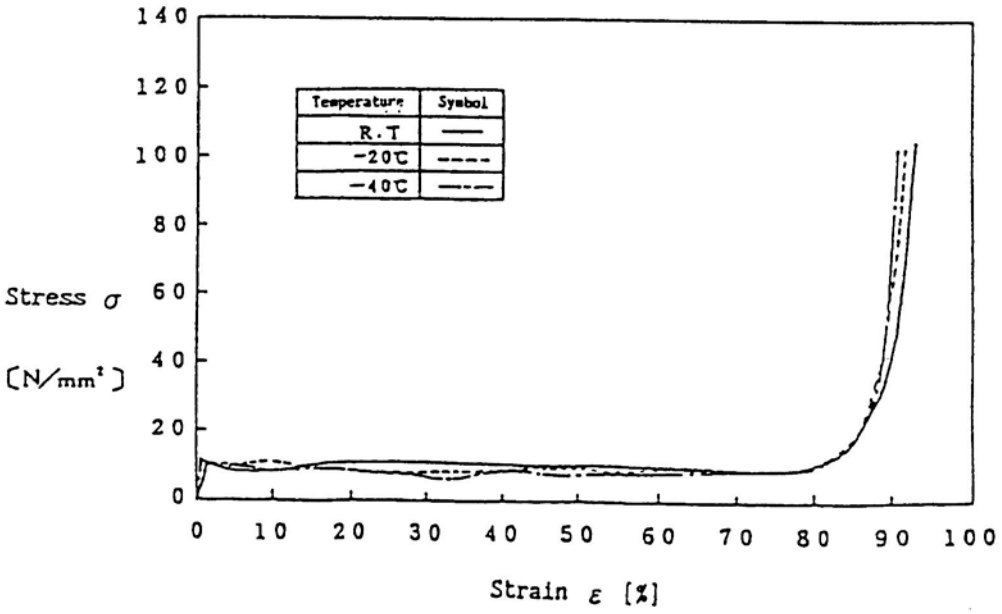

(Ⅱ)-Fig.A.106 Stress/strain characteristics curves for shock absorber at low temperatures[4]

A.10.5　Stress/strain characteristics of hard polyurethane foam

(Ⅱ)-Fig.A.107 shows the stress/strain characteristics of the hard polyurethane foam.

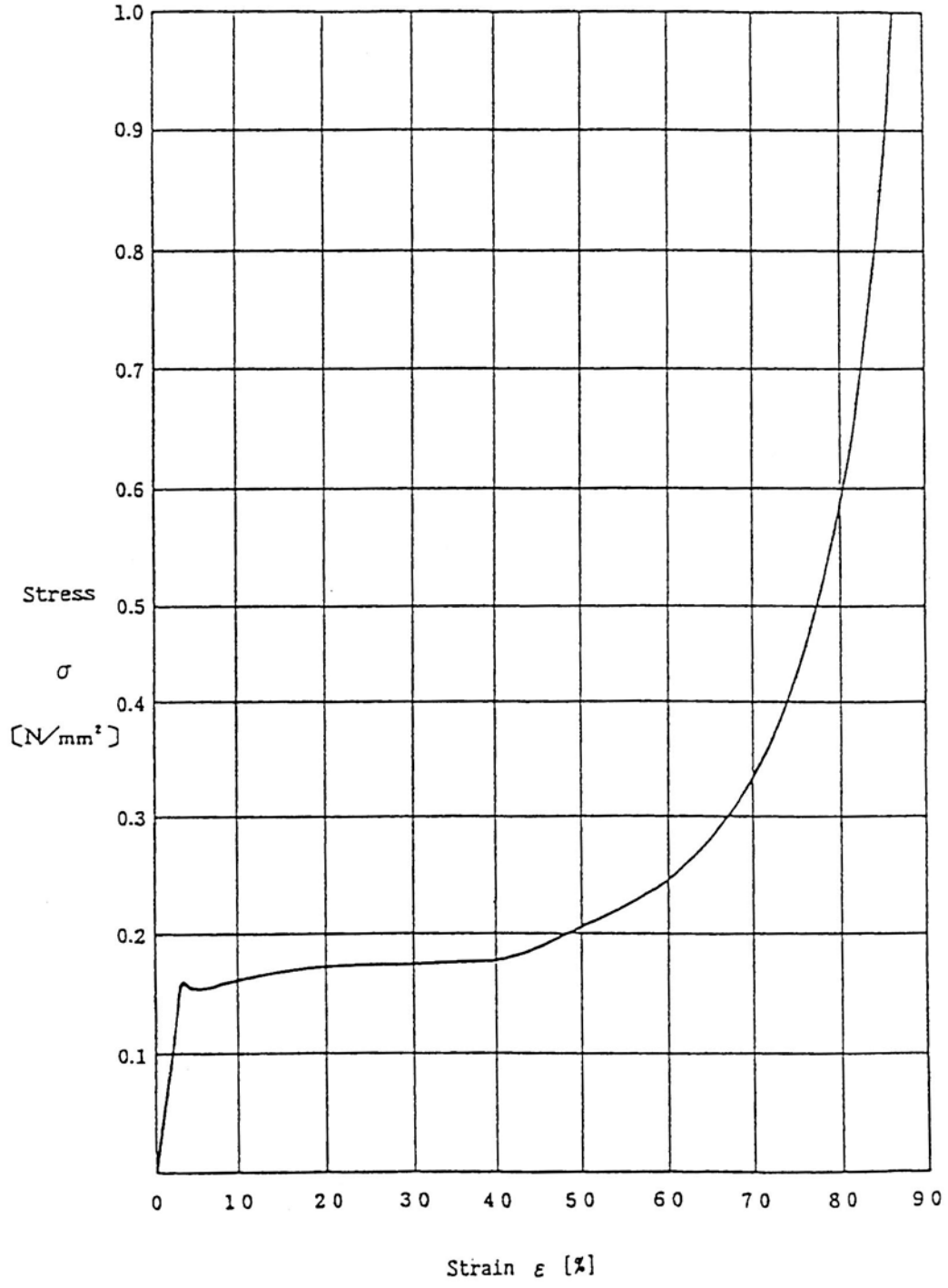

(Ⅱ)-Fig.A.107 Stress/strain curves for hard polyurethane foam[4]

A.10.6 Low temperature strength of SUS 304

(Ⅱ)-Fig.A.108 shows the mechanical characteristics of the material SUS 304 at low temperatures.

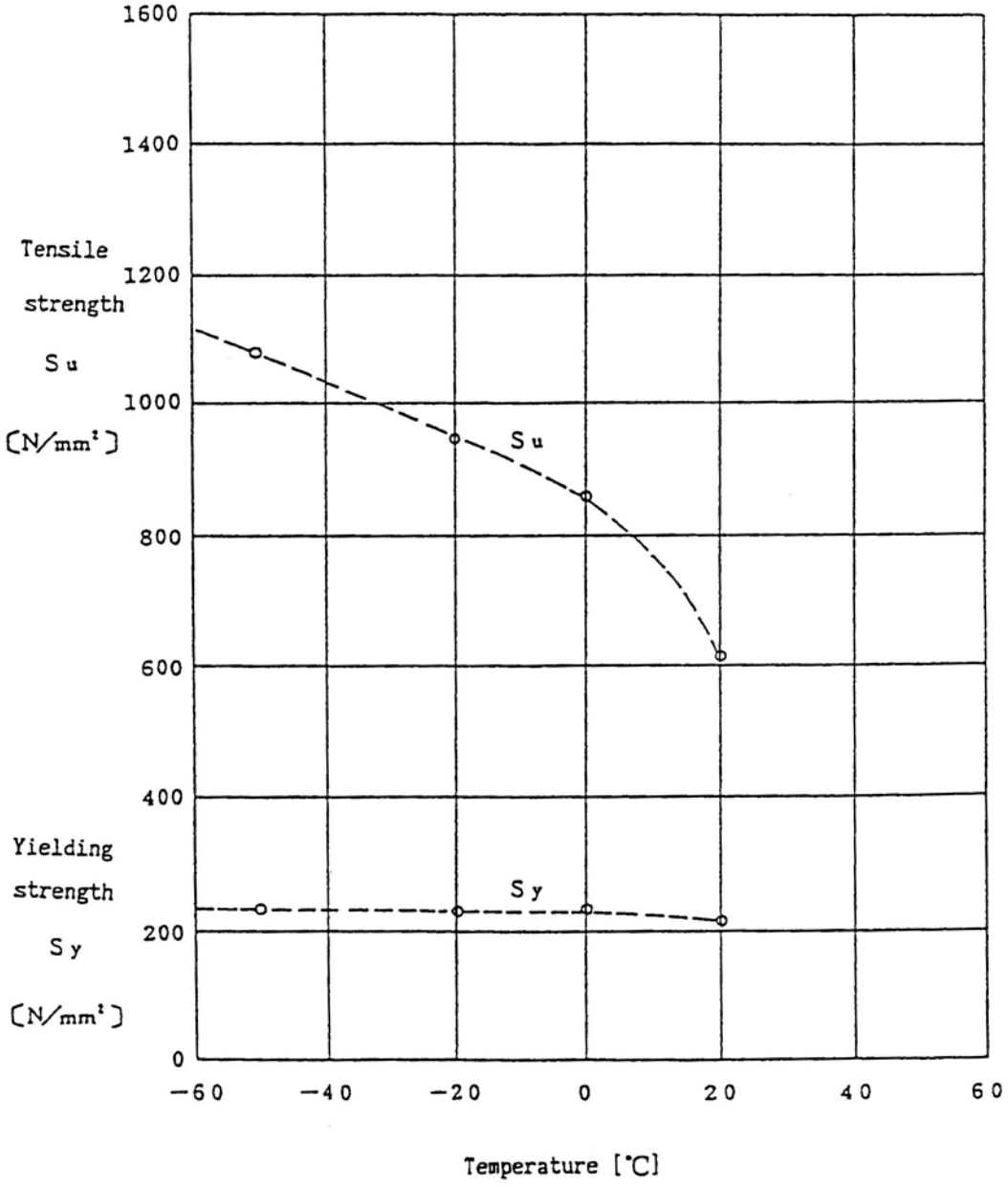

(Ⅱ)-Fig.A.108 Low temperature strength of SUS 304 [16]

A.10.7 Low temperature impact values of SUS 304

(Ⅱ)-Fig.A.109 shows the low temperature impact values of the material SUS 304.

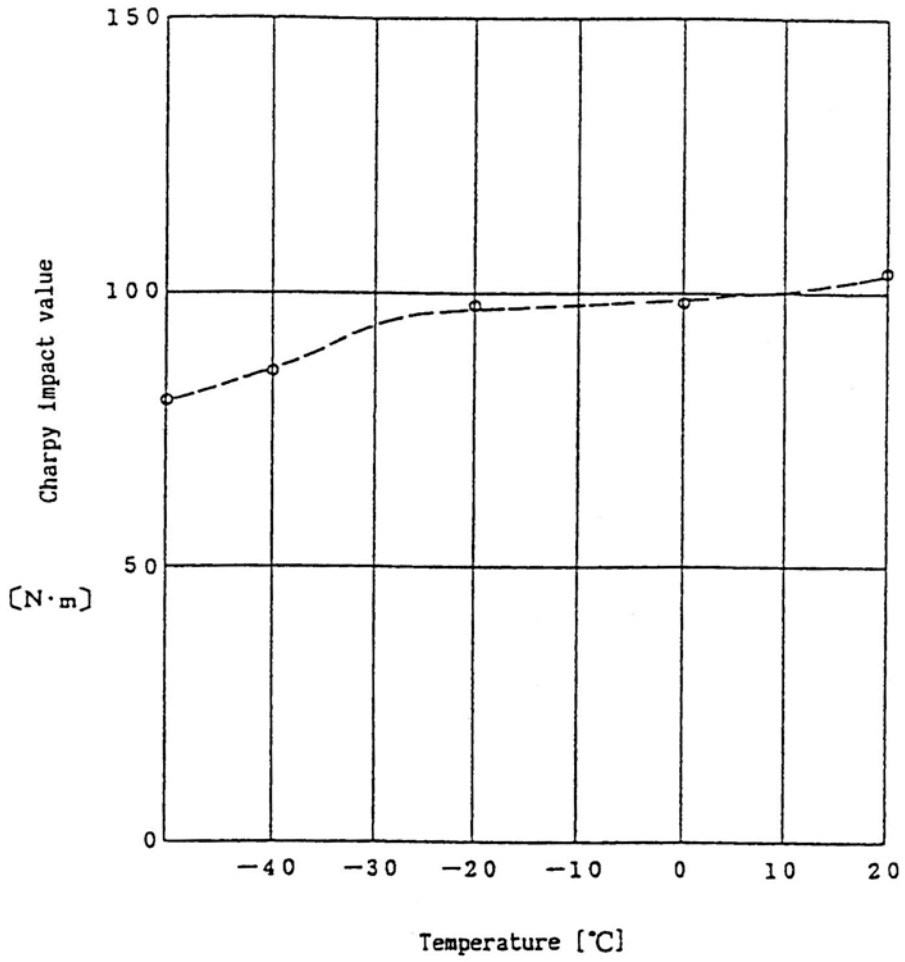

(Ⅱ)-Fig.A.109 Low temperature impact value of SUS 304 [16]

A.10.8 Low temperature impact Value of SUS 630/H1150

(Ⅱ)-Fig.A.110 shows the low temperature impact values of the material.

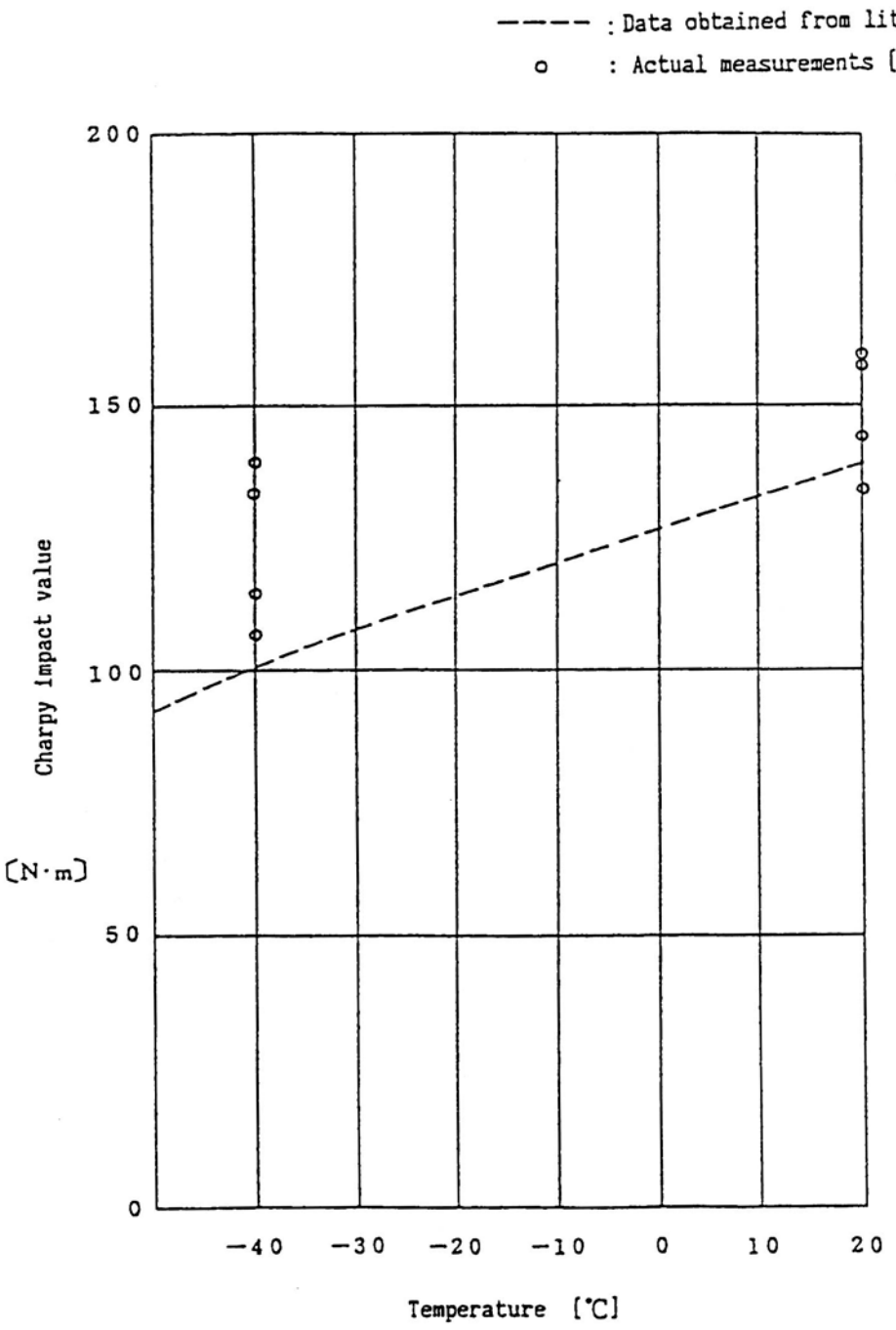

(Ⅱ)-Fig.A.110 Low temperature impact value of SUS 630·H1150 [18]

A.10.9 Method for calculating torque of inner lid clamping bolts

In this section, we will analyze the initial clamping force of the inner lid clamping bolt (called “the bolt” below).

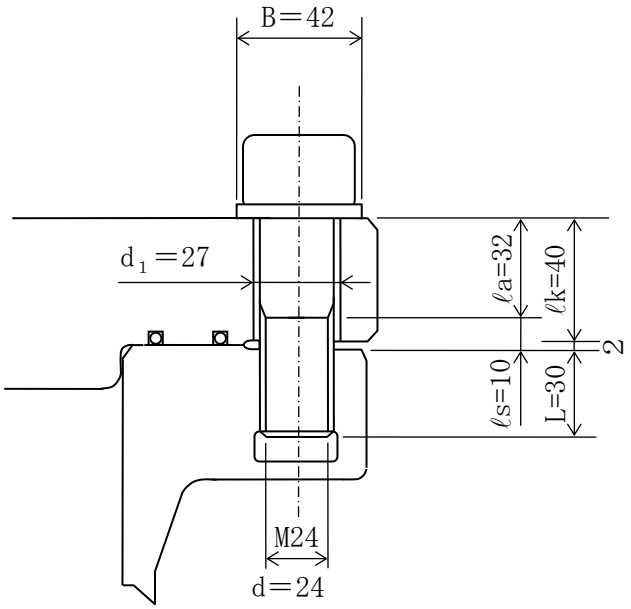

(Ⅱ)-Fig.A.111 Analytical model for initial clamping force of inner lid clamping bolts

The minimum required clamping force for the bolt shown in (Ⅱ)-Fig.A.111 is,

$$F_{min} = F_C + F_G + F_H$$

where

F_{min} : Minimum force required for tightening the bolt [N]

FC : Loss of compressive force in the inner lid when external force is applied [N]

FG : Clamping force assured by the O-rings [N]

FH : Decrease of clamping force due to differential thermal expansion [N]

These three values will be analyzed below.

(1) F_C , the loss of compressive force in the inner lid when external force is applied is

$F_C = (1-\phi)W_a = (1-\phi)(W_1 + W_2)/n$

where

W_a : Axial external force, Wa = (W1 + W2)/n

$= (0.309 + 8.13)\times 105/16 = 5.27\times 10^4$ [N]

W1 : Load due to internal pressure,

$$W_1 = P \cdot \frac{\pi}{4} G_1^2 = 0.175 \times \frac{\pi}{4} \times 474^2 = 3.09\times 10^4 \text{ [N]}$$

where

P: Maximum internal pressure, P = 0.175 [MPa]

G1 : Inner O-ring diameter, G1 = 474 [mm]

W2 : Load occurring at 9 m lid side vertical drop, $W2 = 8.13\times 10^5$ [N]

n: Number of bolts, n = 16

ϕ : Internal force factor of the bolt,

$$\phi = \frac{F_t}{W_a} = \frac{K_t}{K_t + K_C} = \frac{1.50\times 10^6}{(1.50 + 6.92)\times 10^6} = 0.178 \text{ [-]}$$

where

K_t : Tension spring constant of the bolt,

$$K_t = E_b \,/\, \left(\frac{l_a}{A_b} + \frac{l_s + l\delta}{A_s}\right) = 1.45\times 10^6 \text{ [N/mm]}$$

where

l_a : Length of the bolt cylinder, la = 32 [mm]

ls : Length of the thin bolt cylinder, ls = 10 [mm]

Ab : Cross section of the bolt cylinder,

$$A_b = \frac{\pi}{4} d^2 = \frac{\pi}{4} 24^2 = 452 \text{ [mm}^2\text{]}$$

A_s : Effective cross section,

$$A_s = \frac{\pi}{4} d_2^2 = \frac{\pi}{4} 22.051^2 = 382 \text{ [mm}^2\text{]}$$

Where

d_2 : Core diameter of the bolt, d2 = 22.051 [mm]

Eb : Longitudinal modulus of elasticity of the bolt,

Eb = 1.99×10^5 [N/mm^2]

$l\delta$: Length equivalent to the elastic displacement in the fitting parts of the nut, $l\delta$ = 0.57d = 13.7 [mm]

KC : Compression spring constant of the inner lid,

$$K_C = \frac{E_C}{l_K}\cdot\frac{\pi}{4}\ [d_m^2-d_1^2] = 6.68\times10^6\ [N/mm^2]$$

Where

l_K : Tightening length, lK = 40 [mm]

d1 : Diameter of bolt hole, d1 = 27 [mm]

B: Diameter of the contact surface of the bolt head, B = 42 [mm]

dm : Diameter of equivalent cylinder,

$$dm = B + \frac{l_K}{5} = 42 + \frac{40}{5} = 50\ [mm]$$

EC : Longitudinal modulus of elasticity of the inner lid,

Ec = 1.92×10^5 [N/mm^2]

Hence,

$F_C = (1-\phi)\ W_a = (1 - 0.178)\times5.27\times10^4 = 4.33\times10^4$ [N]

The tensile force F_t in the bolt due to external force is,

$F_t = \phi\ W_a = 0.178\times5.27\times10^4 = 9.38\times10^3$ [N]

(2) Clamping force for the O-rings

The clamping force F_G for the O-rings is,

$F_G = \pi(G_1 + G_2)\times q / n$

where

G_1 : Diameter of the inner O-ring, G_1 = 474 [mm]

G_2 : Diameter of the outer O-ring, G_2 = 514 [mm]

q: Linear load of the O-rings, q = 14.3 [N/mm]

Hence,

$F_G = \pi \times (474 + 514) \times 14.3 / 16 = 2.77 \times 10^3$ [N]

(3) Decrease of clamping force F_H due to differential thermal extension

F_H is 0 because the material of the inner lid is the same as that used for the bolts.

Thus, the minimum required clamping force is,

$F_{min} = F_C + F_G + F_H = (4.33 + 0.277 + 0) \times 10^4 = 4.61 \times 10^4$ [N]

(4) The initial clamping force for the bolt

The initial clamping force F_0 of the bolt is a little more than the minimum required force.

$F_0 = 5.89 \times 10^4$ [N] $= 6.0 \times 10^3$ [kgf]

(5) Initial torque for the bolt

The initial torque for the bolt is,

$T = k \cdot d \cdot F_0 = 0.2 \times 24 \times 5.89 \times 10^4 = 2.83 \times 10^5$ [N·mm]

$= 28.8$ [kgf·m]

where k is the torque coefficient (k = 0.2).

(6) Bolt clamping triangle

The above analysis results are shown in the bolt clamping triangle (see (Ⅱ)-Fig.A.112).

The following is the symbols used in (Ⅱ)-Fig.A.112.

F_0 : Initial clamping force of bolt, $F_0 = 5.89 \times 10^4$ [N]

F_{min} : Minimum required force for clamping the bolt, $F_{min} = 4.61 \times 10^4$ [N]

W_a : Axial external force, $W_a = 5.27 \times 10^4$ [N]

F_t : Increment of the bolts tensile force when external force is applied, $F_t = 0.94 \times 10^4$ [N]

F_C : Loss in the lids compressive force when external force is applied, $F_C = 4.33 \times 10^4$ [N]

F_C' : Residual compressive force in the inner lid, $F_C' = 1.56 \times 10^4$ [N]

F_H : Decrease of clamping force due to differential thermal extension, F_H = 0 [N]

F_b : Bolt tensile force, $F_B = 6.83 \times 10^4$ [N]

F_G : O-rings clamping force, $F_G = 0.28 \times 10^4$ [N]

(Ⅱ)-Fig.A.112 shows that the residual compressive force F_C' on the inner lid is higher than the O-ring's clamping force F_G.

Therefore, the containment of the O-rings can be maintained by the initial clamping force F_0.

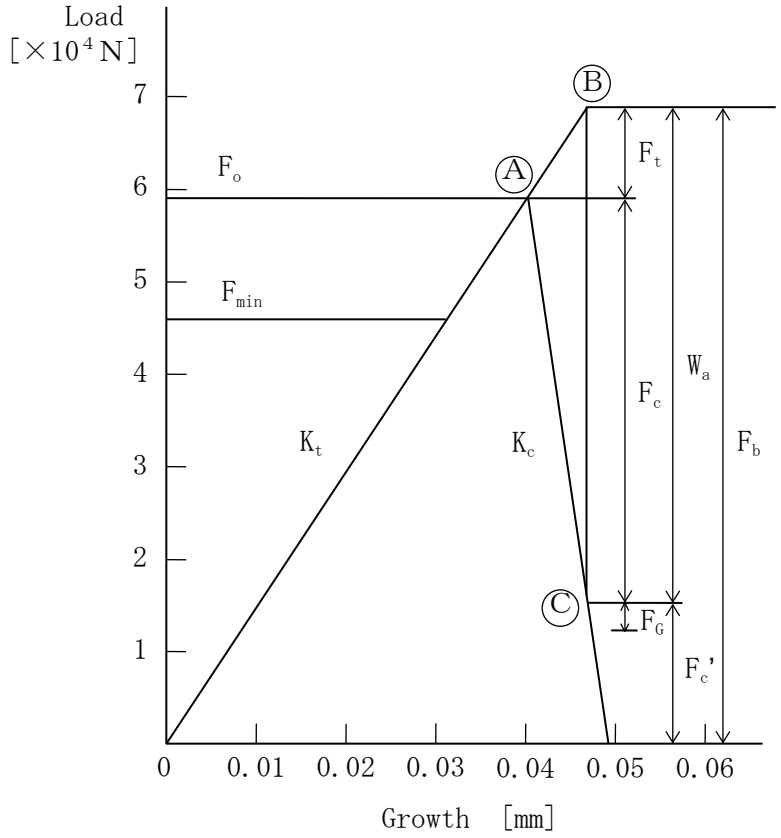

(Ⅱ)-Fig.A.112 Triangle diagram for inner lid clamping bolt

Explanation of (Ⅱ)-Fig.A.112

(1) This illustration shows that even if axial external force W_a acts from the initial clamp force of bolt F_0, the residual compressive force in the inner lid F_C would be larger than O-ring clamping force F_G.

(2) On the axial part of the bolts a tensile force F_o will be imposed by the initial clamping, and on the body to be clamped, (that is the lid part), a compressive force F_o will be generated, two forces being in balance with each other at point Ⓐ, the status of which is shown in the illustration.

(3) When axial external force W_a, acts on any of the bolts in axial direction, the status of the bolt and lid will be moved to point Ⓑ and point Ⓒ.

Point Ⓑ will be removed from Point Ⓐ by means of elongation δ being generated, by a tensile force F_t acting on the bolt axial part, and point Ⓒ will be removed from point Ⓐ to point Ⓒ by means of clamping length being extended as much as δ according to the compressive force, F_C, being lost from

the body to be clamped, (that is the lid part).

(4) That is to say, on the bolt a tensile force Ft is added, from the body to be clamped, (the lid part) a compressive force F_C being removed, and the clamping length will be extended as much as δ where the compressive force remaining on the body to be clamped (The lid part).

A.10.10 Mechanical characteristics of JRR-4B fuel plate

In order to define the analysis criteria by which the plastic deformation will never be generated in the analysis of fuel plate, the proof stress is taken as the analysis standard value.

The proof stress of the JRR-4B fuel plate which is the material for the fuel element (B) shall be specified as given below,

(1) The mechanical property of AG3NE, which is the material of fuel element (A) is shown in IAEA Guide Book, Vol.2 (referential document [14]), in which it is specified that the design yielding point (Sy) is not less than 63.8 N/mm^2 at the evaluating temperature 75℃.

(2) JRR-4B fuel has been subjected to a tensile strength test on the basis of a tensile strength test piece which is manufactured from a sheet of fuel plate sampled from each roll badge, the criteria of the test being 88.3 (N/mm^2) in the tensile strength; that is <9kgf/mm^2>.

This test is considered as one of the subjects of precommissioning test of the nuclear reactor facility.

(3) Besides the above, the results of measurements on 20 pieces of samples in the tensile strength test cited in the proceeding articles (2) are as follows.

	Results of measurements		
	Minimum	Maximum	Average
Proof stress (0.2%) (N/mm^2)	97.1	135	114
Tensile strength (N/mm^2)	108	143	122

(4) H12 materials of JIS 1100P and A1200P, which are the raw materials of JRR-4B type fuel plate cladding material, are deemed to have the strength more than those figures shown in the table given below.

	JIS A 1100P H12 A 1200P H12
Proof stress (N/mm^2)	73.6
Tensile strength (N/mm^2)	93.2～128

(5) Looking from the above, it can be deemed as the safety side estimation that the proof stress for the fuel plate having the tensile strength of 88.3N/mm^2 as previously cited in the article (2) as the proof stress of the mechanical property of JRR-4B type fuel may be adopted as 63.8N/mm^2 (yield point of the design) which is equal proof stress mentioned in proceeding article (1).

A.10.11 Literature

[1] ASME Sec. Ⅲ Subsec. NB (1974).

[2] Technical Standards for Atomic Energy Installation for Power Generation Including Standards for Structure, ministerial Notice No.501, 1980.

[3] Commentary on Standards for the Structure of Boilers and Pressure Vessels, Japan Boiler Association, 1980.

[4] In-house data of Mitsubishi Heavy Industries. Ltd.

[5] Roark, J.R., Formulas for Stress and Strain (4th edition), Mc'Graw-Hill International Book Company, 1965.

[6] Timoshenko, S.P., Theory of Plate and Shell (I); Japanese translation version by Hasegawa, T.

[7] Manual for Mechanical Engineering, 6th revised edition, Japan Society of Mechanical Engineering, 1977.

[8] Den Hartog, J.P., Mechanical Vibrations, Mc'Graw-Hill Book Co.

[9] Mizuhara, A. et al., Handbook for Structural Calculation, Sangyo Tosho Publishing, 1965.

[10] Formulas Used in Structural Dynamics, compiled by Japan Society of Civil Engineering.

[11] Sekiyu, T. et al., Handbook for Flat Structure Strength, Asakura Shorten.

[12] Handbook for Elastic Stability, Long Column Research Committee, Corona.

[13] Report on Development and Arrangement of Structural Analysis of Transport Packaging for Used Nuclear Fuel Ⅱ, Japan

[14] IAEA Guide Book Vol.2: Research Reactor Core Conversion Safety Analysis and Licensing Issues Fuels.

[15] On the Prediction of Deformation and Deceleration of a Composite Cylindrical Body for the Corner Drop Case, CONF-710801 (Vol.2), 1971, pp.733-776.

[16] Hasegawa, M., Manual for Stainless Steel, Nikkan Kogyo Shinbun.

[17] Data Book for Strength Designing, compiled by Editorial Committee for data book for strength designing.

[18] Fujita, T., Thermal Processing for Stainless Steel, Nikkan Kogyo Shinbun.

[19] Timoshenko, S.P., Buckling Theory; Japanese translation version by Naka, I. et al., Corona.

[20] Aluminum Hand Book (4th edition), Light Metal Society, (1990)

[21] Summary of Technology for Hybrid Materials, Industrial Technology Center, 1990

[22] In-house data of Nichias Co.,Ltd

[23] Code for Nuclear Power Generation Facilities: Rules on Materials Nuclear Power Plants (2012 edition) of The Japan Society of Mechanical Engineers

[24] Code for Nuclear Power Generation Facilities: Rules on Design and Construction for Nuclear Power Plants (2012 edition) of The Japan Society of Mechanical Engineers